ESD-TR-66-635

(Final Report)

LASA SIGNAL PROCESSING, SIMULATION,
AND COMMUNICATIONS STUDY

March 1967

DIRECTORATE OF PLANNING AND TECHNOLOGY
ELECTRONIC SYSTEMS DIVISION
AIR FORCE SYSTEMS COMMAND
UNITED STATES AIR FORCE
L. G. Hanscom Field, Bedford, Massachusetts

DISTRIBUTION OF THIS DOCUMENT IS UNLIMITED.

AD655802

LEGAL NOTICE

ESD-TR-66-635

(Final Report)

LASA SIGNAL PROCESSING, SIMULATION,
AND COMMUNICATIONS STUDY

March 1967

DIRECTORATE OF PLANNING AND TECHNOLOGY
ELECTRONIC SYSTEMS DIVISION
AIR FORCE SYSTEMS COMMAND
UNITED STATES AIR FORCE
L. G. Hanscom Field, Bedford, Massachusetts

DISTRIBUTION OF THIS DOCUMENT IS UNLIMITED.

FOREWORD

This research was supported by the Advanced Research Projects Agency. The Electronic Systems Division technical project officer for Contract Number AF 19(628)-5948 is Major Cleve P. Malone (ESL-2). This final report covers the period from February 14, 1966 to January 14, 1967; it is a continuation of the "Large Aperture Seismic Array Signal Processing Study," Contract Number SD-296.

This technical report has been reviewed and is approved.

Paul W. Ridenour, Lt. Col., USAF
Chief, LASA Office
Directorate of Planning and Technology
Electronic Systems Division

ABSTRACT

In this final report, the "LASA Signal Processing, Simulation, and Communications Study" results are described in detail.

A summary of our findings correlates the results with factual detail reported earlier. Signal processing is discussed; further system and simulation studies are reported; suggested system implementation is extended; and the set of simulation programs used in this study is described.

ACKNOWLEDGMENT

CONTRIBUTORS

CONTENTS

CONTENTS (Cont'd)

CONTENTS (Cont'd)

CONTENTS (Cont'd)

ILLUSTRATIONS

ILLUSTRATIONS (Cont'd)

ILLUSTRATIONS (Cont'd)

TABLES

Section 1

INTRODUCTION AND SUMMARY

Work during this study continued and extended signal processing techniques suggested in earlier work[1], evaluated applications of microprogramming, and investigated integrated signal processing and communication systems.

Additional requirements which became obvious during the course of the study resulted in a change in emphasis in several areas. One change was to develop a concept using a signal processing system remote from the array site. Another was to consider integration of the array monitor and control function into the proposed signal processing system. In studying beamforming, it was found that steering delays required for experimental purposes could be obtained by using previously determined arrival times.

Once the anticipated signal gain was verified by data analysis, using conventional processing, additional effort was applied to microprogramming to determine the expected speed gains. Moreover, initial diagnostic and discrimination tests using the experimental beam display encouraged an increase in effort to develop the display as a tool.

As a result of these changes, we de-emphasized the world network communications study and the array geometry synthesis.

The study has provided a definition of the initial system synthesis and an analysis of the functional partitioning of a signal processing system, beamforming requirements, array gain, beam coverage, microprogramming, and event location capabilities. Results were conclusive enough to recommend an equipment and program configuration to process LASA signals, and to designate the logical steps necessary to have a signal processing system operational at an early date. A long-range effort was suggested for improving system operation

and for using the proposed signal processing system as a powerful new tool for research in seismology and large array signal processing.

1.1 SUMMARY OF AREAS AFFECTING THE STUDY

System partitioning and beamforming requirements, array gain and beam coverage, microcoded instructions, array geometry, and event location capability received primary consideration as part of this study. Relevant findings in these areas are summarized in the following paragraphs.

1.1.1 System Partitioning and Beamforming Requirements

The LASA signal processing system concept described herein is partitioned into two functions—detection processing and event processing. Implementation of these functions in two compatible processors provides processor redundancy for the critical functions. The signal processing techniques used are conventional beamforming, frequency filtering, and threshold detection.

The detection processing function is required to perform real time on line surveillance of a significant part of the teleseismic zone (i.e., all land areas and all known seismic regions). To efficiently process in real time, this function should be restricted to the essential task of providing approximate arrival time and event location. A reasonable criterion for initial detection is to ensure a loss of less than 3 dB per beam up to 1.5 Hz and to reject noise by bandpass filtering.

Event processing need not occur in real time, but must be capable of maintaining pace with the average detection output rate. This requirement does not prohibit the processing load for a given event from exceeding the signal history period. Arrivals from a detected event are sorted according to the estimated modes of propagation and to their probable registration relative to the beam pattern. Then, a more detailed investigation of the accomplished detection families is performed with densely packed beams to obtain the best event record and to refine location parameters. The preservation of signal fidelity up to approximately 3 Hz with a loss of less than 3 dB per beam has been adopted as a conservative beam distribution criterion.

1.1.2   Array Gain and Beam Coverage

Analysis and simulated tests using LASA recorded earthquake and nuclear test data, although limited in number, have demonstrated significant enhancement of signal-to-noise ratio through the application of conventional beamforming and appropriate frequency filtering. Conventional beamforming and filtering gains approaching 25 dB for a natural event and 34 dB for a nuclear event, with respect to the unprocessed seismometer output, have been measured and verified by spectral density comparisons.

The number of beams required to cover certain pertinent areas of the teleseismic zone, as seen from Montana and a possible Array II location, was calculated as a function of beam quality. A requirement of several hundred detection beams was inferred for comprehensive real-time surveillance. This requirement is compatible with contemporary computer technology, in that the detection load can be supported by a machine of moderate size.

1.1.3   Microcoded Instructions

Beamforming, filtering, and other repetitive computation requirements can normally be implemented by either a modest special-purpose computer or a slower, and therefore larger, general-purpose machine. Advantages of both modest size and sufficient speed for special purposes can be attained by microcoding standard general-purpose computers; thus, standard machines are equipped with special additional instructions which extend their capability to function as special-purpose processors while retaining their general-purpose capability.

1.1.4   Array Geometry and Event Location Capability

A limited number of simulation runs, using LASA seismic data tapes, indicate that the number of seismometers per subarray can be reduced from 25 to 16 without any loss in array gain. Because of noise coherence properties over the subarray aperture, the gain is in fact improved when the inner ring of seismometers is discarded.

Furthermore, it appears possible to discard the four or eight outer sub-arrays, considerably simplifying the logistics and data transmission requirements. Theory is supported by simulation tests which show that only a one or two dB loss penalty is incurred. While it is true that omission of the outer one or two rings of subarrays will decrease single LASA event location accuracy, this capability may be very modest, even for the full LASA, when compared to accuracies obtainable from a world network of arrays. The implications on location and secondary arrival discrimination have not been completely established.

With the above mentioned array reductions, it would be necessary to reduce slightly both the word length and sampling rate to support the above operations with a total input data rate of less than 50 kilobits per second. This data rate is compatible with commercially available wide-band data transmission service.

1.2   STUDY SUMMARY

The primary purpose of this study has been to identify a method of automating the LASA signal processing system hypothesized previously. We extended this system to include array monitoring and control, and to permit both remote and local operation. Two other areas which we studied were supporting analyses to develop initial system operating parameters, and computer program development to test the processing assumptions with experimental data and to verify expected system operation.

1.2.1   Signal Processing

The system requirements, in terms of the required number of detection and event beams as a function of the number of subarrays used for detection, are based on results reported earlier.[2] The requirements were extended to include those of a possible Array II location as shown in Figure 1-1. These curves provide the base signal processing requirements for both detection and event processing and constitute a system objective. A processing system which meets the experimental and operational objectives is shown in Figure 1-2, and described in some detail in Section 2.

The array field, nominally 21 sets of 25 seismometers, transmits sampled quantized data to an identical pair of interfacing units. The detection interface (DI) system equipment receives parallel data from M subarrays of n seismometers each, and edits and presents data to the detection processor (DP). The DP records Mn seismometer data channels and performs the detection process. The DP output is a queue of detections with identification of arrival occurrence and magnitude appropriately recorded and provided to the event processor (EP). The EP determines the members of the detection queue associated with a single seismic event on the basis of arrival velocity and time relationships which must be satisfied by such members. Required time and velocity relationships as a function of range are stored as approximations to seismic travel-time tables.
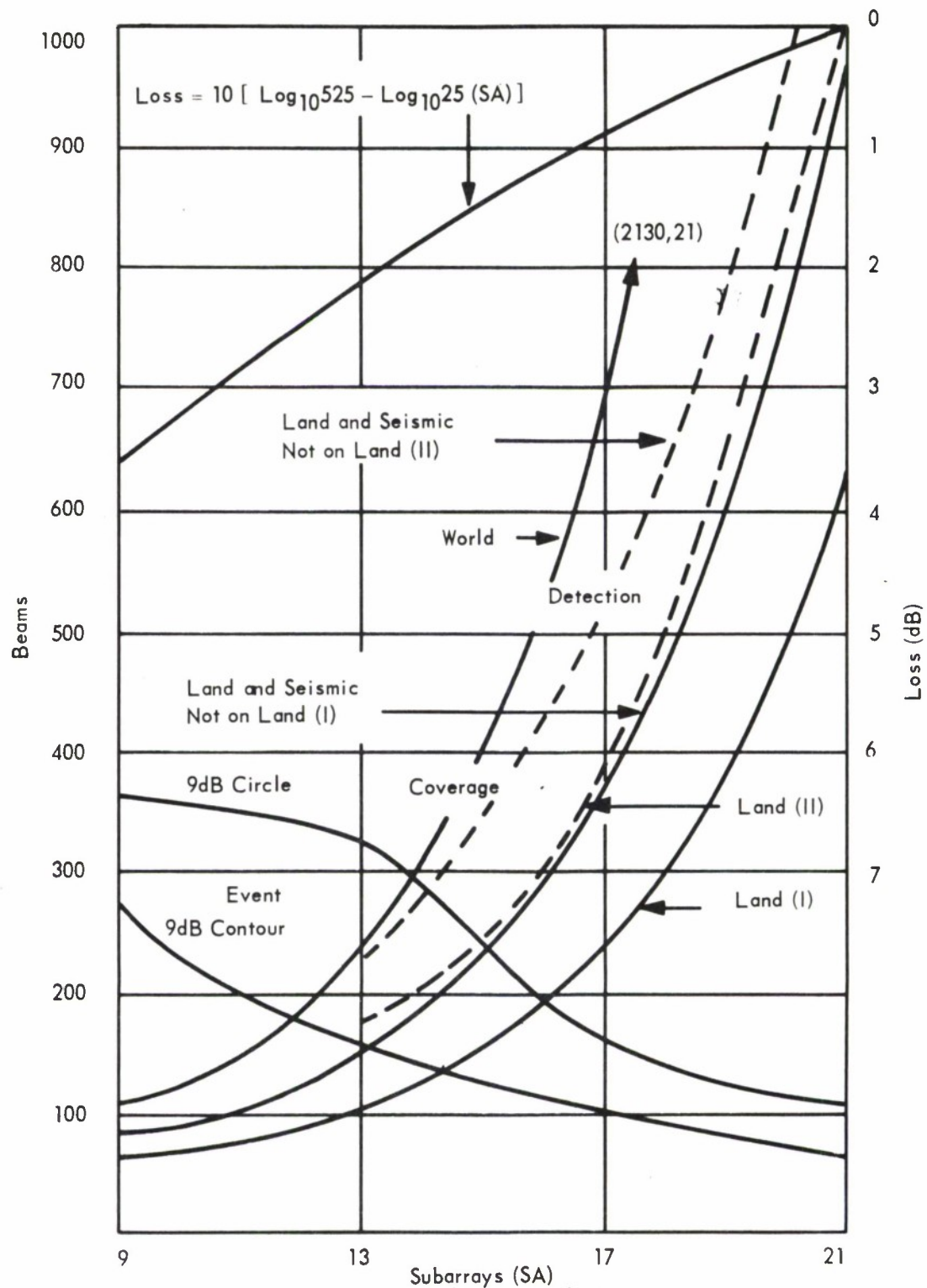
Figure 1-1. Beam Surveillance Coverage Requirement

The figure shows a plot with:
- Left vertical axis: Beams (100 to 1000)
- Right vertical axis: Loss (dB) (0 to 7)
- Horizontal axis: Subarrays (SA) (9, 13, 17, 21)

Labels within the figure:
- Loss = 10 [Log$_{10}$525 − Log$_{10}$25 (SA)]
- (2130,21)
- Land and Seismic Not on Land (II)
- World
- Detection
- Land and Seismic Not on Land (I)
- 9dB Circle
- Coverage
- Land (II)
- Event 9dB Contour
- Land (I)
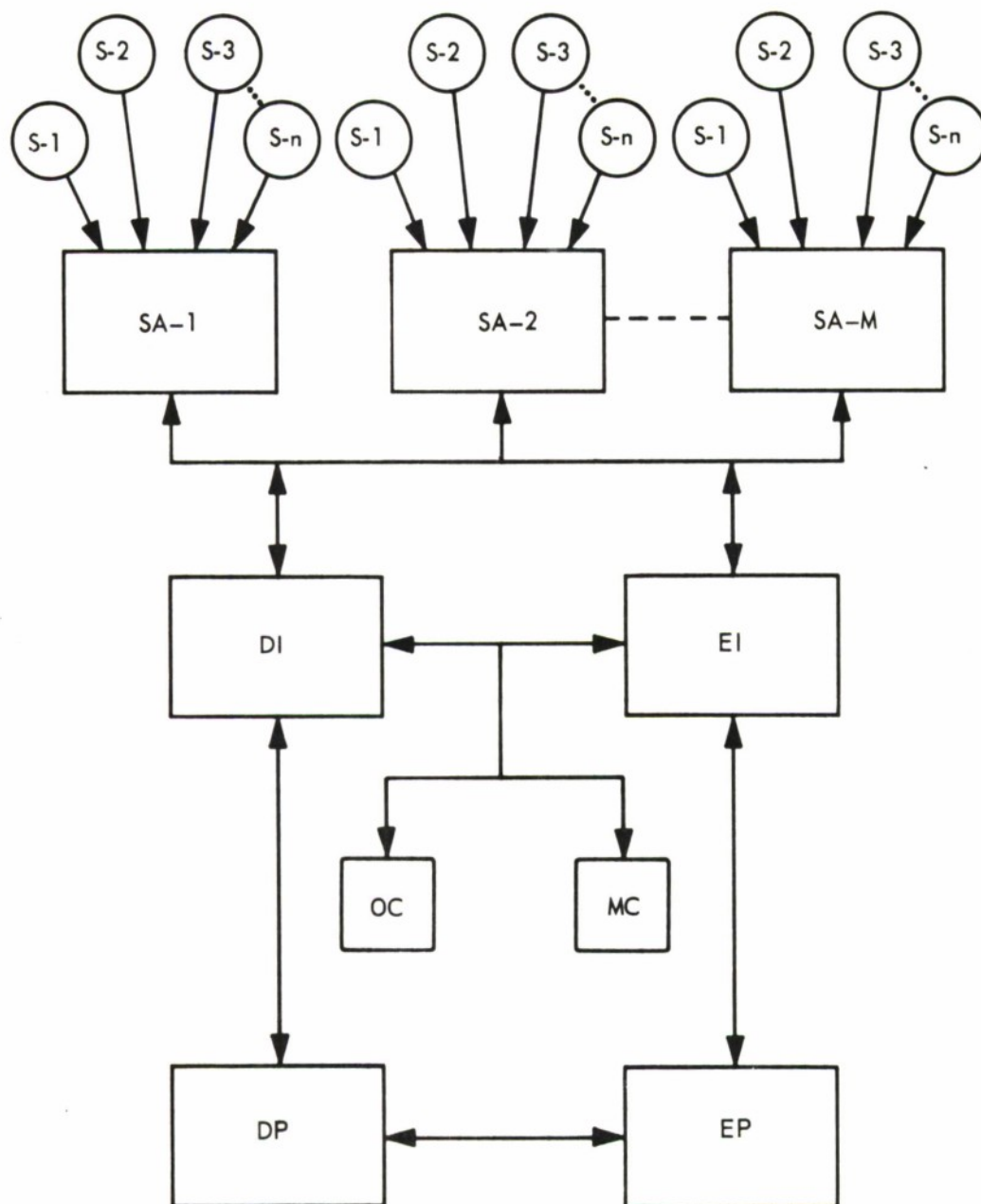
Figure 1-2. A LASA Signal Processing System

For detected arrivals, event beams are formed. If necessary, special processing, including tailor-made steering delays and/or optimum processing, can be included. A seismic bulletin is generated from the resulting events.

The operation console (OC) and the maintenance console (MC) are the operator monitor and array control stations, respectively. The event interface (EI) system equipment supports the array maintenance and control function.

Redundancy considerations are based on a fail-soft philosophy. In case of a DP failure, for example, the EP performs the DP function; hence, an uninterrupted detection processing is provided at the expense of event processing. Similarly, the MC should be designed to function as an OC, and the EI as the DI. This system synthesis requires that the EP, EI, and MC be sufficiently sized to provide a catch-up capability for reasonable values of detection thresholds and maintenance procedures. An auxiliary processing system may be required for supporting classification studies and operations. Although this aspect is discussed in subsequent sections, it is not a principal part of the system concept. The total system implementation plan is identified with options which must be available to cover requirements for both remote and on-site processing system locations (Section 2.1).

A suggested communication system between an array and a remotely located processing system is based on certain array modifications (e.g., not using the B-ring of seismometers in each subarray) that can be made without significant loss in system performance (Section 2.2). Our data analyses (based on a limited sample) and the results of other analyses strongly indicate the validity of this conclusion. Nevertheless, further investigations using larger data samples are warranted. The principal implication of the reduced communication line requirement is that by appropriately scaling a coarse and fine channel and by modifying both the word size and the sampling rate, the total data rate can be reduced to less than 50 kilobits with a total processing loss of one or two decibels. A reduced aperture has little effect on system gain. Its effect on location accuracy is decreased single-LASA capability. However, this capability is modest compared to that of a large baseline world network, so

the loss of accuracy may not be important. In a remotely located processing system, the reduced logistics, reduced communication requirements, and reduced processing load are advantageous.

An explanation of detection and event processing functions, interface and display requirements, and event processing data flow logic (Sections 2.3 and 2.4) indicates that for appropriate integration, a family of software routines which can be individually tested and monitored should be developed.

Effort was directed toward developing evaluation methods and implementation techniques for microcoding a set of signal processing algorithms (Section 2.5). Generally, an average speed increase of the order of seven is expected over assembly language coding, without the loss of general-purpose machine flexibility.

In the system operation and array maintenance and control functions, relative complexity is required to ensure adequate checking of automatic system operation; but the flexibility to permit continued system growth may require computational extension. Therefore, interface equipment and console system concepts for such extension are given (Section 2.6).

An experimental breadboard display which was constructed and tested appears useful for process evaluation, and may be significant in developing discrimination criteria; it warrants further investigation (Section 2.7).

In an analysis of the initial processing program configurations, the system control function which supports the data flow, and the necessary control functions to implement the signal processing system indicates the need for a systems programming approach in the signal processing system (Section 2.8).

1.2.2   System Studies

Supporting studies which were not included in the First[2] or Second[3] Quarterly Technical Reports are discussed in Section 3. A brief summary of relevant earlier results is also given.

Recommendations in these reports for system sampling rates and scaling were based on requirements to adequately process signals below the

saturation level, and to limit gain degradation from round-off and sampling error to less than 1 dB. An extensive discussion of various sources of processing loss, such as beamforming, filtering, sampling, and scaling, was presented. LASA location capability was also discussed. A capability for optimum processing is desirable, but such processing is expected to be used only for special events. A program for ray tracing in a spherically-layered medium was presented and used for approximating the phase speed-range relationship.

Graphs showing beam coverage as a function of signal frequency led to system designs based on a detection frequency of 1.5 Hz. Experience with signal spectra indicates that most of the energy is at a frequency of 1.0 Hz; therefore, the designed detection beam coverage should be adequate.

Beam requirements for the Montana LASA and an estimate of requirements for a possible Array II location are reviewed (Section 3.1). Because the teleseismic region associated with Location II might contain larger land and seismic areas than those of the Montana LASA, approximately 50 percent more detection beams are necessary, subject to frequency requirements.

Array geometry is discussed briefly (Section 3.2), and LASA beam patterns, including phase response, are shown. The programs which generate these beam patterns can be used for future array design.

The event location capability of LASA and of a world network indicates that an investigation of correlation techniques should be made to obtain more accurate relative arrival times, both at LASA and on a worldwide basis (Section 3.3). The effects of finite beamwidth, inaccurate steering delays, and uncertainty in the phase speed-range relationship discussed in this report are likely to cause several-hundred-kilometer event mislocation. Calibration and other processing considerations may reduce this location uncertainty.

The results of a study of array steering delays indicate that the process of referencing arrival time data to plane wavefronts yields delays of a quality comparable to that obtained when using worldwide travel-time tables as a reference (Section 3.4). Because of the convenience of using a self-contained system, we believe that the wavefront method should be pursued. Curvatures are

measurable by a second-order (quadratic) wavefront program. At the subarray level, plane wavefront approximations can probably be used without incurring unacceptable loss, a result believed to be in substantial agreement with results obtained elsewhere.[4] The fact that certain subarrays seem to be consistently high or low in either observed speed or observed azimuth should be investigated further.

In the area of acquisition of arrival time data, simple thresholding is somewhat erratic even for strong events. It is hoped that the addition of re-dundancy logic and careful threshold value selection will provide adequate ac-curacy at least for the stronger events. For weaker events the possibility of correlation processing for time difference measurement should be investigated.

The probability distribution of required steering delays to estimate the processing speed requirements is shown (Section 3.5). Although the maximum delay is governed by the array diameter and by the smallest expected value of horizontal phase speed, most delays which must be implemented will be con-siderably smaller than this maximum.

The experimental beam display and its initial use on the Longshot event and on an earthquake are described (Section 3.6). This display is useful for arrival analysis in that it provides a visual representation of an event oriented in k-space coordinates on many contiguous beams as a function of time. The results of filter formulation, error characteristics, and precision require-ments studies indicate that classical frequency filtering can be readily instru-mented (Section 3.7).

By an analysis of actual seismic data records from five experiments, an evaluation of subarray beamforming, integration time, system gain, scaled signal-to-noise ratios, and power spectra, is made (Section 3.8). The inner ring of the seismometers can be deleted or weighted zero with a slight gain in performance. In addition, when the outer one or two rings of subarrays are deleted, a loss of less than 1 dB or 2 dB is incurred.

The center of gravity and radius-of-gyration calculations to solve two dif-ferent problems are discussed (Section 3.9). The first problem is selecting the event beam which best describes the event; the second is improving the

location of the event within the selected event beam. In the location problem the center-of-gravity method is useful, since errors because of pattern asymmetry are small. For event beam selection the radius-of-gyration result was disappointing. Generally, the first- and second-moment approach appears to be computationally simpler than the originally suggested correlation technique, and for that reason it was investigated. Although the results are inconclusive, beam pattern correlation may yield other performance advantages and, therefore, warrants consideration.

1.2.3   Data Analysis Programs

Computer programs developed during this study are described, and a flow chart of each program is included (Section 4). Generally, the description of the programs relates to a particular version of that program. The experimental nature of the study constantly required program modification to increase general program capability or to conduct a particular experiment.

The available programs provide considerable signal processing analysis capability. A LASA Tape Edit program, which edits the raw seismic data tapes available from LASA, was developed. Programs functionally simulating the signal processing algorithms of subarray and LASA beamforming and filtering were generated. With the pertinent filter characteristics provided, the coefficients required for a given classical filter can be calculated. The ability to compute signal and noise power exists at the seismometer, subarray beam, and LASA beam levels. Power spectrum measurements can also be made at each of the three levels. The time delays required for subarray beamforming are provided through a relatively simple thresholding technique, which is suitable for large events. The time delays required to form neighboring beams at the LASA level are provided by linear or plane wave corrections added to the measured time delays corresponding to the central beam.

Programs necessary to generate tapes in a suitable format for the experimental display were developed. The results of the LASA beamforming function represent the normal display data in natural coordinates.

A pseudo-event tape can be developed from a known event so that the signal-to-noise ratio of the seismometer data of the pseudo event is some binary factor of the known event signal-to-noise ratio. Auto- and cross-covariance routines to process data at both seismometer and LASA beam levels were generated. A plot program exists for generating digital plots of various combinations of seismic data channels. An additional plotting capability that generates inverse velocity space maps is provided.

The programs, in general, were written in FORTRAN IV for the IBM 7090 and require only minor modifications for use on machines supported by a FORTRAN IV programming system capability.

1.3   STUDY RECOMMENDATIONS

Our recommendations for acquiring a LASA signal processing capability concern three categories:

- Configuration of a LASA signal processing system
- Procedure for an early system operational date
- Long-range effort for improving the system operation and for using LASA as a powerful new tool for environmental research.

1.3.1   Configuration of a LASA Signal Processing System

The LASA signal processing system should be built substantially as envisioned in the final report (reference 1) of the original study in this series. Further study (references 2 and 3) and analysis of seismic data performed as part of the present study validate that basic configuration and suggest a need for incorporating certain additional functions. System partitioning into real-time detection and lag-time event processing appears to be appropriate. The degree of processing for any given event should be selectable from minimum real-time detection and rough location through routine event processing (using the finer preformed event beams) to special processing capable of producing maximum enhancement of signal-to-noise ratio and signal fidelity. Routine event processing should include the grouping of arrivals into event families. Special processing should include capabilities for the generation of event-tailored steering delays and optimum processing or equivalent.

Serious consideration should be given to eliminating the inner ring of seismometers in each subarray. If permitted by the location degradation, the elimination of the outer ring of subarrays also warrants further consideration.

Initially, at least, steering delays should be organized for greater simplicity, according to the wavefront technique. The reading of relative arrival times at LASA should be automated by cross-covariance analysis of individual seismometers or subarray beams with the LASA beams.

Microcode simulations verified the efficiency of microcoding and the significant speed improvement attainable when the basic signal processing algorithms

are implemented by microprogramming. In effect, microcoding permits the use of a general-purpose processor as a special-purpose one, while retaining the flexibility of the general-purpose machine.

To ensure against unforeseen needs for processor capability which is either significantly greater or smaller than now expected, leasing rather than purchasing the required processing equipment is advisable.

1.3.2 Procedure for Early Operational Date

If a LASA processing facility is available, the first step in making the system operational is to begin operating the detection processing function of the system with tape data, thereby developing a data base.

Results of the communications study suggest that the system can be located off-site for ready accessibility. Serious consideration should be given to interface system equipment for permitting on-line experimental testing of the system concept. Event processing programs should be written and debugged at an early date.

A rudimentary form of automatic event processing should be attempted at an early date. However, the system should permit sufficient flexibility of the logic flow between individual processors and programs to permit the required operator monitoring and intervention for testing various procedures.

A display should play a central role in correlation experimentation designed to determine the best event beam and, perhaps, the event location within that beam.

Additional work is required to finalize the control and maintenance functions to be instrumented in this system. Some effort should be devoted to testing the long-period instrument contributions to the LASA capability.

1.3.3 Long-Range Effort

The usefulness of cross-covariance calculations for providing improved event locations by correlating signals from a world network of stations with LASA beams should be tested. In an attempt to arrive at the best possible steering delays for large numbers of events, the investigation, systematization, and

improvements of these delays for various world regions should proceed as more events are received.

Experiments should be designed, using LASA as a seismic research tool, to obtain more accurate knowledge of the earth's velocity and geological structure and to investigate earthquake predictions and other important environmental data.

Signal processing system trade-off studies should be extended in an attempt to enhance system performance.

Section 2

SIGNAL PROCESSING

A part of the "LASA Signal Processing, Simulation, and Communications Study" addressed technical topics fundamental to the definition of an experimental real-time system. The signal enhancement processor must be very efficient to allow a sensitive real-time surveillance of large regions, and must have the flexibility essential for seismic research. Process automation, record standardization, documentation control, communications flexibility, reliability, fail-soft modes, system diagnostics, maintenance support, and growth potential must be considered to ensure a direct extension to operational status. As the requirement analysis progressed and preliminary processing experience was acquired, a system concept evolved which accommodated the diverse objectives.

Major components of the implicit system implementation are described in this section. The baseline system configuration assumes on-site processing and incorporates several fail-soft options. A communications extension option is presented to permit remote processing with a reduced channel. Basic architectures for both detection and event processing are included, but considerably more data analysis is required to establish the discriminant processing structure. Implementation of detection and event processing will permit the efficient generation of beam histories to support this research. The topics of microprogramming, communication's interface, display functions, and control programs are also presented to provide a comprehensive definition of critical areas which involve special equipment, and/or significantly affect performance efficiency.

2.1 SYSTEM CONFIGURATION

The objectives of the LASA signal processing system are to

1. Test the validity of proposed seismic processing techniques
2. Establish a real-time facility capable of detecting, discriminating, and documenting seismic activity in the teleseismic zone
3. Obtain system operations experience and methods to identify equipment performance criteria
4. Identify methods of improved seismic signal processing
5. Develop information dissemination and coordination techniques
6. Provide a system dedicated to enhance the body of relevant signal processing knowledge
7. Accomplish the above in a manner to allow for experimental systems change.

Comprehensive surveillance requires parallel processing of real-time seismic information which has a large composite data rate; processing speed and flexibility are critical system parameters. The equipment composition must provide adequate fail-soft backup and support for operational functions such as calibration, diagnostics, array maintenance, and supervision. General-purpose machines can be employed without a loss of inherent flexibility, if predominant algorithms are instrumented as special-purpose instructions. These algorithms allow a range of conventional through optimum processing, augmented by arbitrary digital filtering and detection techniques to be programmed in completely general terms.

The process is partitioned to create functional components for machine task allocation. The detection processor performs comprehensive surveillance and identifies the time-phase velocity window of each arrival satisfying the a priori signal criterion. Scaling pointers are established for subsequent operations. This information is logged on the associated tape complex (see Figure 2-1) and is transferred to the detection queue resident in the event processor.

A consistent arrival family is assembled and analyzed by the event processor. Working disk and tape storage is provided through the signal preprocess
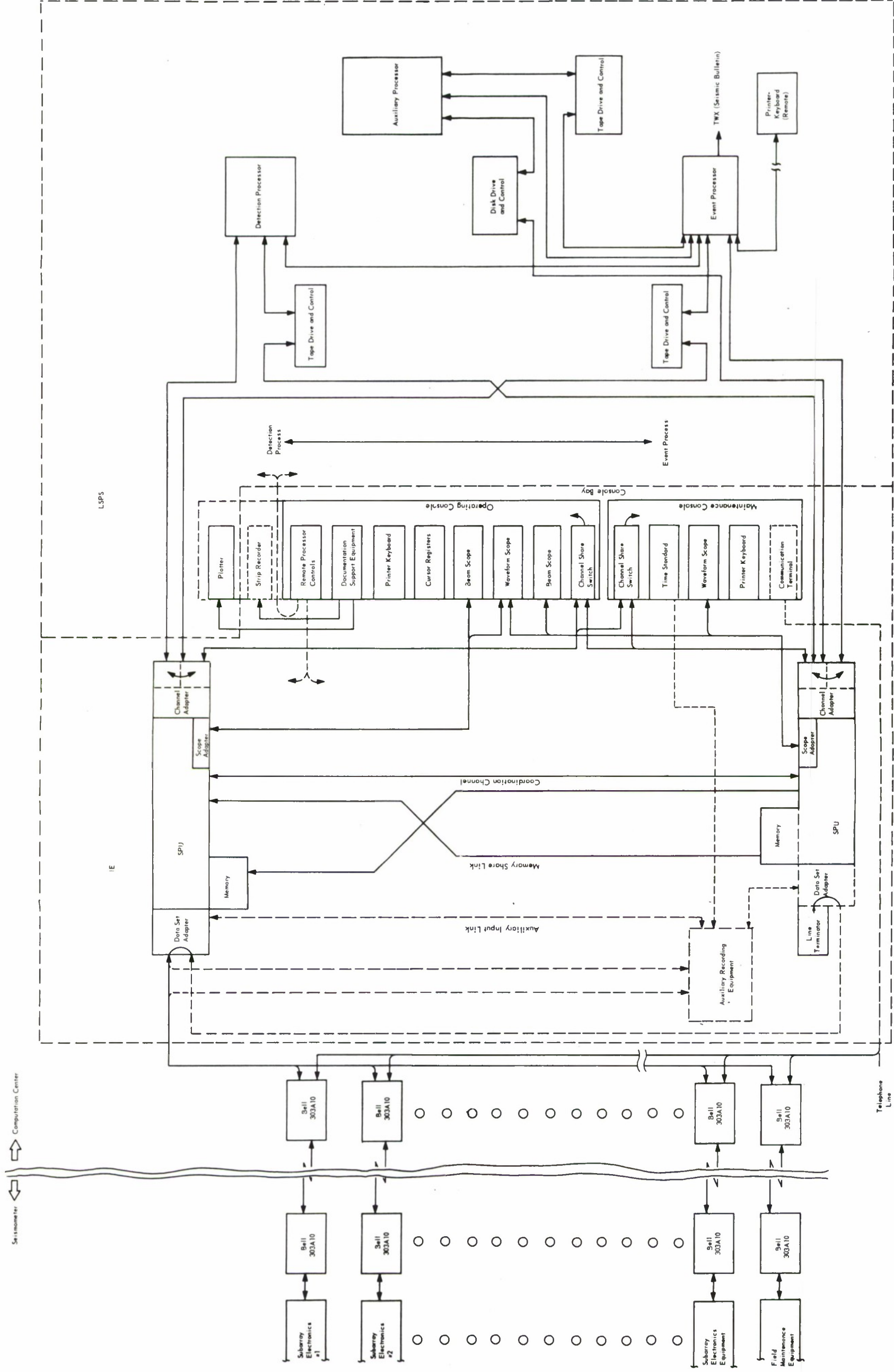
Figure 2-1. Real-Time Equipment Configuration

unit (SPU) channel adapter or by the equipment shared with the auxiliary processor. Additional tailored processing is based on raw data maintained in the event processor tape complex, and characteristic histories are documented. When pertinent, special processing is conducted to extract critical signal parameters and/or update empirical system files. A seismic bulletin is prepared and disseminated to the seismic community by TWX and remote printer-keyboard facilities. Reference data libraries are maintained to permit subsequent processing, documentation, or dissemination as a request service.

An auxiliary, nondedicated, general-purpose scientific processor is also coupled to establish a significant off-line capability, while retaining sufficient intermachine communications for efficient multiprocessor data flow. This capability will be used to analyze signatures for classification, to support seismic data processing research, and to provide the structure for coordinated multiple array operation. Function detail will develop as experience and base data are accumulated.

Raw LASA data is transmitted from each subarray equipment vault to the data processing center as digitally-encoded serial characters with word parity checking. The format is not compatible with general-purpose digital processing terminals; therefore, an interface equipment (IE) requirement exists to preprocess the data. Maintenance and logistics support will be most efficient when the same technology is used throughout the center. Such a concept dictates compatible signal specifications, ensuring a minimum impact in the event of subsequent functional changes or design adjustments.

The basic function of the IE is to buffer communication terminals, multiplex input channels, synchronize message framing, decode characters encountered in transmission, verify message fidelity, and translate the format to be compatible with the detection processor terminal. A secondary function is to time and control each subarray and to implement processing required for a duplex communication capability.

Supporting simultaneous communications through a sufficient number of these channels constitutes a rudimentary requirement which is satisfied by the

data set adapter working with the SPU memory. After message verification, scaling, and blocking, the information is transferred through the channel adapter for processing and documentation. Redundancy can be obtained by adding a second data set adapter on the lower SPU, or by using a special independent recording unit (illustrated with dashed lines).

The principal secondary SPU task is to support display and maintenance functions. Memory share links facilitate the bilateral transferral of seismometer and display data. Substantial histories are retained on disk memory accessible through the channel adapter.

Operations supervision and maintenance are performed from separate consoles. Each is coupled to the system with an automatic channel share switch to permit direct access by either SPU or indirect access by any processor. Discrete sense and indicator facilities are instrumented with standard digital components, although the panel layout is customized for particular operator functions. Printer-keyboards are incorporated to provide flexible control and log facilities.

The maintenance console contains a waveform scope to display array signals and spectrums. A communication terminal permits vocal contact with personnel at the array site to coordinate maintenance activities. Provisions for conference nets should be considered. The system time standard receiver and equipment is incorporated in this console to establish an absolute reference. Either SPU should be capable of maintaining adequate time accuracy for one-day periods to maintain continuity during possible malfunctions.

Overall system monitoring and control is performed at the operations console. A functional description of the display scopes with their associated cursors is given in Section 2-7. Interface equipment supporting hard-copy documentation plotters is contained in this console to permit general data access and to facilitate editing activities. Remote processor controls should be incorporated to centralize device assignment and permit efficient functional reconfigurations.

An examination of the conceptual real-time equipment configuration reveals considerable inherent flexibility in function assignment and data flow.

This flexibility provides adaptability to ensure the initial interface with the dynamic subarray electronics configuration, to permit efficient subsequent upgrading of the subarray channels, and to provide latitude for the system evolution characteristic of R&D efforts. Advanced signal processing features, such as a comprehensive fail-soft response reflex or multi-array coordination, would not significantly alter the system hardware components. In view of anticipated LASA concept extensions, such a growth potential is required to optimize the LASA program design efforts.

2.2   LASA COMMUNICATIONS EXTENSION

Signal processing at the LASA site requires minimum communication of real-time seismic data. However, the potential advantages of performing the computations at a more accessible location during the advanced program development and classification research phases create interest in extending the LASA communication network.

Preliminary sizing of the channel requirements is given in Table 2-1. A direct extension would require both a TELPAK D and a TELPAK A, the latter channel supporting the provision for on-line diagnostics from the maintenance depot at Miles City. The basic sampling rate of 20 Hz and the first submultiple (10 Hz) were combined with various trimmed word structures to investigate the feasibility of narrower, less expensive communication channels. When an excessive loss in array dynamic range resulted, coarse channels at the subarray level were reinserted to maintain a basic LASA large signal capability. Modified subarrays permit a reduction to TELPAK B equipment, but preclude continuity during the interface transition.

Intermediate message format equipment at Miles City would minimize the transition problems and simultaneously provide a more efficient message structure for long-distance communications. No significant operational impact would be present, for the process is deterministic and would require no operator participation. Economically, TELPAK A (or the proposed TELPIPE) service is preferable.

Table 2-1. LASA Communication Extension Costs

Configuration	TELPAK Channel	Capability (Word Size and Sample Rate) (See Note 1)		Installation $	$/Month (Washington Terminal) (See Note 2)	Comments
Direct transmission east	D + A	Complete		2300	104,455 (156,945)	Note 3
	D	No maintenance		1800	78,595 (141,235)	
Modify subarray	C + A	19S/SA	15 bits @ 20 Hz	1500	70,440 (66,530)	Does not include cost of modified subarray
		25S/SA	12 bits @ 20 Hz			
			15 bits @ 10 Hz			
	C	19S/SA	10 bits @ 20 Hz	1000	44,580 (50,820)	Note 3
			15 bits @ 10 Hz			
		25S/SA	8 bits @ 20 Hz			
			15 bits @ 10 Hz			
	B	19S/SA	10 bits @ 10 Hz	1000	35,320	
Intermediate message format equipment	B	19S/SA	10 bits @ 20 Hz	1000	35,320	Does not include format equipment or field communications cost
			15 bits @ 10 Hz			
		25S/SA	8 bits @ 20 Hz			
			15 bits @ 10 Hz			
	A	See Text		500 (400)	25,860 (15,710)	

Note 1: Message structure includes low-frequency channels and additional coarse channels when required to compensate for truncation in array data word dynamic range.

Note 2: Revised tariffs being reviewed by government agencies are indicated in parentheses.

Note 3: All data transmission and multiplexing beyond the subarray is assumed to be by common carrier and therefore bandwidths must be in multiples of 4 KHz.

Two concepts were investigated to understand appropriate reduction techniques which would retain the maximum LASA capability. In the first model, system dynamic range, when restricted to a TELPAK A, is illustrated by Figure 2-2 as a function of the adopted sampling rate and seismometer word size. The model is composed of 19 seismometers per subarray, scaled to cover the dynamic range from 20 dB (relative to one nanometer) to below the background noise. This permits a 12 dB overlap with the one coarse seismic channel per subarray which is scaled to provide a relatively noise-free representation of strong events. Other pertinent assumptions as well as the sampling loss as a function of sampling rate are shown in the figure.

An interpretation of the presented information must consider processing characteristics. When a small signal-to-noise ratio prevails, digital beam-forming extends the observed resolution over that of the sensors in proportion to the number of array elements. This extension illuminates the potential subarray response capability illustrated in Figure 2-2, which is considered adequate for any subsequent process. Coarse channel data integrity can also be maintained beyond the digital range by using high-order truncation with proper interpretation (code wraparound) at the computation center. No initialization problem is encountered since the data has a zero mean.

For the second investigation, array truncation while retaining the established format was considered. An experimental signal (Longshot) was processed according to the tentative system, using a 0.9 - 1.4 Hz bandpass filter. Inner seismometer rings were removed from subarrays, and outer subarray rings were removed from the array. Observed gains are shown in lines A of Table 2-2 for the configuration options investigated. The array truncation loss is summarized in lines B. Note that array performance increases as seismometers are deleted, and decreases as subarrays are eliminated.

A comparative set of theoretical array truncation loss values has been estimated, assuming perfect signal coherence and no noise correlation, in lines (B) of Table 2-2. A comparison of lines B and (B) reveals significant signal and noise characteristics, and suggests improved analytical models for LASA. These tables show that the noise components appear to possess a
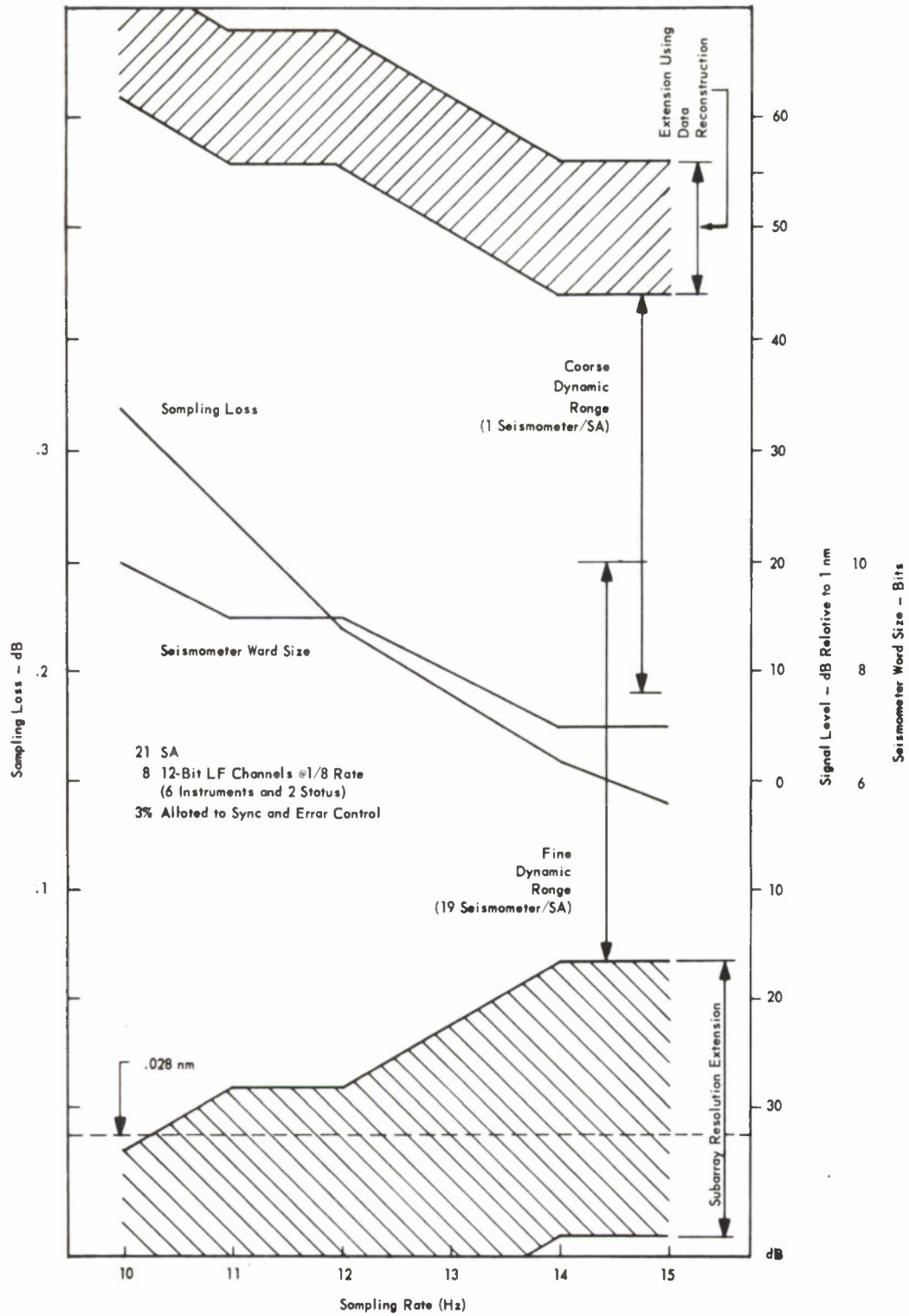
Figure 2-2. TELPAK A Capability

Table 2-2. Array Performance and Communications Requirements

Number of Subarrays		Number of Seismometers Per Subarray		
		25	19	16
21	A	34.0	35.4	35.6
	B(B)	0 (0)	−1.4 (1.20)	−1.6 (1.95)
	C	147	112	94.1
17	A	33.5	34.6	34.7
	B(B)	0.5 (0.92)	−0.6 (2.12)	−0.7 (2.87)
	C	119	90.4	76.2
13	A	32.5	33.6	33.9
	B(B)	1.5 (2.08)	0.4 (3.28)	0.1 (4.03)
	C	91.0	69.2	58.2

A – Observed Processing Gain in dB (Longshot Signal with 0.9–1.4 Hz Filter)

B – Observed Array Truncation Loss in dB

(B) – Theoretical Array Truncation Loss in dB

C – Baseline Data Rate in Kilobits Per Second (14-Bit Words Sampled at 20 Hz)

significant degree of coherence over intrasubarray distances, while some signal coherence loss is evident over the total array.

Decisive conclusions should not be made until a broader data base is analyzed. However, the trends implied by the limited data base available suggest further investigation with additional representative data and consideration of fewer seismometers. The baseline data rate is given in Table 2-2, lines C. Direct application of TELPAK A (proposed TELPIPE) requires a data rate less than 50 kilobits per second, which limits the baseline array to approximately 169 sensors at the 20 Hz sampling rate. A blend of sample rate and word size trimming is therefore anticipated for optimal intelligence transferral. Data requirements of subsequent processes, such as classification, may resolve the tradeoff option.

A functional diagram of the LASA communication equipment is illustrated by Figure 2-3. The intermediate message format equipment, which is composed of the basic data set adapter and a data reduction unit, functionally reduces to a memory containing the proper link word chain. The array interface remains unaltered, while the maintenance function is supported directly as a phantom channel. A keyboard printer has been incorporated to establish a hard-copy communication capability between Miles City and the computation center.

Although the baseline design (solid lines) does not contain redundancy or backup provisions to minimize the probability of losing unrecoverable data, logical upgrading extensions are possible. Redundancy may be achieved by adding a second message format module and long-distance communication channel with the flexibility accorded by the data set adapter concept. An alternate approach is to incorporate an independent asynchronous auxiliary recorder and an associated relative time generator with adequate short-term stability (24 hr). It is assumed that critical tapes would be shipped to the computation center where the catchup function would be handled by the event processor. Both configuration additions are superimposed on Figure 2-3, as the dotted portion of the instrumentation, to illustrate the compatible upgrading features.
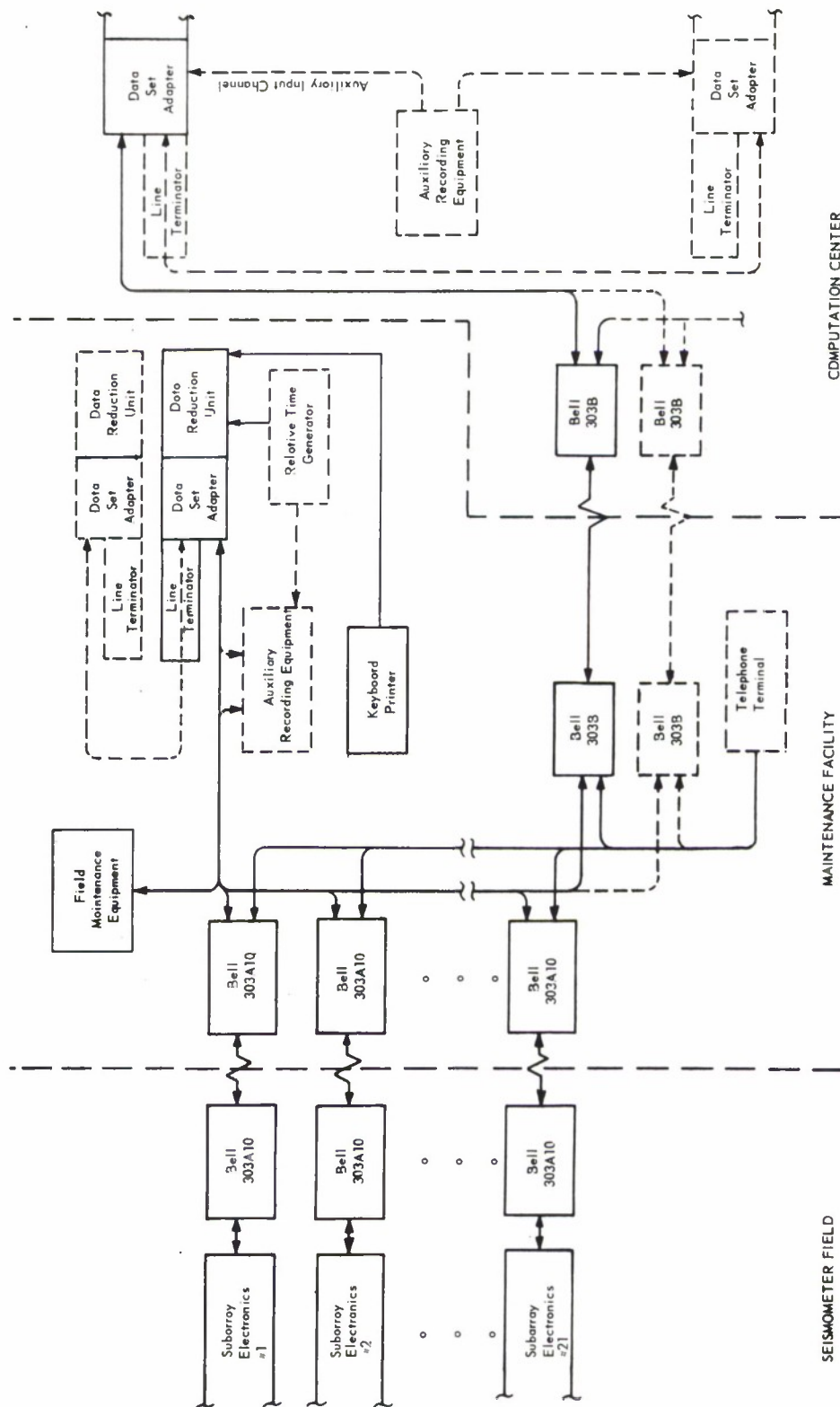
Figure 2-3. LASA Communications Extension

2.3 DETECTION PROCESSING

Detailed analysis of the observations from LASA constitutes a major computer burden, and is accordingly oriented toward a specific time/phase velocity window to minimize the computation impact. Since no significant a priori information is available, continuous real-time surveillance of the teleseismic zone is essential to detect potential windows of investigation. This detection function must digest large amounts of data and extract sufficient information to steer and scale the event process for all activity of interest. Since no deterministic kernel is known, power measurements are the key observables.

Beamforming accomplishes the two rudimentary objectives of phase velocity discrimination and signal-to-noise ratio enhancement by combining the signals in a manner that favors a specific wavefront. However, many wavefronts must be simultaneously considered to monitor any region which is significant, when compared to the main lobe coverage as dictated by the signal frequency, propagation medium, and array geometry. Filtering further improves the process by rejecting those frequency bands which contain an inferior signal-to-noise ratio and/or imply degraded beamforming performance.

Beam interpretation must consider both the processed signal during an observation window and the estimated background noise. The detection criterion structure should have considerable flexibility to accommodate statistical discriminants, if they appear beneficial.

Although the digital implementation of these techniques is not unduly complex, the task of forming and filtering a multitude of beams in real-time is not easily handled with general-purpose digital computers. Fortunately, the required processing is extremely repetitious, and large performance gains can be achieved by instrumenting instructions to efficiently perform the basic signal processing algorithms.

A software controller uses both standard and special instructions to perform the detection process. Since the special functions are representative of general signal processing techniques, rather than a specific program implementation, the processing architecture resident in the controller may be varied

as required. The optimum configuration is dependent on many system parameters such as the number of sensors, the area of surveillance, the required system gain, and the spectral characteristics. The analysis performed throughout this study suggests the configuration portrayed by Figure 2-4. Both the total memory requirements and the number of filter channels are reduced without significant loss of performance when the beamforming process is partitioned at the inherent subarray data module. The high-frequency cutoff properties of the bandpass filter enable a reduction of subsequent sample rates, further reducing memory and execution requirements.

Detection processor inputs can be off-line from tape or on-line from array interface equipment. Each sample-oriented record should contain seismic data and a code relating status changes, such as the addition or deletion of array elements. A header file is also required to establish the initial array status and time.

A separate input subroutine for each input option is available in the controller. Off-line files contain five records for compatibility with the beamforming algorithm batch size, and are synchronously requested to optimize the process. On-line files also contain five records, but are presented asynchronously to the computer. A clock is desired to relate processing requirements with capability.

The subarray buffer memory allocation stores the intermediate results between beamforming and filtering, and is the most efficient location to retain an adequate process time margin. Sufficient filter histories are required in this location and in the filter buffer memory. Any bias developed in the subarray calculations is blocked by the bandpass filter. However, the array data memory should contain a phantom channel to allow a bias compensation to be introduced at the LASA level before the introduction of detection nonlinearities.

The four functions of rectification, integration, noise estimation, and detection criterion are combined in a single algorithm (RIT), enabling efficient coupling of operations with minimum memory accesses. Iterative properties of integration, noise estimation, and detection criterion require buffer memory allocations. A noise estimate inhibit feature is incorporated in the detection criterion algorithm to mask detected signal components.

A software routine is employed to establish maximum envelope amplitude and assemble the detection log parameters which include beam identification, noise level, signal peak, and initial and terminal detection times. Header information should include array status, element masks, threshold criterion, and beam allocations. A detection flag should be available to a display; it can be conveniently located in the sign bit position of the background noise word.

A coordination subroutine must maintain a current portrait of detection status and data time. Array element mask alterations are initiated by this program segment. During off-line operation, proper data sequence is verified and marginal or erroneous data editing is performed in the subarray memory.

Output subroutines must support the communication of detection outputs and beam display data. A capability of monitoring up to eight channels is desirable for maintaining execution confidence and aiding maintenance activities. Graphic presentation of the detection process is a secondary application with intangible utility.

Characteristics of the basic process are given in Table 2-3. A full complement of LASA data is accommodated with minimum preprocessor buffering. Initial parameter selection is based on analytical study and preliminary signal processing experience. Within the projected detection architecture, many parameter options exist, and modifications are anticipated as operating experience is accumulated and signal characterization is improved.

An operational system will require an extension of the outlined controller and implied supervisor. Input/output unit reassignment, automatic process verification, dynamic parameter modification, surveillance editing, transient free-function transferral, and fail-soft configuration responses are anticipated requirements. Although these requirements are not essential during research and advanced development program phases, prudent controller design should incorporate sufficient flexibility to enable a progressive and orderly capability growth.

Figure 2-4. Detection Processor Logic

2-17/18
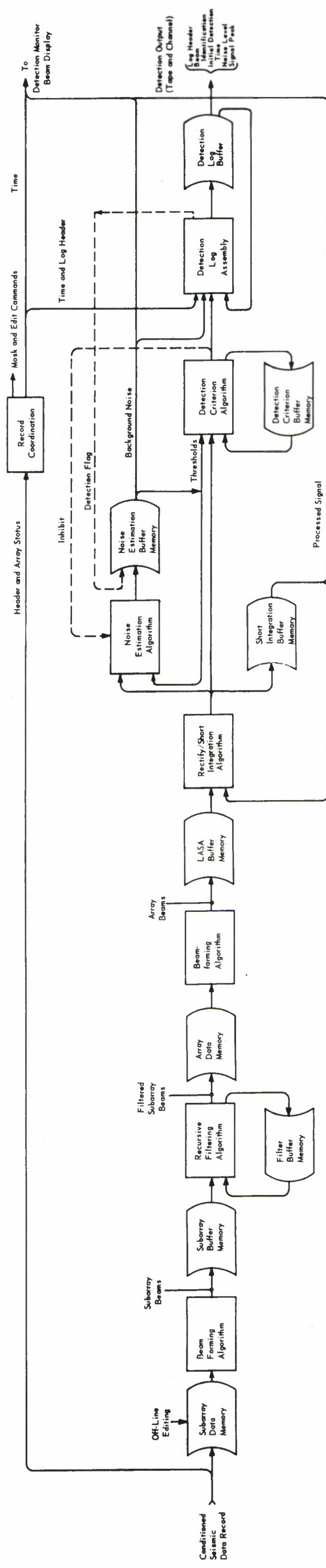
Table 2-3. Basic Detection Process

Functional Operation	Units (Program Characteristics)		Average Execution Rate — Per Second	Time Resolution		Data Channels		Comments
				Input — Second	Output — Second	Input — Nodes	Output — Nodes	
Acquire Data	On-Line		20	0.05	0.05	1	525	Reflects minimum preprocessor buffering
	Tape		2	0.05	0.05	1	525	Read two five-sample records
Subarray Beam Form			2	0.05	0.1	525	105	Five azimuth-dispersed beams per subarray
Filter			10	0.1	0.1	105	105	Sixth degree recursive bandpass filter
LASA Beam Form			1	0.1	0.2	105	B	Number of beams (B) dependent on process parameters and detection controller requirements
RIT	Signal		1.67	0.2	0.6	B	B	Threshold criterion
	Noise		0.56	0.6	1.8	B	B	
Record Coordination	On-Line		20	0.05	0.6	-	-	Time and status
	Tape		2	0.05	0.6	-	-	Time, status, and tape continuity
Detection Log Assembly			1.67	0.6	0.6	-	-	Executed only when one or more beams satisfied the detection criterion

Note: Time measures are relative to data time.

2-19

2.4   EVENT PROCESSING

The central function of the event processor is to form event beams for de-
tected events, and provide necessary filtering, recording, and display. Addi-
tional study indicates that these functions must be supplemented by the functions
of side-lobe and post-P discrimination, the collection of families of arrivals
from a single seismic event, and the additional special event processing of
interesting events. These functional requirements, as well as current thoughts
concerning the required experimental and learning aspects of the system, are
discussed in the following paragraphs.

The resulting arrival detections are expected to include significant num-
bers of side-lobe detections, as well as post-P seismic arrivals, insofar as
the latter possess phase speeds belonging to the P-teleseismic zone. The event
processor will sort out and identify these detections and main-lobe P detections
before event beam processing.

While event processing with preformed beams, using stored delays,
should be adequate for the majority of detected events, some special events will
require maximum obtainable processing gain, even at the expense of considerably
increased computation effort. Experience with studies of arrival times of events
indicates that the variability of such times, even from limited source regions, is
sufficiently great to degrade any set of preformed beams for a given event, as
compared to the gain if a tailor-made set of steering delays were obtainable for
the event. Correlation techniques are expected to permit the determination of
special time delays for individual events. Moreover, the special processing
functions should include a capability for special filtering, including some form
of optimum processing at the subarray level.

The LASA signal processing system, including the event processing
functions, will contain as much autonomous operation as possible, requiring
operator intervention only where judgment is required. After initial checkout
procedures, the system should be capable of a degree of automatic operation.
The final decision logic for processing will depend on experience gained with
seismic factors such as frequency of detection of particular arrival modes and
resolution and degree of predictability of beams for non-P detections, and on

other considerations concerned with the system operation. Autonomous system operation can be continuously improved as more experience is gained; therefore, a reasonable degree of flexibility in the event processing logic is highly desirable. Such flexibility would facilitate the implementation of seismic research use of the system, and provide system testing and calibration functions.

For the above reasons, the event processing function should be considered as composed of a number of computational functions or subroutines to be connected by one of several possible alternative system flows or control programs, permitting maximum flexibility and learning capability during the early operation of the system.

Figure 2-5 shows the major functional information flow of a possible event processing system. The outputs of the detection processing function are collected in a detection queue, clustered, and sorted to form families of arrivals for each seismic event. Routine processing includes event beam formation and event location calculation. For special processing, time delays are obtained adaptively by correlation at the LASA level, while a capability for optimum processing exists at any level.

The detection output is described in Section 2-3. This detection queue can be displayed either before or after an event family has been established. Initially, families are to be established primarily by an operator viewing the queue displays. These displays show the calculated arrival times and velocities of family members (PcP, PP, etc.) corresponding to an assumed P or other detection, along with the actual detected arrivals. As experience is gained in making these groupings, much of this operation can be automated.

The event family function should begin with an operation of clustering detections and assigning velocity space locations and strengths to the clusters. It is hoped that side lobes can be eliminated on the basis of time coincidence and relative geometry with the main lobe. A grouping at equal azimuth can be selected, and a tentative "first arrival" or P wave chosen. The processor can then calculate time and velocity of possible later arrivals, and match these predictions to the actual arrivals. Much of this operation can eventually be made automatic. In an alternative operator-controlled mode (to be used for
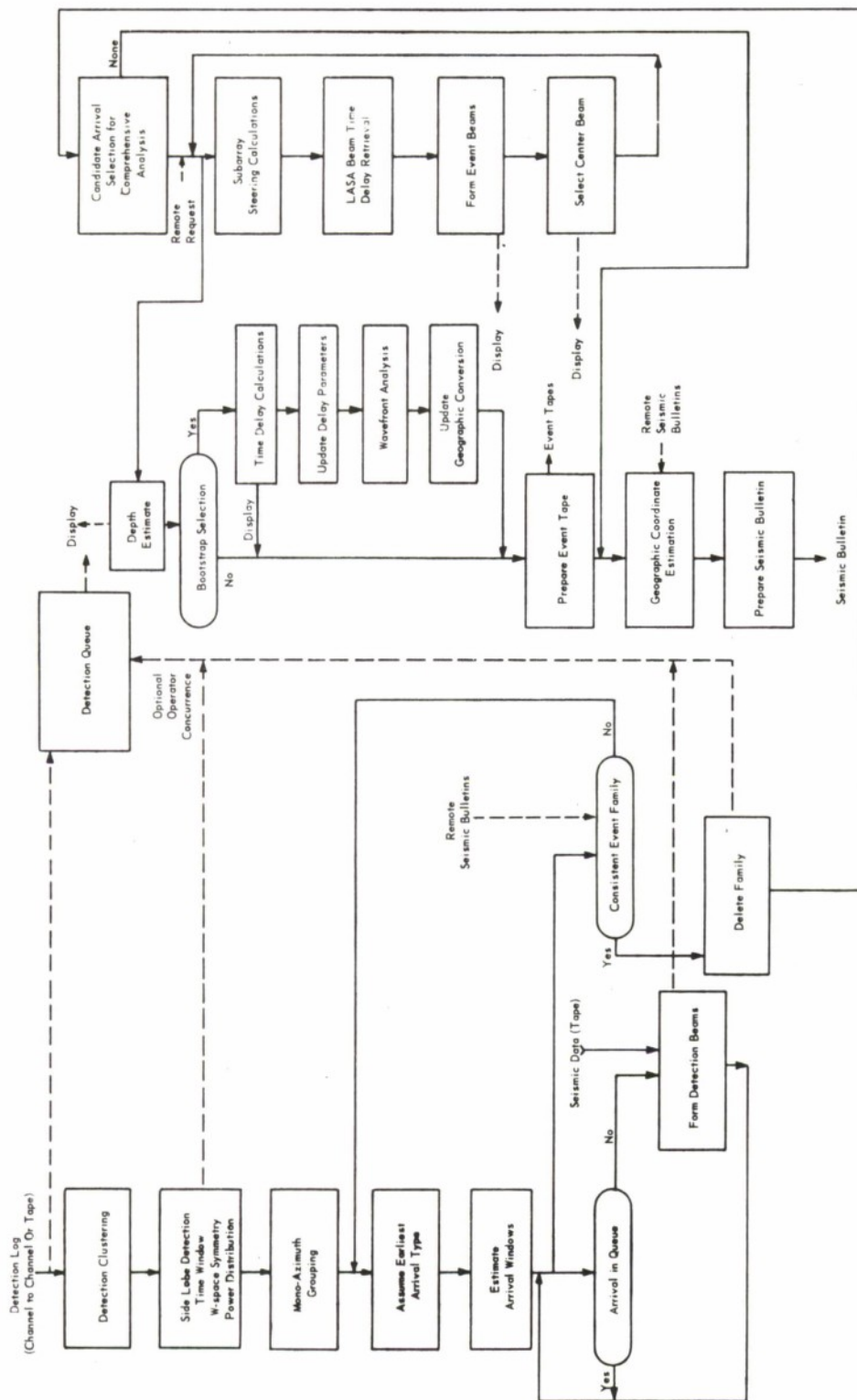
Figure 2-5. Event Processor Logic

initial experiments), the matching can be performed visually with the assistance of the display, providing maximum operator exposure to seismic experience and permitting rational selection of a more highly automatic logic.

As a first step, the predicted delay times and velocities of post-P arrivals for various source depths will be obtained from least squares polynomial fits to the Jeffreys-Bullen Seismological Tables.[5] Eventually, LASA experience should provide more accurate prediction of the required quantities.

The operator should be able to select detected or identified beams for routine event processing. In an automatic mode, it might be required, for example, to always form event beams for the P wave only. Beamforming time delays are to be updated when important new events have been added to the experience list. In the operator-controlled mode, the operator is required to select a tentative P (or other arrival), and then, using the display, compare the actual detections to the predicted arrivals. This procedure can be done on several different assumptions of depth.

The output of the event processor contains an inverse velocity to geographic conversion capability, updated on the basis of velocity experience and world network locations. Location information is expected to be used only for output purposes (seismic bulletin, etc.). Steering delays hopefully can be based on directly measurable velocity information. The event family determination should contain access to a beamforming capability to form detection-density beams outside the P-teleseismic zone whenever required (to search for additional undetected arrivals).

2.5   MICROPROGRAMMING

After the algorithms necessary to implement a signal processing system for LASA were selected and defined, during the first quarter of this study contract, effort was directed at evaluation studies. These studies concluded that the microprogramming approach could provide a significant speed advantage; therefore, further definition was accomplished during the second quarter. In the

final quarter, simulation and testing plans were developed. This section reports on the total effort and the expected implementation results.

2.5.1   Definitions

The algorithm definitions are shown in Figure 2-6 as equations. Some pertinent comments on each algorithm are included in the following sections.

2.5.1.1   Beamforming

Beamforming uses the batching concept in which beam sums are formed in one instruction execution for the present sample period and for the four immediately previous sample periods. A large number of beams $(J \leq 32767)$ can be formed from a large number of inputs $(I \leq 32767)$ during one execution cycle. Input and output data has a precision of 15 data bits with allowable intermediate calculations extending up to 22 data bits. The delay values (τ_{ij}) can have a resolution equivalent to that provided by the input data. The output shift (β) provides scaling capability to minimize overflows in the next process executed.

An additional function of beamforming is to provide optional preshifting of the input data block. This shifting is performed before the beamforming algorithm is executed.

2.5.1.2   Recursive Filter

The Recursive Filter instruction allows feedback filtering to be performed on IJ inputs $(I, J \leq 32767)$ at one instruction execution. A filter of degree $2P-1$ is performed where P can be as large as 127. The coefficients (a_{pij}, b_{pij}) are unique for each term of the filter for each i and each j. All input (f_i, g_{ij}) and output (g_{ij}) data has precisions of 15 data bits with allowable intermediate calculations extending upward to 38 data bits, provided the result before shifting is not greater than 31 data bits. The output shift (γ) allows the 15 output bits to be selected as any consecutive combination of these 31 bits. The second output shift (δ) is optional. When used, it is a right shift applied to the

Beamform

1. $f_i(n\Delta t) = 2^{-\alpha} f_i(n\Delta t)$

2. $B_j(n\Delta t) = 2^{\pm\beta} \left\{ \displaystyle\sum_{i=1}^{I} f_i(n\Delta t - \tau_{ij}) \right\}$; $j = 1, \ldots, J$

Recursive Filter

1. $g_{ij}(n\Delta t) = 2^{\pm\gamma} \left\{ \displaystyle\sum_{p=0}^{P-1} a_{pij} f_i((n-p)\Delta t) + \displaystyle\sum_{p=1}^{P-1} b_{pij} g_{ij}((n-p)\Delta t) \right\}$

2. $g'_{ij}(n\Delta t) = 2^{-\delta} g_{ij}(n\Delta t)$; $i = 1, \ldots, I$; $j = 1, \ldots, J.$

Convolution Filter

1. $g_{ij}(n\Delta t) = 2^{\pm\lambda} \left\{ \displaystyle\sum_{m=0}^{M-1} c_{mij} f_i((n-m)\Delta t) \right\}$;

$i = 1, \ldots, I$; $j = 1, \ldots, J.$

Rectify/Integrate

1. $y_j(n\Delta t) = 2^{\pm\mu_j} \left\{ \displaystyle\sum_{s=0}^{S-1} | B_j((n-s)\Delta t) | \right\}$

Figure 2-6. LASA Algorithm Definitions (Sheet 1 of 2)

2.　　a.　　$\overline{B}_j (n\Delta t) = 2^{\pm \eta_j} \left[y_i (n\Delta t) \right] - 2^{-\sigma_j} \left[\overline{B}_j ((n-1) \Delta t) \right]$

$+ \left[\overline{B}_j ((n-1) \Delta t) \right]$

　　　b.　　$\overline{B}_j (n\Delta t) = \overline{B}_j ((n-1) \Delta t) - y_j ((n-R) \Delta t) + y_j (n\Delta t)$;

$j = 1, \ldots, J$.

For short-term integration, use Equation 1 and either 2a or 2b.

For long-term integration, replace $\overline{B}$ by $\overline{\overline{B}}$, y (optionally) by $\overline{B}$, and use either equation 2a or 2b.

<u>Threshold</u>

1.　　$T_j (n\Delta t) = u_j \overline{\overline{B}}_j ((n-1) \Delta t)$

2.　　$T_j' (n\Delta t) = v_j \overline{\overline{B}}_j ((n-1) \Delta t)$

3.　　Threshold exceeded if $\overline{B}_j (n\Delta t) \geq T_j (n\Delta t)$; $j = 1, \ldots, J$.

4.　　Arrival is declared when threshold is satisfied for Q out of Q' consecutive sample periods. Threshold is changed to T_j whenever an arrival is declared. Threshold is restored to T_j' at the first sample period the criterion is not satisfied.

Figure 2-6. LASA Algorithm Definitions (Sheet 2 of 2)

primary filter output. The time resolution of the input data (f_i) is independent of the rate at which the instruction is executed.

2.5.1.3 Convolution Filter

The Convolution Filter allows filtering to be performed on IJ inputs ($I, J \leq 32767$) at one instruction execution. The filter degree (M) can be as large as 127. The precision characteristics are the same as for the Recursive Filter. No second output shift is provided, since there is no feedback path.

2.5.1.4 Rectify/Integrate and Threshold

Three parts of the Rectify/Integrate and Threshold instruction are

1. Short-time averaging
2. Threshold detection
3. Long-time averaging

Rectify/Integrate and Threshold provides a method for arrival detection. The detection criteria is based on exceeding a particular signal-to-noise ratio for some specified number of samples. The inputs to this instruction consist of beam values of 15 data bits precision. The output signal and noise averages are also 15 data bits. A list is made of all beam numbers on which a change in arrival status occurs during instruction execution. (See Figure 2-6 for the equations referenced below.)

Short-Time Averaging. Short-time averaging is performed as a two-step process. Step one calculates a rectified sum of the LASA beamformer output. This sum is calculated over the last S sample periods. The result (after shifting) forms the intermediate output of short-time averaging. Step two calculates the final short-time average from the intermediate output by using either a binary-scaled exponential equation or a straight summation equation. This final output is used as the input to the threshold detection section.

Threshold Detection. This section performs the actual arrival detection. The final short-time average output is compared with a previously calculated

threshold (the start-arrival threshold). When the short-time average exceeds the start-arrival threshold for Q time samples out of Q' consecutive time samples, an arrival is declared. The relevant beam number is stored and a new threshold (the end-arrival threshold) is introduced. When the short-time average does not exceed the end-arrival threshold for Q out of Q' consecutive time samples, the end of an arrival is declared. The relevant beam number is stored, and the start-arrival threshold is reintroduced. This logic is shown in tabular form in Table 2-4.

When an arrival is in progress on a particular beam, the long-time averaging section is omitted for that beam. At the end of an arrival, long-time averaging is delayed on that beam until the arrival has passed through the array.

Long-Time Averaging. This section calculates an average noise value, and uses it to compute the start- and end-arrival thresholds. Either of two equations is available for long-time averaging: a binary scaled exponential or a summation. The input may be either the intermediate or final output of short-time averaging. The output of the selected equation (the average noise) is multiplied by an 8-bit threshold (u_j). The result is divided by 8, and the resulting number is used as the start-arrival threshold. A similar calculation is performed for the end-arrival threshold (v_j). These two 15-data bit values are not used until the next execution of threshold detection.

2.5.2   Evaluation

Effort on all four algorithms was directed at retaining the flexibility developed during the definition phase. As expected, feedback from the evaluation effort was used to improve algorithm definitions. An example of this is a generated requirement for the beamforming time delays to be organized in a monotonic series.

As a first step, detailed flow charts and programs were developed to simulate the essential arithmetic capabilities of each algorithm. This data was converted into actual microprograms for the IBM System/360 Model 40. Where applicable, new processing approaches and/or hardware were postulated to

Table 2-4. Threshold Detection Arrival Status Determination

Short-Time Average ≥ Threshold	Arrival Detected Previously	Threshold Exceeded Q out of Q' Times	Arrival Status			
			None	Start	Con-tinue	End
No	No	No	X			
Yes	No	No	X			
Yes	No	Yes		X		
Yes	Yes	Yes			X	
No	Yes	Yes			X	
No	Yes	No				X
No	No	Yes	These conditions are not possible			
Yes	Yes	No				

decrease execution time. Some of these approaches resulted in programming restrictions to retain the necessary speed.

At each step, the expected microprogram execution speeds were determined for certain benchmark parameters. These times were compared with both the assembly language version and the projected needs of the detection process. When necessary, new approaches were taken to achieve a minimum execution time for each algorithm. A summary of the anticipated individual execution times for both software and microprogram implementation and the chosen benchmark parameters are shown in Table 2-5.

2.5.3 Simulation

A programming effort was launched to develop software programs which would simulate the microcode operations. The original programs were expanded to reflect new design changes. Some of the exceptional conditions checked by the microcodes were also incorporated into the simulation programs. A standard interface was developed. By using this approach, the simulation programs can be used as substitutes for the microprograms until a machine with the latter is available.

There were two reasons for developing these programs. First, they will allow work to be done on the detection processing program in anticipation of the delivery of the microcoded machines. They can then be carried over and used as part of a dynamic diagnostic scheme to help detect on-line equipment failures. Second, because these programs are identical in function to the microprograms, they can be used for testing purposes to assess the mathematical and special-condition operations of the microcodes.

2.5.4 Test Plans

The planned basis for testing the microprograms requires that the simulation programs be used as a standard. They will be thoroughly checked, using hand solutions. A control program will be written to exercise the simulation

Table 2-5. Expected LASA Algorithm Performance

Process	Assembly Language Program (milliseconds)	Microprogram (msec)	Speed-Up Ratio	Comments
Beamforming	4.5	0.69	6.5	One beam formed from 25 inputs
Recursive Filter	30.2	4.40	6.9	25 filters of degree 6
Convolution Filter	16.2	1.90	8.5	Same as recursive filter
Rectify/Integrate and Threshold	0.7	0.20	3.5	Five values are added to form the short-time average. Every sample period, 10 percent of the input beams experience the start or end of an arrival. An exponential is used for long-term averaging. The time shown is for one beam.

program and the microprograms on identical sets of data. The results will then be compared and any errors in either program tracked down.

Three phases of testing are anticipated: mathematical, special conditions, and interaction. Each phase is described below.

2.5.4.1 Mathematical

This test will determine the mathematical accuracy of the microprogram implementation. For the test, part of the data from the Longshot event will be used. This data will be tested against all the microprograms except Rectify/ Integrate and Threshold.

2.5.4.2 Special Conditions

These tests will exercise a variety of the abnormal conditions and unique data paths within each microcode. The data for this test must be constructed entirely by hand, and will test such operations as overflow handling (both intermediate and final), illegal instruction parameters, and various shifting and output options. Each logical branch of Rectify/Integrate and Threshold will be tested. Testing of all four algorithms is planned for this phase.

2.5.4.3 Interaction

This phase will test the input and output compatibilities of the four routines. Because of the severe speed requirements of the detection process, it is not possible to shuffle data around in storage between microprogram calls. The algorithms will be combined into a program which resembles that being defined for the detection processor. In addition, the data input/computation simultaneity of the microcodes will be tested.

2.5.5 Conclusions

The primary conclusion that can be drawn from the microprogramming work under this contract is that the approach is feasible where high speed is

necessary and the arithmetic load is not too great. Initial estimates show that about 500 LASA beams can be formed in 100 msec whereas, without micro-programming, this formation would require about 700 msec. Table 2-8 confirms that the microprogramming approach will help to solve the LASA processing problem.

2.6   COMMUNICATION INTERFACE

Communication with subarray equipment is a rudimentary requirement for any LASA real-time processing configuration. Commercially available equipment to interface digital processor input/output facilities and wideband data stations is configured primarily for single-terminal applications. Several of these can be employed but the LASA requirement of simultaneously supporting more than 20 duplex channels with nonstandard modulation imposes not only a severe data transfer rate but also a prohibitive processor burden of message formatting. This implies interpretation and generation of coding at the bit level, an operation extremely cumbersome when performed by the parallel logic organization of a general-purpose computer.

2.6.1   Data Set Adapter

A multiplexed data set adapter function is postulated for the interface equipment. This function includes translation between the message structures used in the communication channels and the standardized data word files characteristic of digital storage mediums. Performing this operation at the inherent serial-parallel data representation transition encountered in data set adapters optimizes the translation process. External message character encoding and decoding also reduce the effective processor data rate, alleviating transaction interferences.

Although character definition and rate are basically static parameters of the specific communication channel, word definition may not be constant. Studies of alternate LASA communication configurations reveal potential message formats containing several word sizes to efficiently use the channel when

encountering diverse data resolutions. The format information should reside in a memory large enough to provide adequate message length. An implicit address relationship between data word definition and value is suggested without a loss of message flexibility.

Provisions for chaining the data sequence by word and by block links are desired to provide flexibility in file structure while retaining the potential efficiency of contiguous retrieval or distribution. Variable word size is not required with intelligent message blocking. A single link control word can therefore contain both data word definition and chaining instructions; however, standardization is essential to enable direct coupling of communication facilities for purposes such as echo checking, information distribution, or internal routine cascading.

Operational systems may require the addition of redundant interface equipment to ensure data collection during maintenance and/or failure conditions. The impact of this capability is insignificant if considered during initial design. Parallel data set support using external cable terminations permits a clean, high-speed transferral of the interface functions. Physical cable transferrals would be necessary only when recovering from improbable line transmitter or receiver failures. Theoretical system loss during this recovery transient is shown in Figure 2-7 as a function of the interconnection module size. System degradation is limited to approximately 1 dB when four or fewer data sets are supported by any cable assembly. The implicit module requirement is also graphically indicated to portray the composite design options.

Since neither the communications network nor the geometry of possible future LASA type seismic arrays is firm, moderate equipment flexibility should be incorporated. Modular construction is the most appropriate provision since no significant increase in design effort is encountered. Interface groupings of four data sets appear to be a reasonable selection because of consistency with the maximum interconnection module size and of compatibility with contemporary logic packaging configuration. Six such interface units would satisfy the maximum foreseeable LASA requirement of supporting 21 subarray channels, 1 maintenance channel, and 1 TELPIPE channel. Since an extension
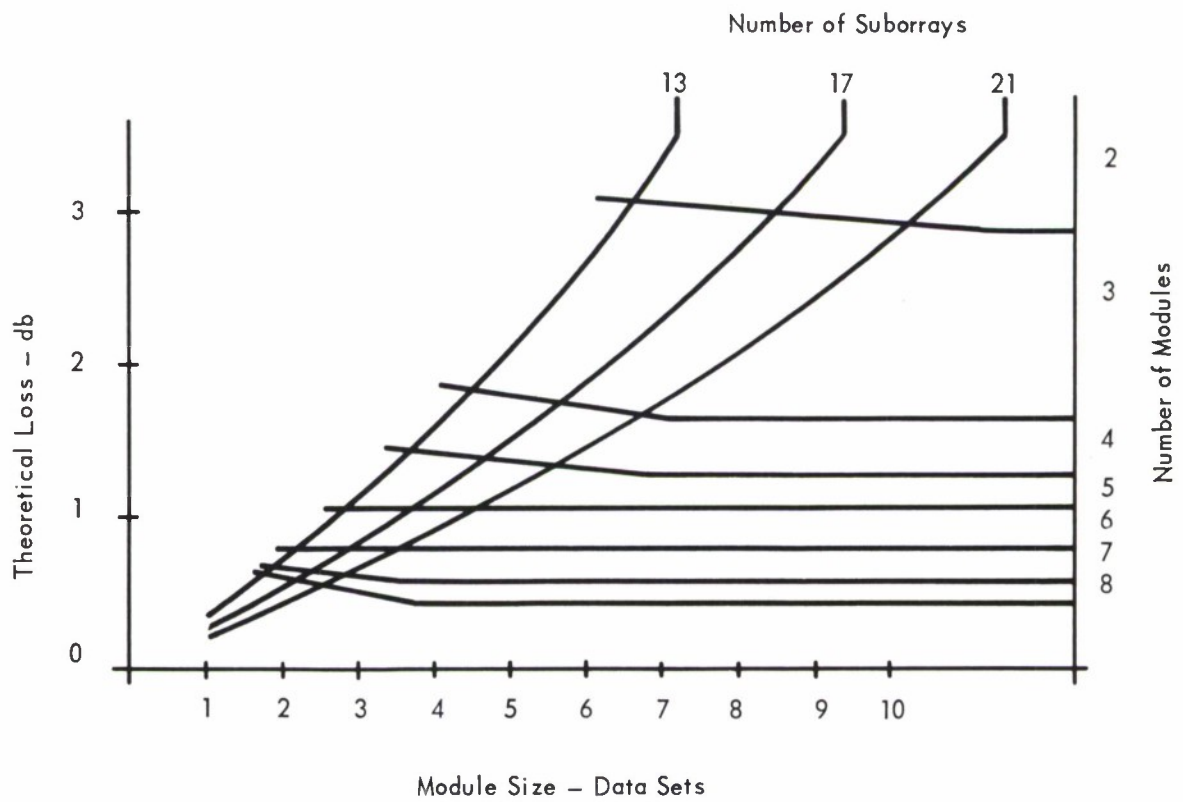
Figure 2-7. Cable Transfer Loss

to eight units would not add to the addressing structure or multiplexer equipment complexity, adequate space and power should be provided.

The conceptual subsystem design is illustrated by the functional data set adapter diagram (see Figure 2-8). Principal components are a data reception unit, a data transmission unit, and from one to eight data set interface units. Since precision message timing implies special internal clock features, the interface equipment timing unit is incorporated in this functional group. Each unit function is detailed by Tables 2-6 through 2-9. A high-speed, cycle-steal access to the signal preprocessor memory with external addressing is employed. Adapter monitoring and control is accomplished with access to several general-purpose registers which serve many preprocessor functions. Table 2-10 characterizes the composite coupling requirement.

2.6.2   Support Processing Requirement

An initial link word must be available in the memory cell permanently allocated to the channel reception pointer. Data and subsequent link words are required to be compatible in format and memory location to obtain proper transmission. Repetitive message formats and optional phases can be distributed by controlling the link word content. Processor interruption at preselectable message phases is desirable to support the subsequent processing of message content. This interruption can be instrumented by monitoring main memory addressing.

Initial message synchronization is assigned as a software function which detects the frame character and alters the format chain to obtain a compatible word distribution. If the message format contains subsequent frame characters, they may be monitored at the appropriate memory location.

Error control, such as parity or polynomial decoding, is not included in the data reception unit. Thus, messages must be processed by a general-purpose algorithm to use and/or delete message redundancies.
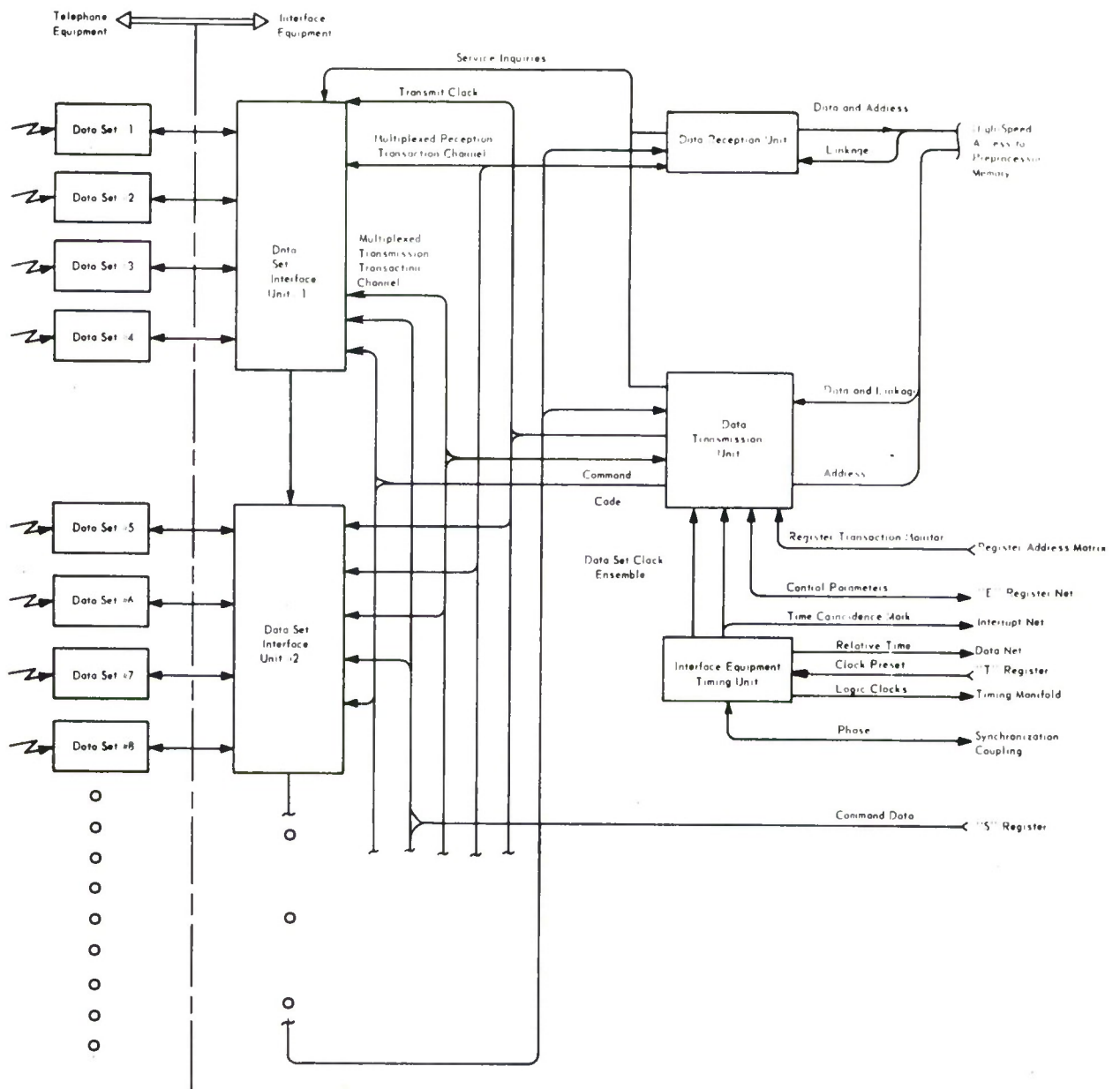
Figure 2-8. Functional Data Set Adapter Diagram

Table 2-6. Bell System 303 Series Data Set, Interface Unit (Sheet 1 of 5)

The communication channel coupling the LASA Data Center and each subarray electronics vault uses scrambled restored polar modulation in conjunction with vestigial sideband modems, and is terminated by Bell System 303-A10 type wideband data sets operating in the synchronous mode. One channel is reserved for maintenance functions. Since the terminal characteristics of the 303 Series data sets are standardized, one universal design will satisfy the electrical interface requirement if the appropriate clock is provided by the timing unit. The following functional specifications reflect the LASA application requirements in which operation is restricted to the synchronous mode.

Hardware Requirements	Functional Specifications		Comments
Modular packaging	4 data sets/module		Module size is limited so that the interface unit can be disconnected from an operating system without imposing a substantial performance transient.
Parallel support of data set	Dual-complementary connectors External line terminations High-impedance drivers and receivers Power sequence isolation		Interface design should accommodate all signals in the high-speed connector group
Electrical compatibility with Bell data set	Line impedance Binary One signal Binary Zero signal Off signal On signal	90-120 ohms 5 ma 23 ma 5 ma 23 ma	Specifications relate to the Bell terminals

Table 2-6. Bell System 303 Series Data Set, Interface Unit (Sheet 2 of 5)

Hardware Requirements	Functional Specifications	Comments
Electrical compatibility with Bell switchgear	Line impedance 3000 ohms Off signal -3 volts On signal 3 volts	Specifications relate to the Bell terminals
Transmit data	Transmit data clock Transmit serial data Phase data and clock transitions Buffer two transmission bits Retain data sector Relay transmission service inquiry or indicate source address for bit replenishment when necessary Set bit buffer from multiplexed transmission bus and cancel bit replenishment request Alter data sector upon command from data transmission unit Relay transmission sector service inquiry or indicate channel address for word replenishment when necessary	Each data set is operationally independent, but the interface module may share an address block

Table 2-6. Bell System 303 Series Data Set, Interface Unit (Sheet 3 of 5)

Hardware Requirements	Functional Specifications	Comments
Receive data	Receive data clock Receive serial data Interpret data at the appropriate clock transition Buffer one received bit Retain data sector Relay reception service inquiry or indicate address for buffer unloading when necessary Drive multiplexed reception bus from data buffer and cancel unloading request Alter data sector upon command from data reception unit Relay reception sector service inquiry or indicate channel address for word unloading when necessary	Received signals must be assumed asynchronous. Each data set is operationally independent, but the interface module may share an address block.
Transmit channel co-ordination signals	Transmit Send Request Transmit Local Test Transmit Remote Test Buffer above signals Initialize above buffers to Off indication	Each data set is operationally in-dependent, but may share co-ordination work structures.

Table 2-6. Bell System 303 Series Data Set, Interface Unit (Sheet 4 of 5)

Hardware Requirements	Functional Specifications	Comments
Transmit channel co-ordination signals (cont'd)	Set above buffers from Register S without switching hazards when addressed Transmit Channel Lock	
Receive channel coordination signals	Receive data set ready Receive AGC lock Drive the parallel data bus with data set status when addressed Interpret AGC lock during the word interval Drive multiplexed AGC lock bus during data buffer unloading	Each data set is operationally in-dependent, but may share co-ordination word structures.
Coordinate channel action	Remember transmission status Advance channel status to Ready and hold with the presence of Send Request and Send Clearance signal Enable reception at or above the ready status Advance channel status to Operate with the coincidence of the Ready status, the Transmission Initiation signal, and the appropriate channel	Each data set is operationally in-dependent, but may share co-ordination word structures. Since the automatic answering feature is not anticipated for any LASA communication branches, related signals should be properly terminated to a central junction bay.

Table 2-6. Bell System 303 Series Data Set, Interface Unit (Sheet 5 of 5)

Hardware Requirements	Functional Specifications	Comments
Coordinate channel initiation	Address resides in Register S of the interface equipment	None
	Initial link address is zero	
	Hold operate status with the Send Clearance signal	
	Return to Off status with the absence of Send Request signal	
	Drive the parallel data bus with Operate status when addressed	
	Slave Channel Lock to Operate status	

Support Processing Requirement

The support processing for this interface control is composed primarily of programmable binary logical operations, relating the control and command discrete signals that are encountered throughout the system. Transmission initiation does require the calculation of appropriate Vernier Time Clock pre-sets to properly phase the message.

2-42

Table 2-7. Data Transmission Unit (Sheet 1 of 4)

Digital communication rates are significantly less than the capability of contemporary technology. Multiplexing the transmission support logic is therefore advantageous to increase interface efficiency. Many message transmission variables are characteristic of a specific channel installation; program control of these parameters is nonessential, and therefore the following functional specifications reflect a Pegboard channel characterization.

Hardware Requirements	Functional Specifications	Comments
Support multiple channels	8 or fewer interface modules	Module address size is consistent with the minimum LASA requirement. Employing fewer modules requires the use of jumper connectors to complete inquiry chains.
Distribute transmission clock timing	32 x 4 Pegboard matrix allocation	Word acquisition can be inhibited for simplex operation by the absence of a peg.
Generate Transmission Initiation signal	Enabled according to code in Register E by the register setting sequence of "E-T" without an interim time coincidence occurring Transmission is initiated with the first subsequent time coincidence signal, if Registers S and T have remained inactive	None
Generate channel characters	Programmable complementary characters for each communication channel 32 x 5 Pegboard matrix allocation Character size selectable from 1 through 16 bits Dotting is optional	LASA communication requirements impose the range of character size.

Table 2-7. Data Transmission Unit (Sheet 2 of 4)

Hardware Requirements	Functional Specifications	Comments
Supply data to the multi-plexed transmission bus	Initiate sequence when response is obtained from the transmission service inquiry	Sequential logic design of the multi-plexed transmission bus controls necessary to efficiently use the transmission unit buffer.
	Employ channel address response to retrieve sector word	
	Generate transmission bit and re-store sector word according to the character generation algorithm	
	Decrement the data word size when a character is completed	
	Alternate the sector if the data word is depleted	
	Originate transmission service inquiry	
Replenish data from main memory	Initiate sequence when no response is obtained from the transmission service inquiry	Proper link word and central memory channel design permit the sharing of a single register for memory addressing and data reception.
	Originate transmission sector service inquiry	
	Retain channel address response as the implicit address segment	
	Obtain the explicit link address segment from the link control word in the appropriate buffer memory cell. The initial explicit address segment is zero	

Table 2-7. Data Transmission Unit (Sheet 3 of 4)

Hardware Requirements	Functional Specifications	Comments
Replenish data from main memory (cont'd)	Originate transmission service inquiry and main memory interrupt	
	Continue replenishment cycle when no response is obtained from the transmission service inquiry and new information is available	
	Store the new information in the appropriate buffer memory cell	
	Set up second replenishment phase and originate main memory interrupt when necessary	
	Originate transmission service inquiry	
	Continue second replenishment phase when no response is obtained from the transmission service inquiry and new information is available	
	Store the new information in the appropriate buffer memory cell	
	Set up third replenishment phase and originate main memory interrupt when necessary	
	Originate transmission service inquiry	
	Continue third replenishment phase when no response is obtained from the transmission service inquiry and new information is available	

Table 2-7. Data Transmission Unit (Sheet 4 of 4)

Hardware Requirements	Functional Specifications	Comments
Replenish data from main memory (cont'd)	Store the new information in the appropriate buffer memory cell Originate transmission service inquiry	
Supervise channel coordination buffers	Interpret Register S without hazards according to code immediately following its insertion in Register E Transmit channel or data set status according to code in Register E as a response to "Read E" addressing	Judicious selection of "E" codes enables efficient monitoring of the transmission initiation process.

Support Processing Requirement

An initial link word must be available in the memory cell permanently allocated to the channel transmit pointer. Data and subsequent link words are required to be compatible in format and memory location to obtain proper transmission. Repetitive messages and optional phrases can be achieved by controlling the link word content. Optional words are directly inserted; this technique appears to be most suitable for the control of LASA subarray modes. Processor interruption at preselectable message phases is desirable to support the transferral of non-repetitive or extremely long messages. This interruption can be instrumented by monitoring main memory addressing. Error control, such as parity or polynomial encoding, is not included in the data transmission unit; messages must be preprocessed by general-purpose algorithms to include these characteristics when desired.

Table 2-8. Data Reception Unit (Sheet 1 of 4)

Digital communication rates are significantly less than the capability of contemporary technology. Multiplexing of reception support logic is therefore advantageous to increase interface efficiency. Many message transmission variables are characteristic of a specific channel installation; program control of these parameters is non-essential, and therefore the following functional specifications reflect a Pegboard channel characterization.

Hardware Requirements	Functional Specifications	Comments
Support multiple channels	8 or fewer interface modules	Module address size is consistent with the minimum LASA requirement. Employing fewer modules requires the use of jumper connectors to complete inquiry chains.
Obtain data from the multiplexed reception bus	Initiate sequence when response is obtained from the reception service inquiry Employ channel address response to retrieve sector word Decode reception bit and restore sector word according to the character decoding algorithm Decrement the data word size when a character is completed Alternate the sector if the data word is depleted Originate reception service inquiry	Sequential logic design of the multiplexed reception bus control is necessary to efficiently use the data reception unit buffer.

Table 2-8. Data Reception Unit (Sheet 2 of 4)

Hardware Requirements	Functional Specifications	Comments
Decode channel characters	Programmable complementary characters for each communication channel	LASA communication requirements imply the range of character size. If excessive sector word bits are required to accommodate character decoding, two bits are sufficient.
	32 x 5 Pegboard matrix allocation	
	Character size selectable from 1 through 16 bits	
	Dotting optional	
	Automatic character synchronization	
	Minimum distance error detection decoding	
Unload data to main memory	Initiate sequence when no response is obtained from the transmission service inquiry	Two registers are required as data and address sources for the memory
	Originate reception sector service inquiry	
	Retain channel address response as the implicit address segment	
	Obtain the explicit link address segment from the link control word in the appropriate buffer memory cell. The initial explicit address segment is zero	
	Originate reception service inquiry and main memory interrupt	

Table 2-8. Data Reception Unit (Sheet 3 of 4)

Hardware Requirements	Functional Specifications	Comments
Unload data to main memory (cont'd)	Continue unloading cycle when no response is obtained from the transmission service inquiry and main memory access is complete	
	Complete first unloading phase transactions	
	Set up second unloading phase and originate main memory interrupt when necessary	
	Originate reception service inquiry	
	Continue second unloading phase when no response is obtained from the reception service inquiry and main memory access is complete	
	Complete second unloading phase transaction	
	Set up third unloading phase and originate main memory interrupt when necessary	
	Originate reception service inquiry	
	Continue third unloading phase when no response is obtained from the reception service inquiry and main memory access is complete	
	Complete third unloading phase transaction	
	Originate reception service inquiry	

Table 2-8. Data Reception Unit (Sheet 4 of 4)

Hardware Requirements	Functional Specifications	Comments
Identify marginal words	Flag 17th word bit when the source message is marginal because of inadequate data set AGC level, or when it contains an improper character Write the data word with illegal memory parity if the source message contains an improper character with a Hamming error distance equal to or greater than one quarter of the code dimension	Marginal words may be included or excluded in the final data file as a programming option which weighs consistency of message redundancies

Table 2-9. Interface Equipment Timing Unit (Sheet 1 of 3)

An integrated timing unit is specified to ease synchronization of the dual interface equipment. This coordination is essential to the smooth transferral of communication functions, so that either interface set can be maintained without operational degradation. Although the LASA requirements support only the two data set clock frequencies of 19.2 KHz and 50 KHz, other standardized digital communication rates can be readily supported. The following functional specifications reflect that flexibility obtainable with no logic penalty.

Hardware Requirements	Functional Specifications	Comments
Precision frequency source	± 0.01 % Phase locking oscillator coupling with isolation from power sequence transients	These standards for all interface timing must be phase-locked to prevent long-term relative drift
Synchronous logic timing	2 MHz clock system	Detailed specifications are consistent with the selected interface technology
Bell System 303A-Series data set timing	19.2 KHz half-group clock 50.0 KHz group clock 230.4 KHz supergroup clock	Data set clocks are distributed by the data transmission unit
Alternate data set expansion capability	1.2 KHz clock 1.8 KHz clock 2.4 KHz clock 4.8 KHz clock	Data set clocks are distributed by the data transmission unit. The alternate clock options may be mutually exclusive.

2-51

Table 2-9. Interface Equipment Timing Unit (Sheet 2 of 3)
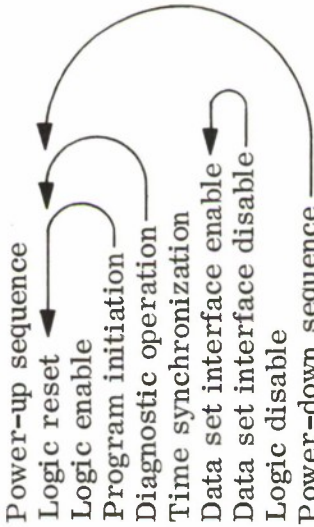
Hardware Requirements	Functional Specifications	Comments
Vernier time clock and marker	10^{-6} second resolution 16-bit clock register Time Coincidence interrupt generated when value coincidence with Register T exists Drive parallel data bus with clock value when addressed	The Vernier time marker is required to phase data set transmissions, and can be used by the programmer to update Greenwich time
Timing unit synchronization	Data set clock generation is synchronized at the initial synthesizer state Vernier time clock is set to Zero at the synchronization instant	Applicable only when bringing up and operating a second timing unit
Diagnostic support capability	Single step and system clock Repetitive operation from program initiation to Time Coincidence interrupt	Any additional specifications which aid maintenance and/or diagnostic tasks should be incorporated
Automatic sequencing	Power-up sequence Logic reset Logic enable Program initiation Diagnostic operation Time synchronization Data set interface enable Data set interface disable Logic disable Power-down sequence	None

Table 2-9. Interface Equipment Timing Unit (Sheet 3 of 3)

Hardware Requirements	Functional Specifications	Comments
Remote operation	Slaved sequence control Function status indicators	A part of the operations control console is allocated to remote centralized system control

Support Processing Requirement

Interval measures relative to Greenwich time and to communication record blocks must be maintained within the signal processor program.

Table 2-10. Data Set Adapter Coupling Requirement

Coupling	Signal Delineation	Baseline Data Rate	Comment
High-speed memory access	1-bit memory interrupt 16-bit address 1-bit read/write code 16-bit data bus 2-bit write parity modifier Appropriate transaction coordination	3.2 KHz transactions (including links)	Highest priority assignment
Register E net	16-bit read bus Several bit command code	Low data rate Continuous monitor	Multiplexed adapter control
Register S	16-bit bus	Low data rate Continuous monitor	Command preset
Register T	16-bit bus	Low data rate Continuous monitor	Clock preset
Register address matrix	2- or 3-bit register write decode	Low data rate Continuous monitor	Command sequence protect
Data net	16-bit bus	Low data rate	Directly addressable data
Interrupt net	1-bit program interrupt	Low data rate	Compatible with preprocessor design
Timing manifold	Several bits	Continuous monitor	Preprocessor basic clock family
Synchronization coupling	Analog oscillator coupling 3-bit synchronization coordination	Continuous monitor	None

2.7   DISPLAY FUNCTIONS

LASA signal processing is concerned principally with manipulating and interpreting signals which are time and spatially dependent. These signals contain information relating seismic observables and characterizing instrumentation and signal processing performance. A real-time operations requirement is to efficiently display this data for system performance verification, diagnostics, unusual occurrence analysis, and data editing. Educational attributes are additional benefits which may contribute significantly to initial development, reveal potential capability extensions, and dynamically present the essence of the process.

A display of waveform traces is conventional and versatile. One unit at the Operations console would support data editing. It would function with the event processor when monitoring or operator concurrence is desired. A second unit at the Maintenance console is suggested to support independently the array and the signal processing diagnostics. Presentation of both time histories and spectral content is required for rapid seismometer calibration, and may be a useful general option.

Comprehensive data addressing is essential to diagnostic monitoring, and keyboard supervision may provide the most flexible control for adequate presentation identification. Multiple traces are required to display parallel channels, significant process modes, or the phasing of multiple arrivals. Eight 500-sample traces appear adequate. Note that the sample interval may vary between traces; thus zero-order hold phase compensation and first-order hold instrumentation are desirable options. Independent waveform translation is required to properly phase the data, and should be composed of an inter-sample vernier and a data file pointer modifier. This composition also enables an efficient and natural data precession to facilitate library scanning, editing, and transient monitoring. Provisions for freezing the display to conduct detailed examination of a local region is implicit.

Although a calibrated graticule can provide gross measures, time and interval marking should be indicated by electronically generated cursors to

maintain proper registration. Center indexing, with waveform phasing directly coupled to the operator intervention cursor registers, is an appropriate display mode. However, the presentation of a complete real-time data field and the measurement of spectrum frequency parameters imply a left margin and a variable index, respectively. These two static and one dynamic cursor modes do not imply major hardware instrumentation, and should be included for operating convenience.

Basic waveform display-oriented functions have been defined. Digital support tasks of record addressing, history supervision, scaling, time coordination, data display refreshing, and cursor register interpretation are required. In addition, hard-copy routines should be coupled and coordinated to provide semiautomatic documentation of data files corresponding to or assembled with the display activity.

Spatial relations of the signal characteristics are not portrayed by the waveform histories. A beam display concept has been postulated which retains the beam allocation geometry in inverse horizontal phase velocity space. It uses intensity modulation to indicate the seismic energy observed on each beam. An experimental display operating from tape data is functioning (Section 3-6), and has verified that detections originating from seismic activity and from communication errors have distinct signatures. In addition, the array beam pattern is distinguishable, and some event-oriented signature intelligence is observable. Two displays are envisioned in an operational LASA installation. One display unit would allow monitoring of the detection process to verify proper system operation. Optional detection accentuation is required for comprehensive process surveillance, and logarithmic scaling may be beneficial in portraying large dynamic ranges. Provisions for freezing the display and for regressing in time to conduct detailed examination without the loss of data are desirable but expendable during system fail-soft modes. Several minutes of history should be adequate.

The second display unit could serve many functions. Observation of the detection queue through adjustable phase velocity-time windows could indicate the rationale of event logic decisions, and establish a qualitative measure of

the event backlog. Trained operators could significantly contribute to system performance by optimally indicating concurrence, and by supervising the processing of weak or otherwise marginal arrivals. Dynamic, two-dimensional presentation of event beams as mosaics of energy content or as a correlation with reference beam patterns could display the data base used to derive event origin. Image cursors should be employed to indicate unambiguously the selected beam direction. Detents should be used only when identifying specific beams. A secondary application of this functional display unit is the indirect supervision of the detection posture. Pertinent parameters such as coverage, background noise, and detection sensitivity can be efficiently interpreted and edited with cursor-referenced instructions. Such action should be automatically documented in the System Log.

The above functions represent different resolution requirements. Four preselected scales are suggested to efficiently use the display field and provide some growth flexibility. Beam-packing is essentially the grouping of circular elements to provide a continuous planar coverage. Figure 2-9 illustrates the implicit hexagonal geometry and the unequal spacing in rectangular coordinates. Sixteen intensity modulation levels are readily packed and instrumented. Although all levels are not clearly distinguishable, low-level detail and display smoothness is obtained.

Event queue presentation and detection monitoring can require mosaic linear dimensions in excess of 64 cells, but always less than 128 cells. Seven counter stages are adequate for vertical indexing, but an eighth horizontal stage must be provided to establish the staggered-line registration. Preselectable operator feedback efficiently controls the mosaic dimensions.

Beam indexing and subraster character generation become difficult with large fields. Adoption of a raster scan establishes a definite deflection waveform, reduces the encountered frequencies, and eliminates registration problems. A 1K bit memory is required to buffer two-line intensity histories if a nondedicated refresher source is employed. However, an additional access margin is gained which will substantially reduce multiplexed device interference.

1.15
Units

0.866
Units

cos 30° = 0.866

1 Unit
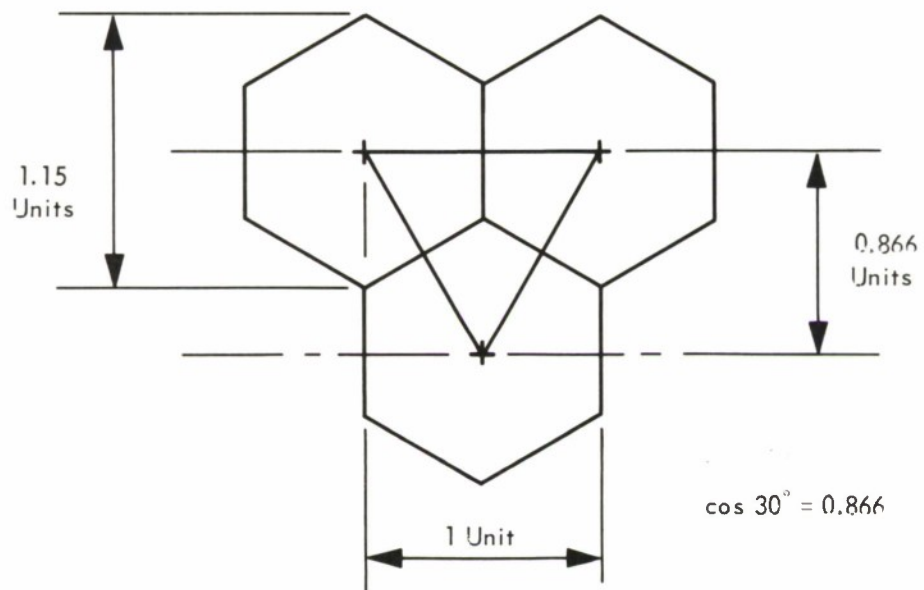
Figure 2-9. Beam-Packing Geometry

Character generation is a simple task when the reflected vertical vernier parameter (β) of Figure 2-10 is employed to bias a threshold detection (L0) of the reflected horizontal vernier. Figure 2-11 illustrates the Boolean functions (Wi) of this threshold parameter, and the two low-order grey code addresses (L2 and L3) which modulate the beam values (Ri).

$$W1 \quad = \quad \overline{L0} \cdot \overline{L2}$$

$$W2 \quad = \quad L0 \cdot \overline{L3}$$

$$W3 \quad = \quad \overline{L0} \cdot L2$$

$$W4 \quad = \quad L0 \cdot L3$$

Correlation displays may be improved with continuous or discrete interpolation. This refinement is required on only one unit, and could be instrumented as an attachment. Figure 2-12 defines an analog weight set which is easily generated. Although relatively high-frequency waveforms are processed, only limiting and gating operations are encountered. Special-purpose discrete interpolation is more involved, but does retain large intensity gradients at the character boundaries. Figure 2-13 illustrates the binary variables which uniquely define trinary weighting functions of the following form:

$$W1 \quad = \quad \begin{cases} 1 & \text{If} \quad \overline{L0} \cdot \overline{L1} \cdot \overline{L2} \cdot \overline{L4} \;=\; 1 \\ 0.5 & \text{If} \quad (L0 \cdot \overline{L2}) + (\overline{L0} \cdot L1 \cdot \overline{L4}) \;=\; 1 \\ 0 & \text{If otherwise} \end{cases}$$

$$L4 \quad = \quad \begin{cases} 1 & \text{if } \beta \geq 1/2 \\ 0 & \text{if } \beta < 1/2 \end{cases}$$

Note that the unity weight value can be instrumented as a composite of two half weights to achieve maximum transition smoothness.

Conventional technologies satisfy all digital and video instrumentation requirements. Relatively high-speed gates are necessary to derive the video from the weighting functions. Transient switching hazards are minimized in this conceptual design by restricting all gate action to periods of zero beam weight. Any residual transients can be masked by establishing the black
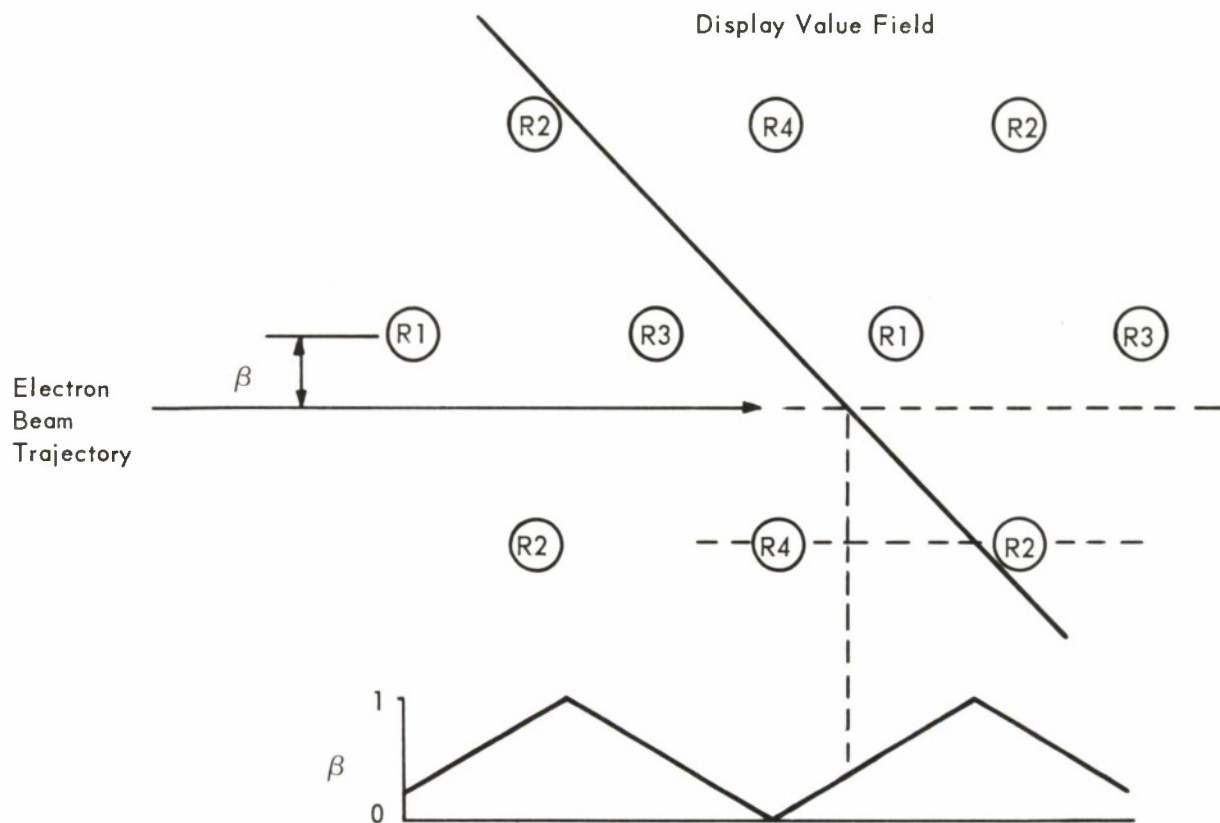
Figure 2-10. Reflected Vertical Vernier Parameter
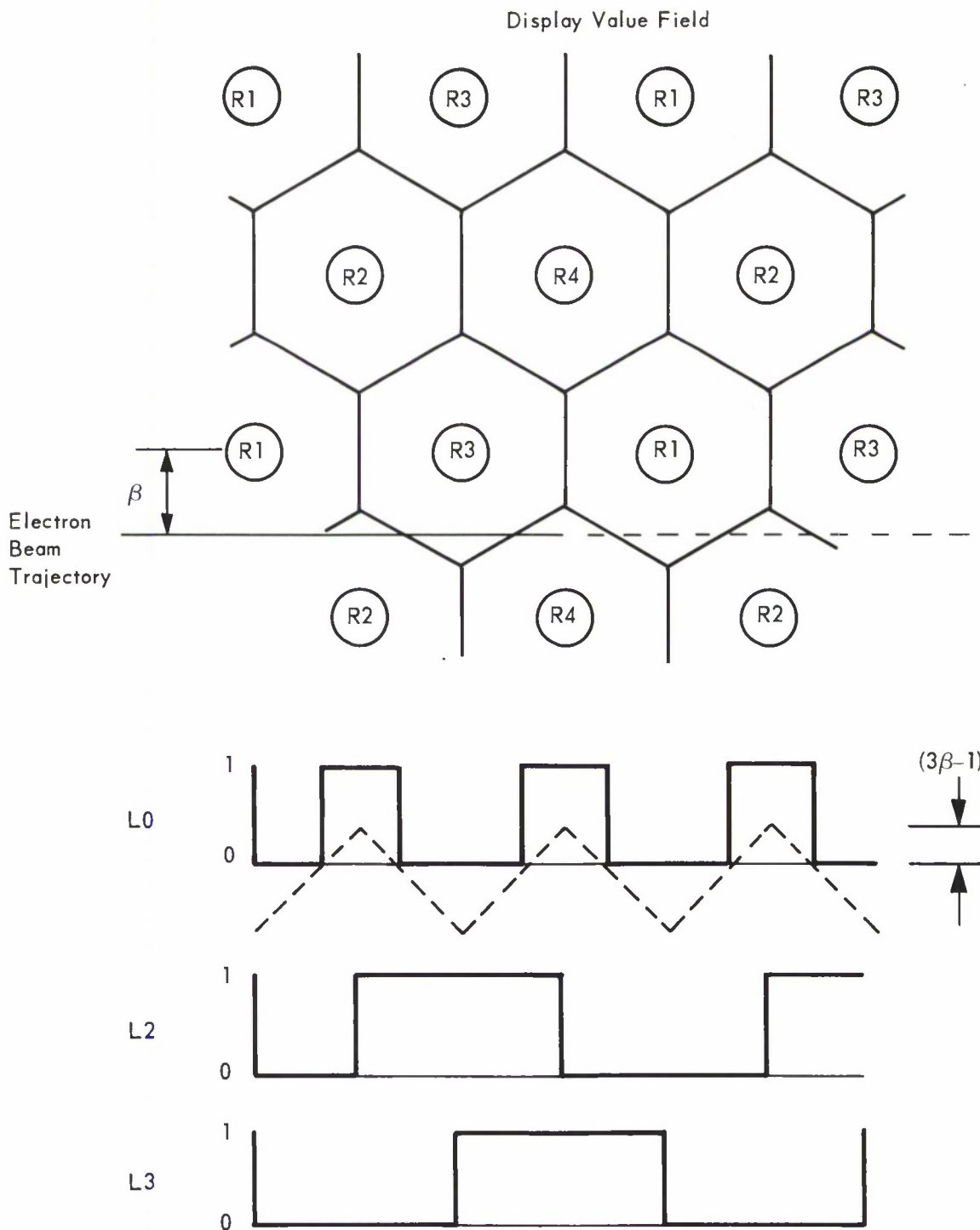
Figure 2-11. Beam Display Switching Parameters
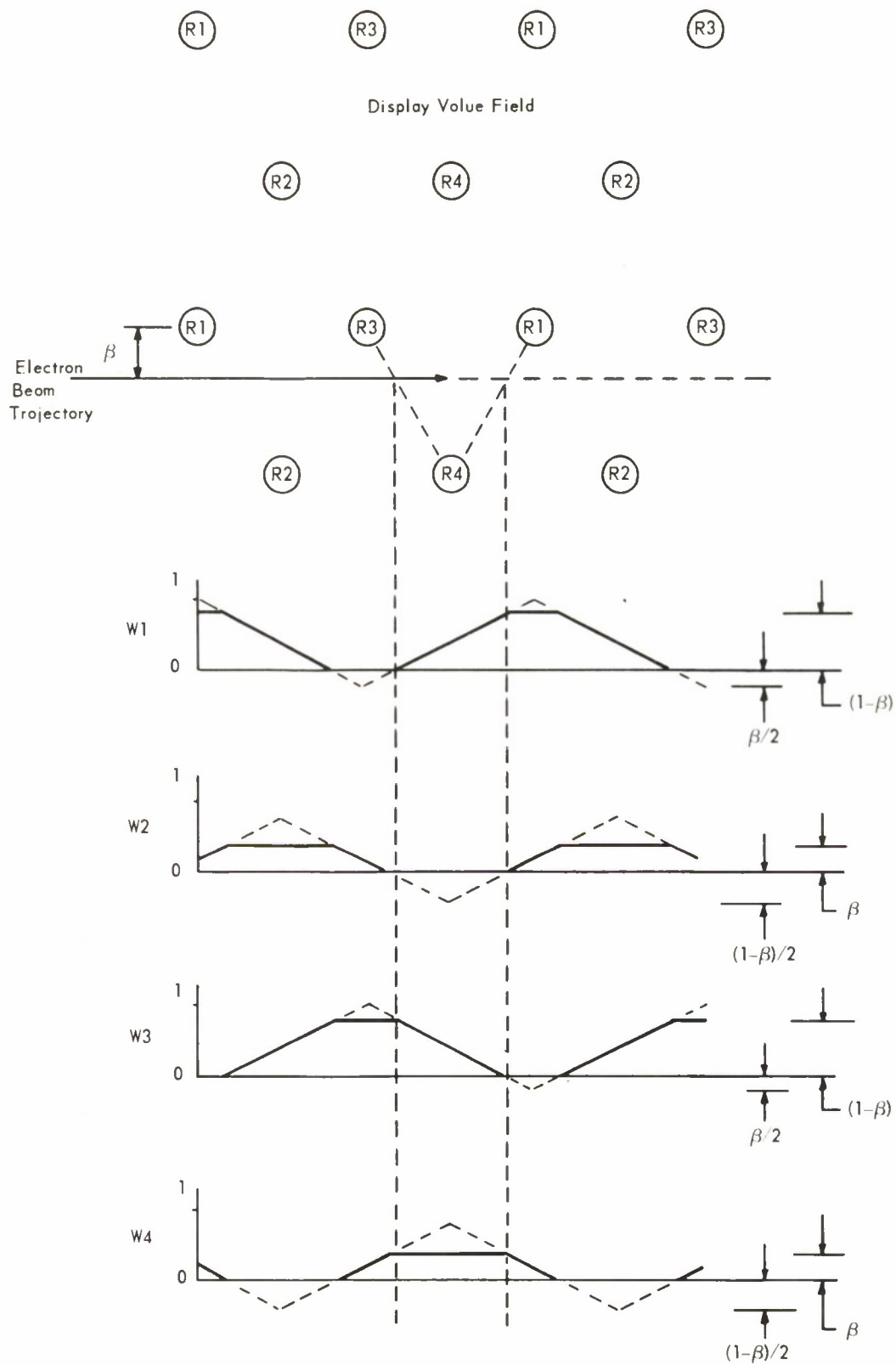
Figure 2-12. First-Order Beam Interpolation
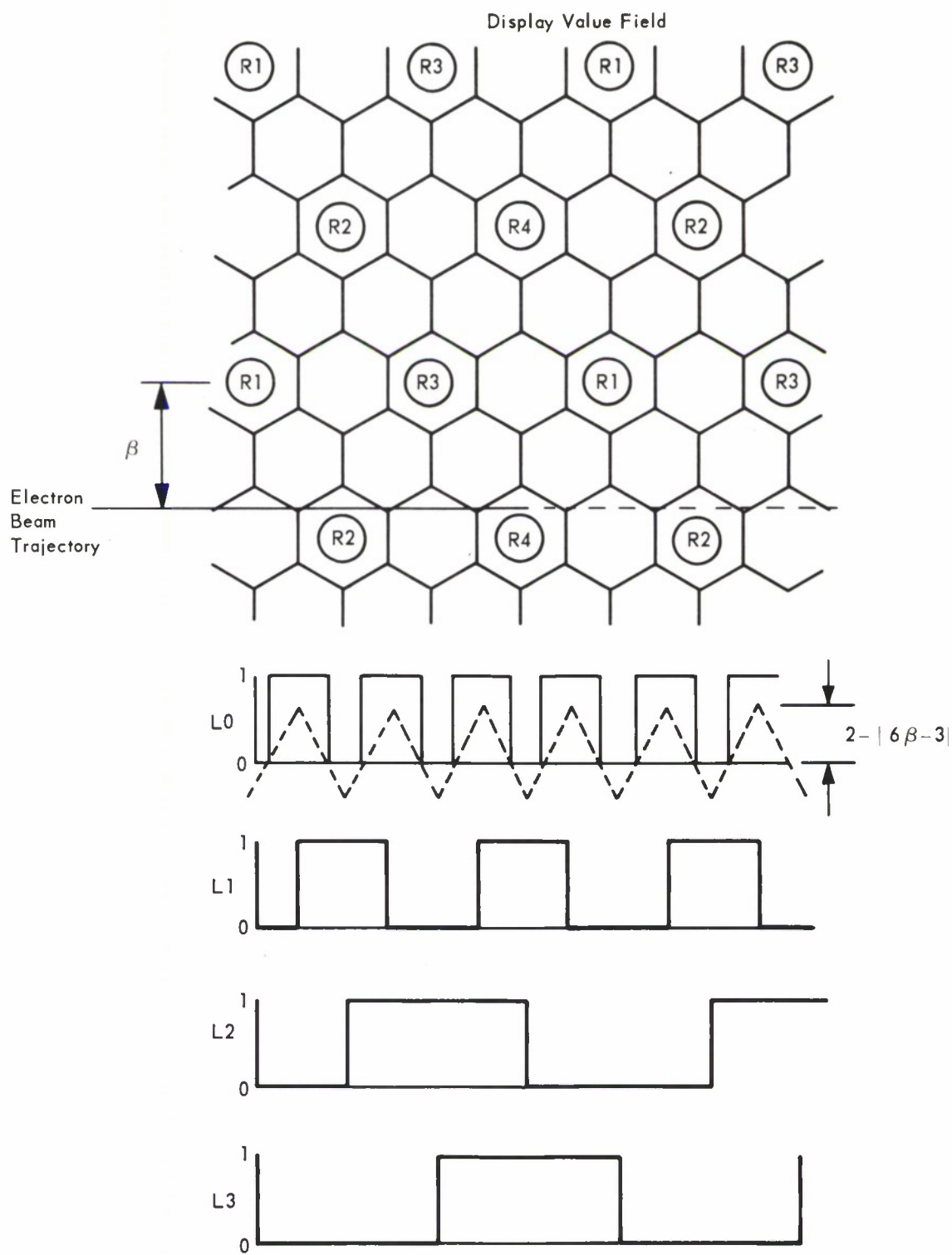
Figure 2-13. Digital Beam Interpolation

pedestal at the node video stage and allowing a negative weighting function excursion. The video generator (see Figure 2-14) is a composite of these configuration concepts, and should provide a clean and stable background field.

Physical display properties are illustrated by Figure 2-15. A hood containing a polarized reflection shield is optimized for intensity pattern viewing. Camera mounting hardware is incorporated to facilitate hard-copy documentation. An optional intensity calibration strip may aid display adjustment and interpretation. Time can be easily coordinated with the image by superimposing a label field of sixteen 5 x 7 dot characters with the addition of a generation matrix. Since the fields are mutually exclusive, digital data distribution and storage facilities can be shared. Table 2-11 lists a convenient character set which is compatible with both the beam format and binary-coded decimal notation.

Record addressing, history supervision, scaling, time coordination, data refreshment, and cursor register interpretation are again the principal digital support tasks. Scaling should occur after the history file for subsequent display parameter manipulation. Figure 2-16 shows the functional processing which allows beam field display of linear signals, logarithmic signals, linear background noise estimates, logarithmic background noise estimates, and logarithmic signal-to-noise ratios. The data communication and processing impact is reduced by maintaining a quasi-static beam roster to distribute only active display intensity values to the refresher buffer. The highly repetitive nonlinear scaling process can be streamlined by using base two arithmetic to establish an integer relationship between the characteristic value and the shift operation. Eight-bit logarithms with four bits allocated to the mantissa provide a 0.375 dB resolution throughout the system's dynamic range. Control of the pedestal and of intensity scaling (shift and limit operation provide adequate product quantization) allows optional presentation for specific characteristics of operator interest, and establishes a direct beam measurement capability (if a pedestal calibration bias parameter is incorporated).

Several decimal words constituting a parameter measurement display will facilitate operational functions such as array calibration, array diagnostics,
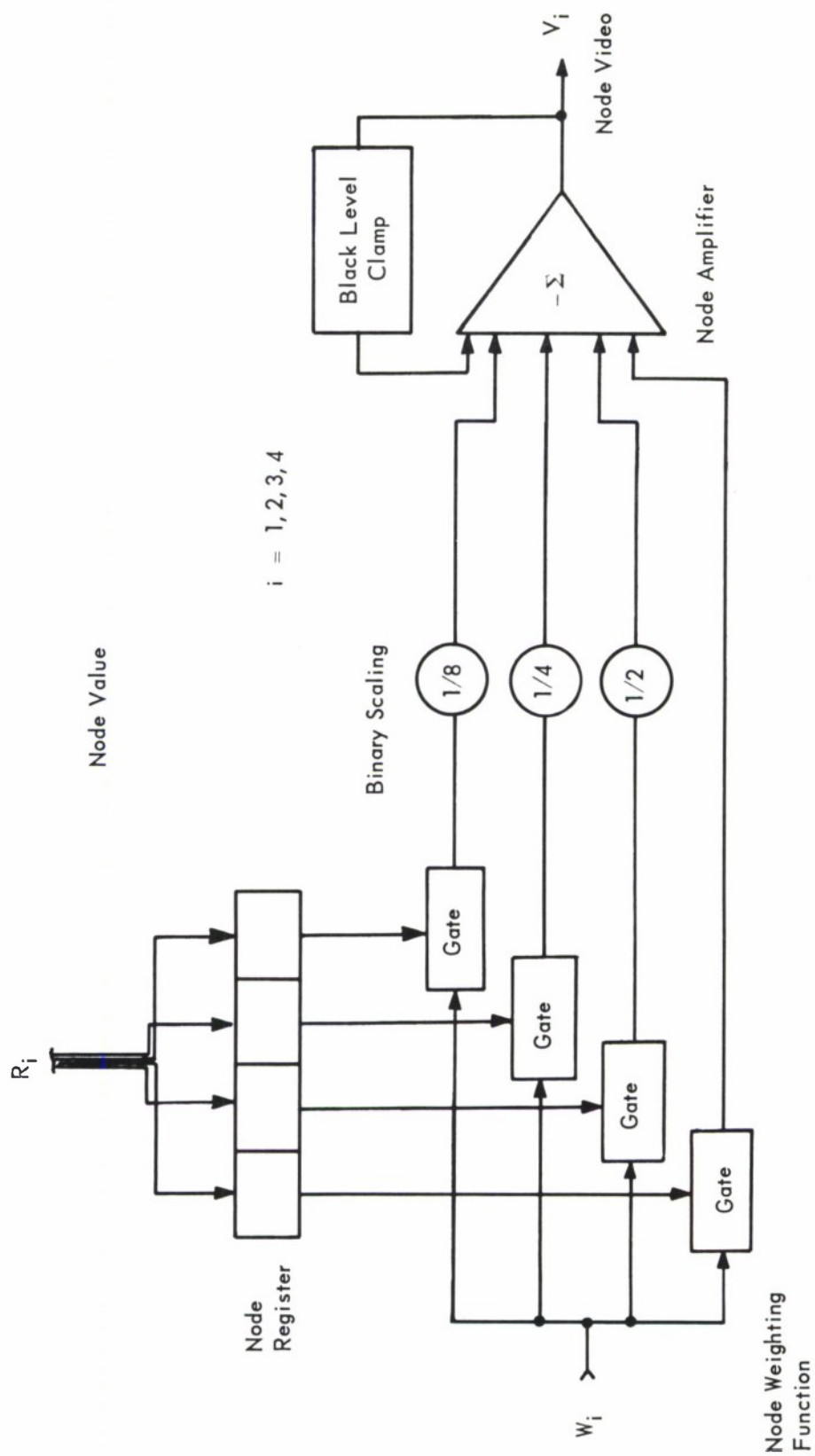
Figure 2-14. Node Video Generation
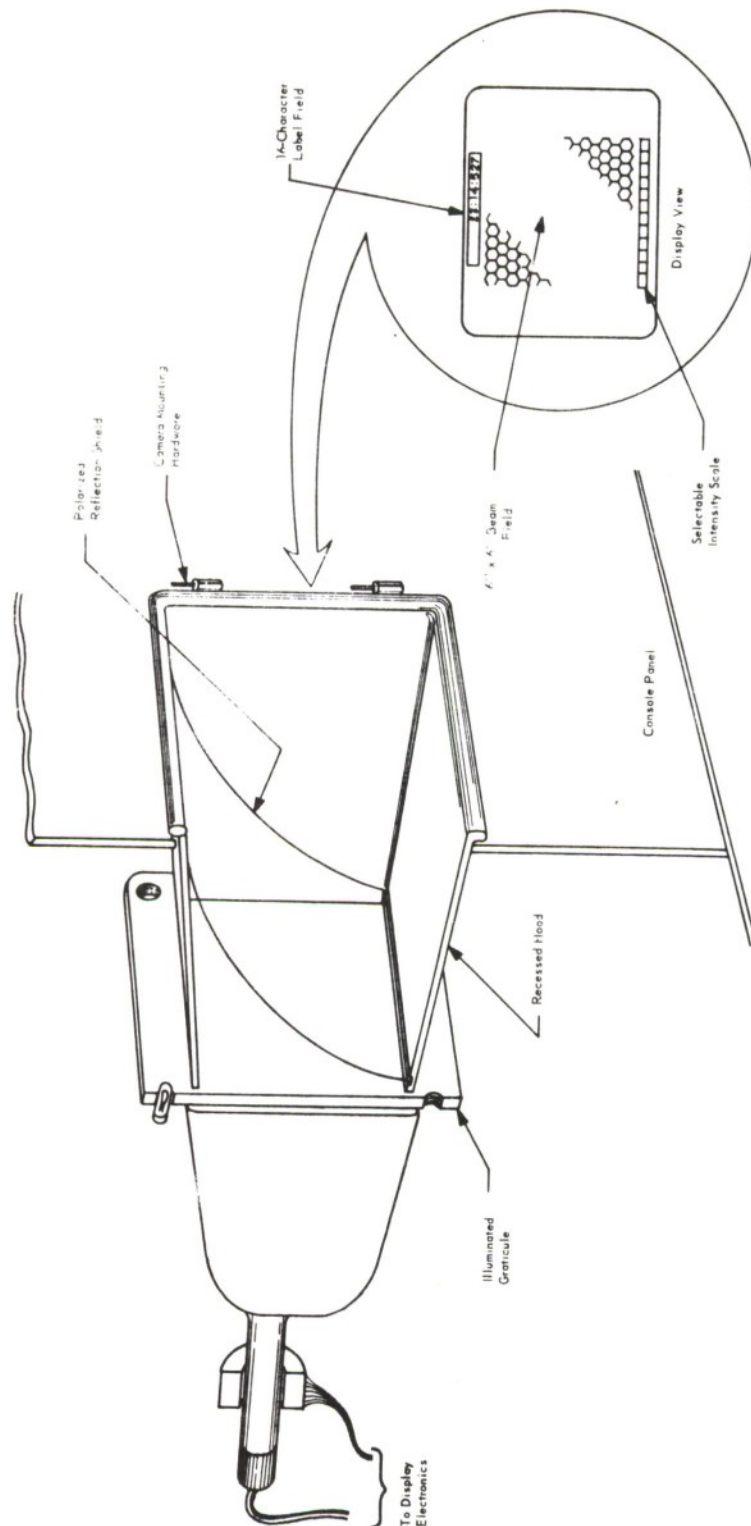
Figure 2-15. Conceptual Beam Scope

14-Character
Label Field

Display View

Selectable
Intensity Scale

Polarized
Reflection Shield

Camera Mounting
Hardware

4" x 4" Beam
Field

Console Panel

Recessed Hood

Illuminated
Graticule

To Display
Electronics

Table 2-11. Beam Scope Label Generation

Half-Byte Code	Character
0000	0
0001	1
0010	2
0011	3
0100	4
0101	5
0110	6
0111	7
1000	8
1001	9
1010	To be defined at
1011	a later date
1100	
1101	period
1110	colon
1111	blank
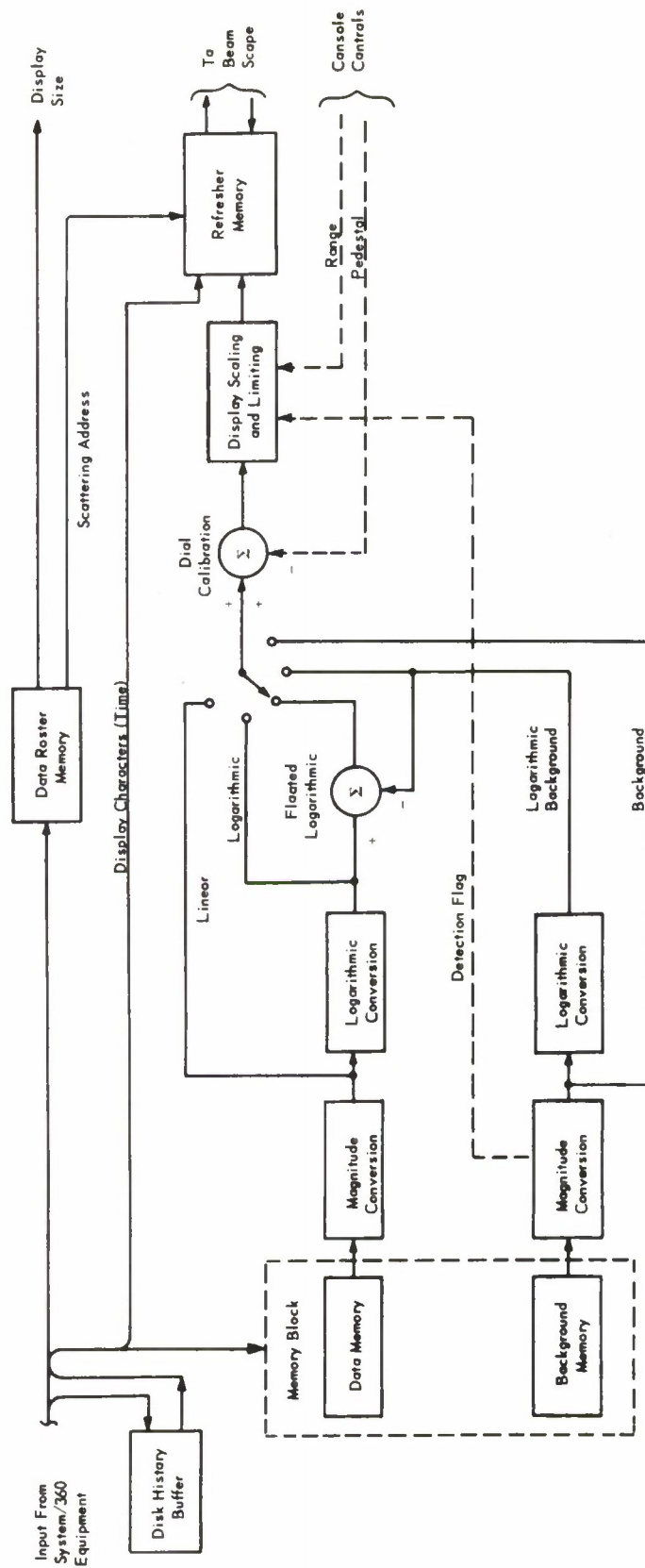
Figure 2-16. Functional Beam Scope Processing

phase velocity coordinate observations, arrival time refinement, data record verification, copy format preparation, and time synchronization. Since source data may originate from any system message or device, this operation should be closely coupled to supervisory structure. Conventional techniques are adequate to multiplex, scale, and present the information. Subsequent definition work should consider character generation techniques to provide adequate quantum and parameter identification.

Conventional real-time system components can satisfy the hard-copy and discrete status display requirements. The conceptual system allocates detection and system logs to console keyboard-printers, and supports a system status indicator array to indicate system posture concisely. The objective is to provide efficient and unambiguous communications with operations during such transition periods as process editing, fail-soft recovery, and shift-changing. The less critical functions of listing and plotting would be performed as an automatic off-line priority sequenced process, which could be forced on-line when critical. One unusual hard-copy requirement is envisioned. Many interested factions of the seismic community have based their data record and analysis capability on photographic signal history documentation. A single recorder would provide an adequate film medium transcription capability to support their operations, if accelerated translations were performed as a request service.

The preceding discussion of display functions provides a concept structure to support equipment selection or design. Flexibility, because of the research nature of this project, should be retained as the implementation detail develops.

2.8   CONTROL PROGRAMS

Each machine in the system requires a set of monitor and control programs to support its operation. The monitor must coordinate all the activities in a given machine, such as program computation, input/output scheduling and interrupts, man-machine communication, and communication with other processors. Those demands on the processor do not occur in a predictable

sequence, but are announced by interrupts. The part of the monitor which handles the interrupts and schedules the sequencing of these activities is the supervisor.

A higher-level coordination of activities is necessary between the detection processor and the event processor. When both processors are operating, one is considered the master coordinator. This function requires logic in both monitors, but is mainly a part of the event processor's monitor because of its capacity and its central position in the configuration. Each processor, however, can manage its activities if the other processor is absent.

2.8.1 Detection Monitor

The detection processor, for control purposes, logically has just one problem program. The core map is essentially static; no programs are brought into memory or removed during processing. This main program accounts for most of the computer time in this processor. It may also request input/output through the supervisor (e.g., build a log of detected arrivals for later use by the event processor).

Another function of the detection processor is to acquire and record input data. This function is accomplished by a monitor program which must use the supervisor to issue its input/output operations.

Communication with external processors, in particular the event processor, may sometimes be of a high priority nature, as when reconfiguring or changing procedure is demanded by a failure. In this situation, a monitor program which has control and which issues its input/output through the supervisor is required.

The supervisor must schedule all input/output requests and service their completions in a central module, the detection input/output control. Input/output may be issued by any of three programs on symbolic devices on any channel. The detection input/output control decides the particular device according to the configuration and mode of operation, and schedules the requests according to the availability of the channels and the priority of the requester.

The scheduling of programs and input/output operations and handling of supervisory call interrupt, external interrupt, and input/output interrupt are interrelated. Handling program interrupts and machine check interrupts is more or less independent of other supervisory operations.

The logical structure of the detection processor programs, showing the organization of the monitor and in particular the supervisor, is shown in Figure 2-17.

2.8.2   Event Monitor

The event processor's principal function is to process arrivals detected by the detection processor. This involves the execution of a sequence of programs, not all of which reside in core memory at all times. The sequence of programming may differ, and the amount of event processing may vary, depending on the character and frequency of the arrivals and the requirements of the user. Where the event processing load is not high, other tasks should be run.

Some of these activities are compute-bound (e.g., event beamforming) and some are input/output-bound. If the computer is being used for some activity of secondary importance and arrivals begin to occur, event processing should start immediately. It would be undesirable to cancel the current job in order to respond; therefore, multiprogramming with three tasks could be done in the event processor with the ability to load programs from disk memory for execution as needed. One program partition can be reserved for the early stages of event processing, so that the processor can respond quickly to the detection of arrivals.

Some of the duties of the event monitor are to

1.   Schedule input/output issued by programs outside the supervisor for all devices on all channels

2.   Schedule queueing and loading of tasks on demand

3.   Initiate event processing on cue from the detection processor

4.   Handle communication between user and system
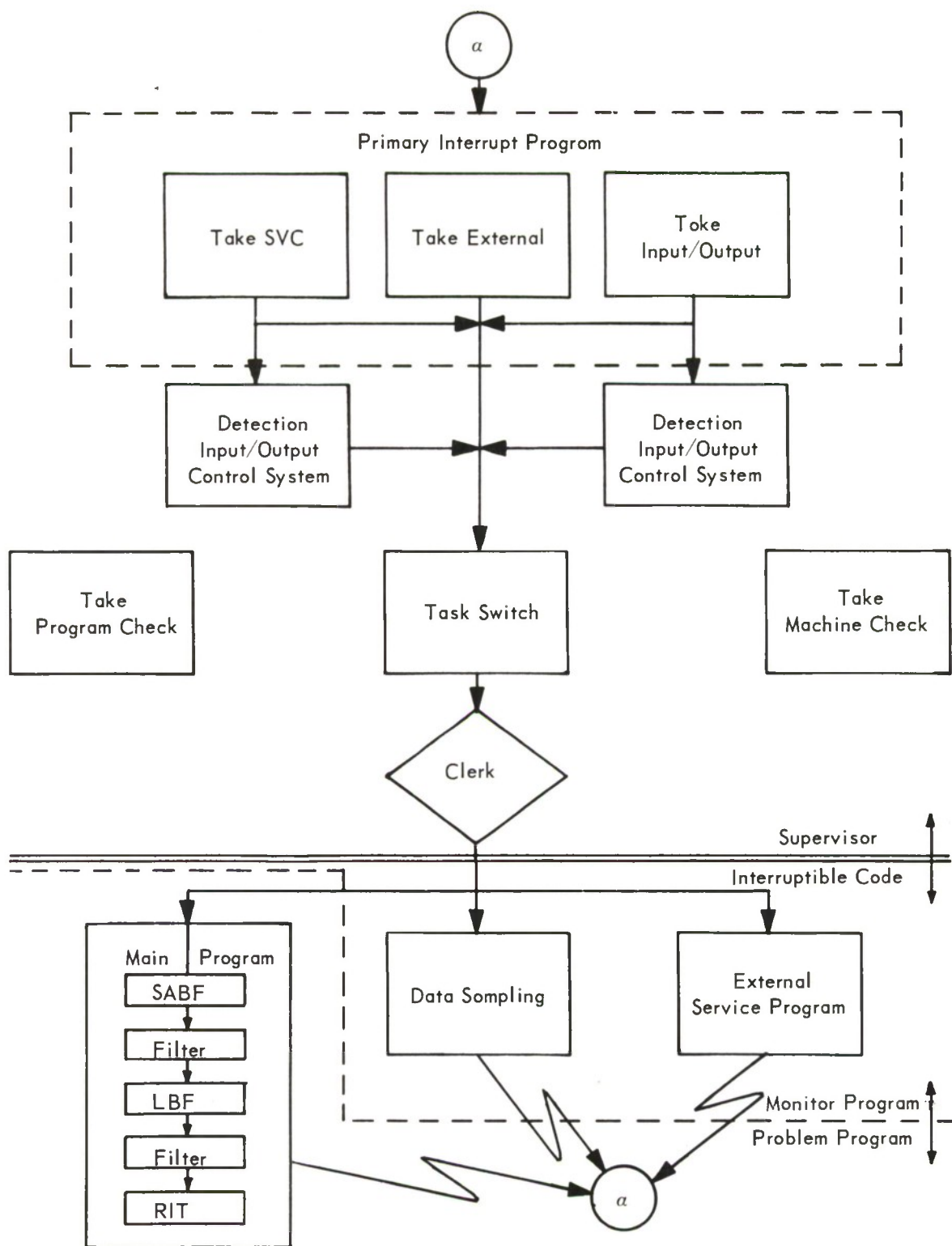
Figure 2-17. Detection Processor, Program Segment

5. Execute several tasks concurrently

6. Schedule tasks automatically

7. Detect failures or deliberate shutdown of detection processor and assume its function

8. Oversee the activities of the whole configuration.

The event monitor must perform certain functions and service devices which cannot be done using currently available standard software packages. It is desirable to have the use of many of the standard utilities and other modules. Therefore the event monitor must be designed primarily around the requirements of the system, but must be compatible with respect to input/output control with the standard systems which support these computers. To a large extent, the event monitor will be constructed around the modules of a standard programming support package.

Figure 2-18 illustrates the programming structure of the event processor, emphasizing the relationship between the three program partitions. The supervisor structure is logically segmented in much the same way as the detection processor supervisor, although the individual modules are quite different in scope and structure.

In the situation where the event processor must take over the function of the detection processor, the three partitions shown in Figure 2-18 will perform the functions of the three interruptible programs shown in Figure 2-17.

Figure 2-18. Event Processor, Program Control Structure

The diagram contains the following elements:

α

Event Supervisor

Supervisor

Interruptible Code

Event Processing Portition

Event Processing — Especiolly functions which use microcoded algorithms.

Support Portition

Progroms which ore o port of event processing or which support operations which ore experimental progroms.
Exomples:
Deloy time colculotion,
Detection beom selection,
Produce event record,
Select event beom,
Plot beom,
Produce seismic bulletin,
Fortron compiler,
Many others.

Monitor Portition

Input/Output to ond from detection processor.
Servicing other reol-time devices.
Operotor Communicotion.

α

It is possible for some fost-running tosks listed under support portition to be run in the event processing portition in periods of low seismic octivity.

Stondord software such os FORTRAN complier must run in support portition.

Figure 2-18. Event Processor, Program Control Structure

Section 3

SYSTEM STUDIES

This section contains Array II beam requirements, discussions of array geometry location capability and steering delays, and a description of the experimental display, filter implementation, and simulation study results.

3.1 BEAM REQUIREMENTS

In Appendix A3 of the Second Quarterly Report (reference 3) a method for determining beam requirements was given. Initial estimates for the LASA beam requirements were verified and presented in the First Quarterly Report (reference 2).

The number of subarray beams to be formed per subarray ranges from six (for worldwide surveillance) to three (for continental land masses only). Intermediate values are required when Pacific Islands or seismic zones are included.

Figure 3-1 shows the number of detection beams required to cover the land areas and the land areas plus seismic zones lying within the P-teleseismic zone as seen from the Montana LASA and from a second array location already considered. The number of beams for each case is shown as a function of beam diameter, D, in inverse velocity space. For the main lobes of the Montana LASA and subarray beam patterns, these beam diameters (in sec/km) are related to the loss (in dB) at the beam perimeter and the signal frequency (Hz) by the following formulas. The particular LASA formula used depends on whether the full LASA (21 subarrays) or a reduced LASA (17, 13, or 9 subarrays when one, two, or three outer rings are weighted zero) is used.
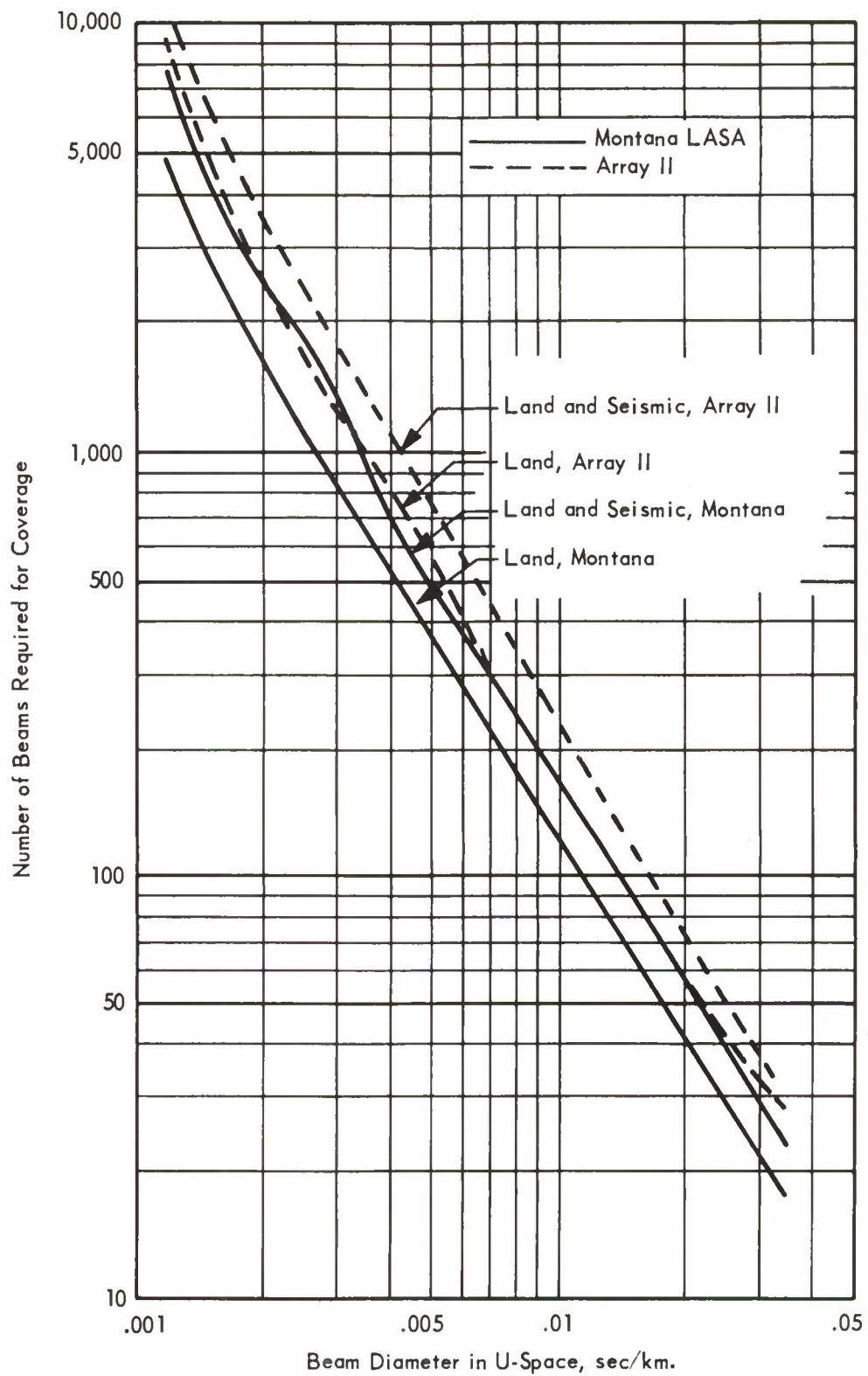
Figure 3-1. Required Number of Detection Beams vs Beam Diameter
in Inverse Velocity Space

$$21 \text{ SA LASA beams:} \quad D = 0.0042 \sqrt{L/f}$$
$$17 \text{ SA LASA beams:} \quad D = 0.0070 \sqrt{L/f}$$
$$13 \text{ SA LASA beams:} \quad D = 0.0118 \sqrt{L/f}$$
$$9 \text{ SA LASA beams:} \quad D = 0.0185 \sqrt{L/f}$$
$$\text{Subarray beams:} \quad D = 0.105 \sqrt{L/f}$$

As a sample calculation, determine the number of detection beams needed to cover land and seismic areas, with an allowance to lose 1.7 dB (in addition to a 1.3 dB subarray beam loss) at 1.5 Hz, using all 21 LASA subarrays.

From the formula for 21 subarrays, the beam diameter is $D = 0.0042 \cdot \sqrt{1.7 / 1.5} = 0.0036$ sec/km. The number of such beams needed to cover land and seismic zones from Montana is N = 900.

3.2   ARRAY STUDIES

A beam pattern program capable of plotting contours of constant phase as well as constant loss—both at a single frequency—has been completed. This program may be useful if it becomes necessary either to try to significantly reduce side lobes of the present LASA by subarray additions, or to synthesize a new LASA configuration.

Figures 3-2 and 3-3 show the dB loss and phase patterns for the Montana LASA configuration. For any future synthesis (i.e., pentagon or heptagon array), the program would be used to evaluate patterns for a single ring or polygon of subarray locations (i.e., five or seven). Hopefully, a desirable side-lobe pattern can be achieved by combining a number of such polygons of varying size and angle of rotation.

Note that in the figures shown, the two major side lobes of LASA are directly crossed by a contour of zero phase angle. If this applies in the regular polygon array synthesis, then a good array with a large main lobe, but small side lobes, might be difficult to achieve by this method, since any side-lobe cancellation would have to be achieved by adding rings having effectively a negative weight, in turn decreasing the main-lobe gain. Therefore, the effectiveness of this method of polygonal array synthesis remains to be established. It has not been determined that side-lobe reduction is in itself a matter of overriding
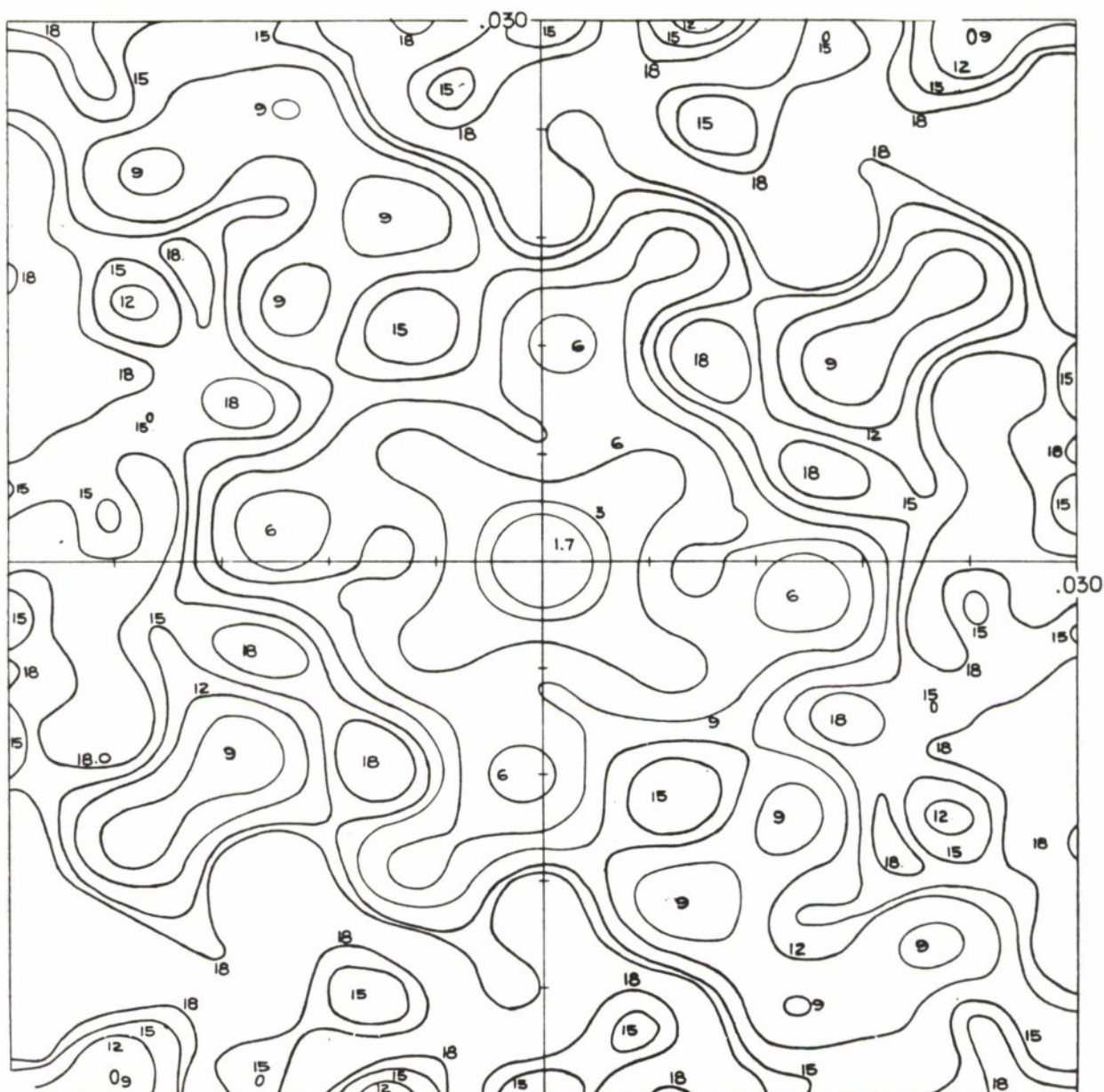
FULL LASA ARRAY, 21 SUBARRAYS
VALUES IN dB

Figure 3-2. Beam Pattern Loss Contours in Wave Number Space
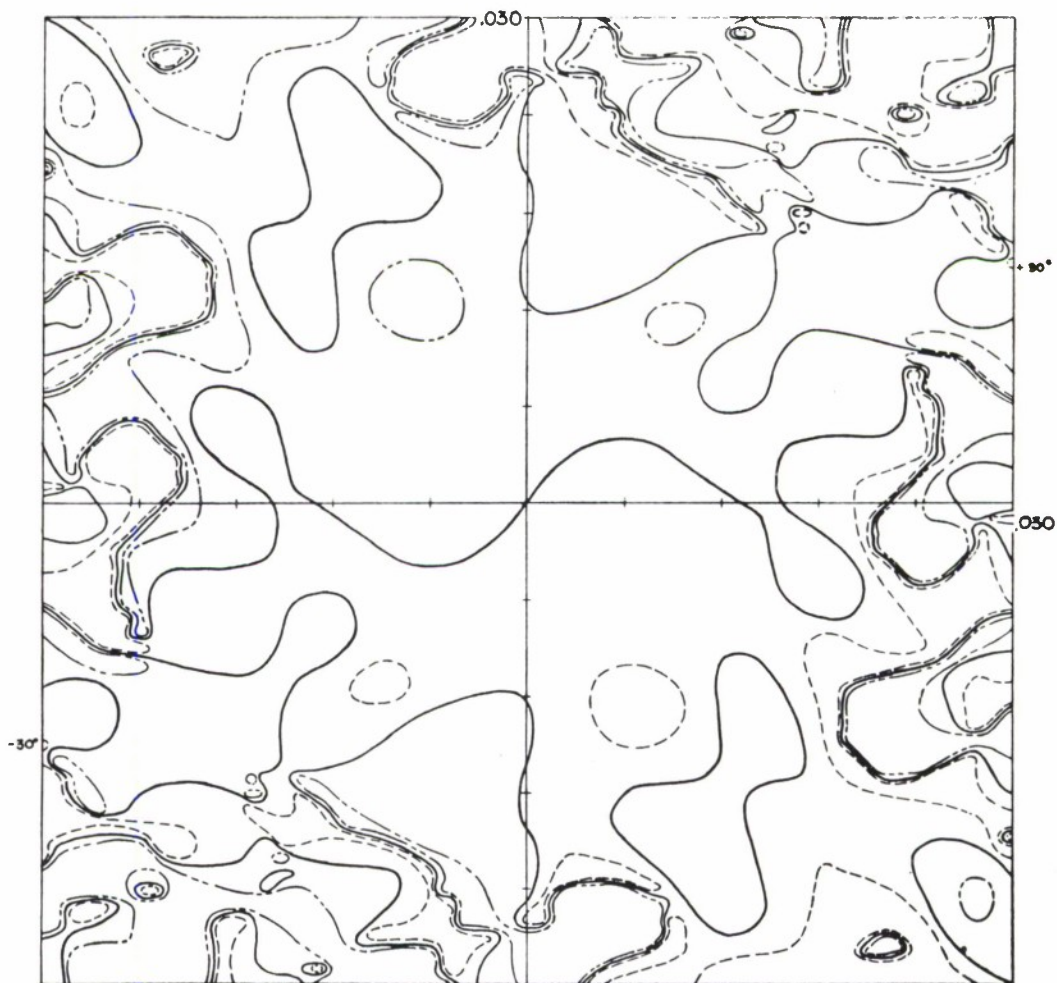
LEGEND

– – – – – –	–30°
————	0°
—— · · ——	+30°

Figure 3-3. Beam Pattern Phase Contours in Wave Number Space

importance (reference 2). For these reasons, any further effort in this direction would be continued on a low-priority basis.

3.3 EVENT LOCATION CAPABILITY

The capability of LASA to locate a seismic event was evaluated in Appendix A of reference 3. The results of that study are briefly summarized here.

The three main sources of location error are expected to be

1. Errors because of finite beamwidth
2. Errors in beamforming because of incorrect steering delays
3. Errors in relating measured phase speed to range.

When preformed event beams are used to locate events, the basic timing error is that of the preformed beams compared to the arrival of the actual wavefront; the resulting error in U-space is numerically about that of a 3 Hz, 3 dB beam radius, or perhaps 50 to 190 km. This assumes the existence of significant energy at 3 Hz, an assumption whose validity is questionable from studies of signal spectra (Section 3.8). However, subsequent beam processing, such as calculating centers of gravity of beam clusters or correlation, should help materially to reduce this source of error (Section 3.9). After a strong event has been treated individually by steering a beam designed adaptively for the event, the corresponding least squares U-space location probably cannot be further improved. The error then is a minimum of 30 km due only to sampling error, but for actual events is more likely to be 50 km to 100 km. The additional error of U-space to geography conversion must be added to both methods of processing. The error can be minimized only for areas where calibration events have been available.

The above estimates refer to the entire 200 km aperture LASA. Reducing the aperture would proportionately increase the factor multiplying timing errors leading to location errors. However, it must be recognized that the location capability of even the full-size LASA is an order of magnitude below that of a world network.

The location capability of a set of two or more seismic stations, one or more of which could be LASAs, is bounded largely by the ability to accurately read corresponding arrival times at such stations. For this reason, it would be desirable to explore the possibility of increasing the accuracy of such relative arrival times by cross-covariance analysis of signals and reception at widely separated stations. For example, signals received for some event at various stations throughout the United States might be correlated against the corresponding LASA beam to determine what improvements might be made over manual methods.

3.4 STEERING DELAYS

The problem of developing a set of steering delays with which to form beams in the LASA signal processing system falls into two interrelated tasks. In the first task, assume that, for a number of seismic events used for calibration of a particular seismic region, arrival times at the various LASA seismometers have been identified. These times, or more particularly the relative arrival times or time differences for each event, must be organized and averaged so that a presteered beam can be formed toward any point in the region of the calibration events. The method must include some means of interpolating steering delays between received events. In the second task, meaningful relative arrival times from the seismic signals are actually measured. Progress in and further plans for completing the solution of these two problems are presented in the following paragraphs.

3.4.1 Organization of Arrival Time Data

The first task, the organization of previously measured time delays, has traditionally been accomplished by defining for each event region and receiver site a travel time anomaly. This anomaly is the difference between the actual travel time and a theoretical one, based on a worldwide travel-time average for events at a given range, such as the Jeffreys-Bullen Seismological Tables (reference 5). The required event range can be obtained for each event from an event

location based on the world seismic network. Time of origin is also determined by this network. The average anomaly for each receiver for a given region is then calculated from a number of events in that region, and used to provide a correction to theoretical travel-time tables to give the required beam steering delays. The LASA system steering error for a given event would then depend on how well the event arrival time differences fit the region averages. Some of the bias in these anomalies can be removed by keeping track of the relative anomalies with respect to a particular receiver (such as the station LA0 in LASA) rather than absolute values. A very interesting and informative study of time anomalies using this method on the LASA array has been completed by E.F. Chiburis (reference 4).

Another possible method of organizing the time delays is to establish a best-fitting plane or second-order wavefront for each event, and to use as anomalies the variabilities of the deviations from this best-fitting wavefront. As in the currently used method, the delays are then based on the anomaly averages for a given region. It is not known which one of these methods might yield better results, but we believe that each has sufficient arguments supporting it to warrant consideration of both.

The major advantage of the presently used method, based on the Jeffreys-Bullen Tables, is that it makes use of world seismic network event locations whose accuracy far exceeds that of the single LASA event location capability. The argument that the organization of arrival time data should be based on this relatively accurate source location information, and that it should be referred to the extensive seismological experience encompassed in the Jeffreys-Bullen Tables (reference 5) and available local corrections to them, cannot be dismissed. Another advantage of the presently used method is that it deals with each station (subarray) individually. Thus, those cases in which arrival times are determined at considerably less than all 21 subarrays can be handled in a straight-forward manner. Conversely, a least squares wavefront is affected by incompleteness of arrival time data.

On the other hand, the wavefront method promises certain advantages, one of which is convenience. If this method can be used, then adjustments to be made in the LASA system steering delays, as a result of a particular received

event, need not wait for completion of a world seismic network analysis. Second, the argument can be made that location information, no matter how accurately determined, should, if possible, be separated from the other problem of providing the best possible steering delays. What an array really measures is not event location but horizontal phase velocity, which is used in the wavefront method. Finally, the wavefront method removes the relatively large weight given by the conventional method to the reference subarray LA0; the wavefront method can treat all elements with equal weight, whereas the current method requires a reference subarray for best results.

The following questions should be answered as a result of wavefront analysis of these and other events received at LASA.

1. If processed events are grouped according to azimuth and inverse phase velocity, and the array is then steered for plane waves corrected by the average deviation from the plane at each subarray for the group of events, will the resulting steering errors be comparable to the corresponding errors incurred when the Jeffreys-Bullen Tables are used as a reference?

2. Can the residuals (deviations from plane) be significantly reduced by iterating with a curvature correction based on an approximate knowledge of curvature dependence on range?

3. Alternatively, can a meaningful measurement of wavefront curvatures be made by using the quadratic wavefront part of the Least Squares Wavefront (LSWF) program?

4. If so, what is the behavior of the curvatures of such quadratic fitting surfaces (arrival time as a quadratic function of array horizontal position coordinates)? Are these curvatures better behaved functions of event location when calculated in and perpendicular to the range direction rather than arbitrarily placed in East-North coordinates? How is their apparent behavior affected by plotting them against inverse velocity rather than actual range? What is the variation of curvature from geographic region to region? Can a trend, beyond just an average bias value of the curvatures, be identified within a region? How badly is the fit of a wavefront's deviations to the average deviations for a group degraded, as the number of subarrays used to determine the wavefront is made significantly less than that used for the rest of the group?

5. Can subarray beams be steered with sufficient accuracy by using time delays corresponding to plane waves? If so, can the same plane wave be used for all subarrays for an event, or are local variations of horizontal phase speed and azimuth over the array so great as to lead to unacceptable subarray steering losses?

3-9

6.   Can thresholding be used, under some circumstances, to obtain arrival time data from incoming events?

Initial conclusions for some of these questions are discussed in Section 3.4.6.

3.4.2   Data Used for Organization Study

A complete set of answers to the above questions requires the availability of a large set of arrival times for seismic events from various regions of the earth. Particularly for the fifth group of questions concerning subarray delay analysis, such arrival times should be known for a significant number of events for all the seismometers in several, if not all, of the subarrays. This information will be easily available only when a large number of received events can be directly processed to obtain the arrival times on the required seismometers. Such events might include particularly strong events (magnitude 6 or over) which have been thresholded and a collection of the more frequent smaller events on which times can hopefully be obtained by correlation processing. Results discussed in the present report are based mainly on optically read arrival time data which has been made available by Seismic Data Laboratories (SDL) of Teledyne Industries, Inc., and the VELA Seismological Center (Air Force Technical Application Center), Alexandria, Virginia.

Several hundred event arrivals were made available in their original form by SDL. These events are part of the Earth Sciences Division (ESD) of Teledyne Industries, Inc. file ranging from Event ESD No. 1 to Event ESD No. 353, and covering several geographic regions. Chiburis of SDL developed this data for the Jeffreys-Bullen analysis.

3.4.3   Least Squares Plane and Quadratic Wavefront Program

This program accepts as inputs the positions, arrival times, and computation weights of up to 25 seismometers (or subarray beams), and calculates three different least squares wavefronts with the actual arrival time deviations from the best fits.

The three fits are a

1. Best-fitting plane wavefront

2. Best-fitting plane wavefront followed by an adjustment of arrival times to consider the expected effect of range upon wavefront curvature, with the above process repeated for any desired number of iterations.

3. A best-fitting quadratic wavefront plus the three derived second derivatives or curvatures, expressed in array coordinates, range coordinates, and the principal coordinates of the quadratic surface.

A description of this and other programs is in Section 4.

Figure 3-4 is a typical computer output for the least squares wavefront analysis of an event arrival. The top five lines are input quantities including run number, world network PDE event identification data, and the ESD number designated for the event. The sixth line gives the inputted coefficients R0, R1, R2, and R3 of a cubic polynomial used to estimate the event range from the computed value of inverse phase speed. RE is the assumed earth radius, and NIT is the number of iterations of range corrections (item 2 above).

The main tabular output shows the seismometer (or subarray center) designation by number (K) and site name (B1, etc.). W is the weight associated with the site in the least squares calculation, while X, Y, and T are the site location (km) and arrival time (sec.) referred to an arbitrary reference point and time (with average values shown in the last line). T-TBAR and TN are the arrival time less the average arrival time, and the modified arrival time after NIT iterations of range correction, respectively. The three columns of DELTAT denote deviations of actual arrival times from the best-fitting plane wavefront, the plane wavefront after NIT iterations of range correction, and the best-fitting quadratic wavefront, respectively. The last time in the DELTAT columns represents the standard deviation of the deviations (SIGMA).

The first three columns at the bottom of the page show the values of inverse velocity components U and V (denoted by Ux and Uy elsewhere in this report), the inverse velocity magnitude W (elsewhere called U), and azimuth AZI, as well as a range estimate, R, based on the cubic polynomial in W previously described. The first column contains the quantitative results from the plane wavefront calculation; the second shows the result after NIT iterations of range correction; and the third gives the corresponding linear coefficients,

QUADRATIC AND LINEAR WAVEFRONT RUN NUMBER 10
KOMANDORSKY   1   LAT.=54.9N   LONG.=165.8E
1/16/66   19:44:39.5   MAG.= 5.6   DEPTH = 15 KM
RANGE = 5859   AZIMUTH = 313   ESD NO.= 125
(C-COMPRESSION   D-DILATATION)
RO = 13528.000   R1 = -46116.000   R2 = -1000000.000   R3 = 0.0   RE = 6370.000   NIT = 5

K	W	X	Y	T	T-TBAR	DELTA T (PLANE)	TN	DELTA TN (PLANE)	DELTA T (QUAD)	SITE
1	1.00	9.825	7.072	55.600	0.262	0.1106	55.599	0.1126	0.0256	B1
2	1.00	4.425	-6.022	55.900	0.562	0.0729	55.900	0.0753	-0.0150	B2
3	1.00	-6.966	-3.273	55.250	-0.088	0.0920	55.250	0.0938	0.0059	B3
4	1.00	-1.419	8.585	55.000	-0.338	0.1164	55.000	0.1188	0.0368	B4
5	1.00	7.157	17.016	55.100	-0.238	0.1904	55.099	0.1920	0.1192	C1
6	0.0	15.860	-2.069	0.0	-55.338	-56.1933	0.000	-56.1907	-56.2831	C2
7	1.00	-2.181	-12.723	56.000	0.662	0.1836	56.000	0.1853	0.0992	C3
8	1.00	-11.646	5.126	54.600	-0.738	0.0475	54.600	0.0499	-0.0319	C4
9	0.0	25.642	16.676	0.0	-55.338	-55.8078	-0.003	-55.8080	-55.8875	D1
10	0.0	16.008	-20.660	0.0	-55.338	-57.0460	0.002	-57.0420	-57.1192	D2
11	1.00	-19.967	-14.761	55.000	-0.338	-0.0597	54.998	-0.0603	-0.1417	D3
12	1.00	-10.757	28.040	53.550	-1.788	-0.0027	53.551	0.0012	-0.0361	D4
13	1.00	12.810	51.881	53.450	-1.888	-0.1438	53.444	-0.1465	-0.1065	E1
14	1.00	65.344	-19.455	59.400	4.062	0.0528	59.407	0.0627	-0.0058	E2
15	1.00	-9.296	-59.941	57.550	2.212	-0.0743	57.544	-0.0792	-0.0334	E3
16	1.00	-52.830	8.091	52.450	-2.888	-0.0009	52.452	0.0023	-0.0536	E4
17	1.00	78.874	76.185	55.550	0.212	-0.0932	55.505	-0.1329	-0.0005	F1
18	1.00	55.964	-86.592	61.650	6.312	-0.3030	61.676	-0.2751	-0.0137	F2
19	1.00	-65.386	-79.613	55.780	0.442	-0.0605	55.741	-0.1002	0.0383	F3
20	1.00	-55.392	80.508	48.750	-6.588	-0.2847	48.774	-0.2580	0.0434	F4
21	1.00	0.0	0.0	55.500	0.162	0.1582	55.500	0.1604	0.0715	A0
SUMWT 18.00	AVG	-0.080	0.007	55.335		SIGMA 0.1403		0.1386	0.0636	

	PLANE	PLANE ITER.	QUADRATIC
U	0.047755	0.047735	0.047992
V	-0.045485	-0.045503	-0.045870
W	0.065950	0.065948	0.066387
R	6137.230469	6137.613281	6059.191406
AZI	313.605	313.628	313.705

QUADRATIC PARAMETERS
P = 55.4244
ALPHA = -0.000002908
BETA = 0.000008667
GAMMA = -0.000043920

2D TIME DERIVATIVES-R/AZI
RANGE = -0.000062292
AZIMUTH = -0.000031365
RANGE-AZI = 0.000041753

2D TIME DERIV - PRINCIPAL
NEAREST R = -0.000091353
NEAREST A = -0.000002304
AZIPRINC-AZI = 34.84

END OF JOB

Figure 3-4. Least Squares Wavefront Analysis of an Event Arrival

assuming a least squares quadratic or second-order wavefront. In the quadratic parameters column, P is the time to be subtracted from the arrival times to get to the t = 0 intercept of the quadratic surface at X = Y = 0; whereas, α, β, and γ are the coefficients of X^2, 2XY, and Y^2 in the polynomial describing the quadratic surface. When the XY coordinate system is rotated into range-azimuth directions, the first-order range coefficient becomes W, the first-order azimuth coefficient becomes zero, and the second-order coefficients assume the values shown in the column labeled 2D TIME DERIVATIVES-R/AZI. The last column gives the second derivative relative to principal directions and the angle between the principal and the range directions.

3.4.4 Numerical Results

The following paragraphs present some numerical results of the time-of-arrival data organization study.

3.4.4.1 Wavefront Deviation From Ideal

In processing the preliminary subarray center arrival times of several hundred events received from the Seismic Data Laboratory, the standard deviation (in seconds) of the deviation of actual arrivals from the least squares plane wavefront was typically on the order of 0.2 seconds. A wavefront analysis was performed for three regions (reference 4) for which most of the arrival times were available. The three regions are Kamchatka-Komandorsky, Kurile Islands-Sea of Okhotsk, and the Fiji Islands.

Detailed results of the time deviation analysis are shown in figures 3-5, 3-6, and 3-7, which are direct printouts of the Seismic Steering Delay Anomalies program.

At the top of the page are the ESD numbers and event regions. The line of numbers from 1 to 21 represents subarray numbers for the time anomalies appearing directly under them. The average deviation AVG (from a plane, rather than quadratic, wavefront) at each subarray for the events used is found on the next level down. The deviation averages are followed by SIG, their standard

SEISMIC STEERING DELAY ANOMALIES
11 WAVE FRONTS WITH COMMON SEISMOMETERS   21 SUBARRAYS.   ALL WEIGHTS ARE # 1.00

DELAYS DELTAIC WERE USED.

THE FOLLOWING WAVEFRONTS WERE USED:
```
ESD EVENT NO-# 125   KOMANDORSKY           125 0
ESD EVENT NO-# 51    KAMCHATKA              51 0
ESD EVENT NO-# 40    KAMCHATKA              40 0
ESD EVENT NO-# 208   KAMCHATKA             208 0
ESD EVENT NO-# 346   E. C. KAMCHATKA       346 0
ESD EVENT NO-# 159   EAST COAST KAMCHATKA  159 0
ESD EVENT NO-# 82    KAMCHATKA              82 0
ESD EVENT NO-# 320   E. C. KAMCHATKA 2     320 0
ESD EVENT NO-# 319   E. C. KAMCHATKA 1     319 0
ESD EVENT NO-# 144   KAMCHATKA CST         144 0
ESD EVENT NO-# 131   KAMCHATKA             131 0
```

```
                  1      2      3      4      5      6      7      8      9     10     11     12     13     14     15     16     17     18     19     20     21

AVG             0.004  0.115  0.105  0.065  0.090  0.031  0.108  0.097 -0.085 -0.028  0.040  0.042 -0.139  0.070 -0.076  0.045 -0.095 -0.212 -0.099 -0.210  0.147
AVG
SIG             0.049  0.056  0.032  0.047  0.048  0.050  0.037  0.040  0.039  0.029  0.051  0.083  0.062  0.043  0.067  0.042  0.021  0.044  0.058  0.031  0.033
SIG

WAVEFRONT WEIGHT # 1.00            SIGMA # 0.06            LOSS OF 0.56 DB AT 1.00 CPS.
1   0.11 -0.04 -0.01  0.05  0.10  0.06 -0.00 -0.05 -0.10 -0.05  0.00 -0.05  0.00 -0.05  0.04 -0.07  0.01

WAVEFRONT WEIGHT # 1.00            SIGMA # 0.04            LOSS OF 0.27 DB AT 1.00 CPS.
2  -0.05 -0.05 -0.01 -0.03 -0.04 -0.04  0.05 -0.02 -0.01  0.04  0.00 -0.02 -0.03 -0.01 -0.06  0.0  -0.03  0.06 -0.01 -0.05

WAVEFRONT WEIGHT # 1.00            SIGMA # 0.04            LOSS OF 0.34 DB AT 1.00 CPS.
3   0.0   0.0   0.0   0.0   0.0   0.02 -0.05 -0.02 -0.03  0.0  0.11  0.0  0.04  0.0  0.03  0.03

WAVEFRONT WEIGHT # 1.00            SIGMA # 0.03            LOSS OF 0.16 DB AT 1.00 CPS.
4  -0.04  0.04 -0.01 -0.02 -0.02 -0.03 -0.04 -0.03 -0.01 -0.04  0.0  -0.02  0.02 -0.02  0.04  0.0  0.03  0.02  0.03 -0.05

WAVEFRONT WEIGHT # 1.00            SIGMA # 0.07            LOSS OF 0.90 DB AT 1.00 CPS.
5  -0.01 -0.07 -0.01  0.0   0.04 -0.05  0.0  0.04 -0.05  0.0 -0.15  0.16  0.0  0.09  0.08  0.06  0.01 -0.01  0.01

WAVEFRONT WEIGHT # 1.00            SIGMA # 0.09            LOSS OF 1.26 DB AT 1.00 CPS.
6   0.03  0.04  0.04  0.01  0.0   0.0 -0.05  0.07 -0.04  0.03  0.03  0.05  0.03 -0.12 -0.02  0.02

WAVEFRONT WEIGHT # 1.00            SIGMA # 0.04            LOSS OF 0.26 DB AT 1.00 CPS.
7   0.0   0.0   0.0   0.0   0.0   0.0  0.07 -0.05  0.01  0.02  0.18  0.05 -0.15 -0.01  0.0  0.0  0.10  0.04  0.02

WAVEFRONT WEIGHT # 1.00            SIGMA # 0.03            LOSS OF 0.20 DB AT 1.00 CPS.
8  -0.02 -0.03  0.02  0.03  0.02  0.0   0.03  0.04  0.01  0.08  0.04 -0.04 -0.03 -0.00  0.00 -0.01 -0.01  0.00

WAVEFRONT WEIGHT # 1.00            SIGMA # 0.03            LOSS OF 0.20 DB AT 1.00 CPS.
9   0.00  0.01 -0.05  0.03 -0.04 -0.04 -0.02 -0.04  0.04  0.03  0.02 -0.02 -0.02  0.04 -0.04 -0.03 -0.03  0.00 -0.04  0.03  0.04
```

Figure 3-5. Kamchatka Region Event Anomalies (Sheet 1 of 2)

```
WAVEFRONT HEIGHT = 1.00    SIGMA = 0.04    LESS OF 0.26 DB AT 1.00 CPS.
10 -0.04 -0.01 -0.03 -0.11 -0.03  0.04 -0.04  0.01 -0.02 -0.00  0.01 -0.02 -0.01  0.03 -0.00 -0.02 -0.00  0.02

WAVEFRONT HEIGHT = 1.00    SIGMA = 0.04    LESS OF 0.23 DB AT 1.00 CPS.
11 -0.06  0.05  0.05  0.01 -0.04 -0.02  0.06 -0.02  0.0  0.0 -0.07  0.03  0.02  0.02 -0.05 -0.06 -0.01 -0.05
```

AVERAGE SIGMA = .047

Figure 3-5. Kamchatka Region Event Anomalies (Sheet 2 of 2)

SEISMIC STEERING DELAY ANOMALIES
25 WAVE FRONTS WITH COMMON SEISMOMETERS   21 SUBARRAYS.   ALL WEIGHTS ARE = 1.00

DELAYS DELTAO WERE USEC.

THE FOLLOWING WAVEFRONTS WERE USED:
ESC EVENT NO.= 10001   KURILE
ESC EVENT NO.= 324   KURILE
ESC EVENT NO.= 81   KURILE IS
ESC EVENT NO.= 70   KURILE IS
ESC EVENT NO.= 10   KURILE IS
ESC EVENT NO.= 160   KURILE
ESC EVENT NO.= 4   NO OF KURILE IS
ESC EVENT NO.= 20   KURILE - A
ESC EVENT NO.= 24   KURILE IS
ESC EVENT NO.= 45   KURILE IS
ESC EVENT NO.= 210   KURILE
ESC EVENT NO.= 231   KURILE IS.
ESC EVENT NO.= 73   OKHLTSK
ESC EVENT NO.= 187   KURILE
ESC EVENT NO.= 41   KURILE IS
ESC EVENT NO.= 10003   KURILE
ESC EVENT NO.= 74   KURILE
ESC EVENT NO.= 10002   KURILE
ESC EVENT NO.= 79   KURILE
ESC EVENT NO.= 11   KURILE IS
ESC EVENT NO.= 100   KURILE IS.
ESC EVENT NO.= 56   KURILE IS
ESC EVENT NO.= 311   KURILE IS.
ESC EVENT NO.= 117   KURILE IS.
ESC EVENT NO.= 206   KURILE

	1	2	3	4	5	6	7	8	9	10	11	12	13	14	15	16	17	18	19	20	21
AVC	-0.011	0.154	0.054	0.033	0.075	0.053	0.172	0.065	-0.055	-0.051	0.043	0.122	-0.175	0.107	-0.147	0.104	-0.103	-0.204	-0.125	-0.206	0.107
SIC	0.053	0.058	0.038	0.047	0.060	0.038	0.037	0.040	0.045	0.058	0.051	0.059	0.065	0.055	0.060	0.051	0.030	0.062	0.051	0.067	0.037

WAVEFONT WEIGHT = 1.00   SIGMA = 0.07   LCSS CF 0.74 CB AT 1.00 CPS.
1 -0.07 0.05 0.07 0.00 0.05 -0.03 0.03 0.01 0.01 0.00 -0.10 0.16 0.06 0.06 -0.01 -0.01 -0.04 -0.08 0.04 -0.12 -0.03

WAVEFONT WEIGHT = 1.00   SIGMA = 0.06   LCSS CF 0.70 CB AT 1.00 CPS.
2 0.06 0.11 0.02 0.03 0.02 -0.02 0.03 0.03 0.01 0.14 0.01 -0.01 0.02 -0.03 -0.06 -0.13 -0.01 0.0 0.04 -0.10 -0.01

WAVEFONT WEIGHT = 1.00   SIGMA = 0.05   LCSS CF 0.44 DB AT 1.00 CPS.
3 0.0 0.0 0.0 0.0 0.03 0.04 0.0 0.05 -0.03 -0.06 -0.02 0.02 0.01 -0.07 0.0 0.03 0.00 0.0 -0.10 0.10 -0.00

WAVEFONT WEIGHT = 1.00   SIGMA = 0.04   LCSS CF 0.28 CB AT 1.00 CPS.
4 0.0 0.0 0.05 -0.00 0.03 0.03 0.0 0.00 0.00 -0.05 -0.03 -0.10 0.02 0.03 -0.05 0.0 -0.04 0.06 -0.00 0.01

WAVEFONT WEIGHT = 1.00   SIGMA = 0.04   LCSS CF 0.30 CB AT 1.00 CPS.
5 0.08 -0.08 -0.08 0.03 -0.05 0.03 -0.02 0.05 -0.02 0.00 -0.02 -0.01 -0.01 -0.01 -0.04 -0.03 -0.00 0.05 0.01 0.01 -0.01

WAVEFONT WEIGHT = 1.00   SIGMA = 0.04   LCSS CF 0.33 CB AT 1.00 CPS.
6 -0.02 -0.12 -0.02 -0.01 0.04 -0.04 -0.04 0.04 0.04 0.01 0.01 -0.04 0.02 0.04 0.10 -0.02 0.03 -0.04 0.03 -0.03 0.01

Figure 3-6. Kurile Islands Region Event Anomalies (Sheet 1 of 3)

Figure 3-6. Kurile Islands Region Event Anomalies (Sheet 2 of 3)

WAVEFRONT HEIGHT = 1.00   SIGMA = 0.04   LOSS OF 0.26 DB AT 1.00 CPS.
23 0.03 0.02 0.04 -0.06 -0.06 0.04 -0.05 0.02 0.01 0.00 0.00 -0.01

WAVEFRONT HEIGHT = 1.00   SIGMA = 0.04   LOSS OF 0.27 DB AT 1.00 CPS.
24 -0.00 -0.01 0.00 -0.04 -0.02 0.05 0.01 0.00 -0.10 0.00 0.04 0.01 0.05 0.01 -0.04 0.03 0.01

WAVEFRONT HEIGHT = 1.00   SIGMA = 0.04   LOSS OF 0.25 DB AT 1.00 CPS.
25 0.05 -0.01 -0.05 0.0 -0.03 0.02 -0.01 0.02 0.0 0.01 0.07 0.04 0.02 -0.03 -0.03 -0.05 0.06 -0.00

AVERAGE SIGMA = .0516

Figure 3-6. Kurile Islands Region Event Anomalies (Sheet 3 of 3)

SEISMIC STEERING DELAY ANOMALIES
17 WAVE FRONTS WITH COMMON SEISMOMETERS   21 SUBARRAYS.   ALL WEIGHTS APF = 1.00

DELAYS DELTATO WERE USED.

THE FOLLOWING WAVEFRONTS WERE USED:

ESO EVENT NO.=	39	FIJI IS
ESO EVENT NO.=	68	FIJI IS
ESO EVENT NO.=	69	FIJI IS
ESO EVENT NO.=	80	FIJI IS.
ESO EVENT NO.=	85	FIJI IS.
ESO EVENT NO.=	90	FIJI IS.
ESO EVENT NO.=	91	FIJI IS.
ESO EVENT NO.=	92	FIJI IS.
ESO EVENT NO.=	127	FIJI IS.
ESO EVENT NO.=	137	FIJI IS
ESO EVENT NO.=	142	FIJI IS
ESO EVENT NO.=	171	FIJI IS
ESO EVENT NO.=	209	FIJI IS
ESO EVENT NO.=	247	FIJI IS
ESO EVENT NO.=	266	FIJI IS
ESO EVENT NO.=	334	SO. FIJI IS.
ESO EVENT NO.=	342	FIJI IS.

	1	2	3	4	5	6	7	8	9	10	11	12	13	14	15	16	17	18	19	20	21
AVG	0.180	-0.035	0.123	0.269	0.165	-0.043	0.067	0.248	0.153	-0.140	0.045	-0.069	-0.087	-0.190	-0.134	0.114	0.065	-0.252	-0.004	-0.557	0.214
SIG	0.032	0.115	0.032	0.059	0.064	0.044	0.053	0.061	0.068	0.049	0.057	0.044	0.069	0.086	0.076	0.084	0.062	0.100	0.040	0.082	0.048

WAVEFRONT WEIGHT = 1.00   SIGMA = 0.07   LOSS OF 0.83 DB AT 1.00 CPS.
1 0.0 0.0 0.0 0.0 0.0 0.0 -0.03 0.03 0.12 -0.04 -0.01 0.0 0.0 0.0 0.11 0.03 0.0 -0.11 0.02 0.05 0.07

WAVEFRONT WEIGHT = 1.00   SIGMA = 0.06   LOSS OF 0.52 DB AT 1.00 CPS.
2 0.0 0.0 0.0 -0.12 0.10 0.06 0.01 -0.02 -0.04 0.03 0.04 -0.05 0.0 -0.03 0.02 -0.02 -0.07 0.03 -0.02 -0.07 -0.06

WAVEFRONT WEIGHT = 1.00   SIGMA = 0.05   LOSS OF 0.35 DB AT 1.00 CPS.
3 0.0 0.0 0.0 0.04 0.0 0.05 0.05 0.0 0.04 0.0 0.07 -0.03 0.03 -0.01 -0.03 0.01 0.04 -0.03 0.07 0.07 0.04

WAVEFRONT WEIGHT = 1.00   SIGMA = 0.09   LOSS OF 1.57 DB AT 1.00 CPS.
4 0.0 0.0 0.0 0.04 0.0 0.01 -0.09 -0.05 0.02 -0.09 -0.06 -0.06 0.04 -0.18 0.0 0.01 0.11 0.0 0.0 0.22 -0.01

WAVEFRONT WEIGHT = 1.00   SIGMA = 0.07   LOSS OF 0.75 DB AT 1.00 CPS.
5 0.0 0.0 0.0 0.14 0.0 0.03 0.06 0.05 0.05 0.0 0.06 0.0 0.10 -0.05 -0.07 0.07 0.02 0.02 -0.02 -0.08 0.00

WAVEFRONT WEIGHT = 1.00   SIGMA = 0.05   LOSS OF 0.45 DB AT 1.00 CPS.
6 0.0 0.0 0.0 0.05 0.03 -0.03 0.03 0.0 0.06 0.00 0.05 0.03 -0.08 -0.06 0.02 0.08 0.06 -0.05 -0.01 -0.10 0.01

WAVEFRONT WEIGHT = 1.00   SIGMA = 0.08   LOSS OF 1.03 DB AT 1.00 CPS.
7 0.0 0.0 0.0 -0.03 -0.03 0.10 0.15 0.0 0.0 0.0 0.12 0.0 0.09 0.03 3.07 0.11 0.05 0.04 -0.03 0.07 -0.00

WAVEFRONT WEIGHT = 1.00   SIGMA = 0.14   LOSS OF 3.24 DB AT 1.00 CPS.
8 0.0 0.0 0.0 -0.05 -0.13 -0.03 -0.03 -0.13 -0.13 -0.05 -0.09 0.0 0.0 0.0 0.0 -0.28 -0.13 0.27 0.00 0.0 -0.12

Figure 3-7. Fiji Islands Region Event Anomalies (Sheet 1 of 2)

WAVEFRONT WEIGHT = 1.00   0.0   0.01 -0.04
SIGMA = 0.04   0.0   0.0 -0.01 -0.01
LOSS OF 0.39 DB AT 1.00 CPS.   0.0   0.02   0.00   0.11   0.01   0.0   0.02   0.08 -0.04   0.02   0.03   0.06

WAVEFRONT WEIGHT = 1.00   0.05   0.11 -0.02 -0.01
SIGMA = 0.06 -0.05 -0.01 -0.03
LOSS OF 0.57 DB AT 1.00 CPS.   0.10 -0.01   0.10 -0.01   0.04 -0.05 -0.05 -0.03 -0.10 -0.04 -0.09   0.01

WAVEFRONT WEIGHT = 1.00   0.01   0.08   0.03 -0.03
SIGMA = 0.04   0.09   0.01 -0.01
LOSS OF 0.27 DB AT 1.00 CPS.   0.05   0.0 -0.02   0.0   0.04   0.0   0.03 -0.06 -0.00 -0.01   0.02 -0.00 -0.05 -0.02   0.0

WAVEFRONT WEIGHT = 1.00 -0.01 -0.05 -0.01 -0.02
SIGMA = 0.03   0.06 -0.01 -0.02
LOSS OF 0.16 DB AT 1.00 CPS.   0.02 -0.00 -0.01 -0.06 -0.02 -0.04 -0.03   0.00 -0.02   0.02 -0.05   0.00

WAVEFRONT WEIGHT = 1.00 -0.02   0.09 -0.02 -0.03
SIGMA = 0.05   0.0 -0.04
LOSS OF 0.44 DB AT 1.00 CPS.   0.04   0.03   0.05   0.0 -0.07 -0.02 -0.03 -0.05 -0.08 -0.06 -0.05   0.03

WAVEFRONT WEIGHT = 1.00 -0.01 -0.02 -0.01 -0.01
SIGMA = 0.03   0.02 -0.05 -0.03
LOSS OF 0.13 DB AT 1.00 CPS.   0.02 -0.00 -0.07 -0.01   0.02 -0.00   0.0   0.01   0.02 -0.05 -0.02 -0.00   0.01

WAVEFRONT WEIGHT = 1.00   0.02 -0.29 -0.07   0.0
SIGMA = 0.14 -0.08 -0.08   0.04
LOSS OF 3.26 DB AT 1.00 CPS.   0.0 -0.12 -0.05   0.0 -0.14   0.25   0.18 -0.09 -0.06   0.21 -0.08 -0.09

WAVEFRONT WEIGHT = 1.00 -0.04 -0.02 -0.01 -0.00
SIGMA = 0.04   0.00 -0.02 -0.03
LOSS OF 0.29 DB AT 1.00 CPS.   0.00 -0.03 -0.02   0.0 -0.03   0.08 -0.11   0.06 -0.01 -0.02   0.07 -0.04 -0.02

WAVEFRONT WEIGHT = 1.00   0.02 -0.01
SIGMA = 0.03 -0.00 -0.01 -0.03
LOSS OF 0.14 DB AT 1.00 CPS.   0.00 -0.06 -0.00 -0.01   0.00   0.02 -0.00 -0.05   0.03 -0.01 -0.02 -0.04   0.04

END OF JOB

AVERAGE SIGMA

N = 17   .063
N = 15 (all except 8 and 15) .053

Figure 3-7. Fiji Islands Region Event Anomalies (Sheet 2 of 2)

3-20

deviation per subarray. The remainder of the page consists of a two-line output for each event or wavefront in the same event order used at the top of the page. The first line gives the weight applied to a specific wavefront in forming the averages, the standard deviation for the wavefront of the difference between deviation and average deviation for the region or group of events, and finally the steering loss in dB incurred at 1.0 Hz for that standard deviation value. The second line gives the event number and the difference at each seismometer (1 through 21) between the actual deviation from the plane and the average deviation for the region.

As an example of the use to be made of these outputs, consider the Fiji Islands group of events. In these two events, ESD Numbers 92 and 266, stood out as having large anomalies from the rest of the data. Their steering loss was over 3dB at 1 Hz, compared to under 1 dB for all the rest. In event 92, the subarray readings which appear to be responsible for the large sigma are subarrays 16 and 18; whereas, in 266 they are 2, 14, and to an extent 18. It is of interest that in the Jeffreys-Bullen analysis of SDL data, event number 92 does not show an especially large value of Shock Sigma. Thus, it appears anomalous when viewed by one method of analysis, and normal when viewed by the other. Figure 3-8 repeats the averaging for the Fiji Island group of events, assigning zero weight to the two seemingly offending events. This figure shows how, as a result, the losses for the anomalous events go to over 4 dB; whereas, steering to the remainder of the group is improved slightly.

The average values of Event Sigma over all events for each region are given in Table 3-1 with the corresponding values of Shock Sigma derived in the SDL report. These values appear to be of roughly the same magnitude. Care must be exercised in comparing these values for two reasons. First, for those events using relatively few subarrays, the present Event Sigma is more optimistic than the SDL Shock Sigma. This situation results because the variance, as defined here, is $\frac{1}{N}$ times the sum of the squares of N station deviations; whereas SDL used $\frac{1}{N+1}$ times. One must also remember that the data was originally divided into the chosen regions according to the Jeffreys-Bullen

DELAYS DELTATO WERE USED.

THE FOLLOWING WAVEFRONTS WERE USED:

ESD EVENT NO.=		
ESD EVENT NO.= 39	FIJI IS	39 0
ESD EVENT NO.= 68	FIJI IS	68 0
ESD EVENT NO.= 69	FIJI IS	69 0
ESD EVENT NO.= 80	FIJI IS.	80 0
ESD EVENT NO.= 85	FIJI IS.	85 0
ESD EVENT NO.= 90	FIJI IS.	90 0
ESD EVENT NO.= 91	FIJI IS.	91 0
ESD EVENT NO.= 92	FIJI IS.	92 0
ESD EVENT NO.= 127	FIJI IS	127 0
ESD EVENT NO.= 137	FIJI IS	137 0
ESD EVENT NO.= 142	FIJI IS	142 0
ESD EVENT NO.= 171	FIJI IS	171 0
ESD EVENT NO.= 209	FIJI IS	209 0
ESD EVENT NO.= 247	FIJI IS	247 0
ESD EVENT NO.= 266	FIJI IS	266 0
ESD EVENT NO.= 334	SO. FIJI IS	334 0
ESD EVENT NO.= 342	FIJI IS.	342 0

	1	2	3	4	5	6	7	8	9	10	11	12	13	14	15	16	17	18	19	20	21
AVG	0.178	0.002	0.132	0.274	0.185	-0.034	0.066	0.263	0.165	-0.146	0.056	-0.069	-0.077	-0.208	-0.149	0.138	0.078	-0.297	0.001	-0.557	0.228
SIG	0.033	0.053	0.022	0.059	0.048	0.040	0.054	0.037	0.058	0.037	0.053	0.044	0.060	0.058	0.059	0.042	0.051	0.044	0.036	0.082	0.031

WAVEFRONT WEIGHT = 1.00   LOSS OF 0.68 DB AT 1.00 CPS.   SIGMA = 0.06

| 1 | 0.0 | 0.0 | 0.0 | 0.0 | 0.0 | 0.0 | -0.03 | 0.01 | 0.12 | -0.04 | -0.02 | 0.0 | 0.0 | 0.0 | 0.13 | 0.00 | 0.0 | -0.07 | 0.02 | 0.05 | 0.05 |

WAVEFRONT WEIGHT = 1.00   LOSS OF 0.57 DB AT 1.00 CPS.   SIGMA = 0.06

| 2 | 0.0 | 0.0 | 0.0 | -0.12 | 0.08 | 0.05 | 0.01 | -0.04 | 0.03 | 0.04 | 0.03 | -0.05 | 0.0 | -0.01 | 0.04 | -0.04 | -0.08 | 0.07 | -0.03 | 0.07 | -0.07 |

WAVEFRONT WEIGHT = 1.00   LOSS OF 0.26 DB AT 1.00 CPS.   SIGMA = 0.04

| 3 | 0.0 | 0.0 | 0.03 | 0.0 | 0.0 | -0.04 | 0.05 | 0.0 | 0.03 | 0.0 | 0.06 | -0.03 | 0.02 | 0.01 | -0.02 | -0.02 | 0.03 | 0.01 | 0.07 | 0.07 | 0.03 |

WAVEFRONT WEIGHT = 1.00   LOSS OF 1.43 DB AT 1.00 CPS.   SIGMA = 0.09

| 4 | 0.0 | 0.0 | 0.04 | 0.0 | 0.01 | -0.09 | -0.07 | 0.01 | 0.0 | -0.08 | -0.07 | -0.06 | 0.03 | -0.17 | 0.0 | -0.01 | 0.09 | 0.0 | 0.22 | -0.02 | |

WAVEFRONT WEIGHT = 1.00   LOSS OF 0.64 DB AT 1.00 CPS.   SIGMA = 0.06

| 5 | 0.0 | 0.0 | 0.14 | 0.0 | 0.02 | 0.06 | 0.06 | 0.03 | 0.0 | 0.06 | 0.05 | 0.0 | 0.09 | -0.03 | -0.06 | 0.04 | 0.01 | 0.06 | -0.03 | -0.08 | -0.01 |

WAVEFRONT WEIGHT = 1.00   LOSS OF 0.34 DB AT 1.00 CPS.   SIGMA = 0.04

| 6 | 0.0 | 0.0 | 0.04 | 0.01 | -0.04 | 0.05 | 0.03 | 0.05 | 0.06 | 0.01 | 0.04 | 0.03 | -0.09 | -0.04 | 0.03 | 0.05 | 0.05 | -0.02 | -0.02 | -0.10 | -0.00 |

WAVEFRONT WEIGHT = 1.00   LOSS OF 1.00 DB AT 1.00 CPS.   SIGMA = 0.08

| 7 | 0.0 | 0.0 | 0.0 | -0.05 | 0.09 | 0.15 | 0.0 | 0.0 | 0.0 | -0.02 | 0.11 | 0.0 | 0.08 | 0.04 | 0.08 | 0.08 | 0.04 | 0.08 | -0.04 | 0.07 | -0.02 |

WAVEFRONT WEIGHT = 0.0   LOSS OF 4.01 DB AT 1.00 CPS.   SIGMA = 0.15

| 8 | 0.0 | 0.0 | -0.06 | -0.15 | -0.04 | -0.03 | -0.15 | -0.14 | 0.0 | -0.05 | -0.10 | 0.0 | 0.38 | 0.0 | 0.0 | -0.30 | -0.15 | 0.30 | -0.00 | 0.0 | -0.13 |

Figure 3-8. Seismic Steering Delay Anomalies (Non-Unity Weights) (Sheet 1 of 2)

3-22

```
WAVEFRONT WEIGHT =  1.00       SIGMA =  0.04       LOSS OF 0.28 DB AT 1.00 CPS.
 9   0.05 -0.07   0.00  0.0    0.0 -0.02 -0.01   -0.03  0.00  0.00    0.00   0.10  0.02  0.0  -0.01  0.07 -0.01  0.01  0.03  0.05

WAVEFRONT WEIGHT =  1.00       SIGMA =  0.06       LOSS OF 0.53 DB AT 1.00 CPS.
10   0.05  0.07  -0.03 -0.01  -0.07 -0.02 -0.03    0.07 -0.08 -0.01 -0.07   0.10  -0.02  0.06 -0.03 -0.07 -0.04 -0.07  0.04 -0.09 -0.00

WAVEFRONT WEIGHT =  1.00       SIGMA =  0.03       LOSS OF 0.17 DB AT 1.00 CPS.
11   0.01  0.05   0.02 -0.03   0.07  0.00 -0.01    0.03  0.0  -0.02  0.0    0.03  -0.07  0.02  0.00 -0.01 -0.02 -0.02 -0.03 -0.0  -0.00

WAVEFRONT WEIGHT =  1.00       SIGMA =  0.03       LOSS OF 0.12 DB AT 1.00 CPS.
12  -0.00  0.01  -0.01 -0.02   0.04 -0.02 -0.02   -0.00 -0.02 -0.01 -0.07  -0.01  -0.03 -0.02 -0.01  0.02 -0.01  0.01 -0.05 -0.01

WAVEFRONT WEIGHT =  1.00       SIGMA =  0.05       LOSS OF 0.40 DB AT 1.00 CPS.
13  -0.02  0.06   0.04 -0.02  -0.05  0.0  -0.04    0.02  0.02  0.06 -0.01  0.0   -0.08 -0.01 -0.02 -0.08 -0.09 -0.05 -0.06 -0.05  0.02

WAVEFRONT WEIGHT =  1.00       SIGMA =  0.03       LOSS OF 0.16 DB AT 1.00 CPS.
14  -0.01 -0.06  -0.02 -0.02   0.00 -0.06 -0.03   -0.02 -0.09 -0.01  0.0  -0.01   0.01  0.02  0.0  -0.01  0.01 -0.01 -0.03 -0.00  0.00

WAVEFRONT WEIGHT =  0.0        SIGMA =  0.15       LOSS OF 4.08 DB AT 1.00 CPS.
15   0.02 -0.33  -0.08  0.0   -0.10 -0.09  0.04   -0.14  0.0   0.13 -0.06  0.0  -0.15   0.26  0.19 -0.12 -0.08  0.25 -0.09  0.0  -0.10

WAVEFRONT WEIGHT =  1.00       SIGMA =  0.04       LOSS OF 0.32 DB AT 1.00 CPS.
16  -0.04 -0.06  -0.02 -0.01  -0.02 -0.03 -0.03   -0.03 -0.01 -0.03 -0.03  0.0  -0.04   0.09 -0.10  0.04 -0.02  0.02  0.06 -0.04 -0.03

WAVEFRONT WEIGHT =  1.00       SIGMA =  0.03       LOSS OF 0.12 DB AT 1.00 CPS.
17  -0.04  0.01   0.01 -0.01  -0.02 -0.02 -0.03   -0.02 -0.07  0.00 -0.03  0.00  0.01   0.01 -0.04  0.00 -0.02  0.01  0.01 -0.04  0.03

END OF JOB

AVERAGE SIGMA =  .049
```

Figure 3-8. Seismic Steering Delay Anomalies (Non-Unity Weights) (Sheet 2 of 2)

Table 3-1. Average Event Sigma and Shock Sigma

Anomalies Run Number	Region Number and Name	Number of Events	Average Event Sigma (Seconds)	Average Shock Sigma (Seconds)
19	9 Kamchatka-Komandorsky	11	0.047	0.065
20	10 Kurile Islands-Sea of Okhotsk	25	0.052	0.057
4	36 Fiji Islands Region	17	0.063	0.060
6	36 Fiji Islands Region with two anomalous events removed	15	0.053	0.057

Note: Average values over all events in a region of Event Sigma and Shock Sigma as calculated by Seismic Data Laboratory.

analysis, whereas these same regions were accepted at face value for the wavefront analysis. As shown by the data for the Fiji Islands group, an event may be a good fit to one method of analysis and a poor one to the other.

Overall, the steering errors corresponding to either method appear to be of comparable magnitude, as shown in Table 3-1.

3.4.4.2 Wavefront Curvature

From the events discussed in Section 3.4.4.1, wavefront curvatures as measured by the second derivative of the least squares quadratic wavefront surfaces were investigated. Tables 3-2 and 3-3 list the events used and their ESD numbers, as well as the parameters, P, α, β, γ, etc., as discussed in Section 3.4.3. D2R, D2A, and D2R/A represent the second derivative of time, with respect to distance referred to East-North coordinates; the next three columns refer to principal axes of the least squares surface. Range is as given by the world seismic network; W is the inverse phase velocity as determined by the quadratic fit; and ΣW_i is the sum of the weights, usually equal to the number of subarrays at which reliable arrival times were available. The curvatures were plotted, to find out whether each region possessed a measurable curvature bias, and whether the curvatures showed any noticeable trend within the regions. A bias for each region does exist, but whether a curvature trend can be established within the regions is somewhat questionable. If these estimates prove to be correct upon examination of more extensive data, the least squares plane wavefront program would seem to serve as well as the quadratic program, because curvature bias would tend to be incorporated in the average values for deviation from plane. On the other hand, between regions, the Quadratic program might still provide a useful method of interpolation.

3.4.4.3 Velocity Analysis by Subarrays

In an attempt to measure the applicability of plane wave delays at the subarray level, the LSWF program has been applied to the individual subarrays for four events. While the inverse phase velocity vector varied among the subarrays for each event, a surprising degree of correlation was found among events at each subarray.

Table 3-2. Curvatures for Wavefront Arrivals from Region 10, Kurile Islands, and Sea of Okhotsk

— Values should be multiplied by 10^{-4} —

ESD	P	α	β	γ	D2R	D2A	D2R/A	D2 near R	D2 near A	Azi Princ. Azi	Range	W(meas)	Σwi
324	21.6175	.0831	.0207	-.5357	-.4650	-.4401	.6201	-1.0727	.1676	44.43	6636	.0614	20
20	35.6286	.2100	.0020	-.5147	-.2491	-.3605	.7226	.4200	-1.029	-42.80	6806	.0600	7
10	17.6352	.2322	-.0744	-.5014	-.0778	-.4608	.7236	.4792	-1.0178	-37.59	6731	.0603	20
11	31.7217	.2590	-.0568	-.5018	-.0647	-.4209	.7483	.5264	-1.0120	-38.31	7462	.0566	12
24	54.7501	.1768	-.1593	-.5754	-.0366	-.7606	.7323	.4182	-1.2155	-31.85	6855	.0595	16
4	57.2887	.4525	-.0375	-.5835	-.1382	-.1238	1.0387	-1.1698	.9078	44.80	6759	.0592	11
41	61.8167	.2684	-.0653	-.5272	-.0484	-.4692	.7782	.5474	-1.0650	-37.44	7347	.0565	13
56	55.1199	.3346	-.0303	-.5550	-.1476	-.2933	.8887	.6712	-1.1121	-42.66	7612	.0551	19
45	16.8419	.0779	-.1032	-.5030	-.1709	-.6793	.5615	.1913	-1.0415	-32.82	6902	.0584	15
70	60.8343	.1885	-.0612	-.6120	-.2981	-.5487	.8000	.3864	-1.233	-40.55	6721	.0598	17
74	61.4232	.0477	-.0570	-.5522	-.2982	-.7107	.5747	.1061	-1.1150	-35.13	7433	.0554	11
79	37.3768	.2935	-.0503	-.5619	-.0596	-.4771	.8356	.5930	-1.1296	-37.99	7450	.0557	17
81	38.1191	.2790	.0262	-.6387	-.3944	-.3243	.9185	-1.2789	.5595	43.92	6655	.0614	14
100	50.7961	.0988	-.0184	-.4790	-.2707	-.4897	.5685	.1987	-.9591	-39.55	7570	.0556	15
117	12.0190	.3359	-.0186	-.5401	-.0790	-.3292	.8678	.6727	-1.0810	-40.90	7634	.0557	20
187	57.9175	.2097	.0130	-.5871	-.3583	-.3965	.7970	.4198	-1.1746	-44.31	7210	.0573	18
206	53.7210	.3223	-.0519	-.5304	-.0388	-.3772	.8422	.6510	-1.0670	-39.32	7678	.0552	19
210	10.7523	2.6629	3.2905	2.8482	-.4038	11.4261	-2.8909	-1.0725	12.0948	-13.02	6913	.0604	17
231	48.6578	.3568	-.0009	-.5737	-.1463	-.2873	.9278	.7137	-1.1473	-42.83	5638	.0582	21
311	38.9109	.4020	-.0250	-.6002	-.0429	-.3534	.9913	.8052	-1.2016	-40.55	7631	.0553	21
160	64.783	.2213	.0305	-.4735	-.2662	-.2381	.6974	-.9497	.4453	44.42	6753	.0599	21

NW 6600 - 7700 KM 311 - 316 AZ

Table 3-3. Curvatures for Wavefront Arrivals from Regions 9 and 36, Kamchatka-Komandorsky, and Fiji Islands

← Values should be multiplied by 10^{-4} →

ESD	P	α	β	γ	D2R	D2A	D2R/A	D2 near R	D2 near A	Azi Princ. Azi	Range	W(meas)	Σwi
40	52.42	-.2659	-.1114	-.4004	-.4504	-.8823	.1454	-.4060	-.9267	-16.98	6199	.0628	10
51	34.90	-.0469	-.0030	-.4260	-.4802	-.4655	.3791	-.8520	-.0937	44.45	5996	.0650	19
131	46.74	.1357	.0256	-.5022	-.3993	-.3336	.6391	-1.0064	.2735	43.53	6570	.0615	17
125	55.42	-.0291	.0867	-.4392	-.6229	-.3137	.4175	-.9135	-.0230	34.84	5859	.0664	18
144	63.04	.1753	.0195	-.4498	-.3018	-.2472	.6257	-.9008	.3518	43.75	6551	.0622	21
159	31.41	.0476	-.0097	-.4434	-.3656	-.4259	.4904	.0956	-.8871	-43.24	6373	.0640	18
208	51.47	.1320	-.0710	-.5004	-.2452	-.4917	.6364	.2798	-1.0166	-39.52	6299	.0634	18
319	39.80	.1314	-.0017	-.4495	-.2947	-.3416	.5804	.2627	-.8990	-43.84	6539	.0622	21
320	39.80	.1571	.0150	-.4646	-.3219	-.2931	.6222	-.9299	.3149	44.34	6534	.0622	20
346	23.23	-.2607	-.0356	-.3004	-.4927	-.6294	.0443	-.4797	-.6425	-16.47	6326	.0639	15
82	44.42	.0836	.0409	-.4715	-.4847	-.2910	.5527	-.9490	.1733	40.03	6386	.0616	12
69	40.28	-.1282	.2346	-.3954	.0093	-1.0565	.0878	.0165	-1.0636	-4.68	10117	.0412	15
68	55.36	-.3061	.1956	-.3029	-.2984	-.9196	.2377	-.2178	-1.0001	-18.71	10135	.0422	17
209	60.99	-.2525	.2202	-.5001	-.2571	-1.2482	.0984	-.2474	-1.2578	-5.61	10148	.0411	19
142	41.15	-.1272	.2325	-.4997	-.0312	-1.2227	.0073	-.0311	-1.2227	-0.35	10148	.0412	19
137	41.64	-.1494	.2565	-.4902	-.0260	-1.2531	.0543	-.0236	-1.2555	-2.53	10155	.0414	21
247	52.20	-.2115	.2403	-.3551	-.0944	-1.0388	.1695	-.0649	-1.0683	-9.88	10141	.0409	19
39	42.41	1.3164	.2883	-.5697	+.7357	-1.2423	-.3735	.8039	-1.3105	10.34	10182	.0423	11
85	58.40	-.2503	.2400	-.4425	-.1920	-1.1935	.1288	-.1757	-1.2098	-7.21	10186	.0406	15
90	62.94	-.1331	.2652	-.4992	.0109	-1.2755	.0391	.0121	-1.2767	-1.74	10205	.0415	18
92	48.59	-1.8140	-.0926	1.6688	-.9214	.6310	3.4003	-3.6330	+3.3425	38.57	10206	.0389	13
80	33.00	-.0075	.3884	-.9929	.2224	-2.2233	-.2812	.2543	-2.2553	6.48	10212	.0403	14
91	50.14	-.1096	.1938	-.3717	-.0144	-.9482	.0287	-.0136	-.9491	-1.76	10213	.0412	14
127	18.74	-.2169	.2598	-.2893	-.0407	-.9717	.2419	.0184	-1.0308	-13.73	10390	.0403	17
342	52.92	-.1118	.2301	-.4452	.0112	-1.1253	-.0124	.0114	-1.1254	0.62	10422	.0405	21
171	31.19	-.1353	.2389	-.4361	-.0072	-1.1355	.0214	-.0068	-1.1359	-1.09	10423	.0407	21
266	46.73	.1196	.0129	-.2254	.0551	-.2667	-.3062	.2401	-.4517	31.14	10441	.0401	17
334	26.31	.0846	.2134	-.5305	.2430	-1.1349	-.2932	.3028	-1.1947	11.53	10718	.0401	20

WSW 10100 - 10725, 239- 246, NW 5850 - 6600, 312 - 315

3-27

For each of the four events listed in Table 3-4—Longshot, Kamchatka, Kazakh, and Novaya—the LSWF program has been used to obtain a best-fitting plane wave for each subarray, thereby yielding 21 values for U* (one for each subarray). From a diagram of the LASA configuration, the least squares values for inverse velocity and azimuth have been listed at each subarray for each of the four events (see figures 3-9, 3-10, 3-11, and 3-12). Each set of 21 values of U has been ranked in size from largest to smallest. The four sets of ranks are shown in Table 3-5. As shown in the table, subarray D4, for example, was ranked fourth for Longshot, seventh for Kamchatka, ninth for Kazakh, and tenth for Novaya.

To determine the correlation, if any, between ranks for each pair of subarrays, a statistic known as Spearman's r is computed. The formula for r is

$$r = 1 - \frac{6\Sigma D_j^2}{N(N^2 - 1)}, \qquad (3.1)$$

where N is the number of ranks being correlated (here, N = 21), and D_j^2 is the square of the difference between ranks for subarray j for some pair of events. Since four events are being considered, there is a total of six different correlation coefficients. The six rank correlations are shown in column 1 of Table 3-6.

The statistical significance of the Spearman r may be tested by using the "t" test where the statistic t is given by the formula

$$t = r\sqrt{\frac{N-2}{1-r^2}} \qquad (3.2)$$

with N - 2 degrees of freedom. The six values of t associated with the six rank correlations are shown in column 2 of Table 3-6.

---

*$U = \sqrt{U_x^2 + U_y^2}$ The computer printout shows this as $W = \sqrt{U^2 + V^2}$.

Table 3-4. Four Events Listing

ESD Number	Date	Location	Latitude	Longitude	Magnitude
180	10/29/65	Longshot	51.44 N	179.18 E	6.1
189	2/13/66	Kazakh SSR	49.8 N	78.1 E	6.3
319	4/08/66	Near Kamchatka	51.2 N	157.7 E	5.9
—	10/27/66	Novaya	73.4 N	54.8 E	6.3
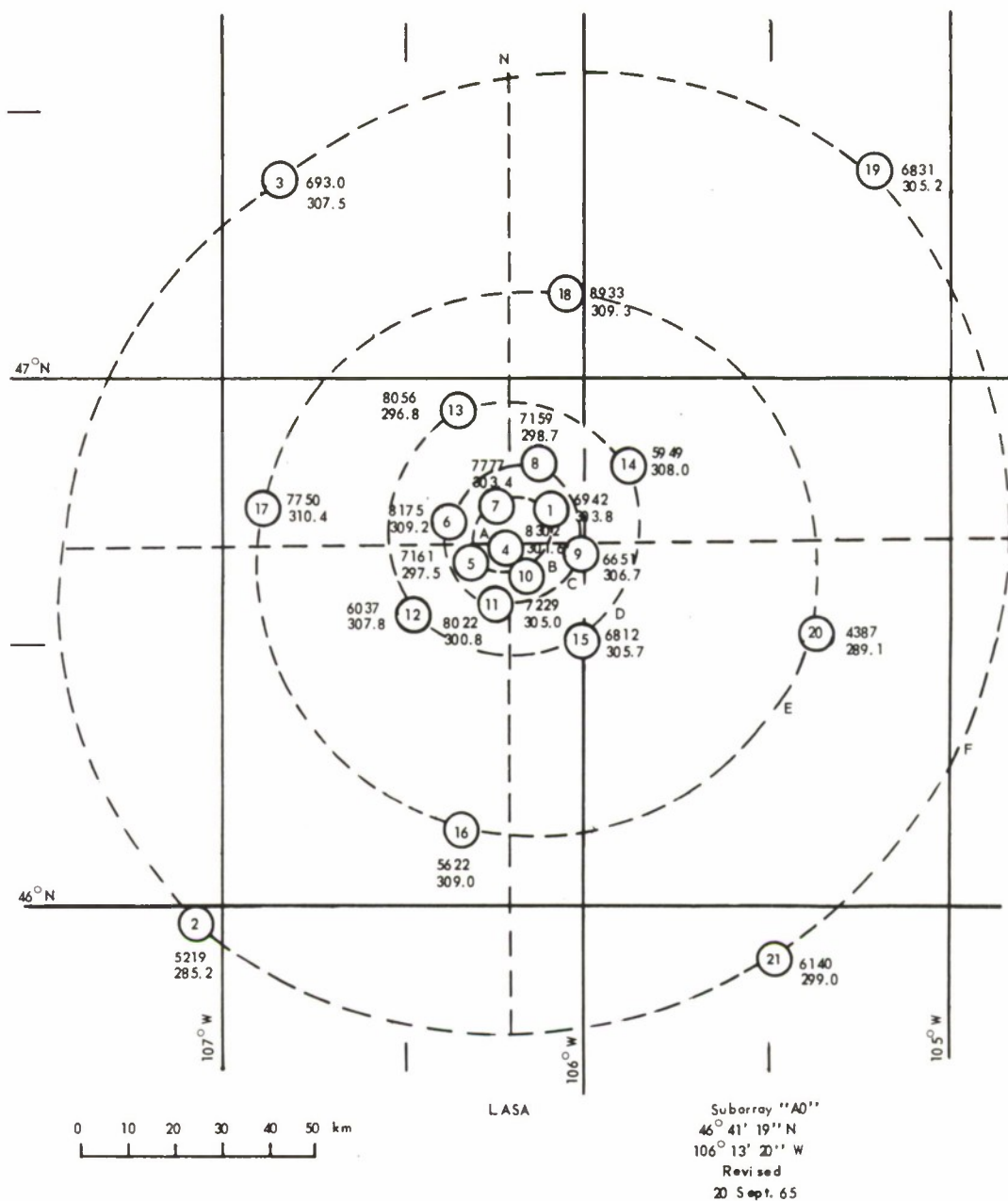
Figure 3-9. Longshot Event, Subarray Analysis
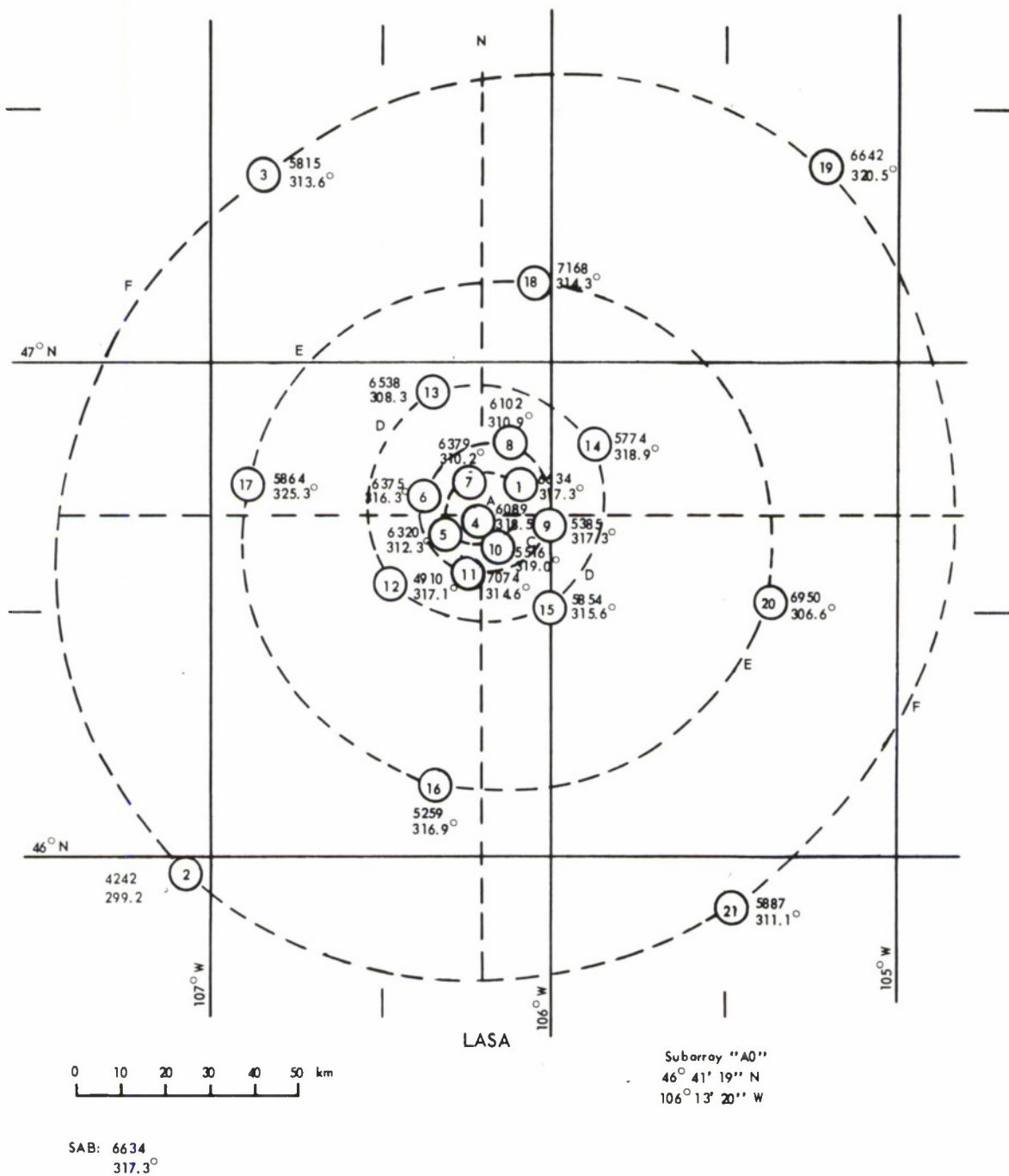
Figure 3-10. Kamchatka Event, Subarray Analysis
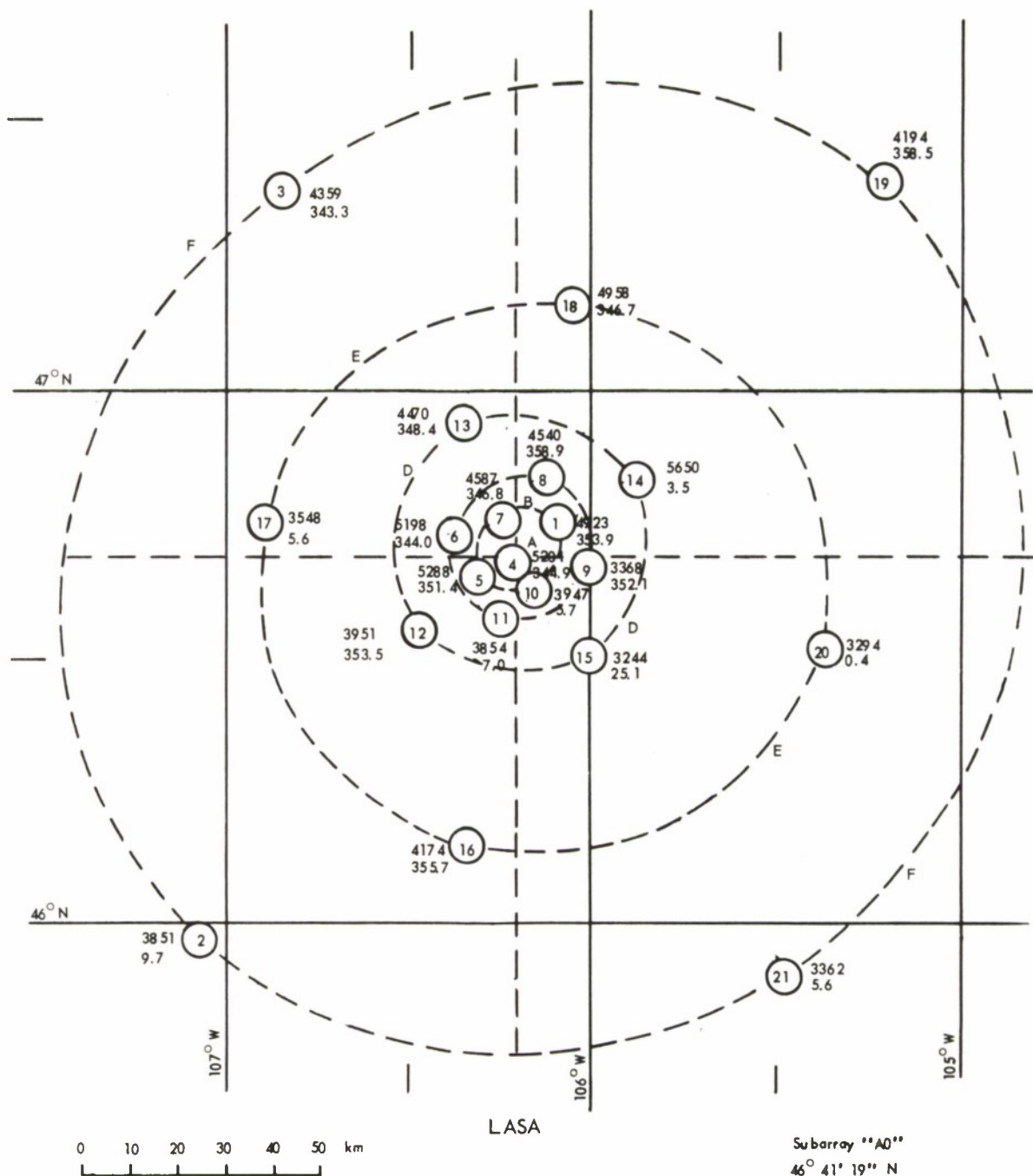
Figure 3-11. Kazakh Event, Subarray Analysis
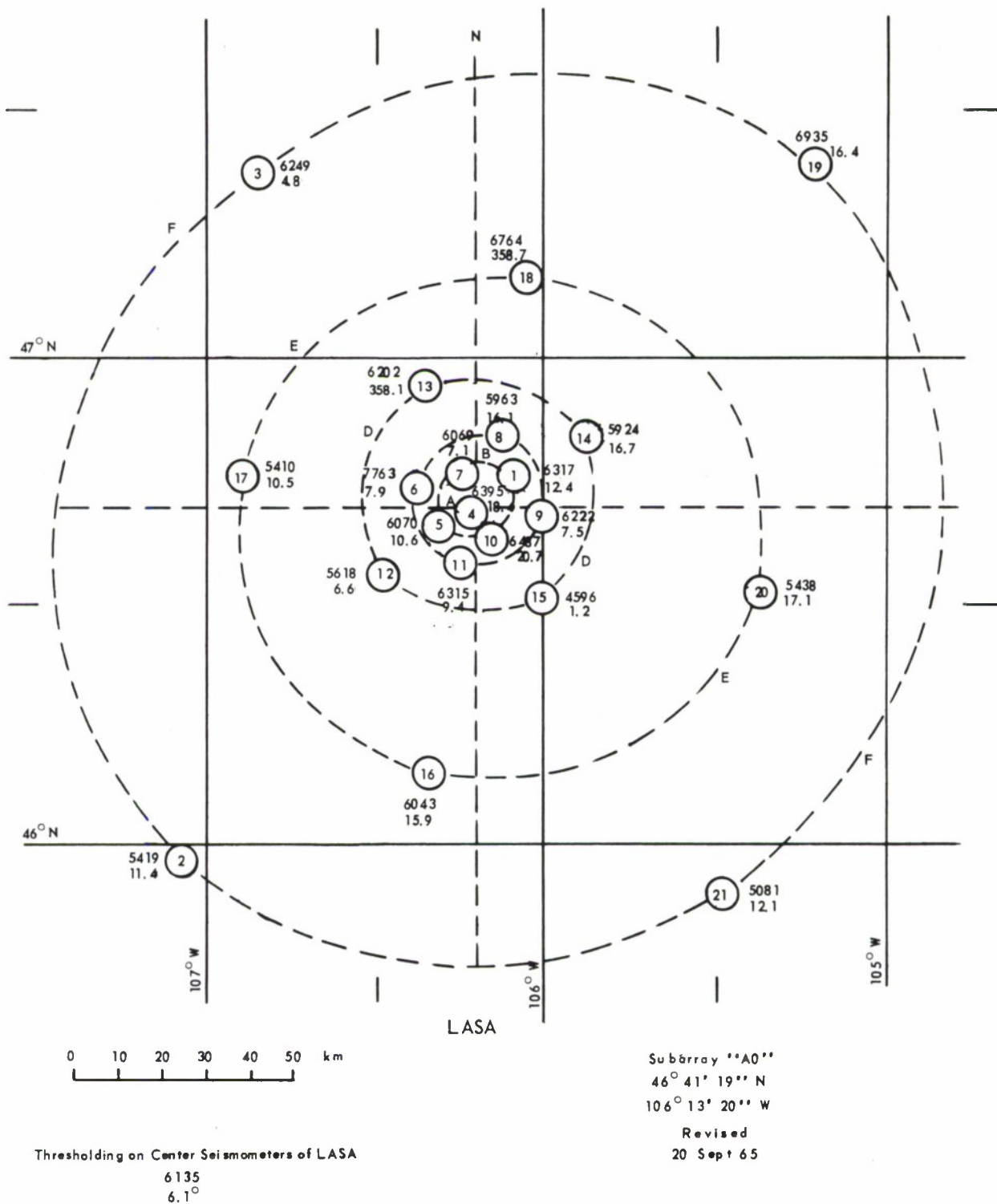
Figure 3-12. Novaya Event, Subarray Analysis

Table 3-5. Subarray Ranking According to the Value of U for the Four Events

Subarray		Longshot	Kamchatka	Kazakh	Novaya
Number	Name				
1	B1	11	6	6	6
2	F3	20	21	16	18
3	F4	12	14	10	8
4	A0	2	4	4	5
5	B3	9	9	3	11
6	C4	3	3	1	1
7	B4	6	8	7	12
8	C1	10	11	8	14
9	C2	15	18	18	9
10	B2	8	17	14	4
11	C3	5	2	15	7
12	D3	17	20	13	16
13	D4	4	7	9	10
14	D1	18	16	2	15
15	D2	14	15	21	21
16	E3	19	19	12	13
17	E4	7	13	17	19
18	E1	1	1	5	3
19	F1	13	5	11	2
20	E2	21	10	20	17
21	F2	16	12	19	20

Table 3-6. Values and Significance of Spearman's r for the Four Events

Rank Correlations	Values of t	Significance at the 5 percent level t_{95} = 2.093 for 19 degrees of freedom
r_{LK} = 0.742	t_{LK} = 4.818	Highly significant correlation between events L and K
r_{LZ} = 0.504	t_{LZ} = 2.544	Definitely significant correlation between L and Z
r_{KZ} = 0.4675	t_{KZ} = 2.305	Significant correlation
r_{YL} = 0.60909	t_{YL} = 3.3476	Highly significant
r_{YK} = 0.6013	t_{YK} = 3.2803	Highly significant
r_{YZ} = 0.5727	t_{YZ} = 3.045	Highly significant

Note: L = Longshot

      K = Kamchatka

      Z = Kazakh

      Y = Novaya

If a 5 percent level of significance is used, then, as shown in column 3 of Table 3-6, the critical value of t for N - 2 = 19 degrees of freedom is t_{95} = 2.093. If a calculated value of t for some pair of events exceeds 2.093, then the correlation r between that pair of events is said to be significant; otherwise it is not significant. As shown in Table 3-6 all six correlations are significant. The correlation between each pair of ranks is too large to be attributed to chance alone. Moreover, in each case the value of t associated with the correlation r is well in excess of the critical t value, so that one may consider the correlations as highly significant. If, as shown in Table 3-7, the six correlation values are ranked, it is evident that the Longshot, Kamchatka, and Novaya events are the most highly correlated, while the Kazakh event is associated with the three smallest values of r. It has not been determined if the reason underlying this significant degree of correlation is inherent in the measurement, or if it reflects a geographical phenomenon. The events differ in azimuth by more than 60°, which would seem to rule out direction as an underlying common factor.

Since the four events all occurred on or near the Eurasian land mass, it would be useful to obtain similar records for events in the Pacific Ocean and in or near South America. Comparison of such events with the present set of four should lead to firmer hypotheses regarding these rank correlation coefficients. Presently, strong events for the Pacific and South American areas are not available.

3.4.4.4   Subarray Losses From Steering a Common LASA Plane Wavefront

To evaluate the signal loss which necessarily results from steering, an analysis has been performed on two events which compares the loss resulting from steering each subarray to its own best plane wavefront with that resulting from steering each subarray to the same plane wavefront. The conclusion is that no significant difference between the two methods of steering exists.

Table 3-7. Ranking of the Six Correlation Values and their Associated Events

r	t	Event Pairs Associated With Each Correlation Value			
		Longshot	Kamchatka	Kazakh	Novaya
0.742	4.818	L	K	-	-
0.609	3.3476	L	-	-	Y
0.601	3.2803	-	K	-	Y
0.5727	3.045	-	-	Z	Y
0.504	2.544	L	-	Z	-
0.4675	2.305	-	K	Z	-

Note: L = Longshot

K = Kamchatka

Z = Kazakh

Y = Novaya

Hence, the presently planned method of steering the array should result in no significant signal loss, as compared with the theoretically optimal method of steering each subarray individually.

For the Kazakh and Novaya events, the LSWF program has been applied to each of the 21 subarrays to produce a best-fitting plane wave through each subarray. With the difference between the expected and the actual arrival time at each seismometer in a subarray treated as an observed value of a random variable, the standard deviation of these differences for each subarray has been computed. The 21 standard deviations for Kazakh are listed in column 1 of Table 3-8, while the 21 for Novaya are shown in column 1 of Table 3-9. Since the plane wavefront for each subarray is best-fitting, these standard deviations are the best value (minimum) obtainable for any first-degree approximation.

For the Kazakh and Novaya events, the LSWF program has also been applied to the center seismometers for each subarray to produce a plane wavefront over the entire array. A set of expected arrival times for the seismometers in each subarray has been computed, based on this LASA plane wave. With these expected arrival times, the standard deviation of the differences between expected and actual arrival times at the seismometers in a subarray has been calculated for each subarray. These standard deviations are listed in column 2 of tables 3-8 and 3-9. Since the values in column 1 are the best values possible, the values in column 2 should be larger, which they are. To obtain a better appreciation of their significance, the standard deviations have been converted to signal loss, measured in decibels. The formula for the loss, L, is given by

$$L = 10 \log_{10} e (2\pi f \sigma)^2,\tag{3.3}$$

where the frequency f is taken as 1 Hz and where σ is the standard deviation in seconds.

The loss figures for Kazakh are listed in Table 3-10, while those for Novaya are listed in Table 3-11.

Table 3-8. Kazakh Event—Standard Deviation of Differences

Subarray		1	2
Number	Name		
1	B1	.0182	.0207
2	F3	.0168	.0256
3	F4	.0169	.0193
4	A0	.0163	.0227
5	B3	.0205	.0248
6	C4	.0159	.0304
7	B4	.0147	.0164
8	C1	.0184	.0205
9	C2	.0175	.0220
10	B2	.0192	.0245
11	C3	.0178	.0244
12	D3	.0166	.0174
13	D4	.0143	.0151
14	D1	.0123	.0279
15	D2	.0194	.0395
16	E3	.0195	.0200
17	E4	.0184	.0252
18	E1	.0163	.0200
19	F1	.0168	.0183
20	E2	.0168	.0235
21	F2	.0177	.0257
Averages		.0172	.0230

Table 3-9. Novaya Event—Standard Deviation of Differences

Subarray		1	2
Number	Name		
1	B1	.0190	.0217
2	F3	.0144	.0194
3	F4	.0140	.0143
4	A0	.0188	.0195
5	B3	.0144	.0161
6	C4	.0473	.0530
7	B4	.0175	.0176
8	C1	.0216	.0266
9	C2	.0239	.0240
10	B2	.0191	.0306
11	C3	.0191	.0200
12	D3	.0151	.0169
13	D4	.0201	.0237
14	D1	.0209	.0271
15	D2	.0274	.0372
16	E3	.0149	.0213
17	E4	.0145	.0191
18	E1	.0205	.0255
19	F1	.0157	.0259
20	E2	.0158	.0248
21	F2	.0182	.0252
Averages		.0196	.0243

Table 3-10. Kazakh Event—Loss

Subarray		1 (dB) Irreducible	2 (dB) Expected	3 (dB) Additional
Number	Name			
1	B1	.0568	.0735	.0167
2	F3	.0484	.1124	.0640
3	F4	.0490	.0639	.0149
4	A0	.0456	.0883	.0427
5	B3	.0721	.1054	.0333
6	C4	.0433	.1584	.1151
7	B4	.0370	.0461	.0091
8	C1	.0580	.0721	.0141
9	C2	.0525	.0830	.0305
10	B2	.0632	.1029	.0397
11	C3	.0543	.1021	.0478
12	D3	.0472	.0519	.0047
13	D4	.0351	.0391	.0040
14	D1	.0259	.1335	.1076
15	D2	.0645	.2675	.2030
16	E3	.0652	.0686	.0034
17	E4	.0580	.1089	.0509
18	E1	.0456	.0686	.0230
19	F1	.0484	.0574	.0090
20	E2	.0484	.0947	.0463
21	F2	.0537	.1132	.0595
Averages		.0507	.0907	.0400

Table 3-11. Novaya Event—Loss

Subarray		1 (dB) Irreducible	2 (dB) Expected	3 (dB) Additional
Number	Name			
1	B1	.0619	.0807	.0188
2	F3	.0356	.0645	.0289
3	F4	.0336	.0351	.0015
4	A0	.0606	.0652	.0046
5	B3	.0356	.0444	.0088
6	C4	.3836	.4816	.0980
7	B4	.0525	.0531	.0006
8	C1	.0800	.1213	.0413
9	C2	.0979	.0988	.0009
10	B2	.0625	.1605	.0980
11	C3	.0625	.0686	.0061
12	D3	.0391	.0490	.0099
13	D4	.0693	.0963	.0270
14	D1	.0749	.1257	.0510
15	D2	.1287	.2373	.1086
16	E3	.0381	.0778	.0397
17	E4	.0360	.0625	.0265
18	E1	.0721	.1115	.0394
19	F1	.0423	.1150	.0727
20	E2	.0428	.1054	.0626
21	F2	.0568	.1089	.0521
Averages		.0659	.1012	.0353

Column 1 of tables 3-10 and 3-11 may be interpreted as the minimal signal loss resulting from steering each individual subarray in an optimal manner. The figures in column 1 might be termed the irreducible losses from best plane wave steering. Column 2 reflects the loss that is to be expected if each subarray is steered to the same LASA plane wavefront. Since it is presently planned to steer the array in this manner, the figures in Column 2 indicate the losses that can be expected from such steering. Column 3 lists the differences between corresponding values in columns 1 and 2. Column 3 might be termed a listing of the difference between the expected loss and the irreducible loss for each sub-array. That is, the figures in column 3 represent the additional loss beyond the irreducible that can be expected because of steering each subarray to the LASA wave.

Examination of tables 3-10 and 3-11 shows that for the Kazakh event the maximum additional loss, as shown in column 3, is experienced by the sub-array D2. This maximum is 0.20 dB. For the Novaya event, the maximum loss is 0.11 dB, also occurring at subarray D2. This loss is to be compared to the average loss of 0.035 dB for that event. Examination of the individual seismometer deviations for this subarray shows that for the Kazakh event no single seismometer is responsible for the large loss. For the Novaya event, both the best fit and the fit to the LASA curve show large deviations at 11 of the 25 seismometers; that is, neither fit is particularly good. For the Novaya event, the irreducible loss and the expected loss for subarray C4 are 0.38 dB and 0.48 dB, respectively, both of which are unusually large. Examination of the individual seismometer deviations indicates that a grossly inaccurate measurement must have been made at one seismometer in the subarray, probably as a result of thresholding.

The data in column 3 in tables 3-10 and 3-11 has been put into histogram form (see Figure 3-13). The histograms display clearly the fact that for both events the additional losses resulting from steering the array are generally much smaller than their respective averages would indicate. In other words, one or two large values have inflated the mean value so that it is not truly
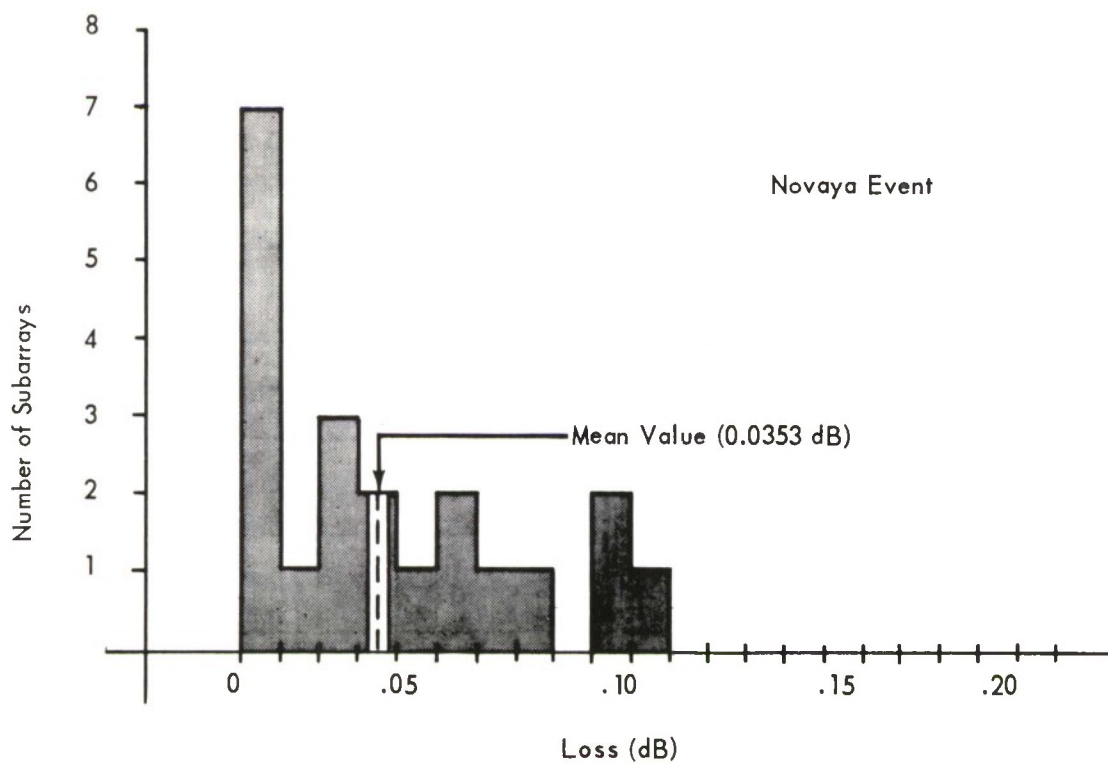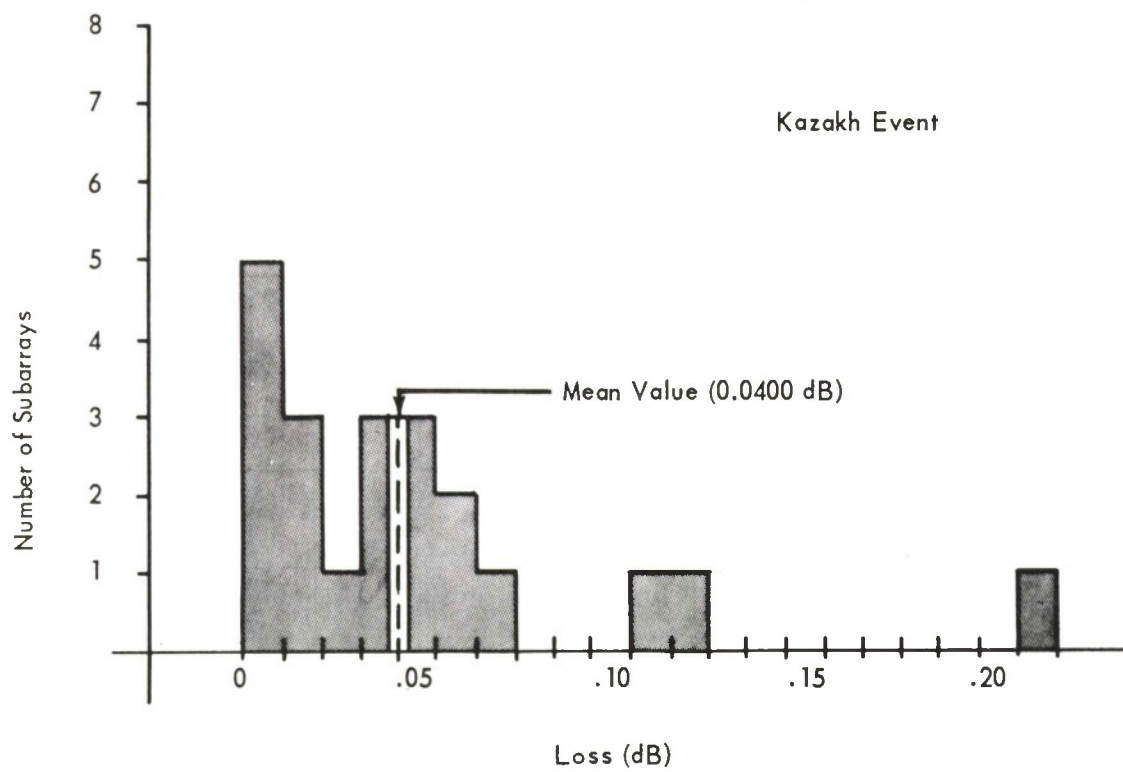
Figure 3-13. Distribution of Additional Loss

representative. From examination of the histograms, it can be concluded that steering each subarray to the same LASA plane wavefront produces an average additional loss of approximately 0.03 dB. Hence, the planned method of steering appears to be reasonable and adequate.

3.4.5 Acquisition of Arrival Time Data

3.4.5.1 Results of Thresholding

The second task in steering delay determination, (Section 3.4), the measurement of the arrival times, has traditionally been accomplished best by manually reading optical (film) records of the seismograms. For very strong events (magnitude 5.9 or greater), processing results obtained from automatic thresholding are usually nearly identical to manually read values. However, even for such strong events, a thresholding method which would consider a detection to have occurred as soon as one record exceeds the threshold would be highly sensitive to erratic fluctuations in the signal onset caused by random noise. For example, for the Novaya event, which was of magnitude 6.3, a false detection because of noise was probably declared at one seismometer (at least) in subarray C4, while at subarray D2, erroneous threshold times were declared at 11 of the 25 seismometers. As previously mentioned, even the best-fitting plane wave at D2 yielded large deviations at these 11 places.

How much thresholding reliability can be improved either by the average of several records or by a majority-type process remains to be determined. Further studies of the time signal plots of subarrays should be made.

For the Kamchatka and Kazakh events listed in Table 3-4, SDL has obtained arrival times at the center seismometer of each subarray for each event. Arrival times have also been obtained by using the Threshold Time Delay program. The threshold-derived arrival times for the two events relative to the arrival time at subarray A0 are shown in column 4 of tables 3-12 and 3-13, while the SDL arrival times, also relative to the A0 arrival time, are shown in column 5.

Table 3-12. Kazakh Event—Threshold Level 2400 q.u.

1 Sub- array Name	2 Threshold Sample Number	3 A0 Related Sample Number	4 A0 Related Sample Number x .05	5 SDL A0 Related Arrival Times	6 ΔT Threshold–SDL (Columns 4–5)
B1	965	–5	–.25	–.24	–.01
F3	1023	53	2.65	2.76	–.11
F4	883	–87	–4.35	–4.22	–.13
A0	970	0	0.0	0.0	0
B3	972	2	.10	.07	.03
C4	962	–8	–.40	–.39	–.01
B4	961	–9	–.45	–.46	.01
C1	956	–14	–.70	–.72	.02
C2	974	4	.20	–	–
B2	977	7	.35	.30	.05
C3	981	11	.55	.53	.02
D3	976	6	.30	.35	–.05
D4	943	–27	–1.35	–1.31	–.04
D1	957	–13	–.65	–.67	.02
D2	985	15	.75	.83	–.08
E3	1012	42	2.10	2.15	–.05
E4	946	–24	–1.20	–1.13	–.07
E1	925	–45	–2.25	–2.24	–.01
F1	905	–65	–3.25	–3.15	–.10
E2	986	16	.80	.85	–.05
F2	1040	70	3.50	3.55	–.05

Total for ΔT: –.61

Table 3-13. Kamchatka Event—Threshold Level 2400 q.u.

1 Sub-array Name	2 Threshold Sample Number	3 A0 Related Sample Number	4 A0 Related Sample Number x .05	5 SDL A0 Related Arrival Times	6 ΔT Threshold -SDL (Columns 4 -5)
B1	3212	1	.05	0	.05
F3	3216	5	.25	.17	.08
F4	3085	-126	-6.30	-6.30	0
A0	3211	0	.0	0	0
B3	3207	-4	-.20	-.30	.10
C4	3195	-16	-.80	-.87	.07
B4	3201	-10	-.50	-.52	.02
C1	3202	-9	-.45	-.55	.10
C2	3225	14	.70	.60	.10
B2	3220	9	.45	.40	.05
C3	3220	9	.45	.43	.02
D3	3204	-7	-.35	-.39	.04
D4	3175	-36	-1.80	-1.85	.05
D1	3216	5	.25	.20	.05
D2	3239	28	1.40	1.42	-.02
E3	3249	38	1.90	1.85	.05
E4	3155	-56	-2.80	-2.88	.08
E1	3172	-39	-1.95	-2.00	.05
F1	3214	3	.15	-.05	.20
E2	3285	74	3.70	3.68	.02
F1	3328	117	5.85	5.82	.03

Total for ΔT: 1.14

For each event, the two sets of arrival times have been compared to determine any discrepancies. Column 6 of tables 3-12 and 3-13 lists the difference, ΔT, between arrival times for each subarray. The standard deviation of ΔT, treated as a random variable, is computed. For the Kazakh event, the standard deviation is $\sigma = 0.049$ seconds, while for Kamchatka, it is $\sigma = 0.046$ seconds.

With these values for σ, the respective losses at frequency $f = 1.5$ Hz have been computed. For Kazakh the loss is 0.93 dB; for Kamchatka the loss is 0.82 dB. These results indicate that for strong events (magnitude 5.9 or better) the SDL and threshold methods yield nearly identical arrival times, subject to the limitations of thresholding mentioned above.

For the Kamchatka event, two LASA beams were formed by the LASA Beamformer program—one beam based on the SDL arrival times and the other based on the threshold arrival times. With S denoting the beam formed using SDL data and T denoting the beam formed using threshold data, it was found by measuring the printed graphs of the two beams that the amplitudes of the respective first peaks were each 196 nm. The maximum amplitudes were measured from the graphs and found to be 203 nm for S and 207 nm for T. A comparison of the smaller amplitude with the larger indicates that the potential gain in decibels (the actual gain difference if the better beam were perfectly steered) may be found from

$$\text{Gain} = 20 \log (\text{larger/smaller})$$

so that here

$$\text{Gain} = 20 \log (207/203) = .1868 \text{ dB.}$$

The gain is evidently negligible. The frequencies, relative to the accuracy of reading the graphic records, were found to be equal.

3.4.5.2   Plans for Correlation Processing

For weaker events, it is hoped that correlation techniques can provide usable delays. There are two criteria for measuring the quality of arrival times which are obtained from this process. First, the times must

lead to significant signal-to-noise enhancement when beams are formed based upon them; second, the times should be sufficiently consistent within a geographic region to permit adequate accuracy of preformed beams. It is expected that because of the relatively large computation time involved, correlation will be carried out only on an experimental basis on one or two presently available events; larger quantitites of data can be analyzed in this way when a processing system becomes operational.

Figure 3-14 is a diagram outlining a method by which correlation can be used to measure relative arrival times for weaker events.

3.4.6   Conclusions

Conclusions from the time of arrival data which has been processed are summarized below. The numbers preceding the paragraphs correspond to the numbers of the series of questions raised in Section 3.4.1.

1.   For the three regions which have been investigated, the steering errors produced by the least squares plane wavefront method of arrival time data organization appear to be comparable in magnitude to the corresponding errors incurred using the Jeffreys-Bullen method. This analysis has been carried out for a limited number of events, and only for the center seismometers of the subarrays. As more data is processed, a more complete evaluation will be possible.

2.   The range iteration method used in an attempt to remove curvature bias from the least squares plane wavefront analysis did not improve the results. The deviations from plane, as well as the inverse phase velocity components, were minimally affected by the iteration of range corrections with least squares plane wavefront routines.

3.   The deviations of actual arrival times from the quadratic wavefront for a given event tend to be from slightly less to about half the value of the corresponding deviations from the plane wavefront for the event. The curvatures as measured by the least squares quadratic wavefront method in any given region exhibit a strong bias.

4.   Whether the curvatures exhibit a noticeable trend as a function of range or inverse phase speed within a region is questionable. A meaningful measure of average curvatures can be made for each source region. The deviations can be reduced in magnitude by applying quadratic corrections. However, the difference between the deviations for an event and the average deviations for the region will
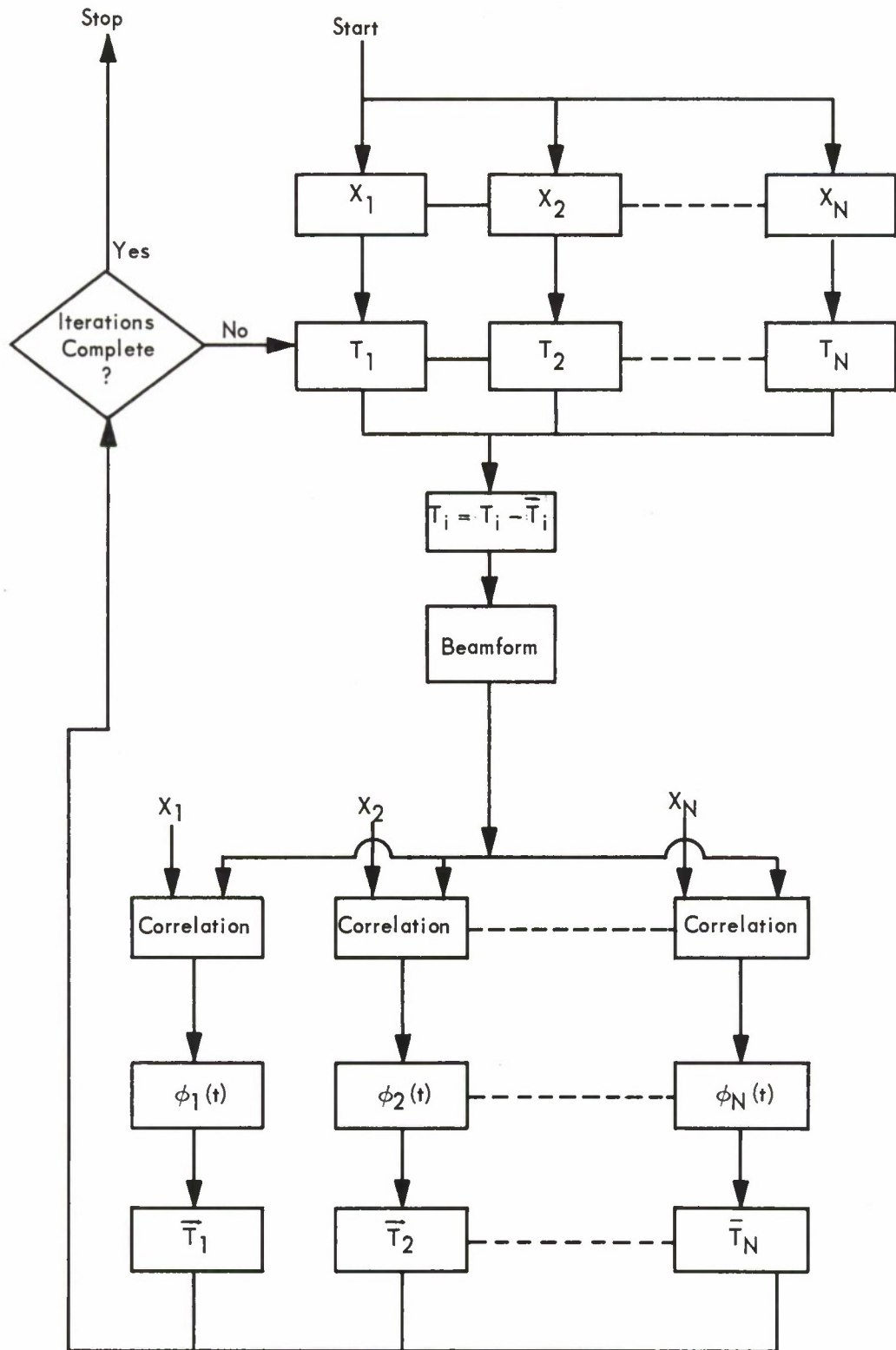
Figure 3-14. Time-Delay Correlation Analysis

probably not be reduced by using the quadratic analysis, as compared to the plane one. They could be reduced if a significant curvature trend could be established within a region. Since this has not happened with any consistency, it is preferable to steer the array by referring the anomalies to plane wavefronts. Nonetheless, the quadratic formulation could be useful for interpolating delays between regions.

For the slight extent to which a curvature trend can be noticed within some regions, this trend appears better established for the range-azimuth derivatives than for the somewhat arbitrary East-North derivative. The trend appears slightly more pronounced when referred to measured inverse phase speed than to world network derived range. No attempt has been made to relate curvatures to interregion variations in source location.

The calculation of a wavefront from arrival times at significantly less than the number of subarrays used for the rest of the region degrades the fit of the event delays to the average delays. Thus, if wavefronts for most events in a region are calculated from 17 to 21 subarray arrival times, an event in that region calculated for 11 to 15 subarrays often exhibits a poor fit, apparently because of the low number of arrival times used. The magnitude of this effect will be strongly influenced by which subarrays are missing.

5.   For a few events for which arrival times were available at all 525 seismometers, the LSWF program was applied individually to each subarray and to the set of subarray center seismometers.

The standard deviation of deviations from the plane at a subarray tended to be on the order of 0.02 sec., indicating, as expected, that the wavefronts are nearer to being plane at a subarray (about one-tenth the deviations) than over the full array. Because of the small subarray aperture, a relatively large variability of azimuth $(\pm 10^{\circ})$ and inverse phase speed $(\pm 40$ percent) for a given event can be expected and was noted. What was somewhat surprising, however, was that, between several events coming from the same general direction, certain subarrays consistently measured a low inverse phase speed and others a high one, compared to the center seismometer beam measurement. The same was true of azimuth measurements. It has not been established whether this phenomenon is a result of a measurement bias at the subarrays, or whether it is caused by geological nonhomogeneities.

The deviations for each seismometer at each subarray were calculated, assuming a common LASA least squares plane wavefront rather than a least squares best fit to each individual subarray. The resulting steering losses were still insignificant, amounting to about 0.10 dB, as compared to the "irreducible" 0.06 dB incurred when each subarray is steered to its own best least squares plane wavefront.

The significance of these preliminary results is that they confirm the validity of the system hypothesis that subarrays can be steered by plane wave delays, and that the direction to which each subarray is steered need not consider any additional subarray "station corrections." In other words, it appears that each subarray can safely be steered to the same point, or be steered according to the principle of dispersed subarray beam steering discussed in Appendix A of reference 3.

6.   Results discussed in Section 3.4.5 indicate that automatic thresholding is not a reliable method of obtaining arrival time data for events below the magnitude of 5.9. Even for events as strong as this, results using just simple thresholding techniques without redundancy checks are erratic. We hope that for strong events such redundancy checks might provide adequate improvement. Investigation of the use of correlation processing to provide time delay for weaker events is planned.

3.5   TIME DELAY PROBABILITY DISTRIBUTIONS

To determine an appropriate set of weights for estimating the number of wraparounds anticipated in the execution of the beamforming algorithms, a study of the time delay distribution for both the LASA and the subarrays was made. Within this section, a three-part study is discussed, and its results given. First, a statistical treatment of the expected time delays as a function of array position was made. Second, an estimate was made of the appropriate weights for each memory wraparound experienced in the execution of the beamforming algorithm. Third, contributors were collected to yield the timing estimate.

3.5.1   LASA Time Delays Distribution Estimates

The parameters for a P wave are u and A, where u is inverse velocity measured in units of seconds per kilometer, and A is the azimuth measured in degrees. If, as shown in Figure 3-15, S denotes a subarray whose azimuth is θ and whose radial distance from the center of the array is r, then a P wave will produce a time delay T at subarray S, relative to the center of the array 0. The
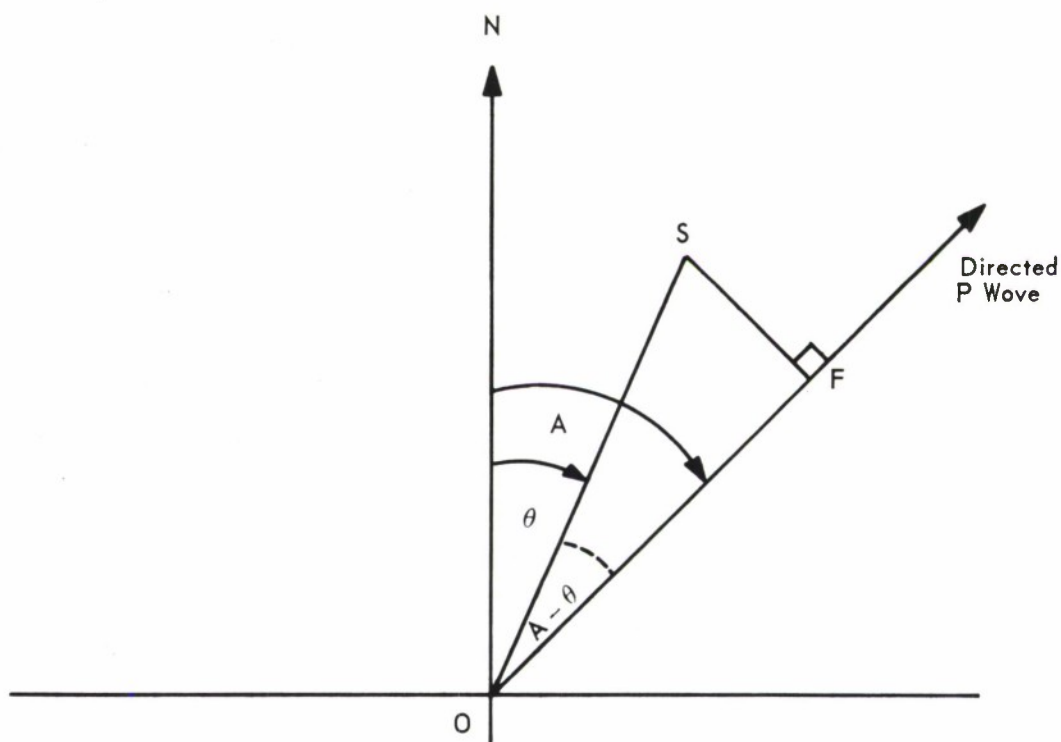
S is Subarray Location

$\tau = \overline{OS}$

$\dfrac{\overline{OF}}{\overline{OS}} = \cos(A - \theta)$

$\overline{OF} = \overline{OS}\cos(A - \theta)$

$\overline{OF} = \tau\cos(A - \theta)$

Figure 3-15. Position of Subarray Relative to a Directed P Wave

time delay T is given by the equation

$$T = ru \cos(A - \theta).$$
(3.4)

As seen from Figure 3-15, the distance $\overline{OF}$ is $r \cos (A - \theta)$; to travel this distance requires $ur \cos (A - \theta)$ seconds.

The parameters u and A are random variables. Moreover, the radial distance r may be treated as a random variable. (As will be shown below, r has an almost trivial distribution.) Consequently, the time delay T is a random variable which possesses distributions both for all the seismometers in LASA and for the seismometers in a subarray.

To determine how time delays are distributed requires some knowledge of the distributions of u and of A. The following assumptions have been made regarding the random variables u and A:

1. A is uniformly distributed over $(0, 2\pi)$. Since θ is a constant, $(A - \theta)$ is also uniformly distributed over $(0, 2\pi)$.

2. Since P waves in the teleseismic range only are being considered, u varies from 0.04 to 0.08 sec/km. Over this range, assume that u is linearly distributed (i.e., the probability that u takes on some value u_0 is cu_0, where c is a constant). This relationship may be expressed as

$$Pr (u = u_0) = cu_0.$$
(3.5)

A distribution for radial distance r may be obtained from the following considerations. There are 21 subarrays in the LASA—one at the center and the other 20 in rings of 4. Although the rings are not concentric, they can be considered as such for the purpose of this study. Since the diameter of LASA is 200 km, there are 4 subarrays whose distance r_2 is 6.25 km, 4 at $r_3 = 12.5$, 4 at $r_4 = 25$, 4 at $r_5 = 50$, 4 at $r_6 = 100$ km, and 1 at $r_1 = 0$.

If it is assumed that any subarray is equally likely to be chosen, then a probability distribution can be obtained from the array geometry. For example, the probability that $r = r_5 = 50$ is 4/21 since there are 4 subarrays at a radial distance of 50 km from the center of the array. The 6 values taken on by r and their respective probabilities are shown in Table 3-14.

Table 3-14. Values and Corresponding Probabilities for Radial Distance r

Value of r_i		Number of Subarrays at Distance r_i	Number of Subarrays at Distance r_i or Less	Probability of a Subarray being at Distance r_i
Kilometers		Relative Frequency	Cumulative Frequency	P_i
r_1	0.0	1	1	1/21
r_2	6.25	4	5	4/21
r_3	12.5	4	9	4/21
r_4	25.0	4	13	4/21
r_5	50.0	4	17	4/21
r_6	100.0	4	21	4/21

To simplify the computations, we decided to approximate the continuous distributions of u and A by discrete distributions. As shown in Table 3-15 the range of u from 0.04 to 0.08 has been divided into 8 subintervals, each of length 0.005; and u accordingly takes on 8 values (u_1, u_2, ... , u_8) when u_j is the midpoint of interval j. Thus, it follows from the second assumption that Pr (u = u_j) = cu_j, where c is a constant. The value of c may be determined by the condition that the probabilities cu_1, cu_2, . . . , cu_8 must have a sum of 1. Hence,

$$cu_1 + \ldots + cu_8 = c(0.0425 + 0.0475 + 0.0525 + \ldots$$

$$+ 0.0775) = c(0.48) = 1 \qquad (3.6)$$

from which c = 1/.48 = 25/12.

A graph of the distribution of u is shown in Figure 3-16.

As A runs uniformly from 0 to 2π, so does (A - θ). Now for any angle D, cos D = cos (-D) so that it is necessary only to consider (A - θ) as running either from 0 to π, or from π to 2π. Since cos (A - θ) increases monotonically from -1 to +1 as (A - θ) runs from π to 2π, this latter range for (A - θ) is used. As shown in Table 3-16, this range has been divided into 10 subintervals, thereby yielding 10 values of (A_k - θ) and 10 values of cos (A_k - θ).

The left endpoint of each interval has been chosen as the value for (A_k - θ). Since the 10 values (A_1 - θ), ... , (A_{10} - θ) are equally likely, the probability associated with each value of cos (A_k - θ) is 1/10; thus, from the notation of Table 3-16,

$$W_k = Pr (\cos (A - \theta) = \cos (A_k - \theta)) = 1/10. \qquad (3.7)$$

From the tables it is seen that a typical time delay value, denoted as T_{ijk}, is given by the formula

$$T_{ijk} = r_i u_j \cos (A_k - \theta), \qquad (3.8)$$

where

i = 1, . . . , 6
j = 1, . . . , 8
k = 1, . . . , 10.

Table 3-15. Values and Corresponding Probabilities for Inverse Velocity u

(Considered a Discrete Variable)

Interval Number	Interval Range	U_j	Value of U_j Over the Interval	P_r $(u = u_j)$ Q_j
1	.040 to .045	U_1	.0425	$25U_1 / 12$
2	.045 to .050	U_2	.0475	$25U_2 / 12$
3	.050 to .055	U_3	.0525	$25U_3 / 12$
4	.055 to .060	U_4	.0575	$25U_4 / 12$
5	.060 to .065	U_5	.0625	$25U_5 / 12$
6	.065 to .070	U_6	.0675	$25U_6 / 12$
7	.070 to .075	U_7	.0725	$25U_7 / 12$
8	.075 to .080	U_8	.0775	$25U_8 / 12$
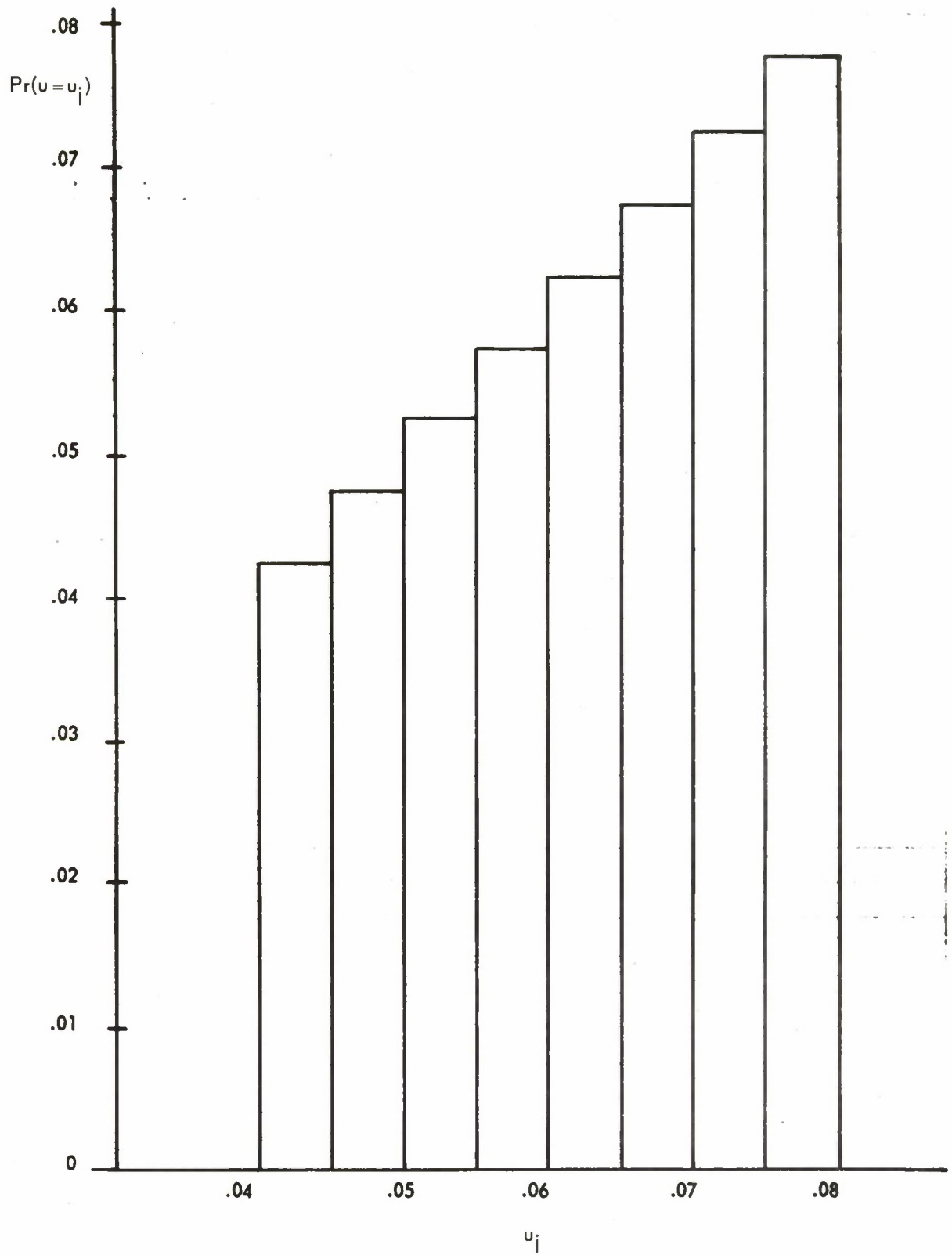
Figure 3-16. Distribution of u, Considered as a Discrete Variable

Table 3-16. Values and Corresponding Probabilities for Azimuth A

(Considered a Discrete Variable)

Interval Number	Value of $(A_k - \theta)$		Equivalent First Quadrant Values	Value of cos $(A_k - \theta)$	W_k
	Radians	Degrees			
1	π	$180°$	$0°$	-1.00000	1/10
2	$\pi + .1\pi$	$198°$	$18°$	-0.95106	1/10
3	$\pi + .1\pi$	$216°$	$36°$	-0.80902	1/10
4	$\pi + .3\pi$	$234°$	$54°$	-0.58779	1/10
5	$\pi + .4\pi$	$252°$	$72°$	-0.30902	1/10
6	$\pi + .5\pi$	$270°$	$90°$	0.0	1/10
7	$\pi + .6\pi$	$288°$	$72°$	+0.30902	1/10
8	$\pi + .7\pi$	$306°$	$54°$	+0.58779	1/10
9	$\pi + .8\pi$	$324°$	$36°$	+0.80902	1/10
10	$\pi + .9\pi$	$342°$	$18°$	+0.95106	1/10

Note: $W_k = P_r [\cos (A - \theta) = \cos (A_k - \theta)]$

Thus, there are $6 \times 8 \times 10 = 480$ values for the random variable T. The minimum value for T is

$$T_{6,8,1} = r_6 u_8 \cos(A_1 - \theta) = 100 \times 0.0775 \times (-1)$$

$$= -7.75 \text{ sec.} \tag{3.9}$$

The maximum value for T is

$$T_{6,8,10} = r_6 u_8 \cos(A_{10} - \theta) = 100 \times 0.0775 \times 0.9511$$

$$= +7.37 \text{ sec.} \tag{3.10}$$

The probability that $T = T_{ijk}$ is computed from Equation (3.8) under the assumption that the variables r, u, and A are independent. Thus, letting $Z_{ijk} = \Pr(T = T_{ijk})$, from Equation (3.8),

$$Z_{ijk} = \Pr(T = T_{ijk}) = P_i \times Q_j \times W_k. \tag{3.11}$$

The numbers P_i, Q_j and W_k may be obtained from tables.

The 480 values for T and their associated probabilities have been grouped into histogram form as shown in Figure 3-17. The histogram consists of 49 intervals, each of length 0.03, over the range -8 to +8. From the histogram, the cumulative distribution has been obtained and is shown in Figure 3-18. Because r_0 is 0 and because $\cos(A_6 - \theta)$ also is 0, an unusual number of values of T are exactly zero. This number can be reduced somewhat by smoothing the cell probabilities. A five-point smoothing formula has been applied to the histogram data of Figure 3-17. The smoothed histogram is shown in Figure 3-19 and the associated cumulative distribution in Figure 3-20.

Analysis of the distribution of time delays shows that the lower quartile value is -1, the median is 0, and the upper quartile value is 2/3. Hence, half of the 480 values are between -1 and 2/3, one quarter are between -8 and -1, and one quarter are between 2/3 and 8. Thus, the time delays for the entire LASA are clustered very tightly about the median value of zero.
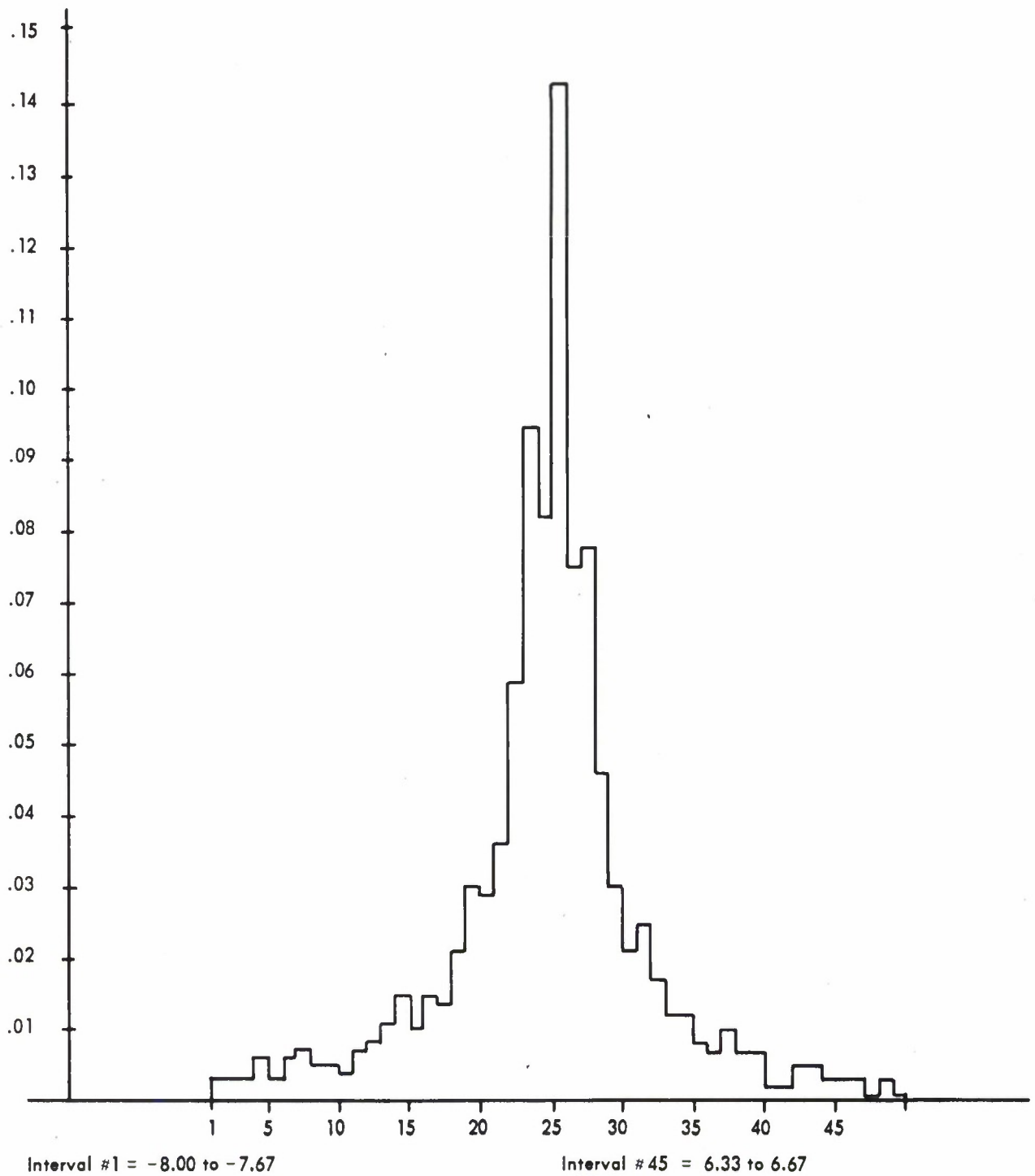
Figure 3-17. Relative Frequency Distribution for LASA Time Delays
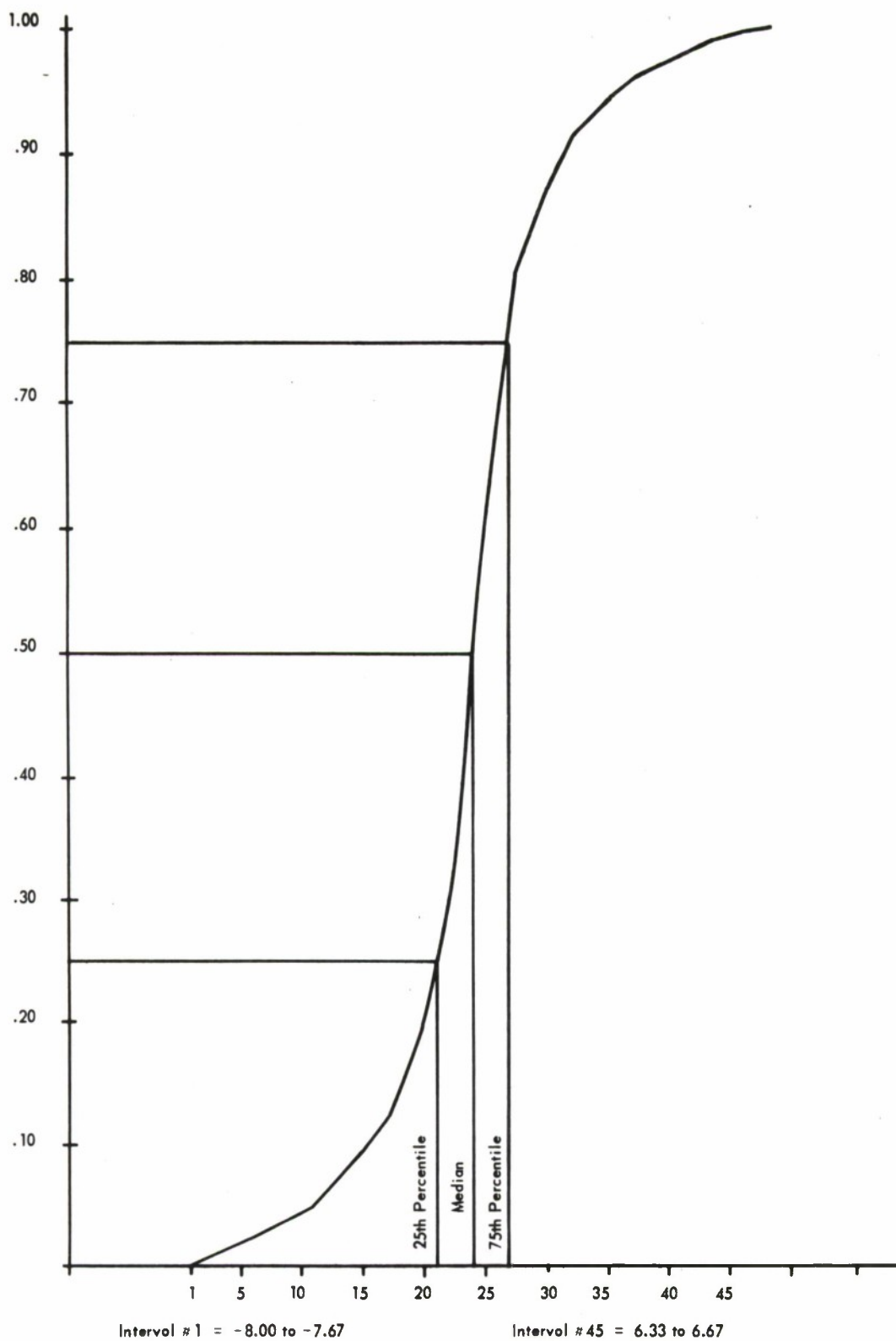
Figure 3-18. Cumulative Distribution for LASA Time Delays

Interval #1 = -8.00 to -7.67   Interval #45 = 6.33 to 6.67
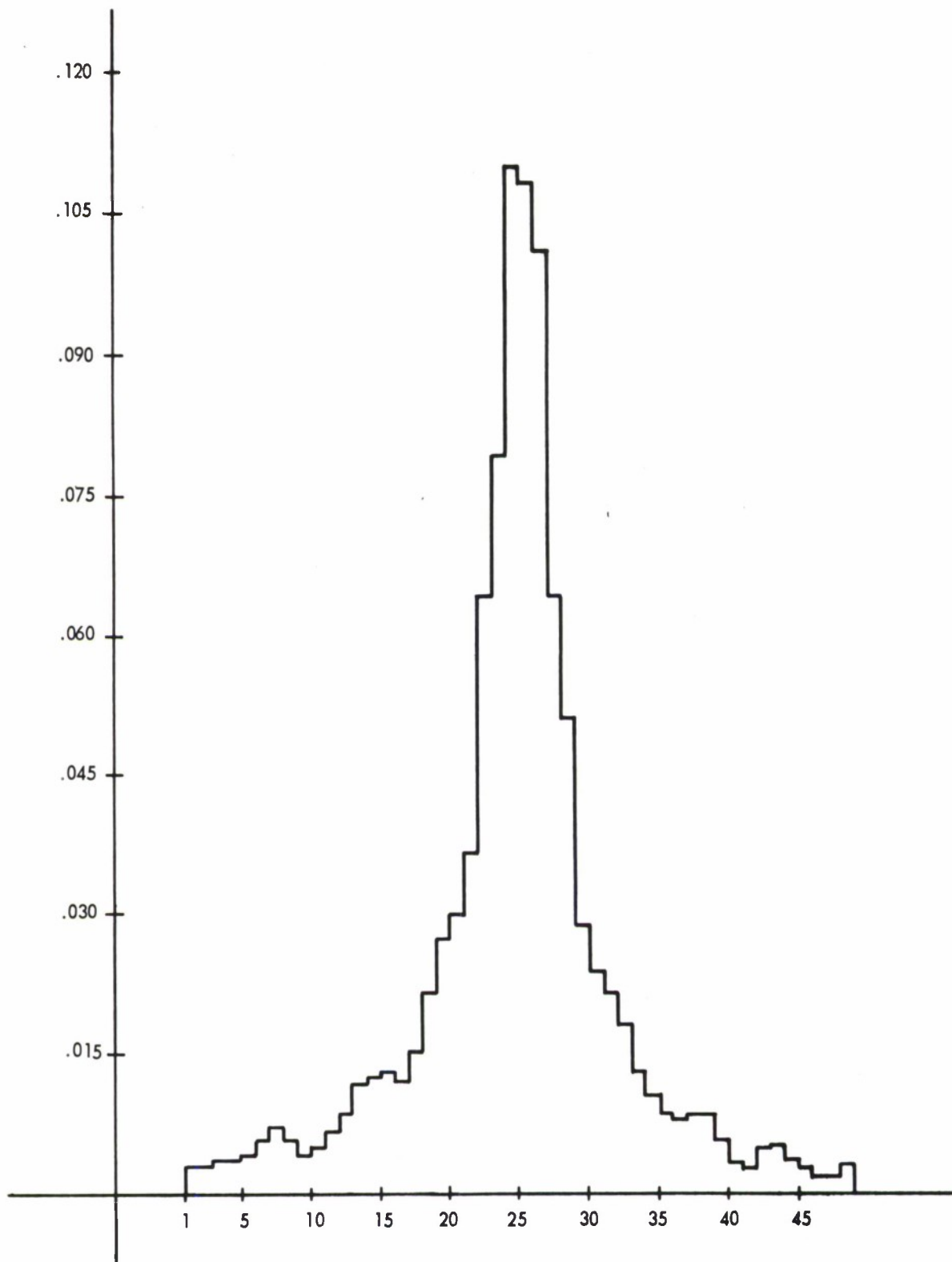
Figure 3-19. Smoothed Frequency Distribution for LASA Time Delays
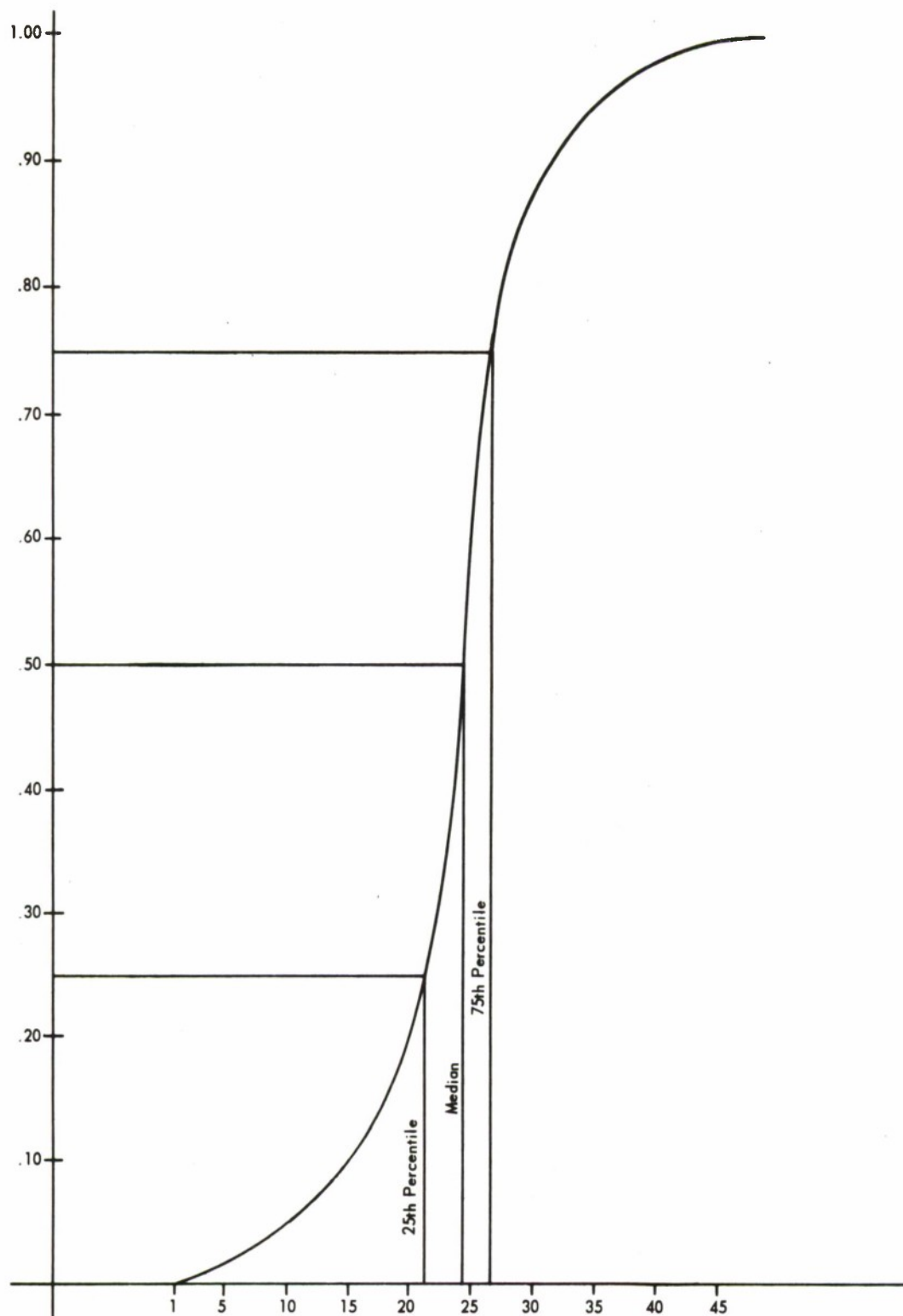
Figure 3-20. Smoothed Cumulative Distribution for LASA Time Delays

3.5.2 Subarray Time Delays Distribution Estimates

To derive a distribution of time delays for a subarray, an equation similar to (3.4) is used as the basic relation

$$t = Su \cos (A - \alpha). \tag{3.12}$$

Here, t is the time delay at a seismometer relative to the center seismometer of the subarray; S is the radial distance of a seismometer from the center seismometer; and α is the azimuth of the seismometer. Again, u and A are the parameters of the P wave.

Since the diameter of a subarray is only 7.5 km, one concludes that the inverse velocity can be considered constant over a subarray. Accordingly, for a subarray, u is fixed and set equal to 0.06 sec/km, rather than varying between 0.04 and 0.08.

Azimuth A is again considered to vary uniformly from 0 to 2π, so that $(A - \alpha)$ from π to 2π only need be considered. In Table 3-16, the column for $\cos (A_k - \theta)$ may be used for $\cos (A_k - \alpha)$.

Since the seismometers in a subarray are essentially equally spaced, it can be shown that S takes on 8 values from 0 through 3.5. These values and their respective probabilities (assuming any seismometer is equally likely to be chosen) are shown in Table 3-17.

Since there are 10 values for $\cos (A_k - \alpha)$ and 8 for S, the random variable t_{ik}, where

$$t_{ik} = S_i u \cos (A_k - \alpha), \tag{3.13}$$

takes on 80 values. If Y_{ik} denotes the probability that $t = t_{ik}$, then under the assumption that variables S and A are independent, Y_{ik} may be obtained from Equation (3.13)

$$Pr (t = t_{ik}) = Pr (t = S_i u \cos (A_k - \alpha)) = 0.06 \, L_i W_k . \tag{3.14}$$

Note that the minimum value for t is

$$t_{8,1} = S_8 u \cos (A_1 - \alpha) = (3.5)(0.06)(-1) = -0.21 \text{ secs}, \tag{3.15}$$

Table 3-17. Values and Corresponding Probabilities for Radial Distance S
of Seismometers

	Value of S_i	Number of Seis-mometers at Distance S_i	Number of Seis-mometers at Distance S_i or Less	Probability of a Randomly Chosen Seis-mometer Being at Distance S_i
S_i	Kilometers	Relative Frequency	Cumulative Frequency	L_i
S_1	0.0	1	1	.04
S_2	0.5	6	7	.24
S_3	1.0	3	10	.12
S_4	1.5	3	13	.12
S_5	2.0	3	16	..12
S_6	2.5	3	19	.12
S_7	3.0	3	22	.12
S_8	3.5	3	25	.12

while the maximum value for t is

$$t_{8,10} = S_8 \, u \cos(A_{10} - \alpha) = (3.5)(0.06)(.95106)$$

$$= 0.20 \text{ seconds.} \tag{3.16}$$

The 80 values for t and their associated probabilities have been put into histogram form as shown in Figure 3-21. The histogram contains 30 intervals, each of length 0.015, covering the range from -0.225 to +0.210 inclusive. The cumulative distribution obtained from the histogram is shown in Figure 3-22. From the cumulative curve it is seen that the lower quartile value is -0.06, the median is 0, and the upper quartile value is +0.045. Here, the subarray time delays are not so tightly clustered as are the time delays for the entire LASA.

3.5.3 Execution Speed Estimates

The term "wrap around" refers to accessing input data for a beamforming operation. The planned data arrangement uses a cyclical storage buffer. In this approach, data is loaded in lines starting from the lowest addressed entry in the block. When the block is filled, the data for the next time period is again placed at the lowest entry in the block. In beamforming, a delay value is subtracted from a time pointer and the resulting storage address is used to access the data. In some cases the storage address developed is below the data block. When this occurs, the block size is added to the developed address, causing a wraparound effect to occur.

From the distribution curves, two cases are of interest. The first assumes a uniform distribution in the phasing of the time pointer in relation to the data block, and the second assumes a worst-case synchronous distribution. Figures 3-20 and 3-22 show that the worst-case mix of the above effects would yield a set of weights for both the LASA and the subarray beamforming process. Both the conditions assumed and the weights are given in Table 3-18. The weights for the subarray case yield the more stringent specification, primarily because the line labeled "Subsequent 5 Wraparounds" has the lowest execution speed of all lines given. These weights are then used to calculate a weighted

Interval # 1 = -.225 to -.210   Interval #30 = .195 to .210
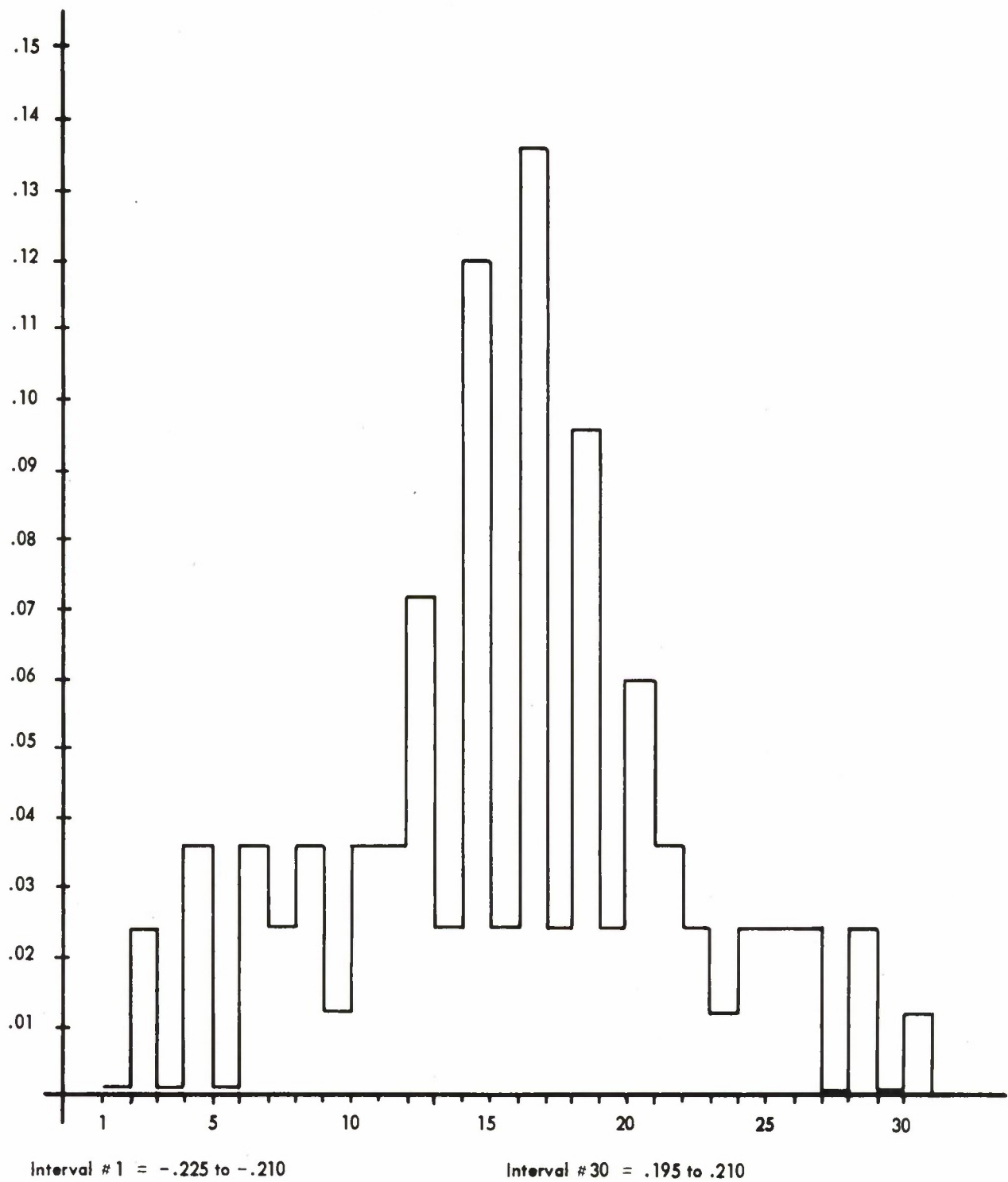
Figure 3-21. Relative Frequency Distribution for Subarray Time Delays
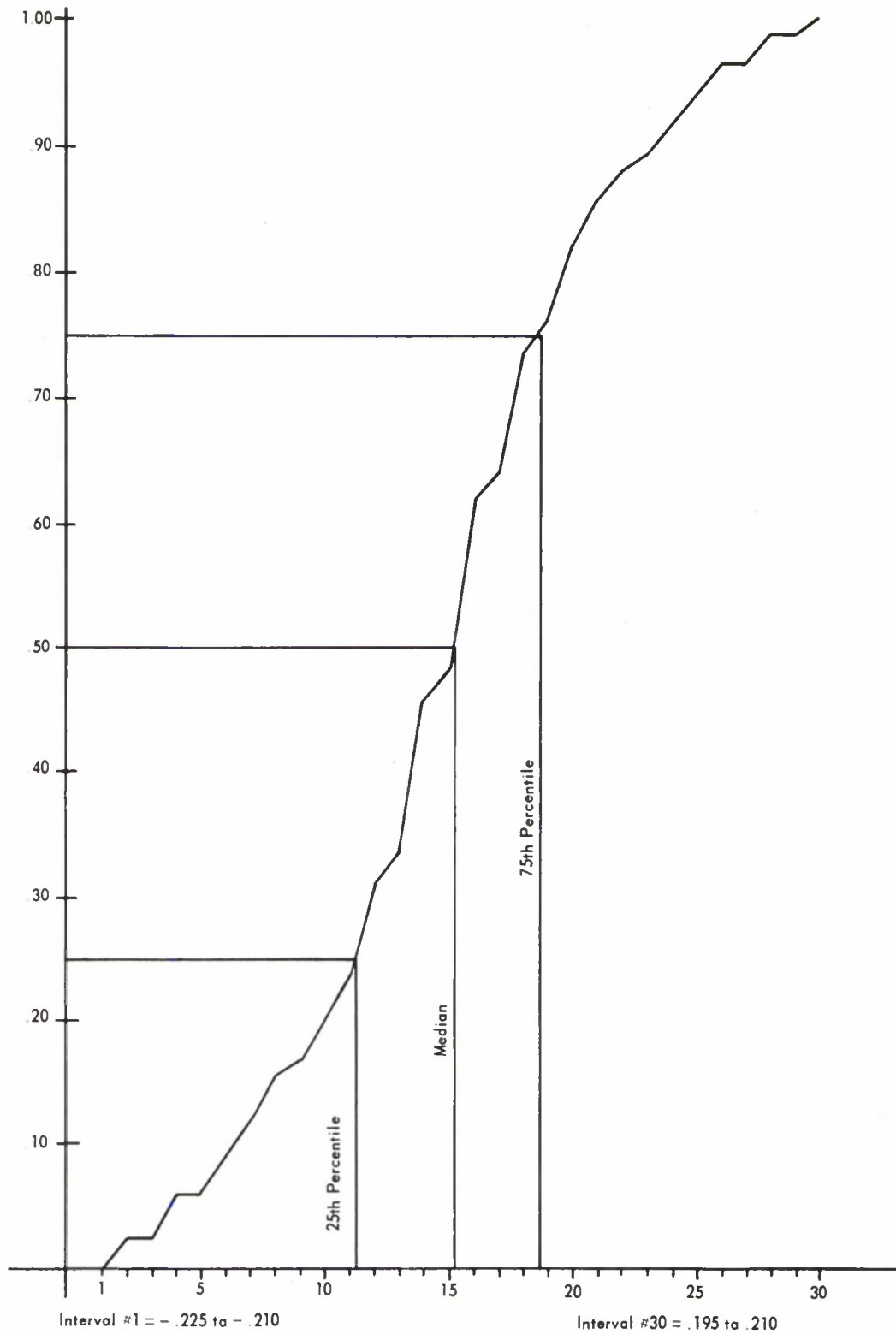
Figure 3-22. Cumulative Distribution for Subarray Time Delays

Interval #1 = -.225 to -.210

Interval #30 = .195 to .210

25th Percentile

Median

75th Percentile

Table 3-18. Beamforming Execution Time Weights

Loop					Weights	
					Subarray	LASA
		0	Wraparounds		0.482	0.482
Poorest of	1, 2, 3, 4		Wraparounds		0.150	0.014
2nd Poorest of	1, 2, 3, 4		Wraparounds		0.076	0.011
2nd Best of	1, 2, 3, 4		Wraparounds		0.075	0.011
Best of	1, 2, 3, 4		Wraparounds		0.016	0.011
First		5	Wraparounds		0.016	0.045
Subsequent		5	Wraparounds		0.185	0.426
					1.000	1.000
Delay Range			(Samples)		0 – 12	0 – 1000
Batch Size					5	5
Batch Increment			(Samples)		2	2
New Data Slots					9	0
Minimum Block Size			(Samples)		30	170

average execution time for the beamforming inner loop. The equation is

$$Time = 0.482 \, (0 \, WA) + 0.150 \, (4 \, WA) + 0.076 \, (3 \, WA)$$
$$+ \, 0.076 \, (2 \, WA) + 0.016 \, (1 \, WA) + 0.016 \, (5 \, WA)$$
$$+ \, 0.184 \, (No \ compare) \hspace{3cm} (3.17)$$

where x WA means that a wraparound occurs on x of the 5 beams being formed. An evaluation of this equation gives an average inner loop time of 24.93 μ sec per point (on all 5 beams). If a beam is formed by 25 inputs, the total execution time is 683.90 μ sec, including all overhead operations.

3.6 EXPERIMENTAL DISPLAY

The experimental beam display provides a visual presentation of beam magnitudes as a function of time. Beams are positioned according to their relationship in the inverse velocity plane. The display is to assist in evaluating techniques for selecting the best beam, identifying the various event arrivals, and verifying the data processing operation.

Initially, the display was operated in an off-line mode with a digital magnetic tape unit. The processed beam intensities are sequenced onto a magnetic tape for input to the display which has the capability of displaying 1024 beams (32 x 32 matrix) in a close-packed configuration. Each beam is currently displayed as a rectangular area. By shifting the odd numbered rows of beams by a one-half beam position, the inverse velocity relationship for close-packed beams is maintained.

A study has been performed to investigate the interface requirements for attaching the experimental display to a processing system. On-line operation should provide a more efficient method for generating and evaluating display presentations; it would allow the operator to participate in amplitude and time-scaling. A functional diagram of the experimental display with the proposed modification for on-line operation is shown in Figure 3-23. Compatibility with the magnetic tape unit for off-line operation will be maintained. The computer will be required to supply beam intensity data at a sufficient data rate to prevent display flicker from pattern fading between writings. A table consisting of a

Common Display Unit for Off-Line and On-Line Operation

CRT

32 x 32 Matrix of Beams

16 Intensity Levels

Display Pattern Regenerated at 58 Frames/Sec

X Axis

Σ

Y Axis

Σ

Z Axis

D/A

5 MHZ osc

.5 MHZ osc

D/A

D/A

Timing and Control

5-Bit Binary Counter

5-Bit Binary Counter

Display Controls

a

Scaling . . . . Pedestal

Time

The display unit should maintain capability for both on-line and off-line operation by moving the input cable

Magnetic Tape Drive and Control Unit

60K Bytes/Sec

Data Output:
Continuous Records of Start Byte Plus 1024 Intensity Bytes

Interface Data Adapter

Computer

Table of Start Byte Plus 1024 Intensity Bytes

Data Transfer:
60K Bytes/Sec

Display controls determine:
table update rate, source of data, data scaling, and pedestal or minimum intensity value for log scaling.

Figure 3-23. Experimental Beam Display

start byte followed by 1024 beam intensities formatted to write from left to right and top to bottom will reside in core storage. Repetitive transfer of the data table will be maintained by chaining the data transfer instructions. The data table will be updated at a rate selected by the operator's time control register, or whenever the operator changes either the scaling or the pedestal control. The pedestal control selects the minimum beam intensity value to be displayed, while the scaling control selects the beam intensity level corresponding to the maximum display intensity. Their interrelationship is shown in Figure 3-24; the pedestal control translates the output/input characteristic line along the output axis, and the scaling controls the slope of the line. Display of a large dynamic intensity range will be evaluated, using a logarithmic relationship between the output and input as illustrated in Figure 3-25. As in the linear case, the pedestal will translate the curve along the output axis, while the scaling controls the effective incremental slope of the curve by varying the display intensity modulation sensitivity.

Beams are positioned on the CRT by counting the beam intensities transferred to the display. The start bit resets the counters to zero before writing each frame, keeping the display synchronized with the data table. The size of the beam is controlled by summing a high-frequency sine wave with both the x and y axis beam position voltages. The experimental display used with a processor will provide a monitor of simulated real-time processing and a valuable method for verifying the detection processing operation.

Display tapes for two events have been prepared. These events are described in Section 3.8 and will be referred to as Longshot and the Earthquake. The number of neighboring beams displayed has been limited to 595—the number of beams that can be formed by one run of the LASA Beamforming program in the IBM 7090 computer with a data rate of 10 samples per second. These beams are close-packed to cover a circle in the inverse velocity plane with a diameter of .052 sec/km. The horizontal and vertical distances between beam centers are .0021 sec/km and .0018 sec/km, respectively. (Irregularities in beamspacing are present because of breadboard electronics.) All presentations are of rectified and integrated LASA beams. Integration is used to indicate a running averaging process using a 2-second time window. Photographs of the first
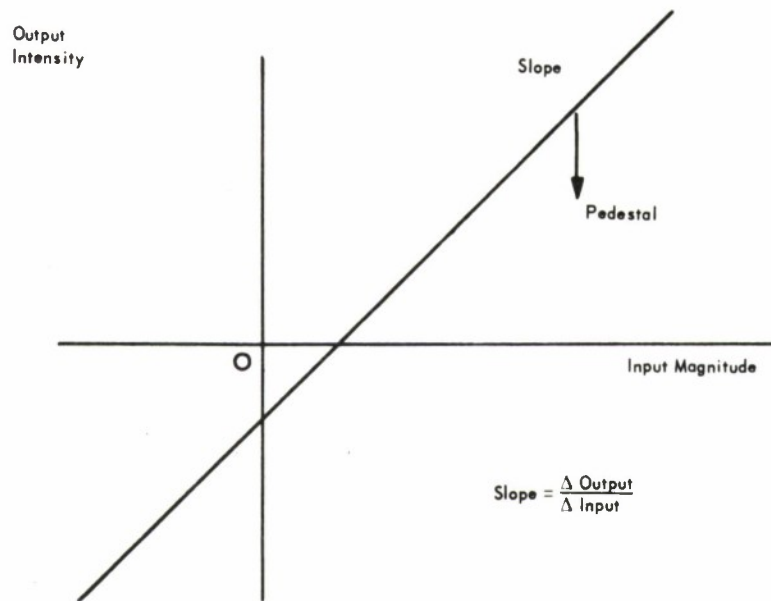
Figure 3-24. Linear Display Scaling Control
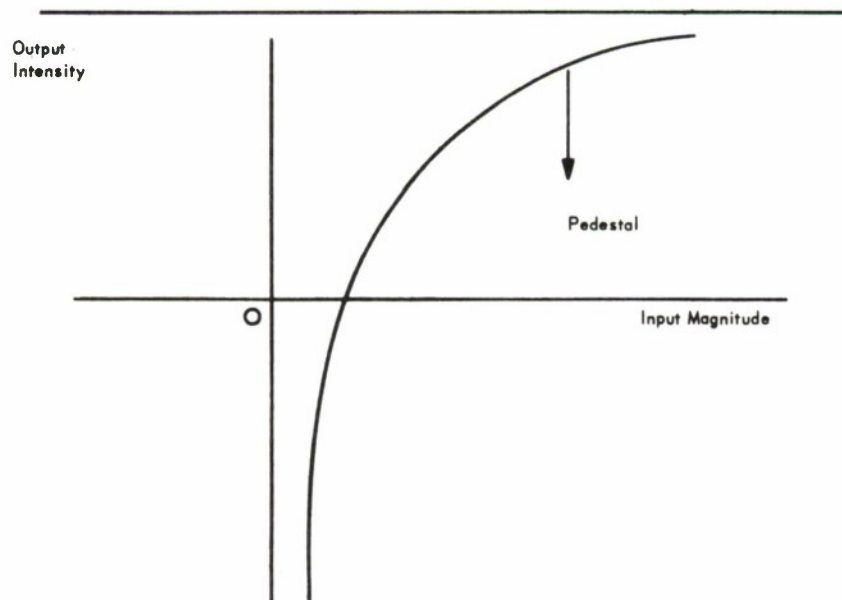
Figure 3-25. Logarithmic Display Scaling Control

arrival for both the filtered and unfiltered LASA beams for the Earthquake and the filtered beams for Longshot are shown in Figure 3-26. A third-order Butterworth bandpass filter was used for both events. The bandpass used for the Earthquake was 0.7 to 1.4 Hz, while the bandpass used for Longshot was 0.9 to 1.4 Hz. A photograph of the neighboring beam presentation for unfiltered LASA beams for Longshot has not been included; however, it would be very similar to the filtered presentation. The fundamental difference between the Earthquake and Longshot display presentations can be attributed to the different frequency spectrum of the signals. Their signal spectra are shown in Section 3.8.5.

To further demonstrate the effect of signal frequency on the neighboring beam pattern, Figure 3-27 shows photographs of the steady-state display presentation for four reference signals from 0.5 Hz to 2.0 Hz. Time delays used for forming these beams are the same as those used for Longshot; therefore, the effect of the LASA array geometry is included in the beam pattern.

The data record preceding Longshot on the raw data tapes contains a number of noise pulses, corresponding to a single time sample, scattered throughout the array. These pulses vary in magnitude up to greater than 20 dB above the maximum value of the seismometer channel output. Although the large magnitude of these pulses would permit their removal during processing, the display presentation they produced is included to demonstrate the capability of discriminating between noise pulse and seismic events. The filtered LASA beam, as a function of time, containing outputs resulting from both the noise pulses and Longshot is shown in Figure 3-28. While the LASA beam outputs appear similar, the display presentations are quite different. The noise pulses produce a pattern which moves across the display as demonstrated by the series of photographs in Figures 3-29 and 3-30. The time interval between photographs is approximately two seconds. Two phases of the pulse pattern are present. The first phase, shown in Figure 3-29, moves across the display from left to right, while the second phase moves from the bottom to the top. Motion across the display does not occur for either Longshot or the Earthquake. The long duration of the noise pulse pattern is a result of the time delay differences for adding signals from different subarrays, and the time response of the filter.
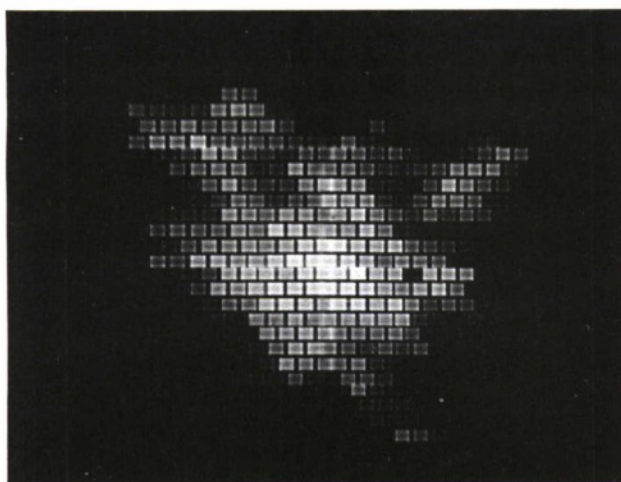
Langshat Filtered, Third-Order Butterwarth
Bandpass, 0.9 ta 1.4 Hz
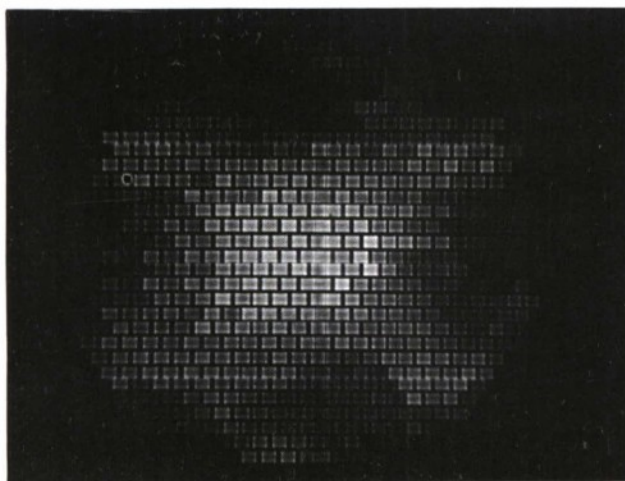
Earthquake Unfiltered
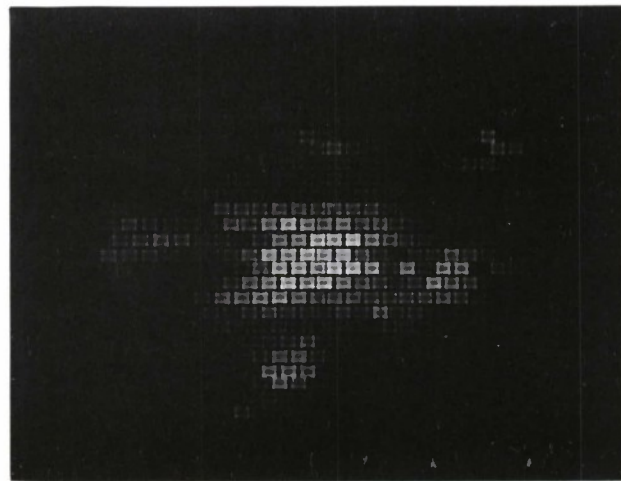
Earthquake Filtered, Third-Order Butterworth
Bandpass, 0.7 to 1.4 Hz

Figure 3-26. Beam Pattern Display, First Arrivals
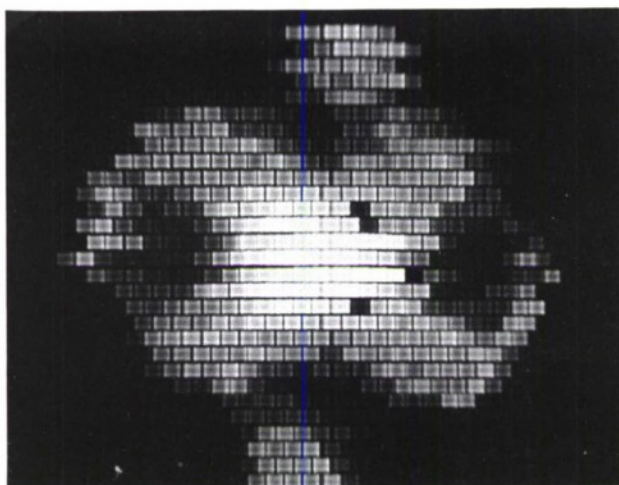
.5 Hz
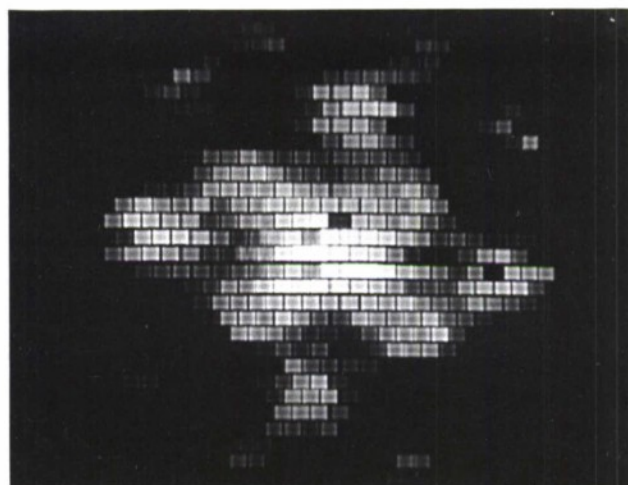
.75 Hz
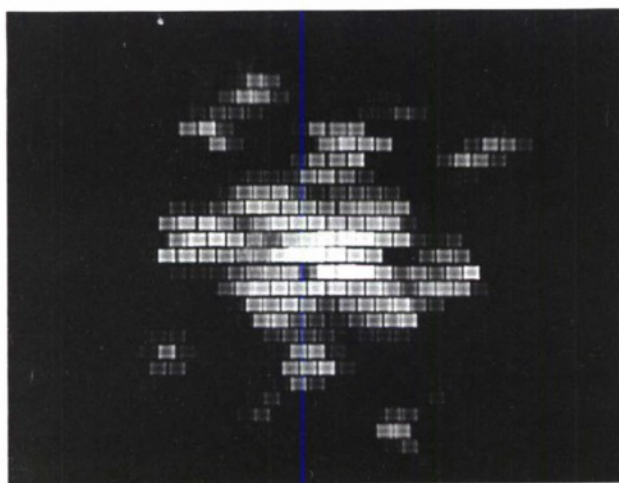
1.0 Hz
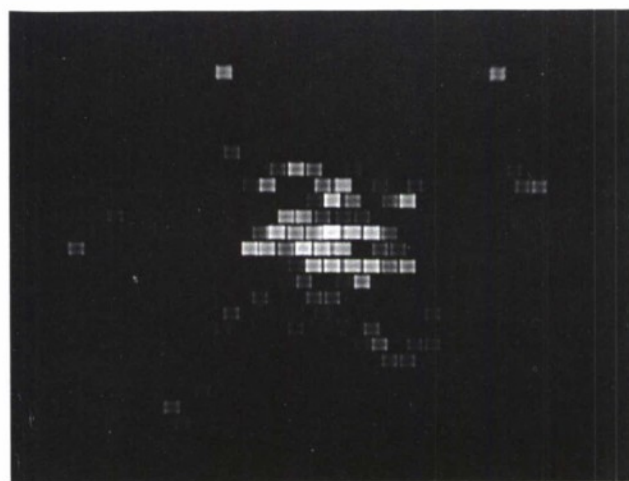
2.0 Hz

Figure 3-27. Reference Signal Display

Longshot

Noise Pulse

Figure 3-28.   Filtered LASA Beam for Scaled Longshot Event
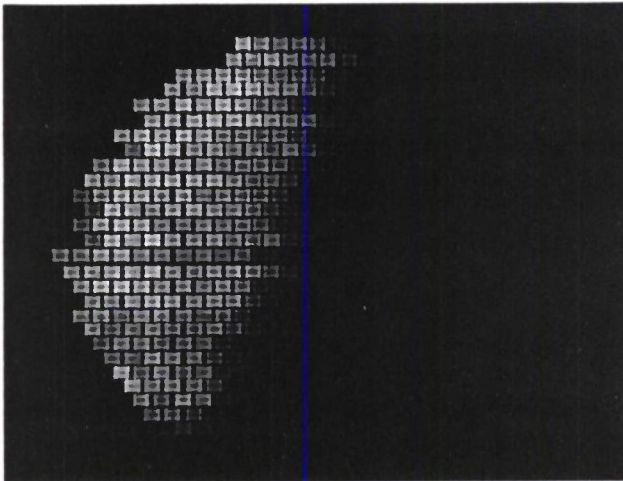
(a)
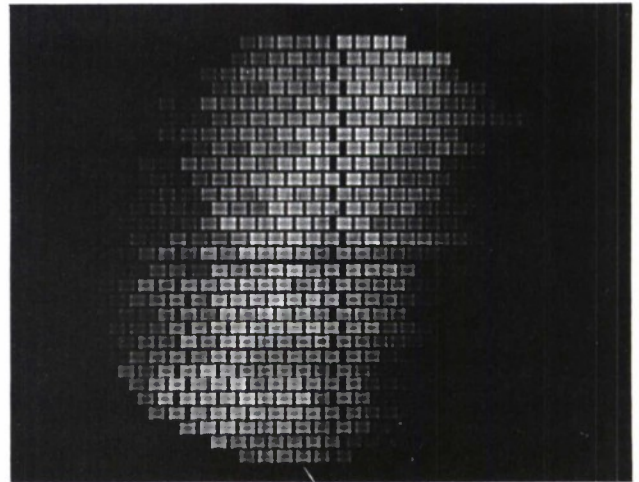
(b)
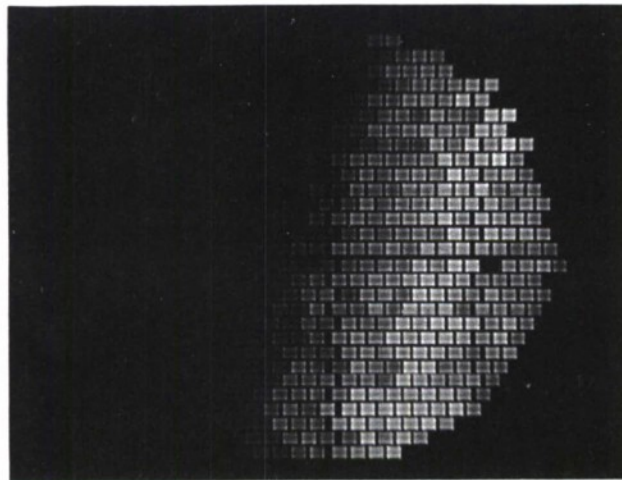
(c)

Figure 3-29. First Phase of Noise Pulse Response
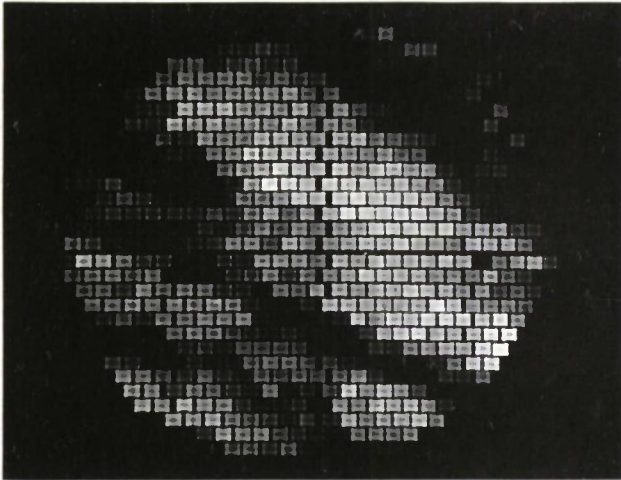
(a)

(b)

(c)

Figure 3-30. Second Phase of Noise Pulse Response

3.7 DIGITAL FILTERING

Among the topics discussed in this particular part of Section 3 are the z-transform treatment of the recursive form of digital filtering and attendant stability considerations (Section 3.7.1). To provide a standard method of synthesizing filters for use in data analysis, the lowpass, highpass, bandpass, and bandreject Butterworth and Tschebyscheff filter types are used. These filter formulations are given in Section 3.7.2. In Sections 3.7.3 and 3.7.4 error considerations and precision requirements are indicated; a number of examples demonstrating the techniques are given in Section 3.7.5. The concluding paragraphs contain some comments on technique limitations and certain extensions. A description of the corresponding computer programs is given in Section 4.4.

The recursive form of the digital filter (references 1, 2, and 3) is given as

$$y_n = \sum_{m=0}^{M} a_m x_{n-m} - \sum_{m=1}^{M} b_m y_{n-m}, \tag{3.18}$$

where x_n and y_n are the input and output quantities, respectively, at the sampling instants n; M is the filter degree; and a_m and b_m are constants. Equation (3.18) may be rewritten [6,7] in the one-sided z-transform notation

$$\frac{Y(z)}{X(z)} = H(z) = \frac{A(z)}{1 + B(z)}, \tag{3.19}$$

where

$$A(z) = \sum_{m=0}^{M} a_m z^{-m} \tag{3.20}$$

and

$$B(z) = \sum_{m=1}^{M} b_m z^{-m}. \tag{3.21}$$

Here z = exp (sT), where s is the Laplace transform complex frequency variable, and T is the sample period in seconds. Of particular interest are the transient and steady-state filter responses.

From Equation (3.19) the filter's amplitude frequency response is

$$|H(\omega)| = 10\log_{10}\left(\frac{P^2+Q^2}{R^2+S^2}\right) \quad dB;$$ (3.22)

the phase response is

$$\phi_H(\omega) = \arctan\left(\frac{PS-QR}{PR+QS}\right) \quad radians,$$ (3.23)

where

$$P = \sum_{m=0}^{M} a_m \cos m\omega T, \qquad R = 1 + \sum_{m=1}^{M} b_m \cos m\omega T,$$

$$Q = \sum_{m=0}^{M} a_m \sin m\omega T, \qquad S = \sum_{m=1}^{M} b_m \sin m\omega T,$$ (3.24)

and ω is the frequency of interest in radians per second.

Defining G(z) as

$$G(z) = \frac{1}{1 + B(z)},$$ (3.25)

the frequency response of the filter denominator is

$$|G(\omega)| = -10\log_{10}(R^2+S^2) \quad dB,$$ (3.26)

and the phase is

$$\phi_G(\omega) = \arctan(S/R) \quad radians.$$ (3.27)

The unit impulse response of the filter is

$$h(nT) = c_n, \tag{3.28}$$

where

$$\sum_{n=0}^{\infty} c_n z^{-n} = \frac{\displaystyle\sum_{m=0}^{M} a_m z^{-m}}{1 + \displaystyle\sum_{m=1}^{M} b_m z^{-m}}. \tag{3.29}$$

The unit impulse response of the denominator of the filter is

$$g(nT) = d_n, \tag{3.30}$$

where

$$\sum_{n=0}^{\infty} d_n z^{-n} = \frac{1}{1 + \displaystyle\sum_{m=1}^{M} b_m z^{-m}}. \tag{3.31}$$

Application of the final value theorem to Equation (3.19) yields the steady-state filter performance for a step input,

$$y_{\infty}^{H} = \sum_{n=0}^{\infty} c_n = \frac{\displaystyle\sum_{m=0}^{M} a_m}{1 + \displaystyle\sum_{m=1}^{M} b_m}, \tag{3.32}$$

and for the filter denominator,

$$y_{\infty}^{G} = \sum_{n=0}^{\infty} d_n = \frac{1}{1 + \displaystyle\sum_{m=1}^{M} b_m}. \tag{3.33}$$

A useful measure (reference 6) of the filter output may be obtained by noting that the sum of the squares of the sampled sequence, $f(nT)$, is

$$S_f^2 = \sum_{n=0}^{\infty} [f(nT)]^2 = \frac{1}{2\pi j} \oint_{\Gamma} F(z) F(z^{-1}) \frac{dz}{z}, \qquad (3.34)$$

where $F(z)$ is the one-sided z-transform of $f(t)$. If the singularities of $F(z)$ lie within the contour Γ, Equation (3.34) may be evaluated by the residue method. It is often convenient to consider the sum of the squares of the filter's unit impulse response,

$$S_h^2 = \sum_{n=0}^{\infty} c_n^2, \qquad (3.35)$$

and the filter's denominator,

$$S_g^2 = \sum_{n=0}^{\infty} d_n^2. \qquad (3.36)$$

3.7.1 Stability and Transformation

Stability considerations here are limited to linear systems and restricted to requiring bounded outputs from bounded inputs at each sampling instant.

It can be shown (reference 6) that the bound criterion is satisfied if the impulsive response, $h(nT)$, of the filter, $H(z)$, is

$$H(z) \leq \sum_{n=0}^{\infty} |h(nT)| \; |z^{-n}| < \infty. \qquad (3.37)$$

If in Equation (3.19) the poles of $H(z)$ are denoted z_{ℓ}, then

$$1 + B(Z) = \prod_{\ell=1}^{m} (z + z_{\ell}) \;, \qquad (3.38)$$

3-84

and stability is assured if

$$|z_\ell| < 1.$$

Consider the bilinear transformation[8]

$$z = \frac{1+W}{1-W},$$ (3.39)

where the real and imaginary components are

$$z = x + jy.$$ (3.40)

By manipulation, the real part of W is

$$\text{Re}\left\{W\right\} = \frac{|z|^2 - 1}{|z|^2 + 2x + 1}.$$ (3.41)

If the magnitude of z is less than unity, the real part of W is always negative; conversely, if the real part of W is negative, z will be less than unity.

Conversion of continuous systems to sampled systems can be obtained by the above mentioned bilinear transformation. If the poles of the continuous system are restricted to the left-half plane (i.e., $\text{Re}\{W\} < 0$), stability under the transformation is preserved. In addition, the imaginary part of W is scaled as follows:

$$V \equiv \text{Im}(W) = \tan\frac{\omega T}{2}$$ (3.42)

where V is the scaled frequency variable.

3.7.2   Filter Formulations

This section gives the filter formulation and the method for specifying the lowpass, highpass, bandpass, and bandreject filter types.

The form used is

$$H(z) = \sqrt{L} \prod_{\nu=1}^{k} \frac{K_{\nu}(A_{\nu}z^2 + B_{\nu}z + 1)}{C_{\nu}z^2 + D_{\nu}z + E_{\nu}}$$ (3.43)

where

$$\nu = 1, 2, 3, ---, k.$$

Equation (3.43) may be expanded in the form of Equation (3.19) as follows:

$$H(z) = \frac{\displaystyle\sum_{m=0}^{M} a_m z^{-m}}{1 + \displaystyle\sum_{m=1}^{M} b_m z^{-m}},$$ (3.44)

where

$$m = 0, 1, 2, ---, M,$$

and where M is the degree of the sampled filter.

For the lowpass and highpass filter types, the 3 dB cutoff frequency is denoted as ω_c; for the bandpass and bandreject types, the 3 dB cutoff frequencies are denoted as ω_1 and ω_2 ($\omega_1 < \omega_2$). The usual relationships for bandwidth, center frequency, and Q are as follows:

$$\Delta\omega = \omega_2 - \omega_1, \quad \omega_0^2 = \omega_1\omega_2 \text{ and } Q = \frac{\omega_0}{\Delta\omega} .$$ (3.45)

The bilinear transformation scales the continuous frequency variable to the sampled frequency variable, V, as follows:

1. Lowpass and highpass

$$V_c = \tan\frac{\omega_c T}{2}$$ (3.46)

2. Bandpass and bandreject

$$V_1 = \tan\frac{\omega_1 T}{2}, \qquad\qquad V_0^{\,2} = V_1 V_2$$

$$V_2 = \tan\frac{\omega_2 T}{2}, \qquad\qquad \Delta V = (1+V_0^{\,2})\tan\frac{\Delta\omega T}{2}. \tag{3.47}$$

For the Butterworth filter[9]

$$W\nu = \exp\left[j\pi(2\nu+k-1)/2k\right] \tag{3.48}$$

where

$$\nu = 1,2,3,---k,$$

and where k is the order of the continuous filter. Set $L = 1$ and use the appropriate set of coefficients listed in Table 3-19. The frequency scaler X in Table 3-19 should be set to unity when using Butterworth filters.

The peak-to-peak ripple amplitude for the Tschebyscheff filter is

$$r = 10\log_{10}(1+\epsilon^2)\ dB, \tag{3.49}$$

where ϵ is a parameter of the filter. Two cases are considered: $|H(\omega)| \le 1$ denoted as T_ϵ and $< |H(\omega)| > \approx 1$ in the band of specification denoted as T_0.

For the Tschebyscheff filter (reference 9)

$$W_\nu = -\sin\frac{\pi\nu}{2k}\sinh\phi + j\cos\frac{\pi\nu}{2k}\cosh\phi, \tag{3.50}$$

where

$$\nu = 1,3,5,---2k-1$$

where k is the order of the continuous filter, and where

$$\left.\begin{array}{c}\cosh\phi\\[4pt]\sinh\phi\end{array}\right\} = \frac{\left[\sqrt{\dfrac{1}{\epsilon^2}+1}+\dfrac{1}{\epsilon}\right]^{1/k} \pm \left[\sqrt{\dfrac{1}{\epsilon2}+1}+\dfrac{1}{\epsilon}\right]^{-1/k}}{2}. \tag{3.51}$$

3-87

Table 3-19. Filter Coefficients

Parameters

Type	K_υ	A_υ	B_υ	C_υ	D_υ	E_υ
Lowpass	$\dfrac{W_\upsilon V_c}{W_\upsilon V_e - X}$	0	1	0	1	$\dfrac{W_\upsilon V_c + X}{W_\upsilon V_c - X}$
Highpass	$\dfrac{W_\upsilon X}{W_\upsilon X - V_c}$	0	1	0	1	$\dfrac{V_c + W_\upsilon X}{V_c - W_\upsilon X}$
Bandpass	$\dfrac{\Delta V W_\upsilon}{\Delta V W_\upsilon - X(1 + V_o^2)}$	1	0	1	$\dfrac{2(V_o^2 - 1) X}{(1 + V_o^2) X - \Delta V W_\upsilon}$	$\dfrac{(1 + V_o^2) X + \Delta V W_\upsilon}{(1 + V_o^2) X - \Delta V W_\upsilon}$
Bandreject	$\dfrac{(1 + V_o^2) X}{(1 + V_o^2) X - \Delta V/W_\upsilon}$	1	$\dfrac{2(V_o^2 - 1)}{V_o^2 + 1}$	1	$\dfrac{2(V_o^2 - 1) X}{(1 + V_o^2) X - \Delta V/W_\upsilon}$	$\dfrac{(1 + V_o^2) X + \Delta V/W_\upsilon}{(1 + V_o^2) X - \Delta V/W_\upsilon}$

If T_ϵ (first case), set $M = L = 1$, when k is odd,
or $M = 1$ and $L = (1 + \epsilon^2)^{-1}$, when k is even; $\hspace{3cm}$ (3.52)

if T_0 (second case), set $M = L = \sqrt{1 + \epsilon^2}$, when k is odd
or $M = \sqrt{1 + \epsilon^2}$ and $L = (1 + \epsilon^2)^{-1/2}$ when k is even, $\hspace{1.5cm}$ (3.53)

and calculate

$$X = \cosh\left[\frac{1}{k}\cosh^{-1}\sqrt{\frac{2M-1}{\epsilon}}\right] \hspace{2cm} (3.54)$$

The remaining values of the coefficients of Equation (3.43) are listed in Table 3-19.

3.7.3 Error Considerations

The use of a digital machine to implement the digital filter introduces not only a sampling error but also a quantization error. Denoting the output of Equation (3.18) as $y_n + \delta y_n$, it can be shown for sufficiently small errors that

$$\delta y_n = \epsilon_n + \sum_{m=0}^{M} a_m \delta x_{n-m} - \sum_{m=1}^{M} b_m \delta y_{n-m}, \hspace{2cm} (3.55)$$

where ϵ_n is the roundoff error[10] and δx_n is the error in the input. In z-transform notation

$$\delta Y(z) = G(z) E(z) + H(z) \delta X(z), \hspace{2cm} (3.56)$$

where $H(z)$ and $G(z)$ are as defined in Equations (3.19) and (3.25), respectively.

Under the ergodic assumption, the autocorrelation function of the sampled stationary sequence, $f(nT)$, is

$$R_f(kT) = \lim_{N\to\infty} \frac{1}{2N+1} \sum_{n=-N}^{N} [f(nT) - m_f] \; [f(nT+kT) - m_f], \qquad (3.57)$$

where m_f is the mean of $f(t)$. The sampled spectral density is the two-sided z-transform of the autocorrelation function

$$\Phi_f(z) = \sum_{k=-\infty}^{\infty} R_f(kT) \; z^{-k} = \frac{1}{T} \sum_{k=-\infty}^{\infty} \Phi_f(s - \frac{2\pi k}{T}). \qquad (3.58)$$

The right side of Equation (3.58) demonstrates the folding effect of sampling. If the units of $f(t)$ are L, the power spectral density is usually taken as

$$S(\omega) = \frac{\Phi(\omega)}{\pi} \qquad L^2 - \text{sec/rad}. \qquad (3.59)$$

The inverse transform of Equation (3.58) is

$$R_f(kT) = \frac{1}{2\pi j} \oint \Phi_f(z) \; z^{k-1} \; dz. \qquad (3.60)$$

Note that $\Phi(z)$ is even, but $R(kT)$ is even and real. $\Phi(z)$ can be considered in two parts. Denote $\Phi^+(z)$ as that part of $\Phi(z)$ which contains the poles of $\Phi(z)$ inside the unit circle ($k \geq 0$), and $\bar{\Phi}(z)$ as that part of $\Phi(z)$ which contains the poles of $\Phi(z)$ outside the unit circle ($k \leq 0$). Then $\Phi(z)$ can be factored as

$$\Phi(z) = \Phi^+(z) \; \bar{\Phi}(z). \qquad (3.61)$$

Equation (3.60) is evaluated as

$$R_f(kT) = \sum_{\text{poles of } \Phi_f^+(z)} \text{Res} \left[\Phi_f(z) \; z^{k-1} \right], \quad k \geq 0$$

and

$$R_f(kT) = \sum_{\text{Poles of } \Phi_{\bar{f}}(z)} \text{Res} \left[\Phi_{\bar{f}}(z) z^{k-1} \right] \quad , \quad k \leq 0 \tag{3.62}$$

where the notation used means to evaluate the sum of the residues of $z^{k-1} \Phi_f(z)$ at the poles of $\Phi_{\bar{f}}^+(z)$ for positive time, and the sum of the residues of $z^{k-1} \Phi_f(z)$ at the poles of $\Phi_{\bar{f}}^-(z)$ for negative time.

When k = 0, Equation (3.57) shows that the autocorrelation function reduces to the mean square value of the sampled sequence

$$R_f(0) = \frac{1}{2\pi j} \oint_{\Gamma} \Phi_f(z) \frac{dz}{z} = \lim_{N \to \infty} \frac{1}{2N+1} \sum_{n=-N}^{N} [f(nT) - m_x]^2, \tag{3.63}$$

where the contour Γ is the unit circle.

The spectral density of the filter output error, δy_n, may be related to the inputs as

$$\Phi_y(z) = |G(z)|^2 \Phi_e(z) + |H(z)|^2 \Phi_x(z), \tag{3.64}$$

where $\Phi_e(z)$ is the spectral density of e_n, $\Phi_x(z)$ is the spectral density of δx_n, and G(z) and H(z) are as defined in Equation (3.56).

If both e_n and δx_n in Equation (3.55) are uncorrelated from sample to sample, the bias in δy_n is

$$\overline{\delta y} = m_x \sum_{n=0}^{\infty} c_n + m_e \sum_{n=0}^{\infty} d_n, \tag{3.65}$$

where the mean is the expected value,

$$E[e_n] = m_e$$

and
                                                                                    (3.66)

$$E[\delta x_n] = m_x;$$

and the variance in δy_n is

$$\overline{\delta y^2} = \sigma_x^2 \sum_{n=0}^{\infty} c_n^2 + \sigma_e^2 \sum_{n=0}^{\infty} d_n^2,$$ (3.67)

where the square of the standard deviation is the variance

$$E[e_n^2] = \sigma_e^2$$

and
                                                                                    (3.68)

$$E[\delta x_n^2] = \sigma_x^2 .$$

   In the model characterized by equations (3.65) and (3.67), the sampling independence assumption may be inadequate. For cascade digital filters, sample-to-sample coherence, no doubt, exists. Consider the system shown in Figure 3-31, where filter number 1 is sampled with period T/n ($n>0$) and filter number 2 is synchronously sampled with period T. The effect in the output, $r(kT)$, because of the input, $p(kT/n)$, and the roundoff errors generated in filter 1, $e(kT/n)$, and in filter 2, $f(kT)$, are of interest. Denote z_n as the z-transform variable of the filter sampled with period T/n (filter 1); then Equation (3.63) shows that the mean square value of $r(kT)$ is

$$R_r(0) = \frac{1}{2\pi j} \oint_{\Gamma} \Phi_r(z) \frac{dz}{z} = \frac{T}{2\pi} \int_{-\omega_s/2}^{\omega_s/2} \Phi_r(e^{j\omega T}) \, d\omega ,$$ (3.69)
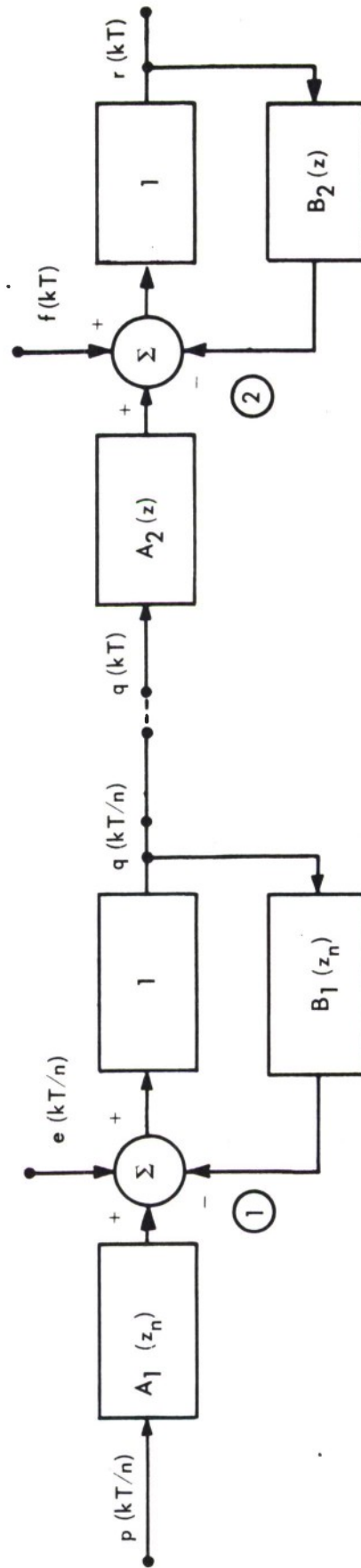
Figure 3-31. Cascade Filter

where the contour, Γ, is the unit circle, and ω_s is the sampling frequency in radians per second.

Now,

$$\Phi_r(z) = |G_2(z)|^2 \Phi_f(z) + |H_2(z)|^2 \Phi_q(z) \qquad (3.70)$$

and

$$\Phi_q(z_n) = |G_1(z)|^2 \Phi_e(z_n) + |H_1(z_n)|^2 \Phi_p(z_n) . \qquad (3.71)$$

Filter number 1 may be considered as n channels, each operating with period T, where the nth channel is delayed by (n-1)T seconds to the extent that the sum of the channel outputs is equivalent to the system operating with period T/n. Superposition permits each channel to be separately interconnected to n identical filters number 2. The outputs of each combined channel, all operating synchronously with period T, can be summed to yield an equivalent output. However, the spectral density of the multirate system may be evaluated in terms of the single rate system as follows:

$$\Phi_q(z) = \frac{1}{2\pi j} \oint_\Gamma \frac{z \Phi(z_n) dz_n}{'z_n(z - z_n^n)} \qquad (3.72)$$

Since $|z^n z^{-1}| < 1$, the contour path need only include the poles of $z_n^{-1} \Phi(z_n)$; therefore the validity of $\Phi_q(z)$ is restricted to the regions satisfying the inequality.

Equation (3.69) can be evaluated in terms of the sampled power spectral density of the sampled sequence r(nt) in that

$$R_r(0) = 2\pi T \int_0^{1/2T} S_r^*(f) \, df \qquad (3.73)$$

where

$$S_r^*(f) = S_r(z), \quad \text{for} \quad z = \exp(2\pi jfT) \qquad \text{and}$$

f is the frequency of interest in Hz.

3.7.4   Precision Requirements

Implementation of the digital filter depends on the data word structure of the particular machine of interest. In floating-point arithmetic, large word-lengths are obtained. In fixed-point arithmetic, execution speed is increased over floating-point arithmetic, but the dynamic range of the variables is restricted. Here, we are concerned with fixed-point arithmetic requirements and limitations necessary to implement Equation (3.18) in a digital machine.

In fixed-point binary arithmetic, the maximum value of the word containing a binary point is essentially $2^{\overline{q}_L}$, where $\overline{q}_L$ is the number of bit positions to the left of the binary point (numbers greater than or equal to unity). The precision of the word is $2^{-\overline{q}_R}$, where $\overline{q}_R$ is the number of bit positions to the right of the binary point (for numbers less than unity). If $\overline{q}_T$ is the data word length independent of sign, then the word is restricted as follows:

$$\overline{q}_L + \overline{q}_R = \overline{q}_T \tag{3.74}$$

In the following paragraphs, the requirements for $\overline{q}_L$ and $\overline{q}_R$ will be determined in terms of the filter parameters. (The bar notation is used here to denote integer values.)

For sufficiently small errors in the coefficients a and b, the relative error in the frequency response is

$$|\Delta H(\omega)| \leq (20 \log_{10} e) \left[\frac{\displaystyle\sum_{m=0}^{M} \delta a_m}{|A(z)|} + \frac{\displaystyle\sum_{m=1}^{M} \delta b_m}{|1 + B(z)|} \right] \text{ dB}, \tag{3.75}$$

where $z = \exp(j\omega T)$ and δa_m and δb_m are the coefficient errors.

For the class of filters considered here, the a_m coefficients are related to each other as binomial numbers; therefore the relative values of the a_m coefficients can be instrumented exactly. The resulting error is one of scale which, if not arithmetically small enough to be neglected, is known and can be

incorporated into the overall process scaling in an inconsequential manner.

However, an error in the b_m coefficients affects the relative accuracy of $|H(\omega)|$. If the error contributions of each coefficient are limited for all frequencies to ΔH_q in dB, then the precision requirement is satisfied if

$$q_R \geq \log_2 \frac{20 \, \overline{G} \log_{10} e}{\Delta H_q},\qquad (3.76)$$

where $\overline{G}$ is the maximum value of $|G(\omega)|$ defined in Equation (3.26).

Generally, the b_m coefficients will have magnitudes which are both greater and less than unity; therefore, the dynamic range requirement will be satisfied if

$$q_L \geq \log_2 \left[|C| + 1 - \sum_{r=1}^{\overline{q}_R} 2^{-r} \right],\qquad (3.77)$$

where C is the maximum value of the coefficients a and b, which are greater than one.

The input, x, may be expressed as

$$x = 2^{q_x} Q,\qquad (3.78)$$

where Q is the scaling of x. To prevent saturation in the input register,

$$q_x \leq \log_2 (2^{\overline{q}_T} - 1).\qquad (3.79)$$

Since the steady-state transfer characteristics of the filters under consideration limit the output to near or less than unity gain, the output scaling is usually taken equal to the input scaling. Using the impulse response as an estimate of the maximum transient response, the output register will not saturate if

$$\widehat{q}_x \leq \log_2 \frac{2^{\overline{q}_T} - 1}{\displaystyle\sum_{n=0}^{\infty} |c_n|}.\qquad (3.80)$$

To avoid undesirable transients in the filter output, the instrumentation should yield an output equivalent to $2^{\overline{q}_T} - 1$, when $q_x > \widehat{q}_x$.

The effect of roundoff errors generated by the fixed-point two's-complement arithmetic implementation of the digital filter is of interest. If sample-to-sample independence is as expressed in equations (3.65) and (3.67), the total mean square error in the output (y_n) is

$$E_y^2 = \overline{\delta y^2} + \overline{\delta y}^2 . \tag{3.81}$$

It is desirable that the internally generated roundoff error contribute a negligible error to the process. If we assume that the input quantization error has a uniform distribution with a total range of 1 bit, the total mean square value of the input is

$$E_x^2 = \sigma_s^2 + \frac{Q^2}{12} + (m_s + \frac{Q}{2})^2 , \tag{3.82}$$

where m_s and σ_s are the mean and standard deviations of the input signal. If the recursive filter is implemented in single-precision arithmetic, the word length needs to be extended an amount q_B bits beyond Q to limit the roundoff error to a specified amount. The number of bits q_B can be expressed as

$$q_B \geq \frac{1}{2} \log_2 \frac{\beta \left[(2M + 1) \sum_{n=0}^{\infty} d_n^2 + 3 \left\{ (2M + 1) \sum_{n=0}^{\infty} d_n \right\}^2 \right]}{1 + \frac{12\sigma_s^2}{Q^2} \sum_{n=0}^{\infty} c_n^2 + 3 \left[\left(1 + \frac{2m_s}{Q} \right) \sum_{n=0}^{\infty} c_n \right]^2} , \tag{3.83}$$

where $\gamma = 10 \log_{10} (1 + 1/\beta)$, M is the filter degree, and γ is the allowable error in dB.

The quantity of 2M + 1 in the above equation is the total number of multiply-accumulate operations required to execute Equation 3.18. Therefore, in single-precision fixed-point arithmetic, 2M + 1 roundoff errors would be committed per filter execution or sample period. It has been suggested (references 2 and 3) that double-precision arithmetic be used to execute each multiply-accumulate operation,

wherein the sum is truncated to the single-precision output before subsequent processing. This procedure requires only single-precision input values, and reduces the number of roundoff errors committed per filter execution to unity. The processing algorithms described in Section 2.5, incorporate this technique.

As in Equation (3.78), the quantity E_x can be expressed as

$$q_E = \log_2 E_x/Q. \tag{3.84}$$

If $q_B \leq q_E + q_R$, the precision error dominates. However, if $q_B > q_E + q_R$ the roundoff error dominates. Either situation can be accommodated by properly selecting the binary-point position in the coefficient data word, or by scaling the arithmetic process. In the former case, q_R is set so that $q_E + q_R$ is forced to be greater than q_B, if the data word restriction (Equation 3.74) is satisfied. However, scaling the arithmetic process requires scaling either the input or the coefficients, or both. Here the instrumentation must retain the scaled values of y_n for the next sample period, and rescale y_n to the desired output scaling before passing the output.

The double-precision sum in terms of the bit assignments will not saturate if

$$\hat{\hat{q}}_x \leq 2\bar{q}_T + 1 + q_E - q_K - \log_2\left[|C| \, (2M + 1) \right] \tag{3.85}$$

and

$$q_K = \begin{cases} q_B & , \; q_B > q_E + q_R \\ q_R + q_E, & q_B \leq q_E + q_R \end{cases}, \tag{3.86}$$

where q_E is the binary equivalent of the total mean square error of the input signal. In the instrumentation suggested in Section 2.5, the total number of double precision bits available is 38. Therefore, the quantity $2\bar{q}_T + 1$ in Equation (3.85) can be taken as 38. In the examples given, it is taken as 31 bits.

When the signal has small statistical values compared to its quantization, q_E tends to be small. This would be the case if m_s and σ_s in Equation (3.83)

3-98

are taken to be zero. For high-degree filters and for filters with large values of C, the intermediate values of the sum may exceed the available bits. In such cases, undesirable transients would occur in the output unless special precautions were taken in the instrumentation.

If the instrumentation notes when q_X exceeds $\widehat{\widehat{q}}_X$, the dynamic range of the double-precision sum may be considerably extended simply by taking advantage of the cyclic nature of two's complement fixed-point arithmetic process. In this manner, the transients encountered in saturation can be minimized by continuing the process to completion. If at completion $q_X > \widehat{\widehat{q}}_X$, the maximum value can be denoted as the output. If $q_X \leq \widehat{\widehat{q}}_X$, q_X can be denoted as the output if $q_X \leq \widehat{q}_X$. This procedure will tend to reduce transients in the overall process, and its restrictions will be of little consequence since the filter scaling is usually such that saturation occurs only when the signal-to-noise ratio is significantly greater than unity.

3.7.5 Examples

In Section 3.8, a limited amount of data analysis results is presented. The digital filter characteristics used in the tabulated gain measurements are presented here.

The filter parameters are listed in Table 3-20. Each filter is a bandpass type filter of order three, where the numerator terms are scaled as

$$A(z) = K(1 - 3z^{-2} + 3z^{-4} - z^{-6}) . \tag{3.87}$$

The Butterworth filter is denoted as B and the Tschebyscheff filter, with 0.5 dB ripple so that $|H(\omega)| \leq 1\,(T_\epsilon)$, is denoted as T. The 3 dB frequencies are given in Hz. The allowable error is limited to 0.5 dB, $q_E = 0$, and $\overline{q}_T = 15$.

In considering the BP-B (0.9 - 1.4) filter with Q or $\frac{fo}{\Delta f} = 2.245$, we note that K = 0.002898, $q_R = 11.78$, and $q_L = 3.18$. Allowing 12 bits for $\overline{q}_R$ and 4 bits for $\overline{q}_L$, we exceed $\overline{q}_T$ by 1 bit. However, only 9 bits are required for q_B. The single-precision output may saturate when the dynamic range

Table 3-20. Filter Parameters

Type Bandwidth (Hz) Order–Sampling (Hz)	BP-B 0.6-2.0 3 10	BP-Te 0.9-3.0 3 10	BP-B 0.7-1.4 3 10	BP-B 0.8-1.6 3 10	BP-B 0.8-1.4 3 10	BP-B 0.9-1.6 3 10	BP-B 0.9-1.4 3 10	BP-Te 0.9-1.4 3 10
$f_o/\Delta f$	0.782	0.782	1.414	1.414	1.764	1.714	2.245	2.245
K	0.041877	0.077174	0.007168	0.010183	0.004751	0.007168	0.002898	0.001489
b_1	-3.238277	-1.684102	-4.150804	-3.765925	-4.118205	-3.714539	-4.081417	-4.263324
b_2	4.906697	1.964237	7.927571	6.792738	7.945605	6.772254	7.955923	8.708174
b_3	-4.502320	-1.695957	-8.752886	-7.245947	-8.927800	-7.347239	-9.092820	-10.443304
b_4	2.669547	1.365187	5.892090	4.836152	6.166726	5.036442	6.444996	7.780241
b_5	-0.949025	-0.634459	-2.292403	-1.905950	-2.479776	-2.051463	-2.677543	-3.402741
b_6	0.159769	0.233542	0.411839	0.361796	0.468312	0.411839	0.532075	0.713734
$\sum_{n=0}^{8} c_n$	0.1003×10^{-7}	0.1698×10^{-8}	0.1644×10^{-8}	0	0.1061×10^{-8}	0.5425×10^{-9}	0	0
$\sum_{n=0}^{8} d_n$	21.557	1.82	28.247	13.726	18.248	9.324	12.3750	12.373
$\sum_{n=0}^{8} c_n^2$	0.2866	0.4096	0.1456	0.1660	0.1250	0.1456	0.1043	0.0997
$\sum_{n=0}^{8} d_n^2$	187.35	7.04	2023.31	561.38	2267.98	619.74	3264.47	11296.53
$\sum_{n=0}^{8} |c_n|$	1.86	1.95	1.69	1.70	1.63	1.63	1.59	1.84
q_R	9.52	7.06	11.44	10.40	11.51	10.50	11.78	12.74
q_L	2.29	0.98	3.13	2.87	3.16	2.88	3.18	3.38
$\hat{q}_x$	14.18	14.04	14.24	14.26	14.30	14.29	14.34	14.11
$\hat{q}_x$	15.49	19.27	12.77	14.04	12.63	13.92	12.33	11.18
q_B	7.73	4.21	8.76	7.88	8.85	7.80	9.08	9.94

of the input exceeds 86 dB; the double-precision sum saturates at 74 dB. If $\overline{q}_R$ is taken as 11 bits to satisfy the data word-length requirement, the relative error in $|H(\omega)|$ is less than 1 dB, and the scaling bias is about 1.6 dB.

Consider scaling the a_m coefficients by 1 bit so that the coefficient scale is 2 K. The error in scale is reduced to 0.8 dB while the dynamic range of both the single- and double-precision words is reduced by only 6 dB.

The theoretical frequency and impulse responses of the BP-B (0.9 - 1.4) filter are shown in Figures 3-32 through 3-34. To interpret the scale of the impulse response curves, replace the normalized ordinate value 1.0 with the number after the scale slash. For example, in Figure 3-33 the first negative peak is approximately 0.50 on the normalized scale. At this point, the filter impulse response output is 0.125 (i.e., 0.25 × 0.50).

3.7.6 Comments

The filters presented are straightforward and typical for standard filtering problems. The design is synthesized in a continuous nonlinear frequency plane and transformed to the discrete process z-plane. Examination of the spectral densities given in Section 3.8 indicates that it may be necessary, in terms of system gain, to identify the filter characteristics from an ensemble of signal and noise spectral characteristics. Such a statistic may or may not be invariant in k-space. In either case, specifications of the filter in sampled space, dependent on an ensemble of signal and noise statistics, may provide optimal detection gain over a frequency band of event spectrums.

It can be seen from the figures showing the frequency and impulse responses that a considerable amount of phase distortion exists for this class of filters. In detection processing, where interest centers primarily on maximizing signal-to-noise ratio, phase distortion is permissible. However, in event processing, where interest centers on signal fidelity, the phase distortion introduced by these filters may not be tolerable. If subsequent experimental work proves this is the case, it may be desirable to introduce linear phase filters for routine event processing.
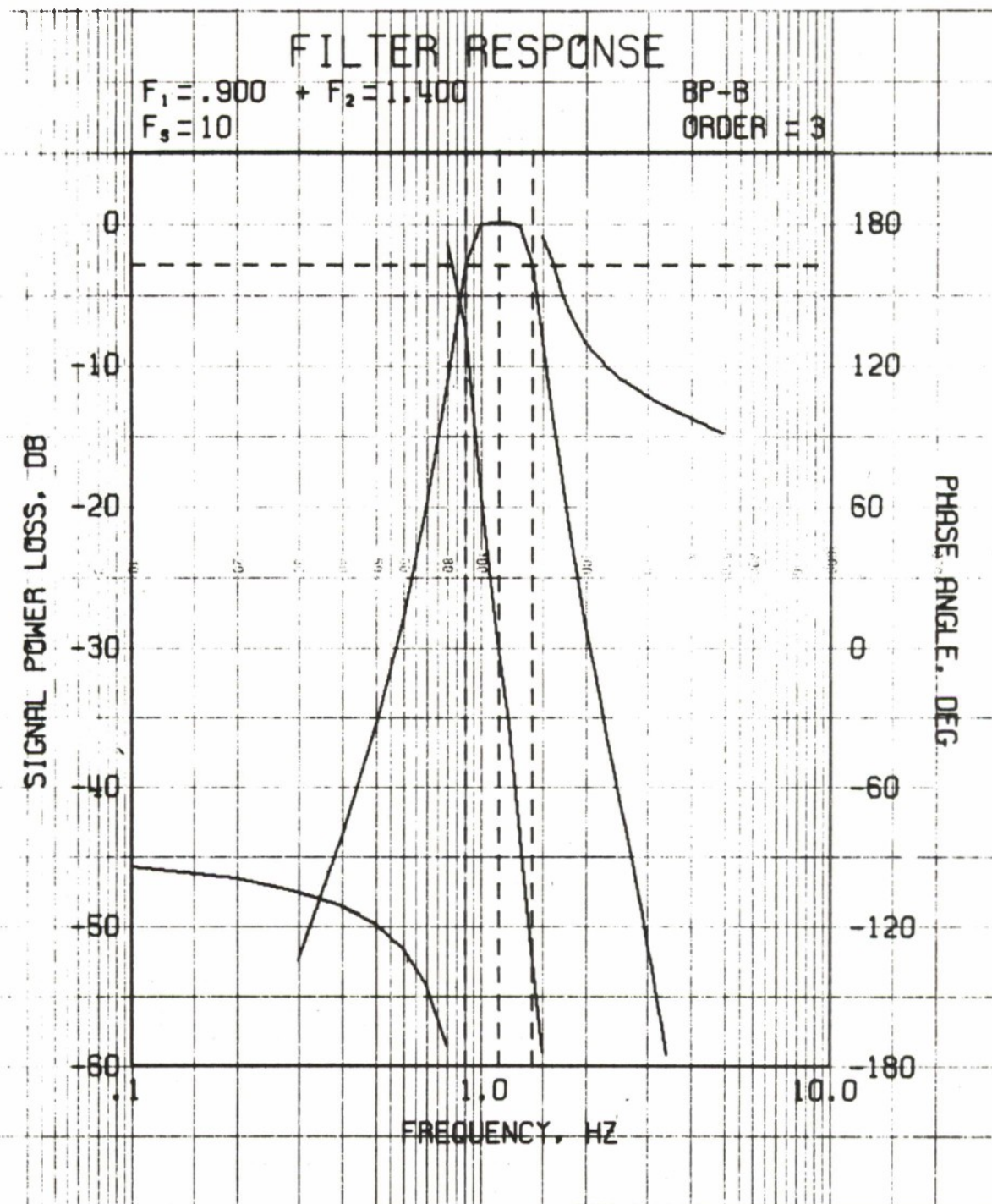
Figure 3-32. Filter Frequency Response

3-102
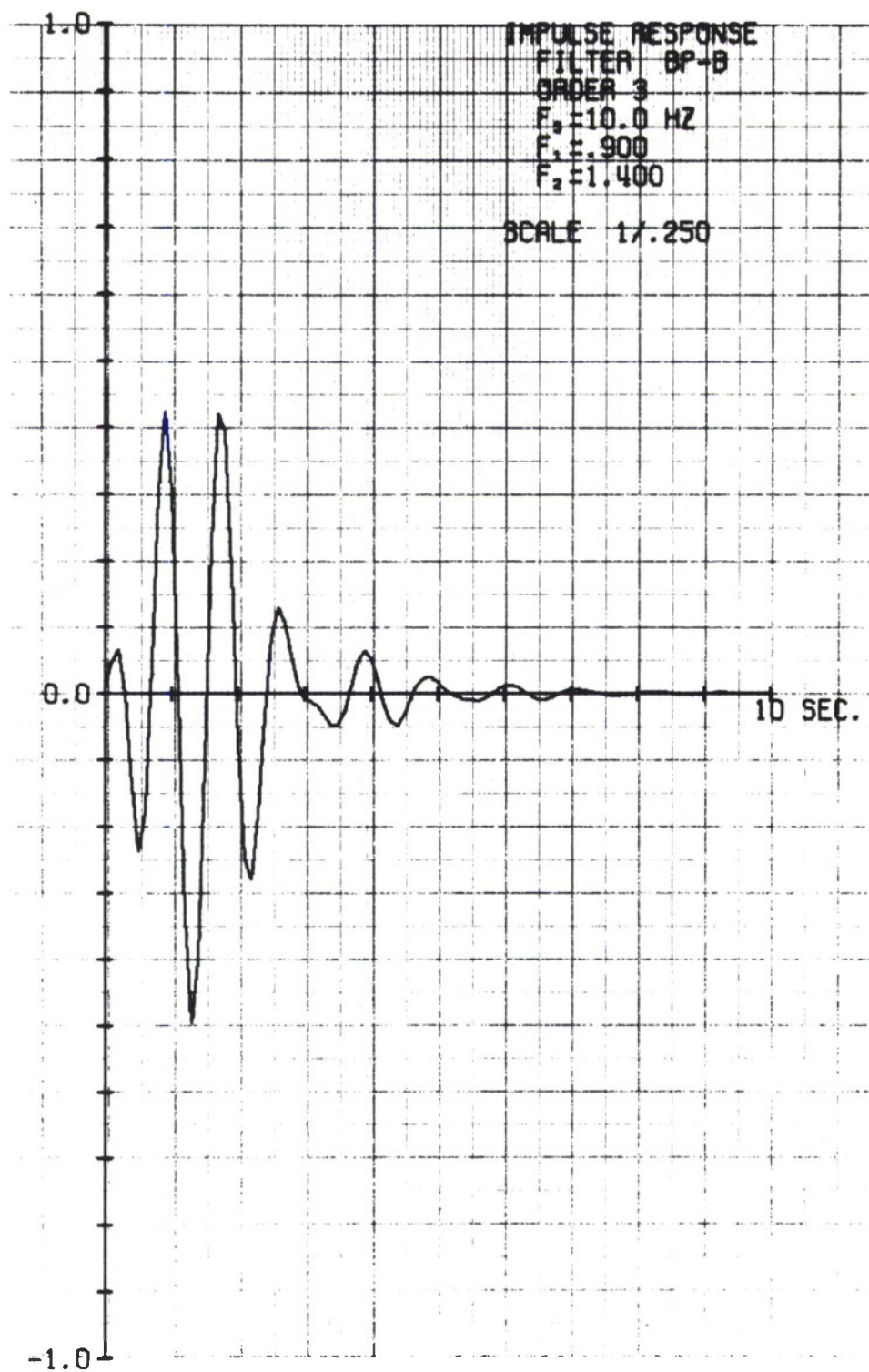
Figure 3-33. Filter Impulse Response
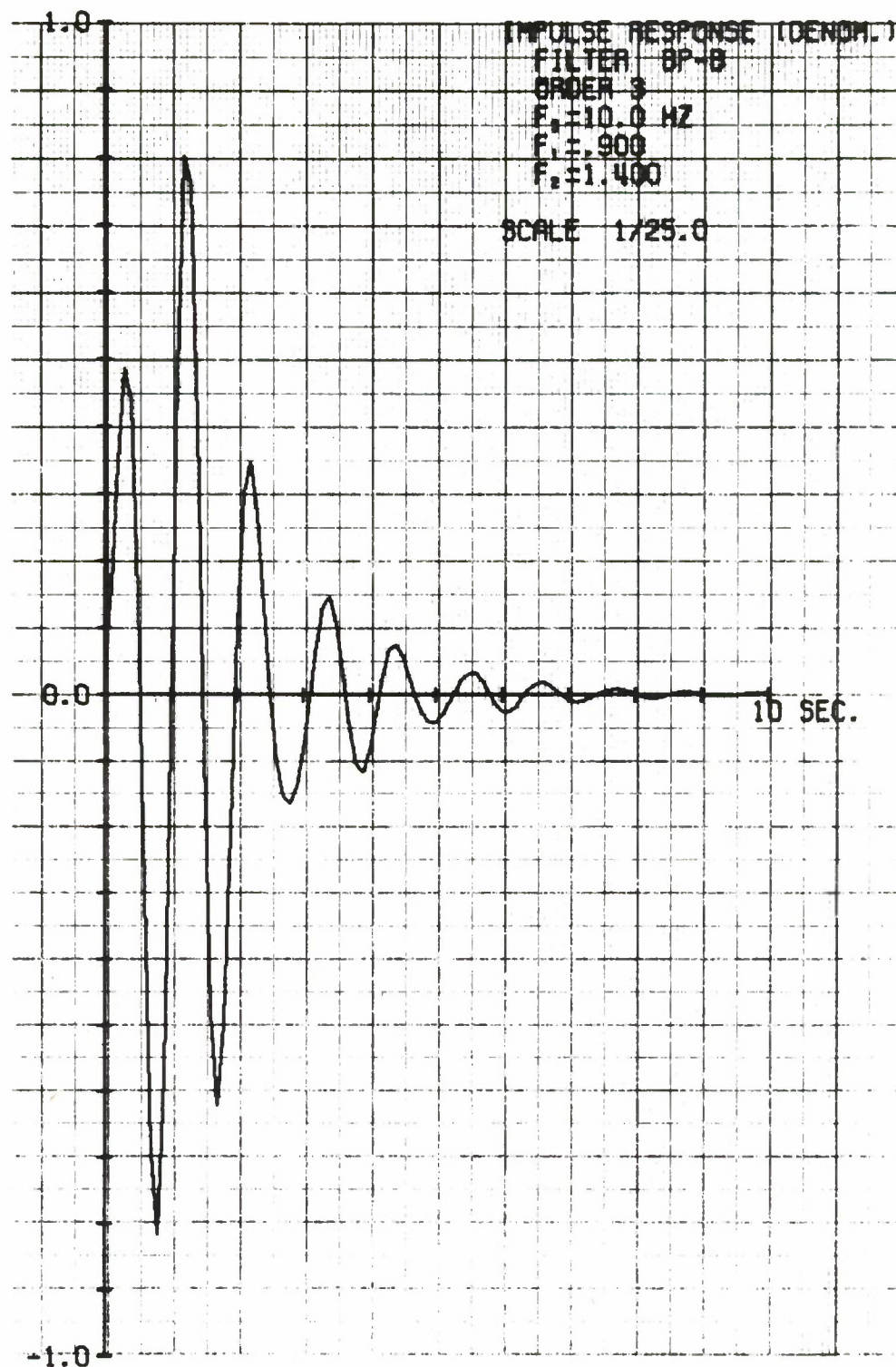
Figure 3-34. Denominator Impulse Response

3.8   DATA ANALYSIS

LASA data analysis studies were primarily concentrated on two seismic events—an underground nuclear event and an earthquake. The analysis performed can be grouped into the following five experiments:

1.   Subarray Beam Filter Analysis
2.   Post-Detection Integration Time Analysis
3.   System Gain Analysis
4.   Scaled Signal/Noise Analysis
5.   Power Spectrum Analysis

Table 3-21 provides pertinent information on the two events considered. Of the five experiments, the nuclear event Longshot provided the pertinent data for experiments 1 and 4. The remaining experiments used data associated with both events. Each of the experiments is discussed in detail.

3.8.1   Subarray Beam Filter Analysis

This experiment is a continuation of the analysis reported in Section B.3 of reference 3.

As before, the 25 seismometers of subarray B1 were conventionally beam-formed, and the sum divided by 25 to obtain the complete subarray beam. Deleting the B-ring of subarray B1 produced the partial subarray beam—the properly delayed sum of the remaining 19 seismometers with the sum divided by 19.

The phasing of the seismometers, before their addition to form the sub-array beam sums, was implemented with a resolution of 20 samples per second. The beam outputs were calculated corresponding to a real-time rate of 10 samples per second.

The complete beam, the partial beam, and the output of the center seismometer, A_0, of subarray B1 were passed through the same digital recursive filter. Noise and signal power were calculated for the three channels from which signal-to-noise ratios were computed. The noise power was obtained by averaging the squares of 850 successive samples (85 seconds) preceding the signal onset for each of the three channels. The average signal power was calculated in the same

3-105

Table 3-21. Event Identification

Longshot	Event	Earthquake
10/29/65	Date	4/8/66
21:08:35.5	LAO Arrival	01:56:40.2
Rat Island	Location	East Coast of Kamchatka
51.44°N 179.18°E	Latitude/Longitude	51.2°N 157.7°E
47.15°	Range	58.81°
304.55°	Azimuth	313.0°
6.1	Magnitude	5.9

manner, but over 50 successive samples corresponding to a 5-second interval. The slight differences noted between Table 3-22 and the table appearing in reference 3, can be attributed to the fact that the signal power reported at that time was computed over a 2.6-second interval, an interval selected to yield maximum average signal power. The signal power calculations for this report were computed over the same real-time 5-second period for each channel considered, and in most cases were not positioned to yield maximum average signal power. The signal-to-noise ratios for each channel were computed according to the definition $10 \log_{10}(S/N)$, where S is the average signal power and N is the average noise power.

The filter gain for the A_0 seismometer was defined relative to the unfiltered A_0 seismometer trace. The subarray gain for a filtered complete subarray beam and partial subarray beam was computed relative to the A_0 trace after passing it through the same filter as that used for the subarray beam. The total gain was taken as the sum of filter and array gains. The seismic noise standard deviation was defined as $\sqrt{N}$.

The results of these calculations for a number of bandpass filters—the same filters used for the table appearing in reference 3—are in Table 3-22. The filters are listed by their 3-dB bandpass, preceded by the designation "Bu" for Butterworth and "Th" for Tschebyscheff. Both fourth- and sixth-degree filter implementations are presented in the table. The Tschebyscheff filters were implemented with a 0.5 dB ripple.

The results are similar to the results reported earlier. Again the partial subarray beam outperforms the complete subarray beam by about 1 dB, except for the Tschebyscheff filter with bandpass from 0.9 Hz to 3.0 Hz. Also, the expected increase in signal-to-noise ratio, as the filter bandwidth is made narrower, is evident. An additional item of interest available in Table 3-22 and not reported earlier, is the effect of using a fourth- instead of a sixth-degree filter. Table 3-22 indicates that a loss of up to 1.5 dB in total gain in relation to a sixth-degree filter would be the result if we wished to reduce the computational burden of the filtering process by using a fourth-degree filter.

Table 3-22. Experimental Longshot Subarray B1 Data

Filter Type and Bandpass (Hz)	Noise Standard Deviation (nm)						Filter Gain (dB) for A_0		Subarray Gain (dB)				Total Gain (dB)			
	A_0 Seismometer		Complete Beam		Partial Beam				Complete Beam		Partial Beam		Complete Beam		Partial Beam	
	4th Degree	6th	4th	6th	4th	6th	4th	6th	4th	6th	4th	6th	4th	6th	4th	6th
Unfiltered	2.74		2.03		1.76		0.0		1.9		2.9		1.9		2.9	
Bu 0.6-2.0	.96	.90	.50	.43	.45	.38	8.7	9.3	5.0	5.8	5.6	6.5	13.7	15.1	14.3	15.8
Th 0.9-3.0	.74	.67	.30	.27	.31	.27	10.9	11.4	7.0	7.5	6.8	7.1	17.9	18.9	17.7	18.5
Bu 0.7-1.4	.75	.73	.33	.29	.28	.25	10.3	10.6	6.4	7.2	7.4	8.4	16.7	17.8	17.7	19.0
Bu 0.8-1.6	.66	.64	.27	.24	.24	.21	11.7	12.1	6.9	7.6	7.8	8.7	18.6	19.7	19.5	20.8
Bu 0.8-1.4	.63	.61	.25	.23	.21	.19	11.9	12.3	7.2	7.8	8.3	9.0	19.0	20.0	20.2	21.3
Bu 0.9-1.6	.54	.51	.21	.19	.19	.17	13.3	13.8	7.3	7.7	8.0	8.4	20.5	21.5	21.3	22.2
Bu 0.9-1.4	.49	.46	.19	.18	.17	.15	13.9	14.4	7.4	7.7	8.4	8.9	21.3	22.1	22.3	23.3
Th 0.9-1.4	.49	.45	.19	.17	.16	.14	14.3	14.5	7.5	7.8	8.5	9.0	21.8	22.3	22.8	23.5

3.8.2 Post-Detection Integration Time Analysis

This analysis was suggested in Section B.3 of reference 3. Its purpose is to provide pertinent experimental data relative to selecting a post-detection integration time which might be suitable (an acceptable loss in signal-to-noise ratio) for many seismic events.

If the seismic noise is a stationary process with a small correlation time, compared with the post-detection integration time, the analysis is performed to maximize the expression $\sqrt{T}\, S$, where T is the post-detection integration time and S is the maximum average signal power for a given T. Based on the preceding assumption, the value of T, for which $\sqrt{T}\, S$ is maximized, is the proper choice for the post-detection integration time for a given event.

Figure 3-35 reflects the results of this analysis for the two events described previously. The analysis is performed at the subarray and LASA beam levels for both events. The signal power S is defined as

$$ S = \frac{1}{T} \sum_{t=1}^{T} A^2(t), $$

where A is a beam amplitude (either a subarray or LASA beam) measured in nanometers, and T is the integration time in seconds.

The subarray beam was formed at a 10 Hz rate with a 20 Hz resolution by adding the 25 properly delayed seismometer traces from subarray B1. The LASA beam was formed at a 5 Hz rate with a 10 Hz resolution by adding the 21 properly delayed subarray beams. The $\sqrt{T}\, S$ quantity is presented in Figure 3-35 in dB relative to one nanometer.

Figure 3-35 indicates that for the earthquake, a post-detection integration time of 6.5 to 7.5 seconds appears appropriate. An integration time of 2 seconds for Longshot seems ideal. If we decided to select an integration time suitable for both of these events, a 3-second, post-detection integration time would provide an average signal power within 1 dB of the maximum signal power for both events.
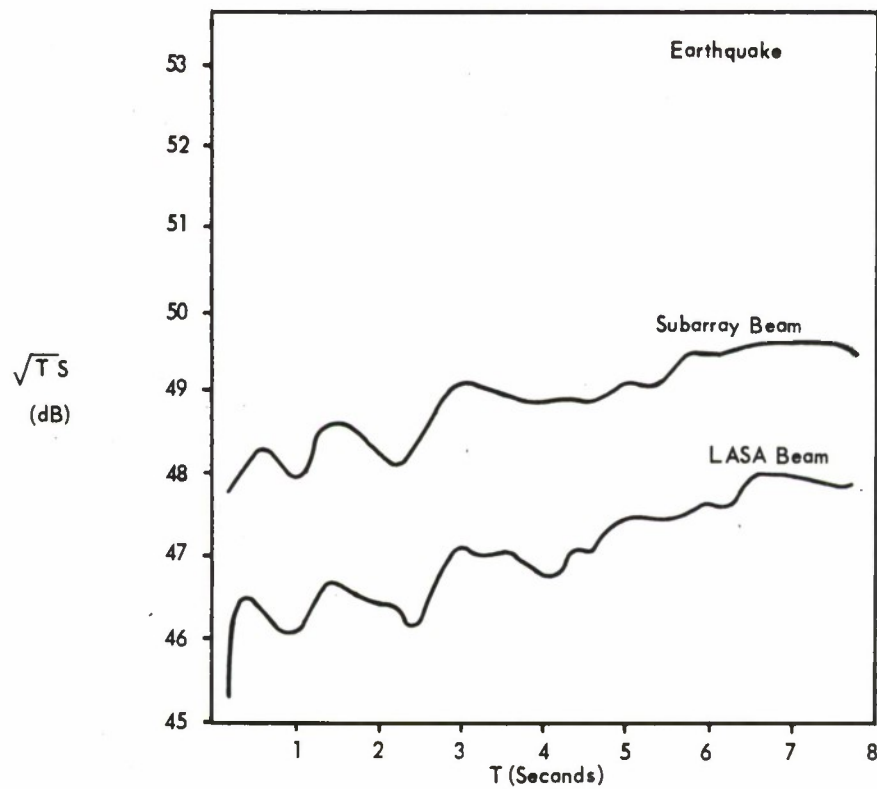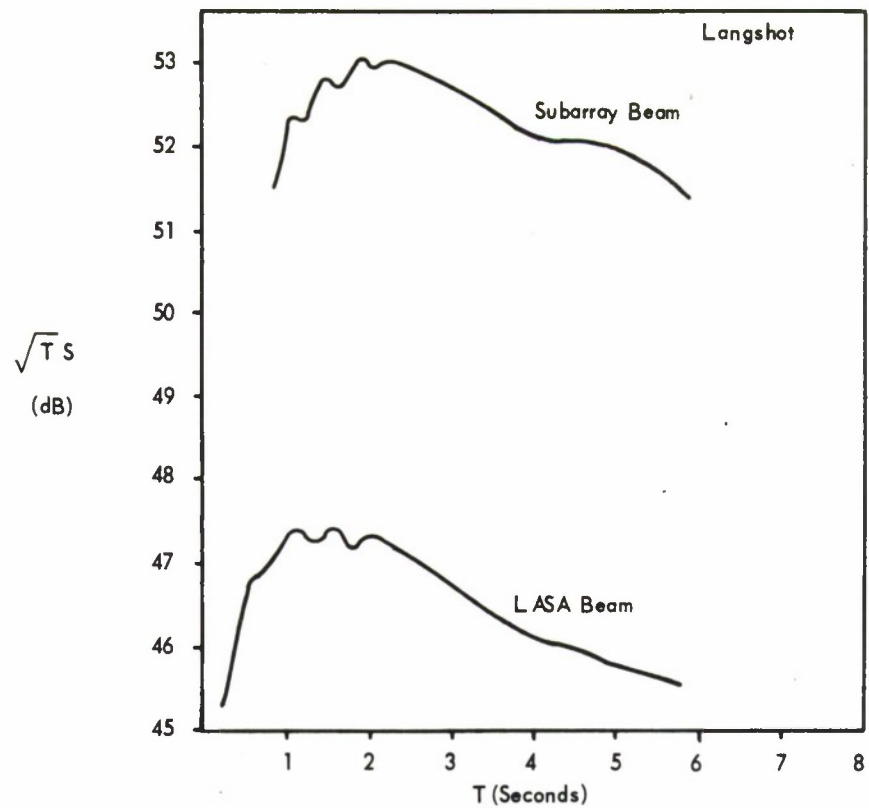
Figure 3-35. Post-Detection Integration Analysis

3.8.3   System Gain Analysis

The purpose of this experiment was to obtain the effect on system gain by varying several pertinent parameters in processing LASA seismic data. The signal-to-noise ratios at the seismometer, subarray beam, and LASA beam levels were calculated for several array configurations. System parameters which were varied are

1.   The number of seismometers per subarray beam
2.   The filter applied to the subarray beams
3.   The number of subarray beams per LASA beam.

Figure 3-36 presents the logic flow of this experiment, using the appropriate data analysis programs. Subarray beams were formed by the properly delayed sum of either the 25 or 19 seismometers within each subarray. The subarray beams formed by 19 seismometers reflect the deletion of the six seismometers in the B-ring of each subarray. All subarray beams were formed at a 10 Hz rate with a resolution of 20 Hz. The filters evaluated were applied to the subarray beams.

LASA beams were formed by the properly delayed sum of either 21 subarray beams, 17 subarray beams (outer subarray ring deleted), or 13 subarray beams (the two outer subarray rings deleted). The LASA beams were formed at a rate of 5 Hz with a 10 Hz resolution.

As indicated by Figure 3-36, signal and noise power were calculated at the seismometer level and at the subarray level for both unfiltered and filtered LASA beams. Signal power was calculated over a 5-second interval and noise power over an 85-second interval.

The results of this experiment are given in Tables 3-23 through 3-26, which in general reflect signal-to-noise ratios and resultant gains. All signal-to-noise figures are in dB relative to one nanometer. Gain figures are also expressed in dB, and are relative to the average seismometer signal-to-noise ratio. The first column in the tables is the subarray identification. The second column gives the average signal-to-noise ratio of the 25 seismometers in the associated subarray. The succeeding pairs of columns show signal-to-noise ratios and gain values for the subarray beam produced by each subarray. The

Figure 3-36. System Gain Analysis, Experiment Logic Flow

Table 3-23. Longshot—25 Seismometers/Subarray

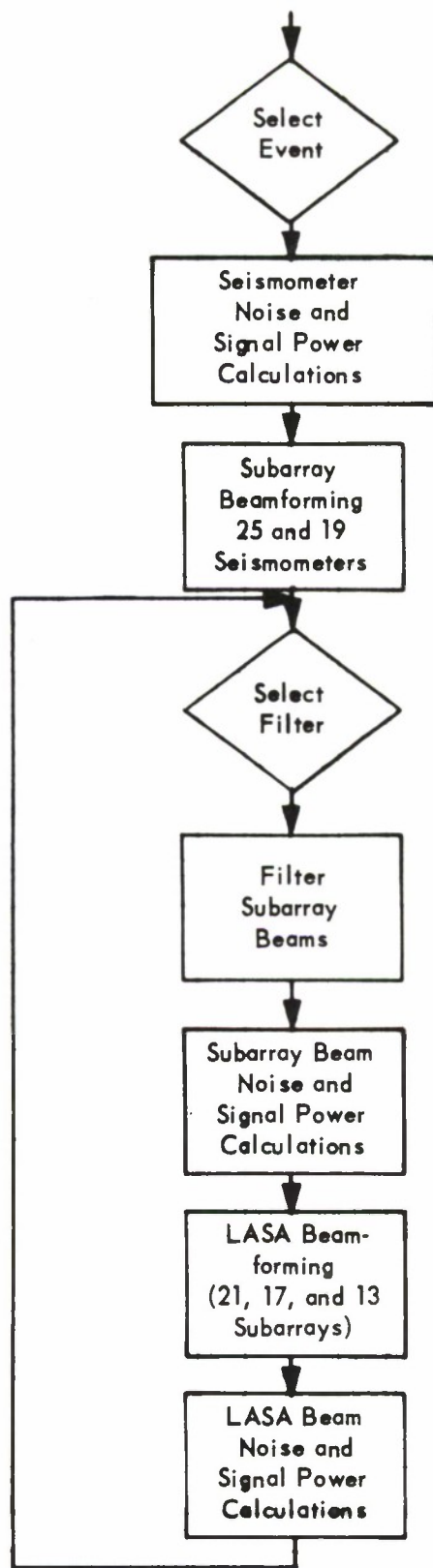|	Avg S/N 25 Seis/SA	Unfiltered		BP-B .6-2.0		BP-T .9-3.0		BP-B .7-1.4		BP-B .8-1.6		BP-B .8-1.4		BP-B .9-1.6		BP-B .9-1.4		BP-T .9-1.4	
		S/N	Gain	S/N	Gain	S/N	Gain	S/N	Gain	S/N	Gain	S/N	Gain	S/N	Gain	S/N	Gain	S/N	Gain
1	31.5	35.6	4.1	48.8	17.3	52.5	21.0	51.6	20.1	53.4	21.9	53.7	22.2	55.2	23.7	55.9	24.4	56.0	24.5
2	32.2	35.0	2.8	48.4	16.2	53.1	20.9	51.3	19.1	53.7	21.5	53.9	21.7	56.1	23.9	56.5	24.3	56.8	24.6
3	34.5	37.3	2.8	49.6	15.1	53.3	18.8	50.9	16.4	53.2	18.7	52.8	18.3	54.8	20.3	54.2	19.7	54.0	19.5
4	29.0	32.1	3.1	44.5	15.5	49.6	20.6	46.9	17.9	49.6	20.6	49.5	20.5	52.1	23.1	52.2	23.2	52.5	23.5
5	28.9	31.4	2.5	44.2	15.3	50.2	21.3	46.5	17.6	49.3	20.4	48.9	20.0	51.3	22.4	50.9	22.0	51.0	22.1
6	29.2	33.3	4.1	46.3	17.1	48.0	18.8	48.6	19.4	51.0	21.8	50.8	21.6	53.2	24.0	53.6	24.4	54.1	24.9
7	27.3	33.4	6.1	43.9	16.6	45.4	18.1	46.2	18.9	48.8	21.5	49.1	21.8	50.8	23.5	51.8	24.5	52.1	24.8
8	31.9	36.0	4.1	47.9	16.0	49.4	17.5	50.3	18.4	51.8	19.9	52.0	20.1	53.5	21.6	53.9	22.0	53.7	21.8
9	30.5	34.0	3.5	48.0	17.5	50.0	19.5	50.7	20.2	52.3	21.8	52.6	22.1	53.6	23.1	53.9	23.4	53.9	23.4
10	32.2	36.1	3.9	48.8	16.6	51.7	19.5	51.6	19.4	54.1	21.9	54.4	22.2	56.4	24.2	56.9	24.7	56.9	24.7
11	31.5	34.5	3.0	47.8	16.3	52.3	20.8	50.4	18.9	52.5	21.0	52.8	21.3	54.2	22.7	54.5	23.0	54.6	23.1
12	32.3	35.5	3.2	47.9	15.6	54.0	21.7	51.3	19.0	53.8	21.5	54.1	21.8	55.7	23.4	56.1	23.8	56.3	24.0
13	30.5	33.6	3.1	44.6	14.1	48.8	18.3	46.4	15.9	48.5	18.0	48.5	18.0	50.2	19.7	50.3	19.8	50.4	19.9
14	31.3	36.0	4.7	48.6	17.3	51.7	20.4	50.9	19.6	52.4	21.1	52.7	21.4	53.6	22.3	54.0	22.7	53.7	22.4
15	27.7	35.3	7.6	45.7	18.0	44.7	17.0	49.9	22.2	51.1	23.4	52.1	24.4	52.3	24.6	53.7	26.0	53.6	25.9
16	30.3	33.5	3.2	44.9	14.6	49.5	19.2	47.1	16.8	49.2	18.9	49.1	18.8	51.1	20.8	51.3	21.0	51.4	21.1
17	33.3	37.3	4.0	46.1	12.8	50.7	17.4	48.9	15.6	51.3	18.0	51.5	18.2	53.5	20.2	54.1	20.8	54.4	21.1
18	26.6	33.5	6.9	45.8	19.2	45.5	18.9	47.5	20.9	48.6	22.0	48.9	22.3	50.1	23.5	50.9	24.3	51.0	24.4
19	20.3	25.6	5.3	36.2	15.9	36.1	15.8	40.7	20.4	39.6	19.3	42.1	21.8	40.1	19.8	43.8	23.5	44.4	24.1
20	29.9	34.9	5.0	46.2	16.3	48.7	18.8	48.9	19.0	50.1	20.2	50.5	20.6	51.4	21.5	51.9	22.0	51.8	21.9
21	27.4	33.1	5.7	43.7	16.3	44.1	17.0	44.9	17.5	47.2	19.8	46.5	19.1	48.6	21.2	47.8	20.4	47.4	20.0
Avg	29.7	34.2	4.5	46.2	16.5	48.1	18.4	48.9	19.2	50.5	20.8	50.9	21.2	52.1	22.4	52.9	23.2	53.0	23.3

Avg Seis S/N

	Avg Seis S/N	Unfiltered		BP-B .6-2.0		BP-T .9-3.0		BP-B .7-1.4		BP-B .8-1.6		BP-B .8-1.4		BP-B .9-1.6		BP-B .9-1.4		BP-T .9-1.4	
		S/N	Gain	S/N	Gain	S/N	Gain	S/N	Gain	S/N	Gain	S/N	Gain	S/N	Gain	S/N	Gain	S/N	Gain
L8 Power (21)	29.7	45.1	15.4	56.6	26.9	58.9	29.2	59.6	29.9	61.3	31.6	61.6	31.9	63.1	33.4	63.7	34.0	63.6	33.9
L8 Power (17)	29.7	44.0	14.3	55.9	26.2	58.9	29.2	58.8	29.1	60.9	31.2	61.0	31.3	62.9	33.2	63.2	33.5	63.1	33.4
L8 Power (13)	29.7	43.3	13.6	54.6	24.9	58.0	28.3	57.8	28.1	60.0	30.3	60.2	30.5	61.8	32.1	62.2	32.5	62.0	32.3

Table 3-24. Longshot—19 Seismometers/Subarray

	Avg S/N 25 Sets/SA	Unfiltered S/N	Gain	BP-B .6-2.0 S/N	Gain	BP-T .9-3.0 S/N	Gain	BP-B .7-1.4 S/N	Gain	BP-B .8-1.6 S/N	Gain	BP-B .8-1.4 S/N	Gain	BP-B .9-1.6 S/N	Gain	BP-B .9-1.4 S/N	Gain	BP-T .9-1.4 S/N	Gain
1	31.5	36.6	5.1	49.4	17.9	52.1	20.6	52.7	21.2	54.4	22.9	55.0	23.5	55.9	24.4	56.9	25.4	57.2	25.7
2	32.2	35.7	3.5	48.9	16.7	52.5	20.3	51.6	19.4	53.9	21.7	54.2	22.0	55.9	23.7	56.5	24.3	56.8	24.6
3	34.5	37.6	3.1	49.6	15.1	52.6	18.1	51.0	16.5	53.1	18.6	52.8	18.3	54.4	19.9	54.0	19.5	53.7	19.2
4	29.0	32.8	3.8	45.6	16.6	50.0	21.0	48.5	19.5	51.2	22.2	51.3	22.3	53.7	24.7	54.2	25.2	54.6	25.6
5	28.9	32.2	3.3	45.5	16.6	50.9	22.0	48.0	19.1	50.9	22.0	50.5	21.6	52.5	23.6	52.0	23.1	52.0	23.1
6	29.2	34.2	5.0	47.3	18.1	46.7	17.5	50.5	21.3	52.4	23.2	52.6	23.4	53.8	24.6	54.4	25.2	54.6	25.4
7	27.3	34.3	7.0	45.1	17.8	44.4	17.1	48.2	20.9	50.2	22.9	51.0	23.7	51.7	24.4	53.2	25.9	53.5	26.2
8	31.9	36.9	5.0	48.3	16.4	48.5	16.6	51.6	19.7	52.6	20.7	53.3	21.4	53.7	21.8	54.7	22.8	54.5	22.6
9	30.5	34.3	3.8	48.3	17.8	49.1	18.6	51.6	21.3	53.5	23.0	54.0	23.5	54.6	24.1	55.1	24.6	55.2	24.7
10	32.2	36.6	4.4	49.7	17.5	50.9	18.7	53.1	20.9	55.5	23.3	56.0	23.8	57.7	25.5	58.5	26.3	58.7	26.5
11	31.5	35.0	3.5	48.4	16.9	52.0	20.5	51.2	19.7	53.3	21.8	53.6	22.1	55.1	23.6	55.5	24.0	55.7	24.2
12	32.3	36.0	3.7	48.4	16.1	53.9	21.6	52.1	19.8	54.5	22.2	54.9	22.6	56.4	24.1	56.9	24.6	57.0	24.7
13	30.5	34.4	3.9	45.5	15.0	48.8	18.3	47.9	17.4	50.0	19.5	50.1	19.6	51.4	20.9	51.7	21.2	51.7	21.2
14	31.3	37.2	5.9	49.6	18.3	51.5	20.2	52.3	21.0	53.5	22.2	54.0	22.7	54.7	23.4	55.4	24.1	55.2	23.9
15	27.7	36.1	8.4	47.4	19.7	48.7	21.0	50.8	23.1	52.4	24.7	53.3	25.6	53.5	25.8	54.6	26.9	54.5	26.8
16	30.3	34.0	3.7	45.5	15.2	49.9	19.6	48.2	17.9	50.3	20.0	50.3	20.0	52.2	21.9	52.5	22.2	52.7	22.4
17	33.3	37.9	4.6	46.6	13.3	50.2	16.9	49.5	16.2	51.6	18.3	52.1	18.8	53.5	20.2	54.4	21.1	54.6	21.3
18	26.6	33.1	6.5	46.1	19.5	44.7	18.1	48.3	21.7	49.0	22.4	49.6	23.0	50.1	23.5	51.1	24.5	51.3	24.7
19	20.3	26.1	5.8	35.6	15.3	34.9	14.6	41.5	21.2	39.7	19.6	43.2	22.9	39.9	19.6	44.7	24.4	45.5	25.2
20	29.9	35.6	5.7	46.7	16.8	48.3	18.4	49.5	19.6	50.6	20.7	51.2	21.3	51.8	21.9	52.7	22.8	52.7	22.8
21	27.4	33.9	6.5	44.9	17.5	44.3	16.9	46.9	19.5	49.0	21.6	48.5	21.1	50.1	22.7	49.5	22.1	49.0	21.6
Avg	29.7	34.8	5.1	46.7	17.0	47.7	18.0	50.0	20.3	51.3	21.6	52.1	22.4	52.6	22.9	53.8	24.1	53.9	24.2

Avg Sets S/N

		S/N	Gain	S/N	Gain	S/N	Gain	S/N	Gain	S/N	Gain	S/N	Gain	S/N	Gain	S/N	Gain	S/N	Gain
LB Power (21)	29.7	45.4	15.7	57.2	27.5	59.0	29.3	60.8	31.1	62.4	32.7	63.0	33.3	63.9	34.2	65.1	35.4	65.0	35.3
LB Power (17)	29.7	44.3	14.6	56.5	26.8	59.0	29.3	60.0	30.3	62.0	32.3	62.3	32.6	63.7	34.0	64.3	34.6	64.1	34.4
LB Power (13)	29.7	43.7	14.0	55.2	25.5	58.2	28.5	58.9	29.2	61.1	31.4	61.4	31.7	62.8	33.1	63.3	33.6	63.1	33.4

Table 3-25. Earthquake—25 Seismometers/Subarray

	Avg S/N 25 Seis/SA	Unfiltered		BP-B.6-2.0		BP-T.9-3.0		BP-B.7-1.4		BP-B.8-1.6		BP-B.8-1.4		BP-B.9-1.6		BP-B.9-1.4		BP-T.9-1.4	
		S/N	Gain	S/N	Gain	S/N	Gain	S/N	Gain	S/N	Gain	S/N	Gain	S/N	Gain	S/N	Gain	S/N	Gain
1	31.9	35.5	3.6	44.6	12.7	42.4	10.5	47.1	15.2	46.9	15.0	47.2	15.3	45.5	13.6	45.7	13.8	45.1	13.2
2	33.2	37.6	4.4	45.0	11.8	43.8	10.6	47.1	13.9	48.1	14.9	48.0	14.8	48.0	14.8	47.5	14.3	47.0	13.8
3	31.5	36.0	4.5	43.2	11.7	37.5	6.0	44.9	13.4	45.6	14.1	45.5	14.0	45.6	14.1	45.3	13.8	44.8	13.3
4	32.3	36.6	4.3	44.5	12.2	43.3	11.0	46.9	14.6	47.7	15.4	47.9	15.6	47.2	14.9	47.2	14.9	46.8	14.5
5	35.9	38.2	2.3	45.7	9.8	48.1	12.2	47.5	11.6	48.5	12.6	48.3	12.4	48.0	12.1	47.4	11.5	46.8	10.9
6	33.7	35.6	1.9	45.2	11.5	49.0	15.3	46.5	12.8	48.3	14.6	47.7	14.0	49.2	15.5	48.2	14.5	48.0	14.3
7	31.6	34.0	2.4	44.8	13.2	46.6	15.0	46.8	15.2	48.1	16.5	47.9	16.3	48.7	17.1	48.4	16.8	48.5	16.9
8	31.5	34.4	2.9	46.9	15.4	44.2	12.7	49.5	18.0	49.4	17.9	50.0	18.5	48.5	17.0	49.3	17.8	48.9	17.4
9	32.4	35.2	2.8	42.1	9.7	41.9	9.5	43.2	10.8	43.8	11.4	43.4	11.0	43.0	10.6	41.5	9.1	40.4	8.0
10	33.1	36.7	3.6	45.5	12.4	44.4	11.3	46.7	13.6	47.6	14.5	47.2	14.1	47.4	14.3	46.7	13.6	46.5	13.4
11	36.8	39.1	2.3	47.7	10.9	51.8	15.0	48.8	12.0	50.7	13.9	50.0	13.2	50.9	14.1	49.4	12.6	48.9	12.1
12	32.4	35.7	3.3	45.0	12.6	41.3	8.9	46.9	14.5	47.4	15.0	47.4	15.0	46.5	14.1	46.2	13.8	45.6	13.2
13	32.7	36.4	3.7	46.0	13.3	42.6	9.9	48.6	15.9	48.5	15.8	49.3	16.6	47.2	14.5	48.1	15.4	47.8	15.1
14	29.3	32.0	2.7	40.0	10.7	39.0	9.7	39.5	10.2	40.1	10.8	39.2	9.9	40.0	10.7	37.7	8.4	36.5	7.2
15	32.9	37.0	4.1	46.1	13.2	44.0	11.1	48.1	15.2	47.9	15.0	48.0	15.1	46.5	13.6	46.4	13.5	45.8	12.9
16	32.4	34.7	2.3	42.6	10.2	43.2	10.8	44.0	11.6	45.0	12.6	44.9	12.5	45.5	13.1	45.5	13.1	45.4	13.0
17	34.6	36.5	1.9	46.6	12.0	48.3	13.7	48.1	13.5	49.2	14.6	49.0	14.4	48.9	14.3	48.2	13.6	47.4	12.8
18	27.4	30.0	2.6	41.7	14.3	39.4	12.0	43.4	16.0	43.4	16.0	43.4	16.0	42.5	15.1	42.1	14.7	41.3	13.9
19	26.3	30.4	4.1	36.4	10.1	32.2	5.9	36.7	10.4	37.9	11.6	37.0	10.7	38.1	11.8	35.9	9.6	34.7	8.9
20	32.6	35.2	2.6	42.9	10.3	42.7	10.1	44.2	11.6	44.8	12.2	44.6	12.0	43.9	11.3	43.3	10.7	42.6	10.0
21	33.6	36.0	2.4	44.7	11.1	46.1	12.5	46.9	13.3	47.7	14.1	47.7	14.1	47.3	13.7	47.3	13.7	47.0	13.4
Avg	32.1	35.3	3.2	44.6	12.5	43.4	11.3	46.4	14.3	47.1	15.0	47.0	14.9	46.6	14.5	46.2	14.1	45.8	13.7
LB Power (21)	32.1	46.8	14.7	54.2	22.1	54.2	22.1	55.8	23.7	56.5	24.4	56.7	24.6	56.8	24.7	56.9	24.8	56.5	24.4
LB Power (17)	32.1	46.1	14.0	53.4	21.3	54.2	22.1	55.1	23.0	56.0	23.9	56.2	24.1	56.3	24.2	56.4	24.3	55.9	23.8
LB Power (13)	32.1	44.3	12.2	52.5	20.4	53.5	21.4	54.4	22.3	55.3	23.2	55.5	23.4	55.8	23.7	55.9	23.8	55.5	23.4

Table 3-26. Earthquake—19 Seismometers/Subarray

	Avg S/N 25 Seis/SA	Unfiltered		BP-B.6-2.0		BP-T.9-3.0		BP-B.7-1.4		BP-B.8-1.6		BP-B.8-1.4		BP-B.9-1.6		BP-B.9-1.4		BP-T.9-1.4	
		S/N	Gain	S/N	Gain	S/N	Gain	S/N	Gain	S/N	Gain	S/N	Gain	S/N	Gain	S/N	Gain	S/N	Gain
1	31.9	36.0	4.1	44.7	12.8	41.4	9.5	47.6	15.7	47.1	15.2	47.7	15.8	45.7	13.8	46.1	14.2	45.6	13.7
2	33.2	38.2	5.0	45.6	12.4	44.2	11.0	47.7	14.5	48.8	15.6	48.6	15.4	48.7	15.5	48.2	15.0	47.7	14.5
3	31.5	36.7	5.2	43.9	12.4	41.3	9.8	45.6	14.1	46.3	14.8	46.3	14.8	46.4	14.9	46.1	14.6	45.6	14.1
4	32.3	36.9	4.6	45.1	12.8	43.3	11.0	47.8	15.5	48.6	16.3	48.8	16.5	48.1	15.8	48.2	15.9	47.9	15.6
5	35.9	38.5	2.6	46.2	10.3	48.1	12.2	48.2	12.3	49.1	13.2	48.9	13.0	48.5	12.6	47.9	12.0	47.3	11.4
6	33.7	36.1	2.4	45.9	12.2	49.0	15.3	47.3	13.6	49.1	15.4	48.6	14.9	50.0	16.3	49.2	15.5	48.9	15.2
7	31.6	34.7	3.1	45.6	14.0	46.4	14.8	47.8	16.2	49.1	17.5	48.9	17.3	49.6	18.0	49.5	17.9	49.6	18.0
8	31.5	34.7	3.2	47.5	16.0	43.7	12.2	50.3	18.8	50.2	18.7	50.8	19.3	49.1	17.6	50.0	18.5	49.7	18.2
9	32.4	35.5	3.1	42.1	9.7	40.8	8.4	43.3	10.9	43.4	11.0	43.2	10.8	42.3	9.9	40.8	8.4	39.7	7.3
10	33.1	36.9	3.8	45.5	12.4	42.5	9.4	46.9	13.8	47.7	14.6	47.4	14.3	47.3	14.2	46.8	13.7	46.6	13.5
11	36.8	39.6	2.8	48.1	11.3	51.8	15.0	49.3	12.5	51.1	14.3	50.5	13.7	51.2	14.4	49.9	13.1	49.3	12.5
12	32.4	36.0	3.6	45.5	13.1	39.3	6.9	47.5	15.1	47.8	15.4	47.9	15.5	46.6	14.2	46.7	14.3	46.1	13.7
13	32.7	36.8	4.1	46.2	13.5	41.5	8.8	49.4	16.7	49.1	16.4	50.0	17.3	47.6	14.9	48.7	16.0	48.4	15.7
14	29.3	32.4	3.1	40.4	11.1	38.4	9.1	40.3	11.0	40.7	11.4	40.0	10.7	40.4	11.1	38.3	19.0	37.1	7.8
15	32.9	37.2	4.3	45.9	13.0	42.8	9.9	48.1	15.2	47.5	14.6	47.8	14.9	45.8	12.9	45.8	12.9	45.2	12.3
16	32.4	35.1	2.7	43.0	10.6	42.4	10.0	44.8	12.4	45.7	13.3	45.8	13.4	45.9	13.5	46.0	13.6	45.9	13.5
17	34.6	36.6	2.0	46.6	12.0	47.4	12.8	48.4	13.8	49.2	14.6	49.2	14.6	48.6	14.0	48.2	13.6	47.4	12.8
18	27.4	30.6	3.2	42.3	14.9	38.6	11.2	44.4	17.0	44.2	16.8	44.3	16.9	43.2	15.8	43.0	15.6	42.1	14.7
19	26.3	30.9	4.6	36.5	10.2	30.8	4.5	37.5	11.2	38.3	12.0	37.9	11.6	38.4	12.1	36.8	10.5	35.7	9.4
20	32.6	35.6	3.0	42.9	10.3	41.7	9.1	44.3	11.7	44.7	12.1	44.5	11.9	43.5	10.9	43.0	10.4	42.3	9.7
21	33.6	36.3	2.7	45.1	11.5	46.1	12.5	47.6	14.0	48.2	14.6	48.4	14.8	47.7	14.1	47.8	14.2	47.5	13.9
Avg	32.1	35.7	3.6	44.9	12.8	42.8	10.7	46.9	14.8	47.4	15.3	47.5	15.4	46.8	14.7	46.6	14.5	46.2	14.1
LB Power (21)	32.1	47.1	15.0	54.4	22.3	53.7	21.6	56.2	24.1	56.9	24.8	57.1	25.0	57.0	24.9	57.1	25.0	56.8	24.7
LB Power (17)	32.1	46.3	14.2	53.5	21.4	53.3	21.2	55.5	23.4	56.4	24.3	56.6	24.5	56.6	24.5	56.8	24.7	56.3	24.2
LB Power (13)	32.1	44.5	12.4	52.6	20.5	52.8	20.7	54.7	22.6	55.7	23.6	56.0	23.9	56.1	24.0	56.3	24.2	55.9	23.8

gain value is defined as the difference between the signal-to-noise ratio of the subarray beam, and the signal-to-noise ratio of the average of the 25 seismometers in the associated subarray. The gain figures give the total subarray gain—filter gain plus beamforming gain—experienced by processing the seismic data through several different filters (including the single unfiltered case). Generally, each pair of signal-to-noise and gain columns represents a computer run through the Subarray Beamformer program and the necessary power calculations. All filters were bandpass sixth-degree filters, and either Butterworth (BP-B) or Tschebyscheff (BP-T). The filters are further identified by their cutoff frequencies in Hz. A detailed description of each of the filters is found in Section 3.7.

The single line toward the bottom of the table gives average signal-to-noise figures. The first column represents the average signal-to-noise ratio of all 525 seismometers in the LASA array. The succeeding pairs of columns present the average signal-to-noise ratios and gains for the 21 subarray beams produced for the filters considered.

The final three rows in each table are the resultant array gains experienced by forming LASA beams (from 21, 17, and 13 subarrays) by the delayed sum of the subarray beams generated in each of the cases considered. Note that the first column again presents the average signal-to-noise ratio of all 525 seismometers in the LASA array. All gain figures for the LASA beams are defined as the difference between the signal-to-noise ratio of the LASA beam and the signal-to-noise ratio of the average of all 525 seismometers.

Table 3-23 contains Longshot data using 25 seismometers per subarray; Table 3-24 also contains Longshot data, but for 19 seismometers per subarray. Tables 3-25 and 3-26 contain data for the Earthquake for 25 and 19 seismometers per subarray, respectively.

As indicated previously, the average seismometer signal-to-noise ratios were computed on a subarray basis for 25 seismometers, and on an array basis for 525 seismometers. No attempt was made to provide new average values for the reduced array (i.e., 19 seismometers, 17 and 13 subarrays) considered.

An investigation of the tables provides additional statistics supporting the fact that deleting the inner or B-ring of each subarray in subarray beamforming

actually improves the signal-to-noise ratio. For Longshot (tables 3-23 and 3-24), an improvement is noted for all cases at both a subarray and LASA level, except at the subarray level for the Tschebyscheff filter with bandpass from 0.9 Hz to 3.0 Hz. This improvement in signal-to-noise ratio is from 0.1 dB to 1.4 dB at the LASA beam level.

Similar signal-to-noise improvement is noted for the Earthquake (tables 3-25 and 3-26) except for the same Tschebyscheff filter at both a subarray and LASA level. The improvement is from 0.2 dB to 0.5 dB at the subarray level, and from 0.2 dB to 0.4 dB at the LASA level.

Another experimental result readily obtained from the tabular data is the selection of the best filter with respect to system gain for the two events considered. The filter which yields the best gain figure for Longshot is the Tschebyscheff 0.9 Hz to 1.4 Hz bandpass filter at the subarray level, and a Butterworth 0.9 Hz to 1.4 Hz bandpass filter at the LASA level. The best gain figures for the Earthquake are produced by the Butterworth 0.9 Hz to 1.4 Hz bandpass filter at the LASA level.

The effect on system gain of deleting the outer one or two rings of the LASA array is directly evident in the tabular data. As stated earlier, the elimination of the outer ring entails the deletion of 4 subarrays, and the elimination of the two outer rings entails the deletion of 8 subarrays. Deleting these rings causes a loss in system gain relative to the gain experienced using the full array. For Longshot, this loss, relative to the full array for filtered LASA beams, does not exceed 0.9 dB for the 17 subarray configurations, or 2.0 dB for the 13 subarray configurations. Associated figures for the Earthquake are 0.9 dB for the 17 subarray and 1.8 dB for 13 subarray configurations.

Note that for the filter which produced the best gain, the 17 subarray configuration yielded a loss relative to the full array of 0.8 dB for Longshot and 0.3 dB for the Earthquake, while the 13 subarray configurations for the best filter yielded a loss, again relative to the full array of 1.8 dB for Longshot and 0.8 dB for the Earthquake.

3.8.4 Scaled Signal/Noise Analysis

To present a graphical presentation of the capabilities of processing seismic data through subarray beamforming, filtering, and LASA beamforming, an experiment was designed to process seismic events for various signal-to-noise ratios. To obtain these events for varying signal-to-noise ratios, a seismic data tape containing an event, Longshot, of known signal-to-noise ratio was processed through the Signal-to-Noise Ratio Control program. The function of this program is to take a selected event, record sufficient noise data previous to the signal, scale the signal by a preset factor, add this scaled signal to the noise, and generate a tape containing original noise traces followed by scaled signal plus noise traces. Since the original signal-to-noise ratio and the scaling factor are known, the resultant event has a signal-to-noise ratio which is also known. In addition, the time delays required for subarray and LASA beamforming are known, since the event we chose to scale to produce these other events was of sufficient magnitude to provide them.

Five seismic data tapes were generated for the experiment. The scale factor α, applied to the original trace, assumed values of 2^0, 2^{-2}, 2^{-4}, 2^{-6}, and 2^{-8}. The 2^0 value provides the results of processing the original unscaled Longshot seismic data. The remaining values provide a range of events of several signal-to-noise ratios.

Each of the five tapes was processed through subarray beamforming, filtering, and LASA beamforming. Signal-to-noise ratios were calculated at the seismometer and LASA beam levels, and a plot of a typical seismometer and a filtered LASA beam was produced. Subarray beamforming was executed at a 10 Hz rate with 20 Hz resolution. The subarray beams produced were passed through a sixth-degree Tschebyscheff bandpass filter (0.9 Hz – 1.4 Hz) at a sampling frequency of 10 Hz. LASA beamforming was executed at a 10 Hz rate with a resolution of 10 Hz.

The signal and noise power calculations were executed over a 2- and 85-second integration period, respectively. Power calculations at the seismometer level are from the A_0 seismometer of subarray B1.

Table 3-27 gives the signal-to-noise ratios at the seismometer and LASA beam levels for each of the five events. Note that at both the seismometer and LASA beam levels the noise power is constant for all cases at the respective levels. The application of a 2^{-2} scale factor would effect a decrease of 12 dB from the signal power of the original signal. Note the 12 dB decrease for each subsequent scale factor and the corresponding decrease in the signal-to-noise ratio. The signal-to-noise ratio for the last two events is less than one.

At the LASA beam level the 12 dB loss from the original signal power and signal-to-noise ratio is again evident. The final column in the table represents system gain and is defined as the difference between the signal-to-noise ratio of the filtered case at the LASA beam level and the signal-to-noise ratio at the seismometer level. Each of figures 3-37 through 3-41 presents a typical seismometer plot and the resultant filtered LASA beam plot. Note the scaling for each plot. The scaling for the beam is the same as for the seismometers, but reflects the fact that it was scaled at the subarray and LASA beam levels by a division equal to the number of channel inputs.

The earlier disturbance preceding the Longshot arrival which becomes noticeable in the LASA beam trace in Figure 3-38 ($\alpha = 2^{-2}$), and which dominates the LASA beam trace in Figure 3-41 ($\alpha = 2^{-8}$) is due to a noise pulse appearing in the data at the seismometer level. The noise pulse appeared on several seismometers during the same sample period. The magnitude of this pulse varied among the affected seismometers, with the maximum magnitude being some 20 dB above the maximum seismometer output capability.

The apparent arrival develops by processing this noise pulse as if it were valid seismic data. The pulse does not appear on the seismometer trace presented simply because the particular seismometer was not affected.

An additional discussion of this noise pulse, including the appearance of the pulse on the experimental display, appears in Section 3.6.

3.8.5   Power Spectrum Analysis

System design and performance are strongly dependent on the spectral content of the processed waveform. A preliminary study of these characteristics

Table 3-27. System Gain Summary

Scale α	Seismometer			LASA Beam			System Gain
	N Noise Power (dB)	S Signal Power (dB)	S/N Ratio (dB)	N Noise Power (dB)	S Signal Power (dB)	S/N Ratio (dB)	(dB)
0	8.8	44.3	35.5	-29.5	40.3	69.8	34.3
2^{-2}	8.8	32.3	23.5	-29.5	28.2	57.7	34.2
2^{-4}	8.8	20.2	11.4	-29.5	16.1	45.6	34.2
2^{-6}	8.8	8.3	-0.5	-29.5	4.1	33.6	34.1
2^{-8}	8.8	-3.7	-12.5	-29.5	-8.1	21.4	33.9

Note: System Gain measured with respect to raw data (unfiltered)
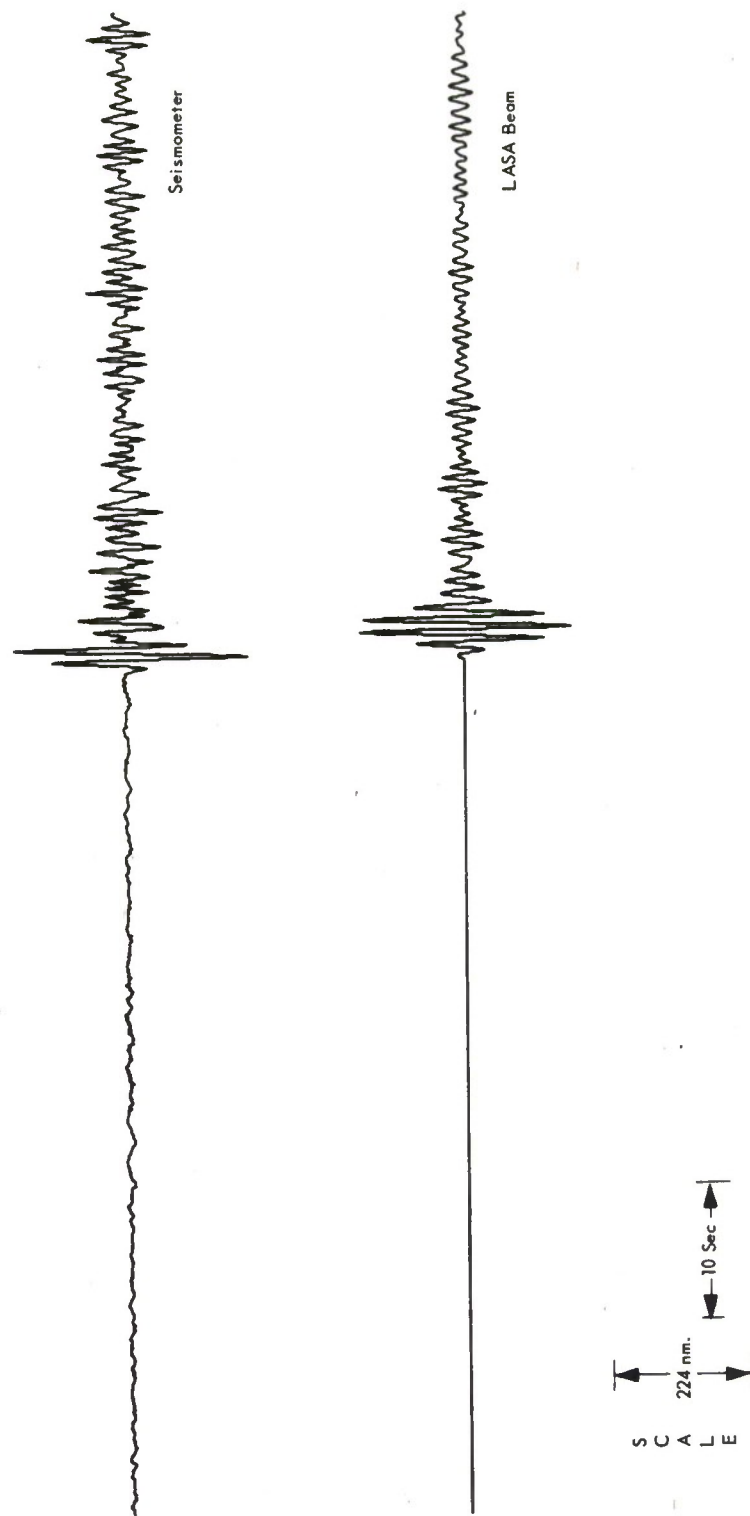
Figure 3-37. Longshot Event—Signal Scaled 2^0
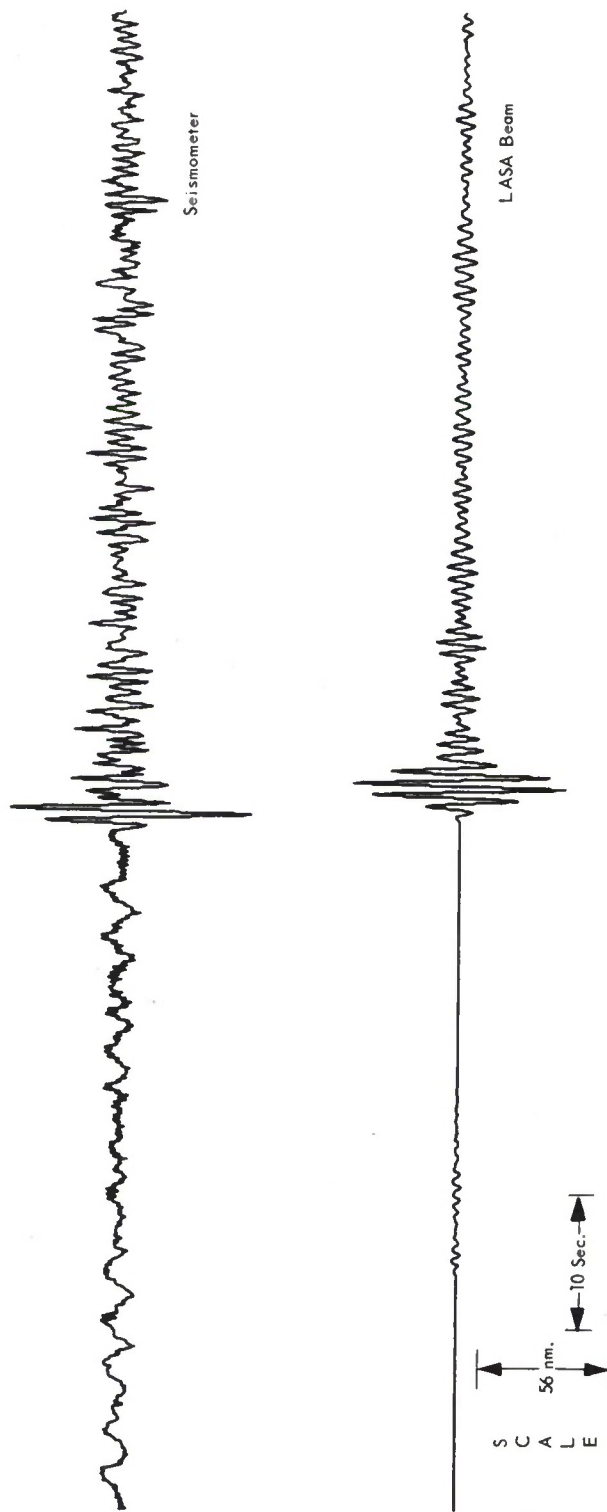
Figure 3-38. Longshot Event—Signal Scaled 2^{-2}

Seismometer
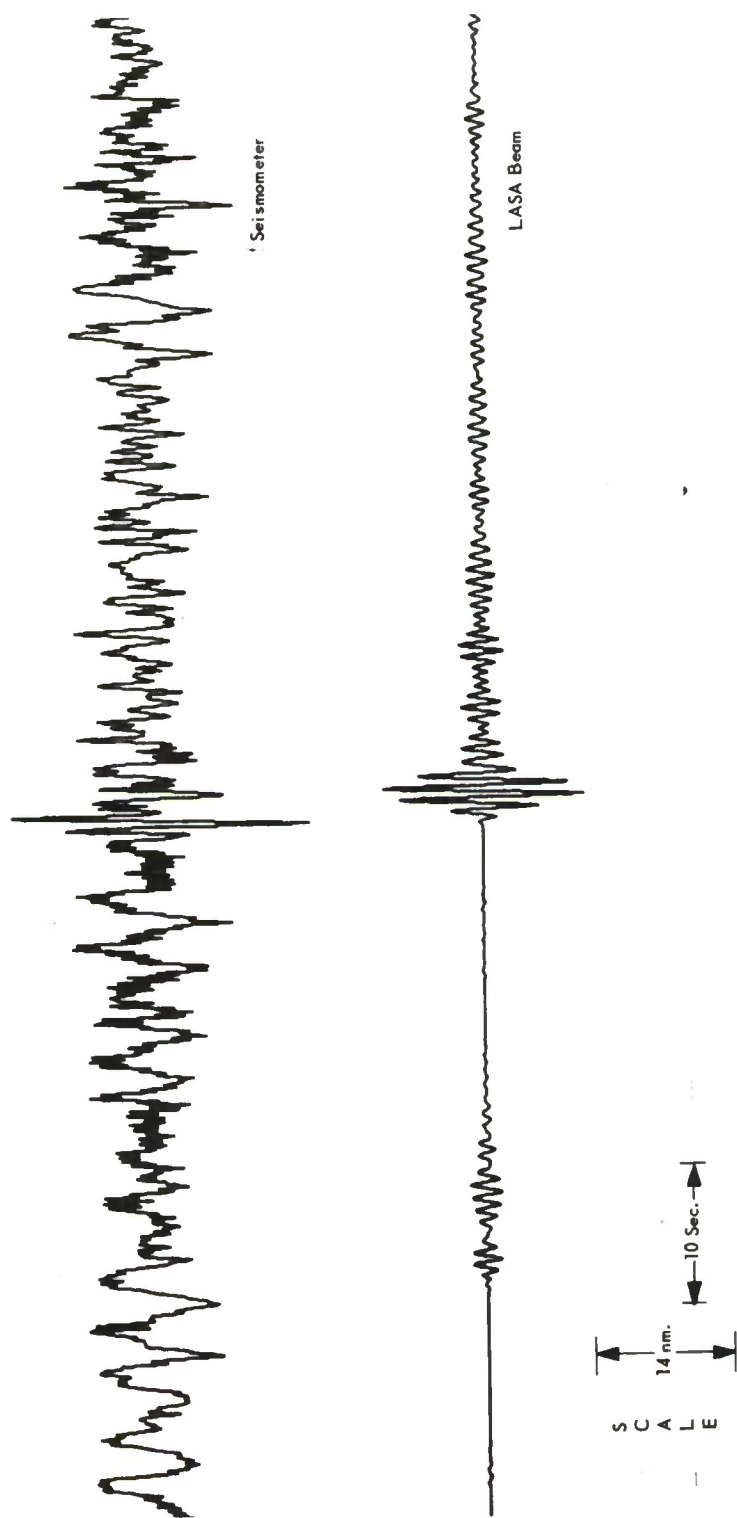
LASA Beam

S
C
A
L
E

56 nm.

10 Sec.

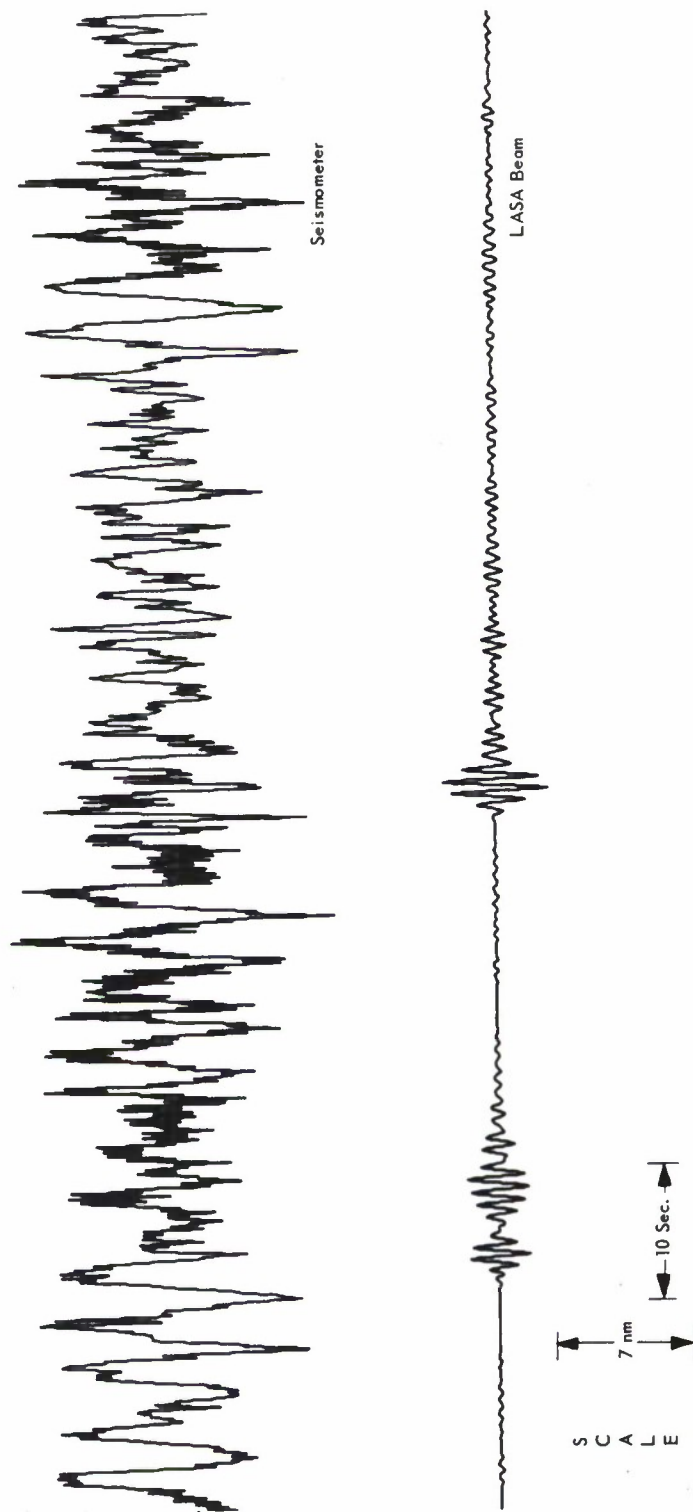Figure 3-39. Longshot Event—Signal Scaled 2^{-4}
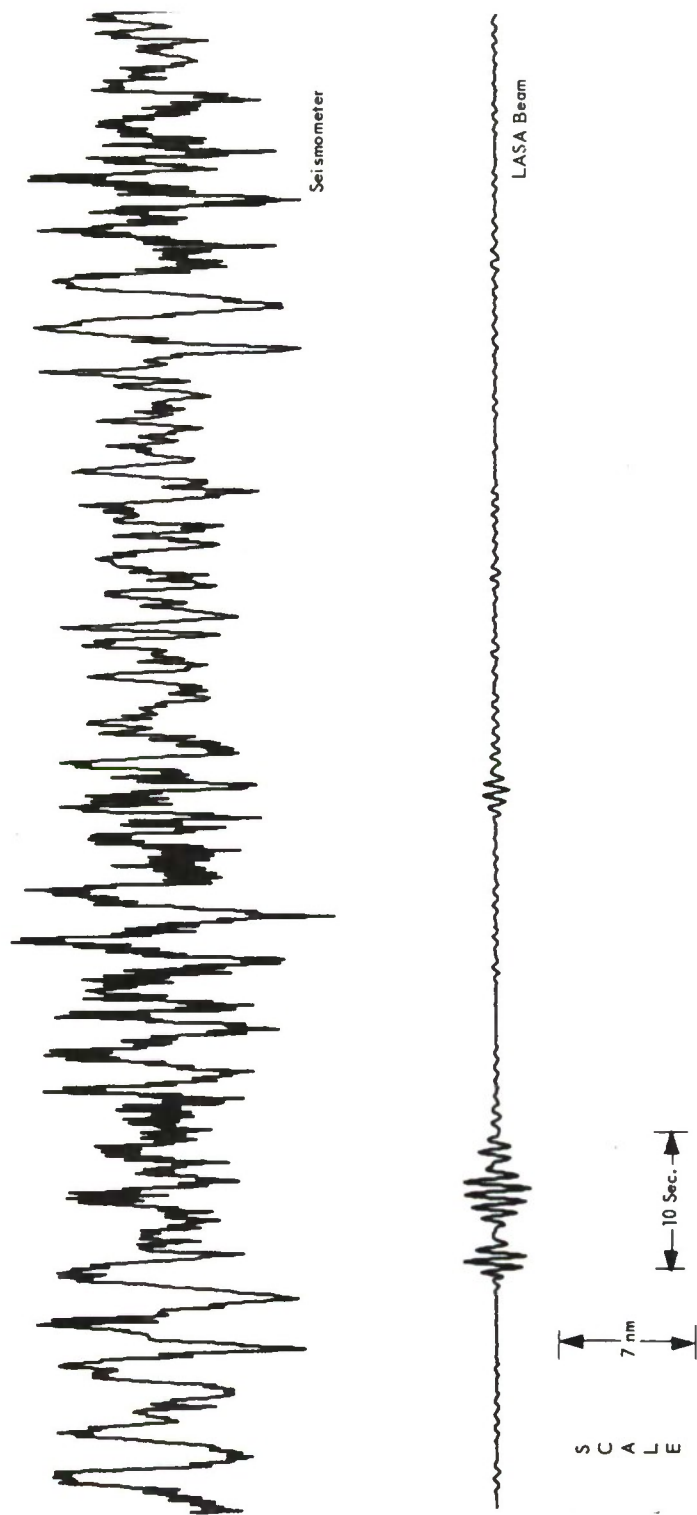
Figure 3-40. Longshot Event—Signal Scaled 2^{-6}

Figure 3-41. Longshot Event—Signal Scaled 2^{-8}

has been conducted to establish an initial data base and to gain processing insight. The Cooley-Tukey[11] formulation was cascaded with a smoothing routine to efficiently estimate spectral density functions. Since considerable roughness is evident, averaging the ensemble of available channels and/or time windows should be considered for future investigation. This capability is being incorporated in the spectrum program package as an optional mode.

Unfiltered subarray and array beams were formed with Longshot and the Kamchatka earthquake (April 8, 1966) to provide an exemplary comparative set. Since ensemble averaging was not conveniently available, subarray B1 and seismometer B1 of this subarray were arbitrarily selected as representaitve elements. Comparative broadband power measurements are displayed in Table 3-28. Excellent consistency (i.e., 0.2 dB) is observed for the earthquake; however, only fair consistency (i.e., 2.0 dB) is observed for Longshot. Note that presently no spectral consistency is certain.

Figures 3-42 and 3-43 present the signal-to-noise ratios observed at the seismometer, subarray, and array nodes. A predominant Longshot spectrum ratio centered at approximately 1.2 Hz is evident, while the Earthquake spectrum ratio has a broad characteristic. A corresponding beam pattern difference is evident when observing the experimental display. This may be a discriminant signature component, but no conclusions should be drawn until a statistically significant base is established through the analysis of many alternate events.

Several additional data comparisons were made to gain coherence insight. Although conclusive results were not obtained, the investigation is presented to indicate both the present status and the direction of subsequent work. Some of the spectrum excursions can not be rationalized, and may be primarily a result of the uncertainty of the spectral density estimate. Ensemble averaging should resolve many of these interpretive problems.

Effective array gain for both signal and noise are shown in figures 3-44 and 3-45. The signal performance trend is flat, but an 8 dB per decade noise attenuation trend is evident in both events. This consistency suggests the feasibility of establishing an empirical coherence model with both frequency and distance dependencies to support future array design efforts. With properly

Table 3-28. Comparative Power Measurements

Event	Parameter	Unfiltered Power (dB)					
		Seismometer		Subarray		Array
		B1	Average	B1	Average	
Longshot	S	43.0	41.0	41.7	40.5˙	39.0
Nuclear	N	11.3	11.3	6.1	6.3	-6.4
Event	S/N	31.7	29.7	35.6	34.2	45.4
Kamchatka	S	40.7	40.5	40.1	40.2	39.4
Earthquake	N	8.5	8.4	4.7	5.0	-7.5
(4/8/66)	S/N	32.2	32.1	35.4	35.2	46.9
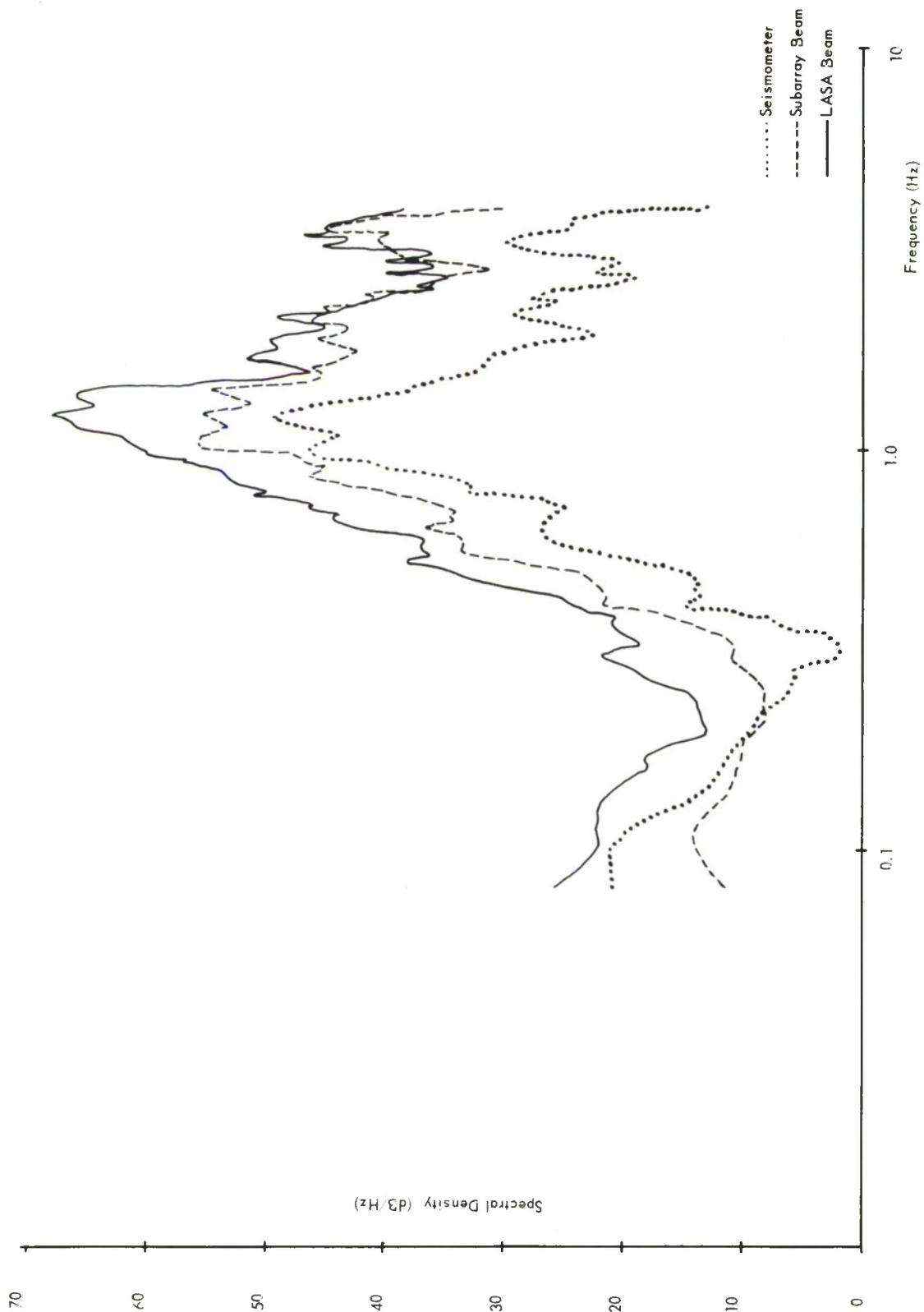
Figure 3-42. Longshot S/N Spectrum

Figure 3-43. Kamchatka S/N Spectrum

Seismometer
Subarray Beam
LASA Beam

Frequency (Hz)

Spectral Density (dB/Hz)
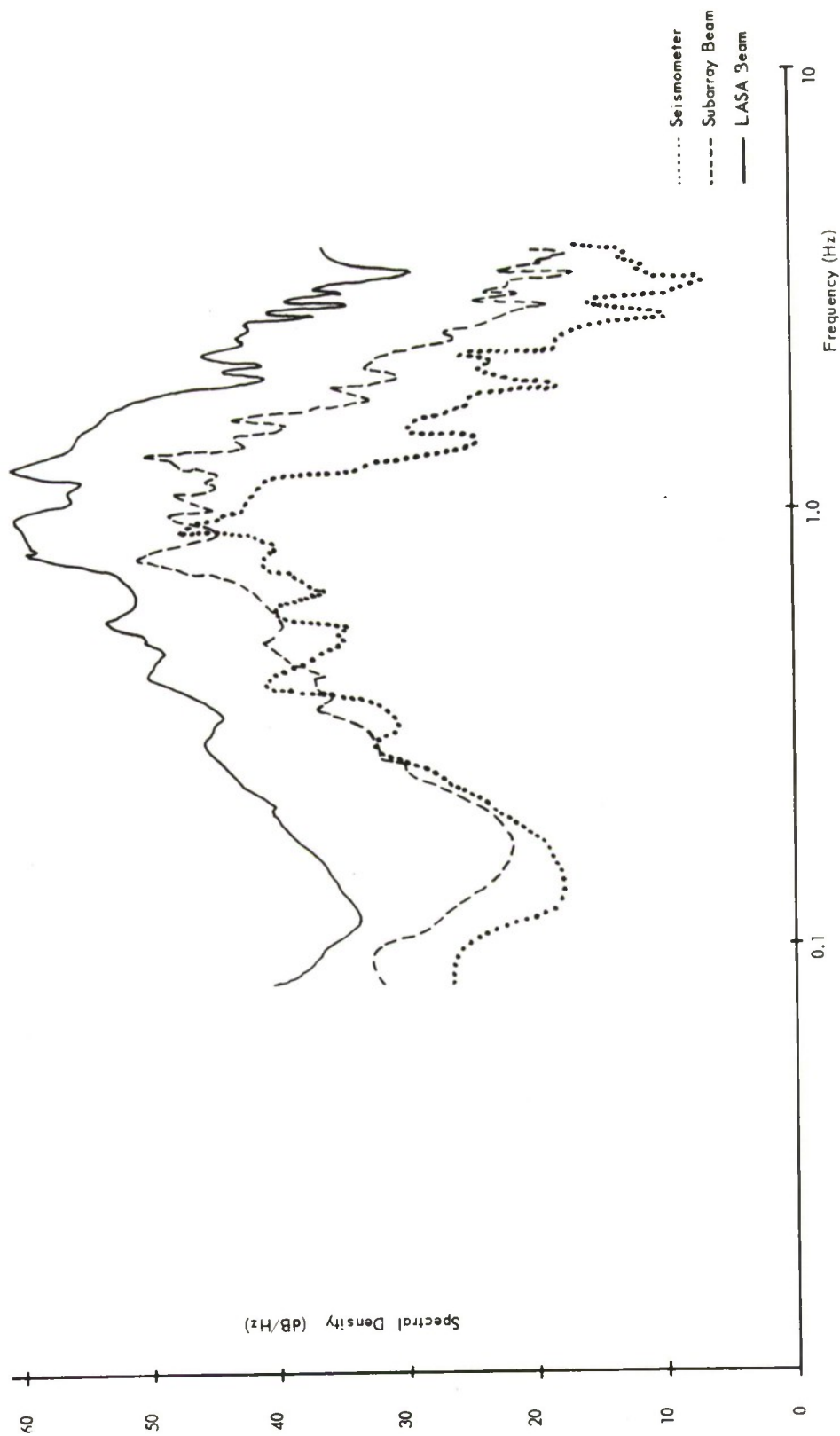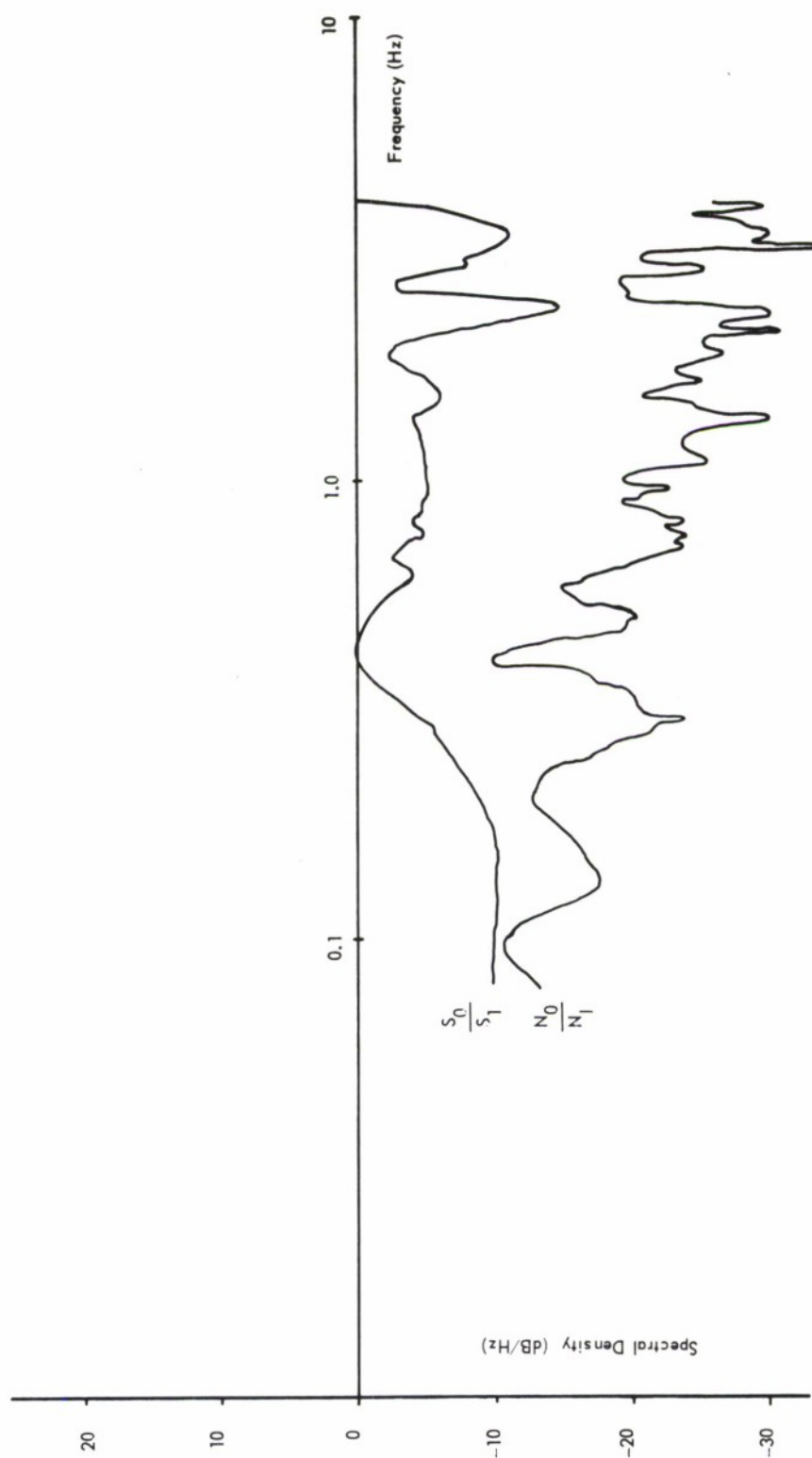
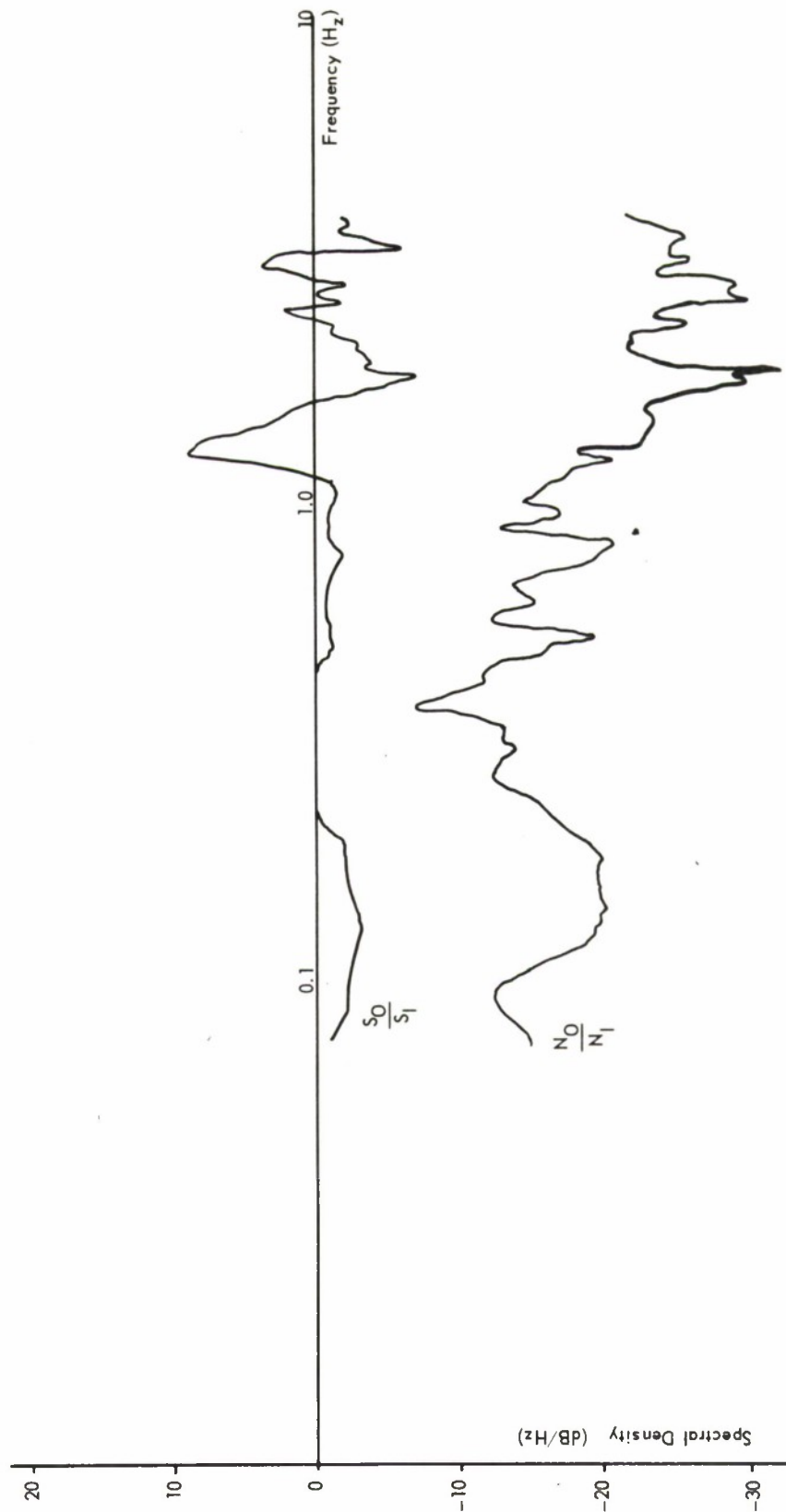Figure 3-44. Longshot Array Gain

Figure 3-45. Kamchatka Array Gain

selected and combined sensors, an exhibit can be generated to portray the frequency and distance realm encountered in LASA.

Beamforming gain was also shown as a function of frequency. Note that an observed gain beyond the theoretical value is realistic for coherent noise component rejection. This performance characteristic is extremely sensitive to the specific steering delays; inherent spectrum estimate uncertainty indicates that speculation should be restricted to trends. Ensemble averaging could be used in future analysis to improve the spectrum estimate and thereby increase interpolation confidence. Examination of the Earthquake arrival (see Figure 3-46) reveals reasonable subarray gain beyond 1.25 Hz and good composite subarray gain beyond 0.14 Hz. These cutoff frequencies are probably representative of the waveform coherence properties as viewed with the Montana LASA geometry.

The Longshot arrival appears to have quite different properties (Figure 3-47). Subarray gain is significant at a lower frequency, and composite subarray gain deteriorates beyond 1.5 Hz. Such diverse observations may not be representative of the physical situation, but rather of the spectrum uncertainty, the beam steering difficulties, or the significantly different signal bandwidth.

Obviously, the present study does not constitute an adequate statistical sample. Subsequent work should use the insight gained to systematically extend the knowledge of sensed seismic waveform properties. Process performance may be extended when a data base exists to tailor the frequency filter. This refinement can involve bandwidth, ripple, and many more subtle parameters. For example, a filter with nonsymmetrical skirts, with z-plane zeros at locations other than ± 1, or with a shaped bandpass may outperform a classical Butterworth or Tschebyscheff filter of the same order. An adjustment of coefficients accommodates such changes; they are then compatible with the microcode algorithm implementation.

Signal modeling can support other LASA activities. If consistent directional noise sources are evident, beam pattern adjustment may be worthwhile. Observation of the background field on the beam display should disclose any significant signature and indicate the feasibility of further study. Both the
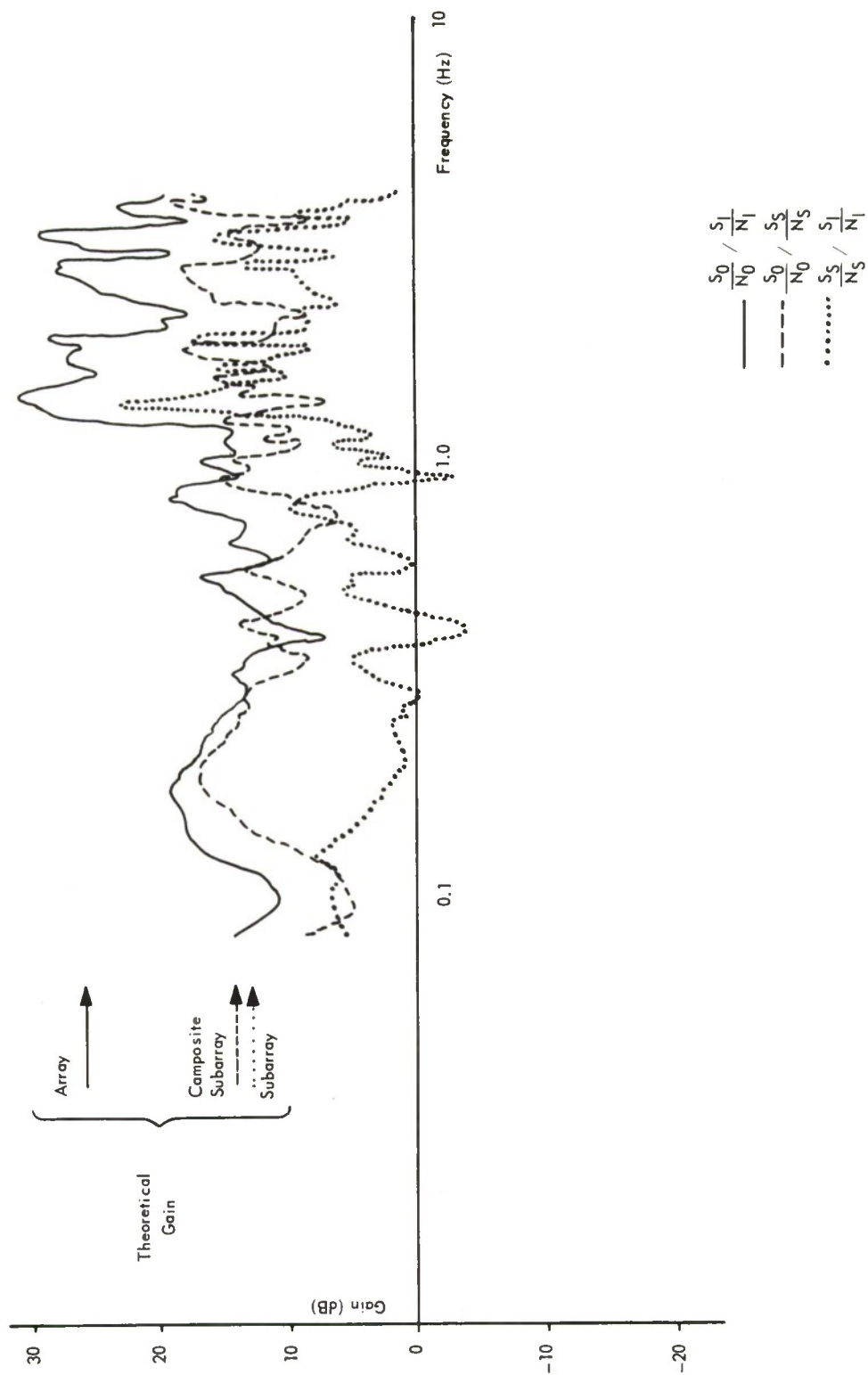
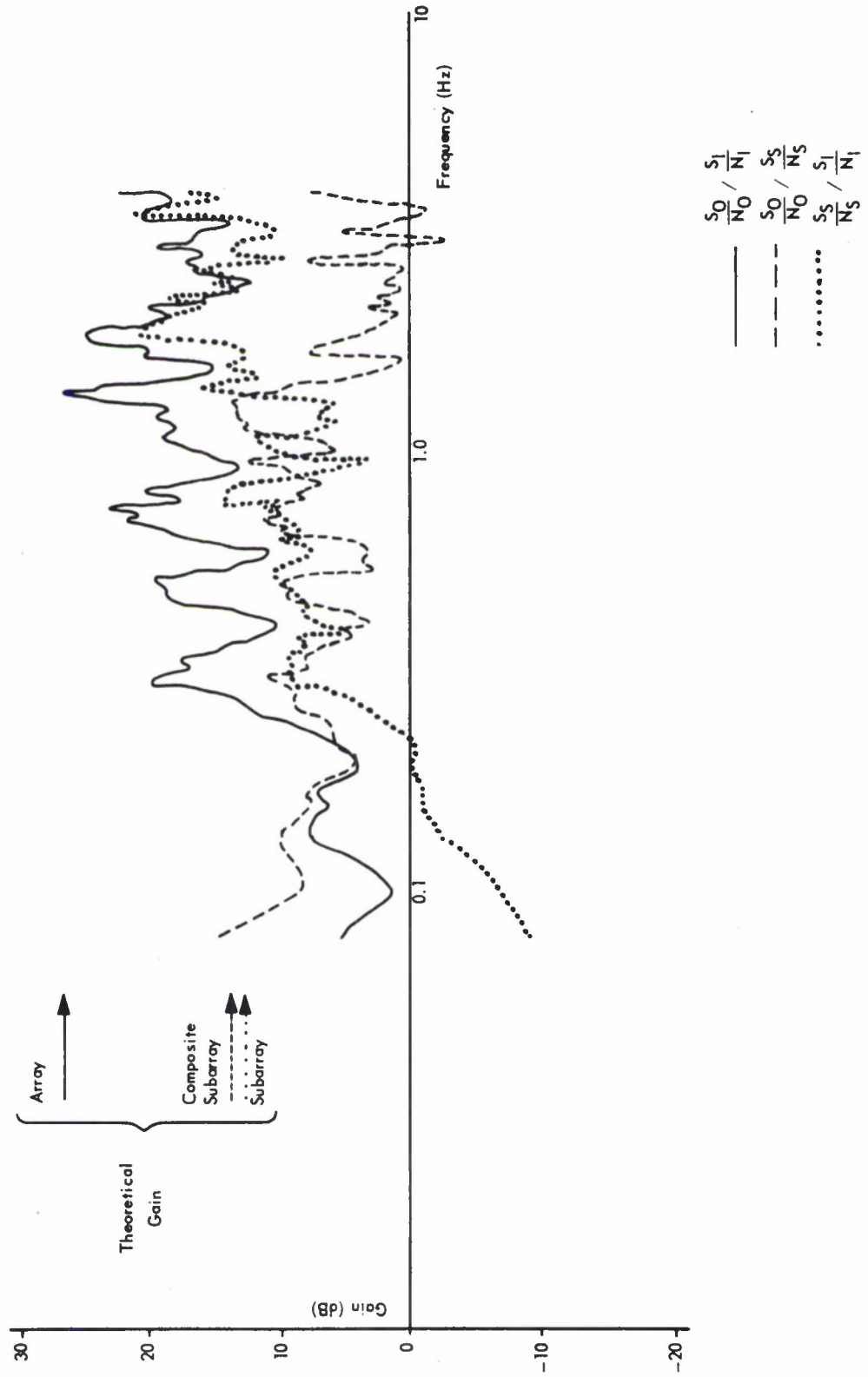Figure 3-46. Kamchatka Beamforming Gain

Figure 3-47. Longshot Beamforming Gain

techniques and the Montana signal characteristics may contribute to the design of future seismic array geometry.

3.9 EVENT BEAM SELECTION BY CENTER OF GRAVITY AND RADIUS OF GYRATION

This experiment will evaluate the accuracy of best beam selection, using the center of gravity and radius of gyration of the event beam pattern. Center of gravity and radius of gyration are defined, respectively, by the first and second moment arms of the beam power in the beam field. For these calculations the center of gravity is located relative to the geometric beam field center, and the radius of gyration is the second moment arm about the center of gravity. These relationships may be expressed as

$$\bar{r}_{CG} = \frac{\sum_{n=1}^{N} P_{Bn} \bar{r}_n}{\sum_{n=1}^{N} P_{Bn}} \qquad RG = \sqrt{\frac{\sum_{n=1}^{N} P_{Bn} \left| (\bar{r}_n - \bar{r}_{CG}) \right|^2}{\sum_{n=1}^{N} P_{Bn}}} \, , \quad (3.88)$$

where $\bar{r}_{CG}$ is the first moment vector which locates the center of gravity relative to the reference point, RG is the second moment arm which corresponds to the radius of gyration about the center of gravity, P_{Bn} is the short-term average beam power of the nth beam in the beam field of N beams, and $\bar{r}_n$ is the vector denoting the nth beam in the beam field.

If the center of gravity of the beam field is to correspond to the center of the event beam pattern, the event beam pattern must be symmetrical and the intensity of the background noise small compared to the event. The effects of both nonsymmetrical event patterns and background noise will be examined. When the radius of gyration about the center of gravity is minimum, the ratio between the intensities of the beams near the event center and the remaining beams in the beam field is maximum. This ratio may provide an indicator of the time period for selecting the best beam using the center of gravity. The minimum magnitude of the radius of gyration will be a function of signal

frequency, of signal-to-noise ratio, and of the size of the geographic area in which the event originates.

To predict the effect of noise on the center of gravity, the following model will be examined. Assume that the noise in the beam field is an ergodic signal (each member of the ensemble possesses identical statistical characteristics, and the statistical characteristics of the ensemble members are independent of time). For ergodic signals, the geometric center of the beam field will be, statistically speaking, the center of gravity of the signal field. Therefore, for this center-of-gravity calculation, the noise will be considered as the sum of the beam noise power throughout the beam field concentrated at the geometric center of the beam field.

The event will be considered symmetrical about the event center and contained within the beam field, allowing the event to be represented as the sum of event signal power on the beams in the beam field concentrated at the event center. Then the error in event selection may be calculated as

$$
r_{E_x}' = \frac{P_N r_{nx} + P_E r_{Ex}}{P_N + P_E}
$$

$$
r_{E_y}' = \frac{P_N r_{ny} + P_E r_{E_y}}{P_N + P_E}
$$

(3.89)

where P_E and P_N are the respective beam power sums for the event and noise. The vector relationships of these sums is shown in Figure 3-48.

The center of gravity for the combined signal fields of P_N and P_E is defined by the vector $\bar{r}_E'$ relative to an arbitrary coordinate system, and the error in event selection (ε) is the difference between $\bar{r}_E$ and $\bar{r}_E'$. The distance between beam field center and event center is represented by $\overline{\Delta r}$.
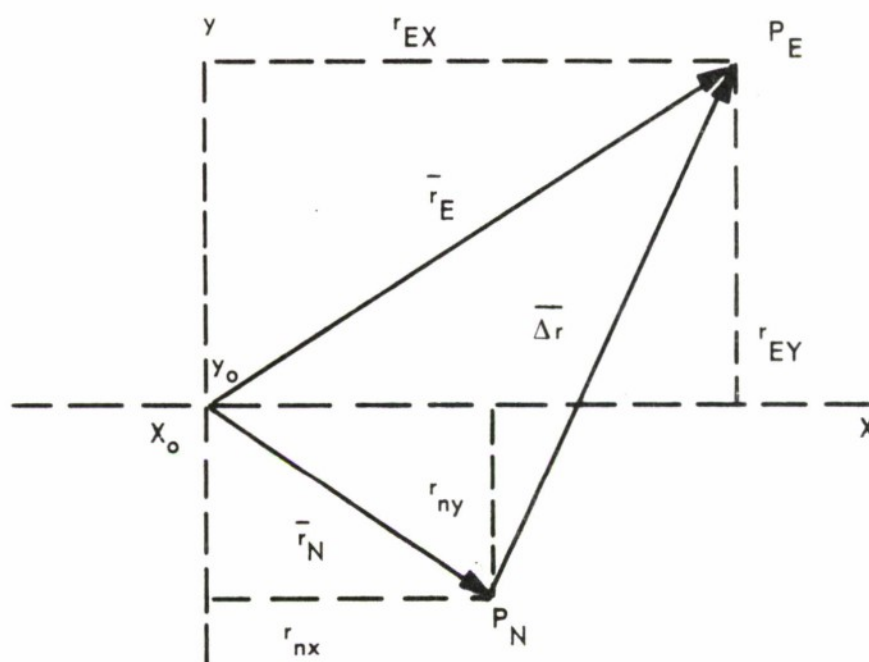
Figure 3-48. Center of Gravity, First Moment Vector Relationship

$$\varepsilon_y = r_{E_y} - r'_{E_y} = \frac{P_N}{P_E + P_N} \Delta r_y$$

$$\varepsilon_x = r_{E_x} - r'_{E_x} = \frac{P_N}{P_E + P_N} \Delta r_x \qquad (3.90)$$

$$\varepsilon_{Total} = \left[\frac{P_N}{P_E + P_N} \right] \overline{\Delta r}$$

The above example shows that for an ergodic noise signal field the error in event center selection is a function of the distance of the event center from the beam field center.

The nonsymmetrical event pattern for center-of-gravity calculations may be the result of nonsymmetry in the event pattern, or the result of a small beam field with a geometric center different from the event center. The loss of pattern symmetry from using a limited noncentered beam field is illustrated in Figure 3-49. In this example, the beam field represents an area in inverse velocity space covered by 255 close-packed event beams (diameter of .0024 seconds per kilometer). For a 1 Hz signal, both 6 dB side-lobes are not included within the beam field. Lower frequency signals would be even more severe, since the loss contours would move out proportionately while the size of the beam field would remain constant. A similar beam field containing 1000 beams would not cover both 6 dB side-lobes of a 0.5 Hz signal. This suggests a pedestal to set all beams with values below a specified loss level to zero, and/or the requirement of an iterative process to position the beam field center nearer the event center. As a demonstration of the error resulting from a nonsymmetrical event pattern within the beam field, Figure 3-50 shows the center of gravity as a function of time for Longshot, with the beam field of 151 beams centered at the event center; Figure 3-51 shows the center of gravity as a function of time for Longshot, with a beam field of 255 beams centered 3 beam positions away from the event center (same as illustrated in Figure 3-49.) Figure 3-51 also shows the radius of gyration about the center of gravity and
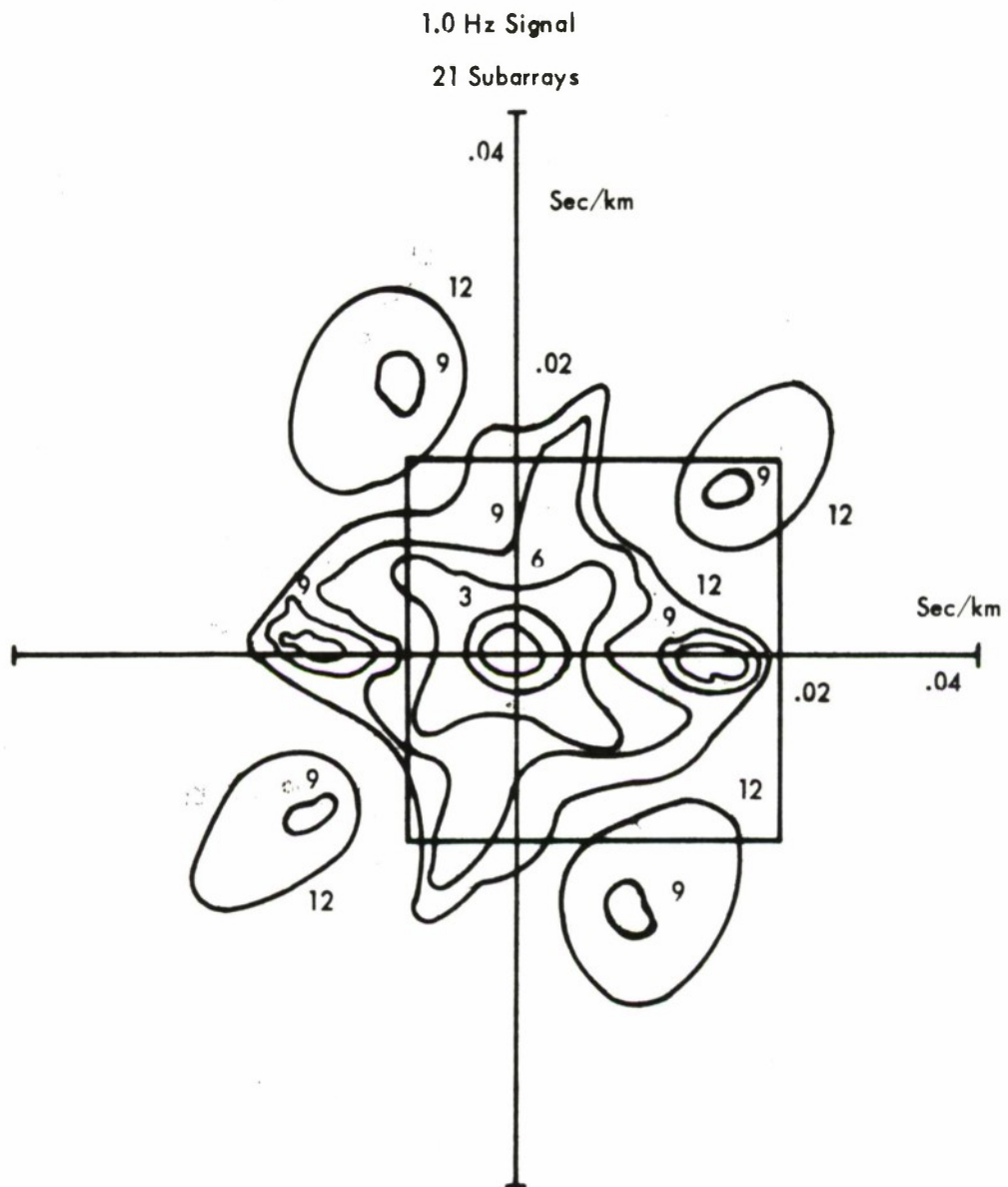
Figure 3-49. Beam Pattern of Full LASA Array
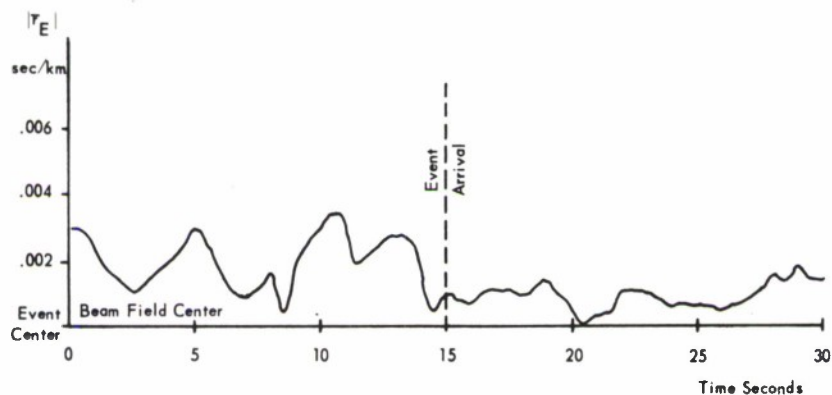
τ_E = Vector from event center to the center of gravity computed for short-term average Beam Power over two-second interval.

Figure 3-50. Longshot Beam Field of 151 Beams

τ_E = Same as Figure 3-50

RG = Radius of Gyration about Center of Gravity

$\overline{B}_{EC} = [\overline{P}_{EC}]^{1/2}$

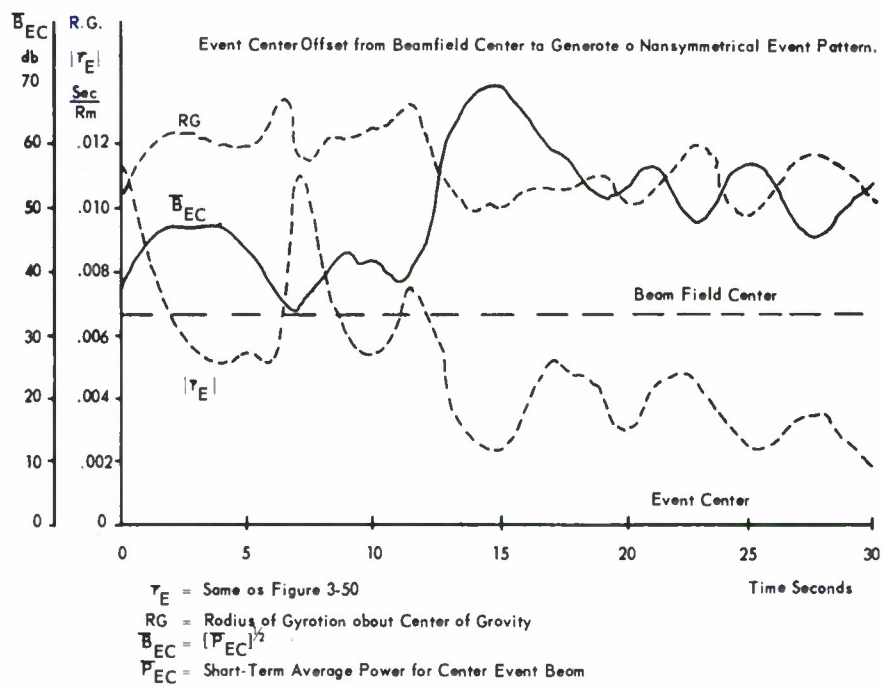$\overline{P}_{EC}$ = Short-Term Average Power for Center Event Beam

Figure 3-51. Longshot Beam Field of 255 Beams

the short-term average magnitude of the center event beam as functions of time.

This initial experiment indicates that it may be possible to locate the event center within one event beam or less, using the center of gravity of the beam pattern. The change in the radius of gyration about the center of gravity resulting from the event arrival was not so significant as originally anticipated. Although modifying the number of beams in the beam field may increase the change in the radius of gyration, another method for detecting the event arrival may be required. Additional analysis on a sufficiently large statistical sample of events must be performed to examine the errors from both nonsymmetrical event patterns and noise, before any conclusion about the use of the center of gravity and the radius of gyration to select the event center can be drawn.

Section 4

DATA ANALYSIS PROGRAMS

This section gives a general description and a flow chart for each of the Data Analysis programs developed during this study.

The programs are generally written in FORTRAN IV and are easily adaptable for processing on various machines. Although some of the programs are written specifically for the IBM System/360, the majority are currently being executed on an IBM 7090 under the IBSYS Operating System.

The IBSYS tape unit assignments used for the IBM 7090 programs are

FORTRAN Logical Unit	Mode	Physical Unit
1	BIN	A3
2	BIN	B3
3	BIN	A4
4	BIN	B4
5	BCD	A2
6	BCD	B1
7	BIN	B1
8	BCD	A5
9	BCD	A3
10	BCD	B3
11	BCD	A4
12	BCD	B4
13	BIN	A6
14	BIN	B2

FORTRAN Logical Unit	Mode	Physical Unit
15	BIN	A5
16	BCD	A6
17	BCD	B2

The standard IBSYS system input/output assignments are

System Unit	Physical Device
SYSLB1	A1
SYSIN1	A2
SYSUT1	A3
SYSUT3	A4
SYS OU1/OU2/PP1	B1
SYSLB2/CK2	B2
SYSUT2	B3
SYSUT4	B4

Several of the programs generate magnetic tapes in a format suitable for off-line plotting. These tapes are always generated on tape unit A6 of the IBM 7090 and recorded at 200 BPI on a 1200-foot reel. These recording restrictions are imposed by the off-line Calcomp plotting systems (Models 563 and 565) used.

4.1   LASA TAPE EDIT (Figure 4-1)

Purpose

This program converts LASA raw data tapes into IBM 7090 FORTRAN IV compatible binary tapes. All 651 channels present in the raw data tapes, or any part thereof, may be selected for editing.

Description

Input

Program input consists of edit processing control cards and from one to three LASA raw data tapes.

Card Input. The control cards are used to indicate to the program the number of (1) records to be skipped before initiating the editing process, (2) records to be edited, (3) channels to be edited, (4) LASA raw data tapes to be mounted, their respective names and reel numbers, and (5) each channel to be edited. Card inputs are

Data Card 1

Card Column	Field Specification	Variable Name	Sample Value
1 - 6	I6	NRSKP	4000
7 - 12	I6	NRED	6600
13 - 18	I6	NCH	525
19 - 24	I6	NOTAPE	3
31 - 36	A6	NAME (1)	Tape 1
43 - 48	A6	NAME (2)	Tape 2
55 - 60	A6	NAME (3)	Tape 3

where

NRSKP   Number of records to skip before editing (each record contains data for two sample periods)

NRED   Number of records to edit

NCH   Number of channels to edit

NOTAPE   Number of input tapes

NAME (I)   Six-character tape description

Data Card 2-N

Card Column	Field Specification	Variable Name	Sample Value
1 – 5	I5	ICH (I)	1
6 – 10	I5	ICH (I)	2
⋮	⋮	⋮	⋮
66 – 70	I5	ICH (I)	14

where

ICH(I)   Specifies channels to be edited. Fourteen channel numbers are recorded per card so the number of data cards required is directly related to the number of channels.

Tape Input. Each LASA raw data tape is a binary tape recorded at 800 BPI and composed of 18-bit words with extended sign and odd parity. Negative numbers are in two's-complement notation. A record on a raw data tape consists of (1) a four-word header containing the date-time data, (2) two frames each containing 651 words representing one data sample from each of the 651 channels, and (3) a seismometer status trailer, when required. All trailer data is ignored during the editing process. The raw data tapes must be mounted in the following order:

One Reel   Unit A4

Two Reels   First B3, Second A4

Three Reels   First A3, Second B3, Third A4

Computation

Each record on the raw data tapes is unpacked and placed in individual IBM 7090 words. The data channel values (seismometers) are converted to floating-point notation. The data is then arranged in memory for subsequent recording.

Output

Program output consists of an off-line printout and as many FORTRAN compatible LASA edit tapes as are required during the editing process.

Printed Output. The off-line printout lists all the information supplied on the input control cards. It contains the (1) number of logical records on the output LASA edit tapes, (2) raw data tape record numbers where read checks occurred, if any, (3) locations of unexpected end-of-files on the raw data tapes encountered before the specified number of records are edited, and (4) data from the header record written on the first LASA edit tape as described below.

Tape Output. Each LASA edit tape from unit B4 is a high-density (800 BPI) tape with each data word 36 bits in length. Each logical record on a LASA edit tape will consist of from 1 to 651 data words. Because these logical records are written in FORTRAN, each will be subdivided into physical records of no more than 256 words. The first logical record is a header record which contains in consecutive order the year, day, hour, minute, second, and millisecond of the first data sample record which follows the header; it also contains the number of edited channels and their respective channel numbers. The header words are in fixed-point form. Each logical record which follows the header record consists of a floating-point data sample for all the channels selected for editing. As raw data tapes are recorded, four data samples are lost during reel switching. To compensate for these lost records, four logical records of the last available data will be recorded when an end-of-file is reached on all but the last raw data tape.

Program Interaction

The edited tapes generated by this program form the input for the Subarray Beamformer (SABF) and Seismometer Power programs.

Program Restrictions

This program expects only one end-of-file per LASA raw data tape. Because LASA raw data tapes do not contain a year in their header, an NYEAR card must be inserted in the Read 1 Subroutine. The present deck has NYEAR = 1966.

Comments

This program is designed for the IBM 7090 computer under IBSYS supervision and is written in FORTRAN IV and MAP. All reading is done by Library IOCS and writing by FORTRAN IV.
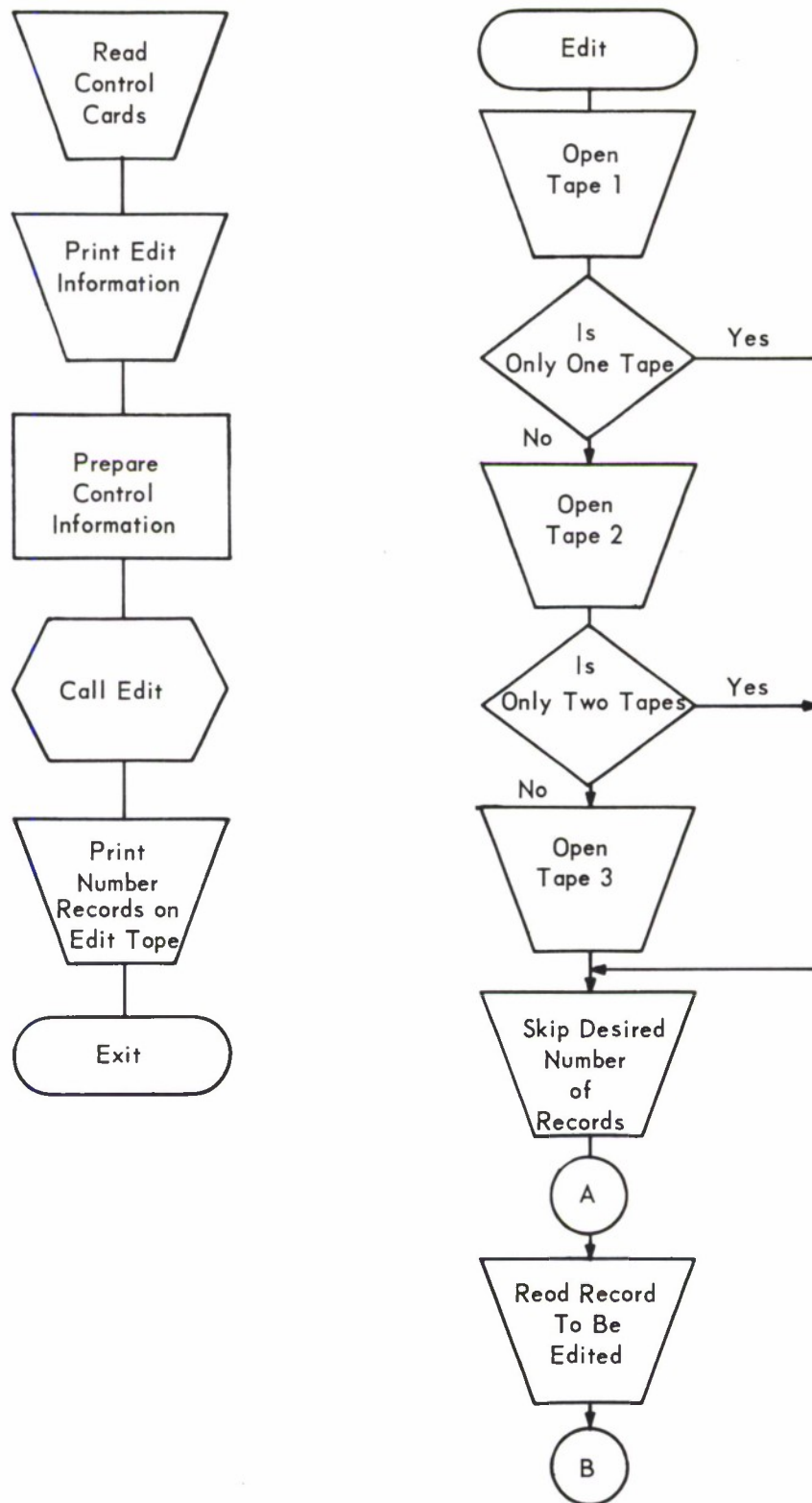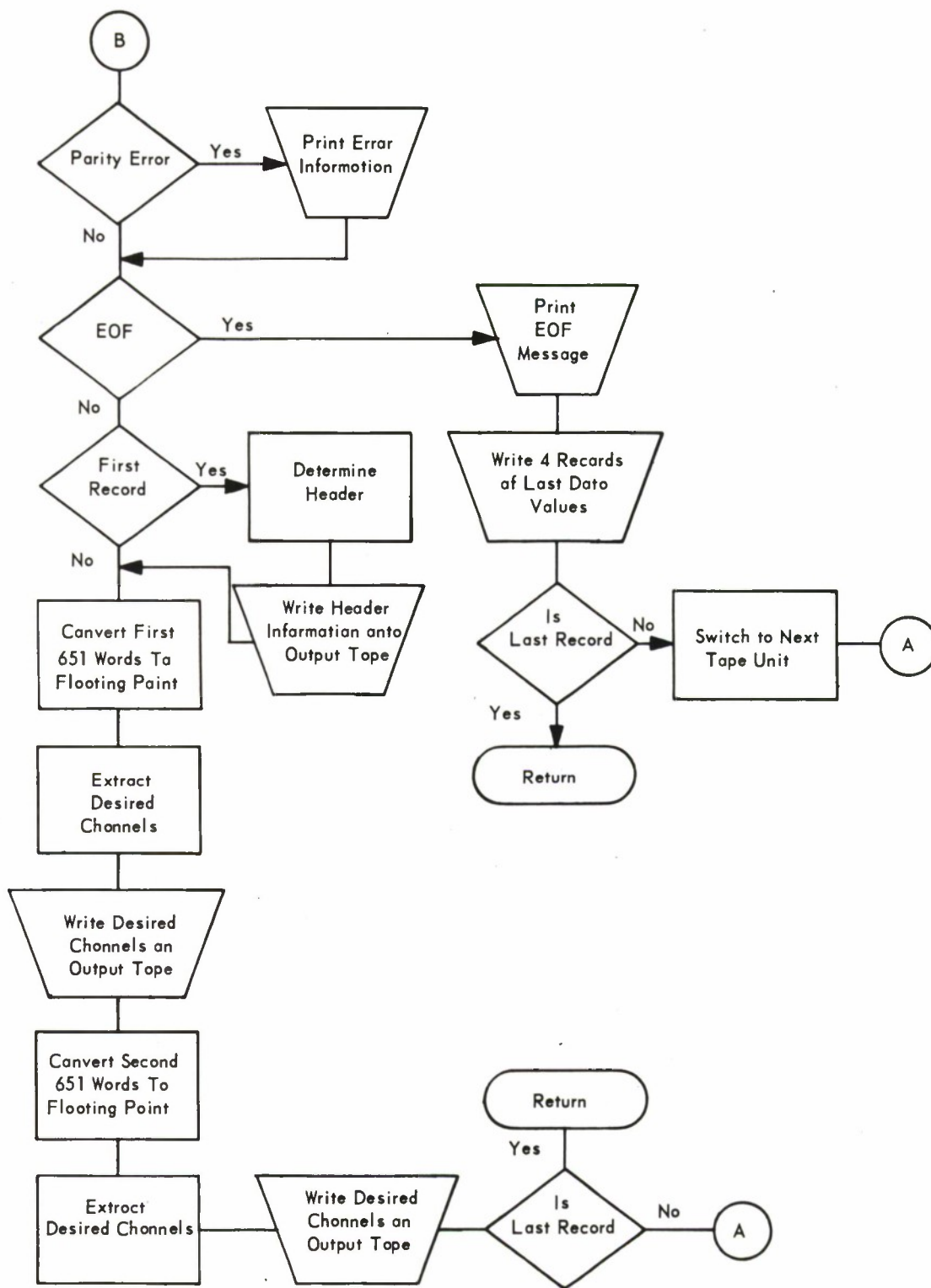
Figure 4-1. LASA Tape Edit (Sheet 1 of 2)

Figure 4-1. LASA Tape Edit (Sheet 2 of 2)

4.2   SIGNAL-TO-NOISE RATIO (Figure 4-2)

Purpose

This program constructs a LASA data tape containing a specified number of noise samples; these samples are followed by a specified number of signal samples, each of which has been multipled by a unique scaling factor and added to a noise sample. The overall effect is the generation of a magnetic tape containing an event in which the signal-to-noise ratio can be controlled. This tape is then available for processing through pertinent data analysis programs.

Description

Input

The program reads a LASA edit tape from unit B3 and extracts segments of noise samples and signal samples. If multiple input tapes are used, they are mounted alternately on units B3 and A3. Control cards provide the capability to choose precisely the portions of noise and signal samples to be used by the program in generating a pseudo-event tape with a known signal-to-noise ratio. Scaling factors for each seismometer present on the input tape are provided by card input.

Card Inputs

Data Card 1

Card Column	Field Specification	Variable Name	Sample Value
1 - 5	I5	NCH	525
6 - 10	I5	NSKP	1000
11 - 15	I5	NNOISE	6000
16 - 20	I5	NMSKP	5
21 - 25	I5	NSIG	3000
30 - 35	A5	NID	1/4
36 - 40	I5	NREEL	2

4-9

Card Column	Field Specification	Variable Name	Sample Value
45 - 50	A5	NBLNK	EVENT

where

NCH	Number of channels on input reel(s)
NSKP	Number of noise samples to skip
NNOISE	Number of noise samples to use
NMSKP	Number of samples to skip between noise and signal
NSIG	Number of signal samples (NSIG < NNOISE)
NID	Scaling factor identification
NREEL	Number of input reels
NBLNK	Signal data identification

Data Card 2

Card Column	Field Specification	Variable Name	Sample Value
1 - 5	I5	NOSF	525

where

NOSF	Number of scaling factors that follow on subsequent card(s)

Data Card 3-N

Card Column	Field Specification	Variable Name	Sample Value
1 - 14	F14.0	BSI(I)	.25
15 - 28	F14.0	BSI(I)	.25
⋮	⋮	⋮	⋮
57 - 70	F14.0	BSI(I)	.25

where

BSI(I)   Scaling factor for the Ith channel. Five scale factors are
           recorded per card so the number of data cards required is
           directly related to the number of channels.

Computation

The program skips noise on the LASA edit input tape to a specified sample
period. It then reads noise samples and immediately writes them onto the output
reel, until the point at which the signal is to be added to the noise samples is
reached. The noise from this point to the last of the specified noise samples
is read and written on an intermediate tape. The edit reel is then positioned,
if necessary, to the first signal sample.

The scaling process is then begun and entails the following for each
channel: read a signal sample; read a noise sample from the intermediate
tape; multiply the signal by the appropriate scale factor; add the noise sample;
and write the scaled signal plus noise value onto the output tape. This process
is continued for the desired number of signal samples.

Output

Output tapes are written on unit B4 in the same format as the input tapes,
and contain the same number of channels. The intermediate tape is on unit A4.

Program Interaction

The input and output tapes are in the LASA edit format. Therefore,
signal-to-noise ratio can be adjusted on any tapes of that format.

Program Restrictions

Each channel (seismometer) must have a distinct scaling factor. If there
are more channels than scaling factors, the remaining channels will be scaled
by a factor of one.

The number of noise samples must be greater than the number of signal samples. The difference will be the number of noise samples at the beginning of the output tape.

Comments

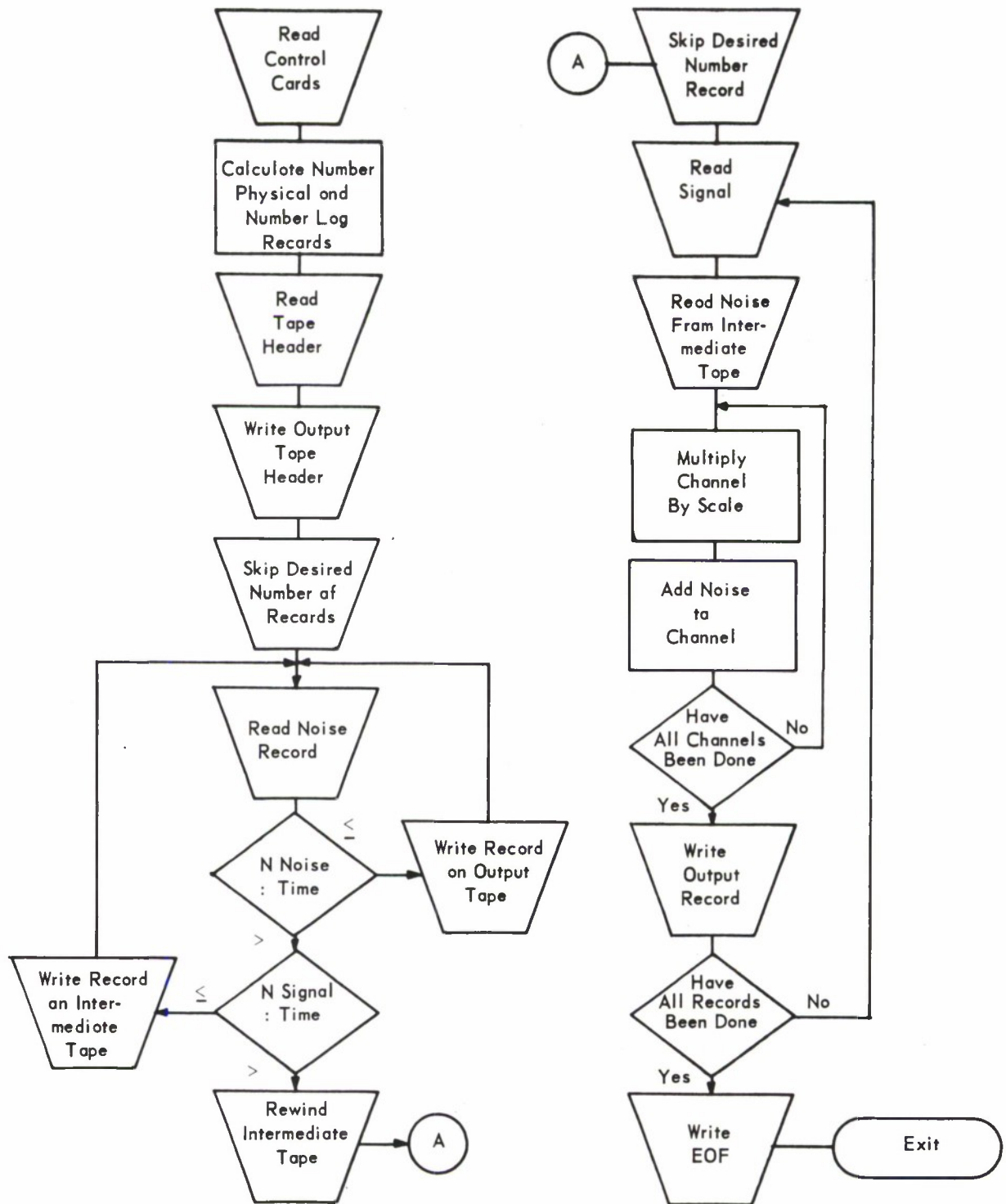This program is written in FORTRAN IV and MAP for the IBM 7090.

Figure 4-2. Signal-to-Noise Ratio

4.3   INVERSE VELOCITY SPACE-MAPPING (Figure 4-3)

Purpose

This program prepares inverse velocity space maps of the world land areas and seismic zones and lines of constant geocentric latitude and longitude.

Description

Input

Two forms of input acceptable are (1) Mode 0—Initial latitude and longitude coordinates and an incremental value for each to generate coordinate lines for inverse velocity space-mapping, or (2) Mode 1—Pairs of latitude and longitude to be mapped into inverse velocity coordinates.

Card Inputs (Mode 0)

Data Card 1

Card Column	Field Specification	Variable Name	Sample Value
1	I1	MODE	0

where

MODE   Equal to 0 for mode 0

Data Card 2

Card Column	Field Specification	Variable Name	Sample Value
1	I1	L	1

where

L   Number of title cards to be printed on plot (limited to a maximum of 9 cards)

Data Card 3

Card Column	Field Specification	Variable Name	Sample Value
1 - 48	8A6	BCD(1) – BCD(8)	TITLE

The comment in columns 1 - 48 will be the title on the Calcomp plot. Up to 9 cards may be provided at this point.

Data Card 4

Card Column	Field Specification	Variable Name	Sample Value
1 - 9	F9.4	PHIO	-106.221
10 - 18	F9.4	THETA0	46.6886
19 - 27	F9.4	RE	6370.
28 - 31	F14.0	A	13528.
32 - 45	F14.0	B	-46116.
46 - 59	F14.0	C	-100000.
60 - 61	I2	KON	0
62 - 63	I2	IRAN	0

where

PHIO	Longitude of receiver location in degrees (PHIO is negative if West)
THETA0	Latitude of receiver location in degrees (THETA0 is negative if South)
RE	Radius of the earth in kilometers
A, B, C	Constants in quadratic equation relating range and inverse phase velocity
KON	= 0, write out inverse phase velocity and azimuth < 0, write out the x and y components of inverse phase velocity
IRAN	= 0, omit range in printout ≠ 0, include range in printout

Data Card 5

Card Column	Field Specification	Variable Name	Sample Value
1 - 4	F4.3	WMAX	.1
5 - 8	F4.3	WMIN	.03

where

WMAX   Maximum value of inverse phase velocity to be plotted on map

WMIN   Minimum value of inverse phase velocity to be plotted on map

Data Card 6

Card Column	Field Specification	Variable Name	Sample Value
1 - 9	F9.4	PHI1	- 180
10 - 18	F9.4	DELPHI	5
19 - 22	I3	NPHI	64

where

PHI1   Initial longitude value in degrees

DELPHI Longitude increment in degrees

NPHI   Number of longitude values to be used (must be multiple of 18)

Data Card 7

Card Column	Field Specification	Variable Name	Sample Value
1 - 9	F9.4	THETA1	-90
10 - 18	F9.4	DELTHT	5
19 - 22	I3	NTHETA	32

where

THETA1 Initial latitude value in degrees

DELTHT Latitude increment in degrees

NTHETA Number of latitude values to be used

Mode 1 accepts as input a magnetic tape which was provided by the US Navy Oceanographic Office; this tape contains world map latitude and longitude coordinates to help prepare an inverse velocity space map, and must be mounted on FORTRAN logical unit 8.

Card Inputs (Mode 1)

Data Card 1

Card Column	Field Specification	Variable Name	Sample Value
1	I1	MODE	1

where

MODE   1 for Mode 1

Data Card 2

Card Column	Field Specification	Variable Name	Sample Value
1 – 9	F9.4	PHI0	–106.221
10 – 18	F9.4	THETA0	46.6886
19 – 27	F9.4	RE	6370.
28 – 31	F14.0	A	13528.
32 – 45	F14.0	B	–46116.
46 – 59	F14.0	C	–100000.

where

PHI0   Longitude of LASA in degrees (PHI0 is negative if West)

THETA0   Latitude of LASA in degrees (THETA0 is negative if South)

RE   Radius of the earth in KM

A, B, C   Constants in quadratic equation relating range and inverse phase velocity

Data Card 3

Card Column	Field Specification	Variable Name	Sample Value
1 – 4	F4.3	WMAX	.1
5 – 8	F4.3	WMIN	.03

where

WMAX   Maximum value of inverse phase velocity to be plotted on map

WMIN   Minimum value of inverse phase velocity to be plotted on map

Data Card 4

Card Column	Field Specification	Variable Name	Sample Value
1 – 5	I5	NBR	999

where

NBR   Number of latitude-longitude pairs to be read from input tape (choose NBR = 999 for the coordinate tape from US Navy Oceanographic Office)

Data Card 5

Card Column	Field Specification	Variable Name	Sample Value
1 – 3	I3	IPNT	50

where

IPNT   Program generates output for every IPNTth point transformed into an inverse phase velocity map

Computation

The equations used in the program are discussed in Appendix A of the Second Quarterly Technical Report (reference 3).

Output

Both Mode 0 and Mode 1 produce a printout with the following variables:

PHI0, THETA0, RE, A, B, C (input variables described in the input portion of this program writeup).

If C = 0, the header also contains

WM   Inverse phase velocity corresponding to the largest range obtainable from the equations in Section A.2.1 of the Second Quarterly Technical Report.

RM   Largest possible range from the same equation.

WO   Inverse phase velocity for range = 0 according to the same equation.

WM, RM, WO are useful for checking values of A, B, and C.

Mode 0 also records longitude values down the page and latitude values across the page. As noted in the input section of this program writeup, values for range will be printed if IRAN $\neq$ 0. If KON = 0, the magnitude and azimuth of inverse phase velocity will be recorded. If KON < 0, the (x, y) component values of inverse phase velocity will be recorded.

Mode 1 also records values of longitude, latitude, range in km., magnitude and azimuth of inverse phase velocity, and (x, y) component values of inverse phase velocity for every IPNTth point transformed.

Both Mode 0 and Mode 1 generate a Calcomp plot tape.

Program Interaction

None

Program Restrictions

Internal looping of the program requires the total number of lines of latitude formed to be a multiple of 18. There is no restriction on the number of longitude lines formed.

Comments

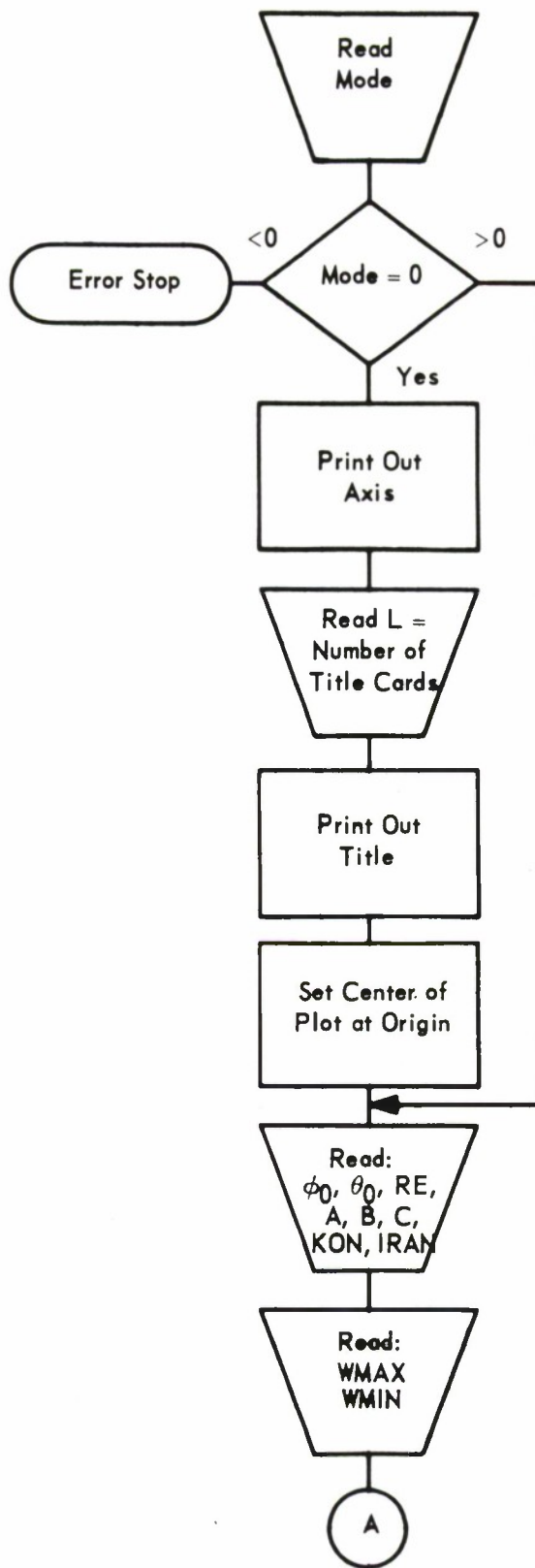This program is written in FORTRAN IV for the IBM 7090.

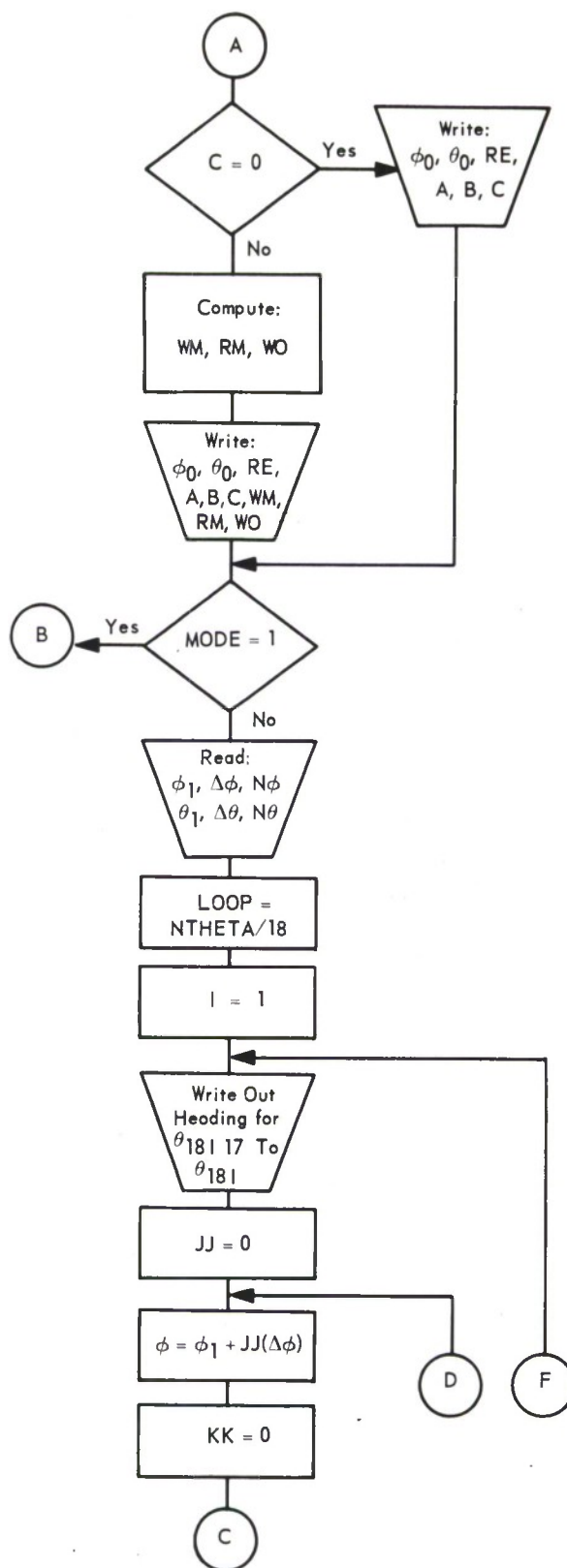Figure 4-3. Inverse Velocity Space-Mapping (Sheet 1 of 6)

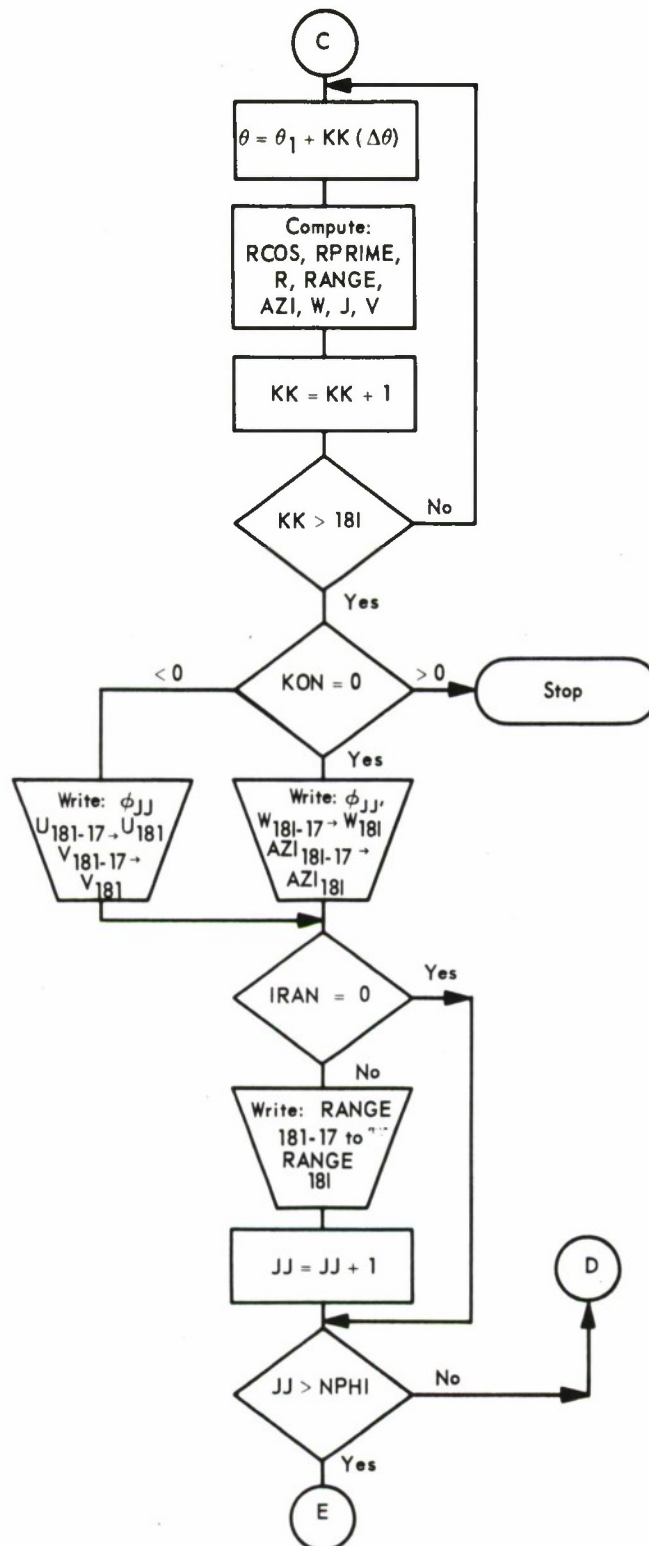Figure 4-3. Inverse Velocity Space-Mapping (Sheet 2 of 6)

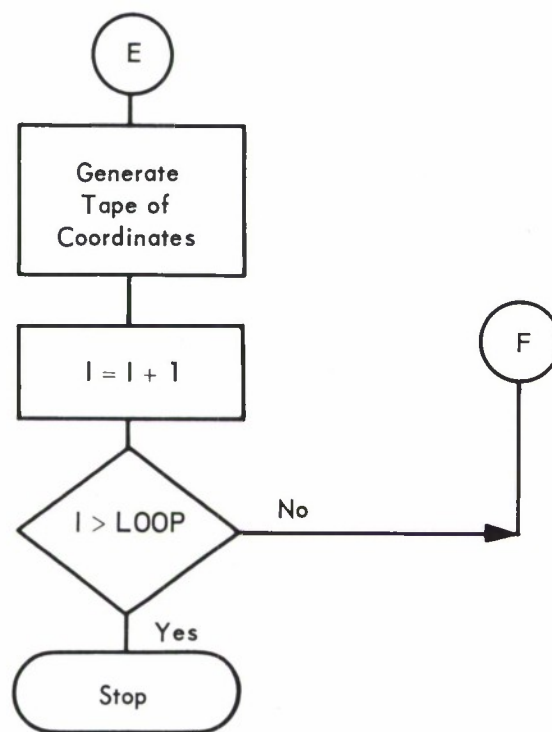Figure 4-3. Inverse Velocity Space-Mapping (Sheet 3 of 6)

Figure 4-3. Inverse Velocity Space-Mapping (Sheet 4 of 6)
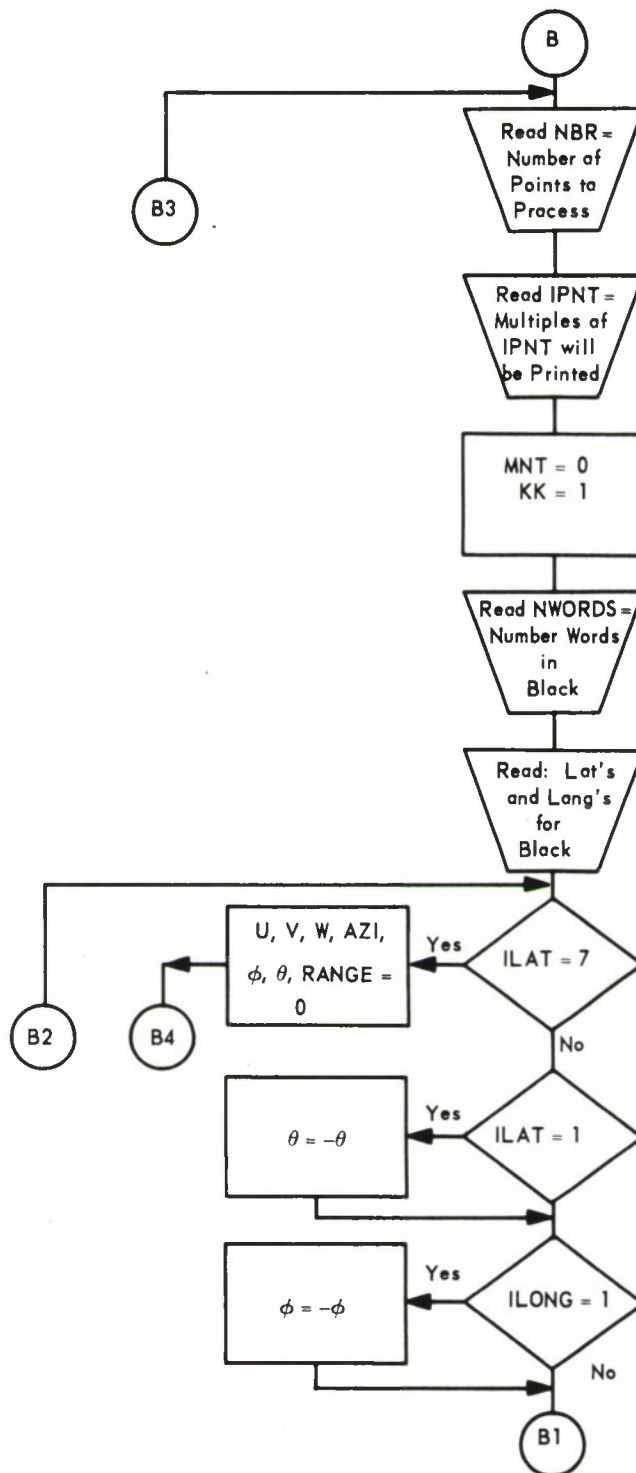
Figure 4-3. Inverse Velocity Space-Mapping (Sheet 5 of 6)

4-24
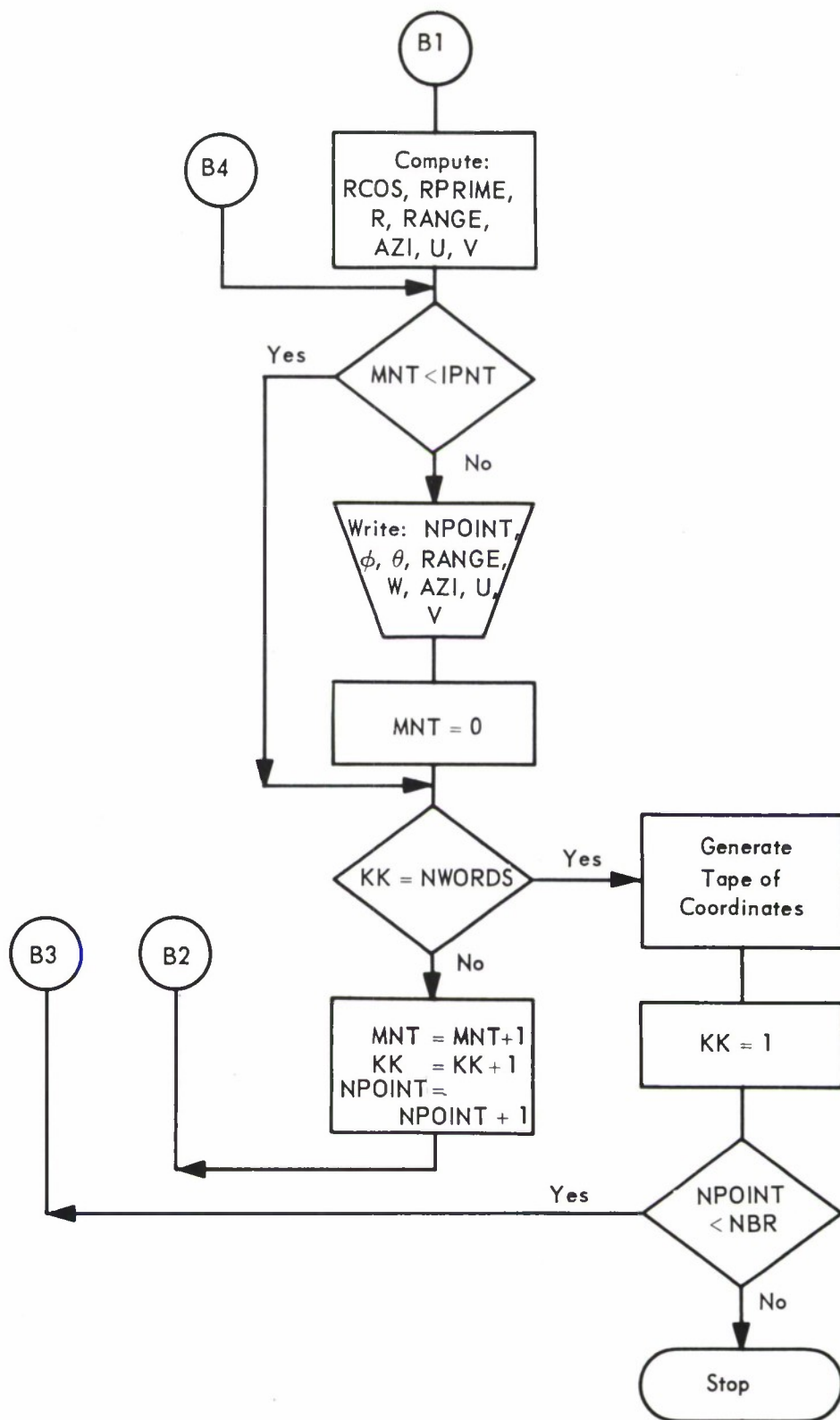
Figure 4-3. Inverse Velocity Space-Mapping (Sheet 6 of 6)

4.4 FILTER COEFFICIENT (Figure 4-4)

Purpose

This program generates recursive filter coefficients for a given lowpass, highpass, bandpass, or bandreject Butterworth or Tschebyscheff filter; it has the option of calculating a frequency response, an impulse response of both the filter transfer function and its denominator, and corresponding bias and variance coefficients. The frequency response and impulse response can also be plotted.

Description

Input

The desired filter variables (type, kind, order) must be specified with sampling rate and center and/or cutoff frequencies.

Card Inputs

Data Card 1

Card Column	Field Specification	Variable Name	Sample Value
1	I1	LC1	3
2-11	F10.5	F1	0.7
12-21	F10.5	F2	1.4
42-51	F10.5	FS	10.0
57-61	F5.3	RT	0.5
62-67	A6	TYPE	BP-TE
68-70	I3	K	1
71-72	I2	NCF	5

where

LC1	1/2/3 condition. LP filter (F1 input)/HP filter (F2 input)/BP or BR filter (F1 and F2 input)
F1	Frequency (see LC1)
F2	Frequency (see LC1)
FS	Sampling rate (Hz)

RT	Ripple on Tschebyscheff filter (dB)
TYPE	Alphameric filter description
K	Filter order
NCF	(Optional) Calculate coefficients for order K through NCF. If NCF is blank, only coefficients for order K will be computed.

Data Card 2

Card Column	Field Specification	Variable Name	Sample Value
1-5	F5.0	GAPS	0.1
6-10	I5	IPLOT	1
11-15	F5.0	ALPHAI	-
16-20	I5	MERROR	-
21	I1	KIMPLS	1
22	I1	IMPPLT	1
23-27	F5.0	QBITS	-
28-32	F5.0	DELTAH	-
33-40	F8.0	RHO	-

where

GAPS	(Optional-Call FREQR) 0/Value condition. Do not calculate full frequency response/Give frequency response incrementing frequency between calculations by GAPS. (Note: IMPLS must be called if FREQR is to be called.)
IPLOT	(Optional-Call FRQPLT) 0/1 condition. Do not write plot tape for frequency response/Write plot tape for frequency response. Tape should be mounted on A6 at 200 BPI (ring in). (Note: FREQR must be called if FRQPLT is to be called.)
ALPHAI	0/Value condition. Use ALPHAI = 5.0 set by program/Override program value with ALPHAI.
MERROR	0/Value condition. Use MERROR = 25 as set by program/ Override program value with MERROR. (Note: ALPHAI and MERROR determine how far the impulse response is carried out. The larger value of MERROR or $\frac{(ALPHAI)\ (F_S)}{F}$ is used where F_s is sampling rate and F = F1 for lowpass filter, F2 for highpass filter, and $\sqrt{F1 * F2}$ for bandpass or bandreject filter.

KIMPLS   (Optional–Call IMPLS) 0/1 condition. Do not calculate
         impulse response/Calculate impulse response.

IMPPLT   (Optional) 0/1 condition. Do not write tape to be used by
         Impulse Response Plot program/Write tape for use by Impulse
         Response Plot program. Tape should be mounted on B2 at 800
         BPI (ring in). (Note: IMPLS must be called if tape is to be
         written.)

QBITS   0/Value condition. Use QBITS = 27 (Number of bits in floating
         numbers)/Override program value with QBITS.

DELTAH   0/Value condition. Use $\Delta H = 0.5$/Override program value with
         ΔH = DELTAH.

RHO   0/Value condition. Use ρ = .001/Override program value with
         ρ = RHO.

Computation

The computations are discussed in Section 3.7 of this report.

Output

This program produces for off-line printout the a [A(N)] and b[B(N)] filter
coefficients and an abbreviated frequency response [20 Log H (db)] with phase
angle [H(DEG)] for the filter. When the option for an expanded frequency re-
sponse is exercised, the frequency response of the roundoff spectrum [S(dB/HZ)]
and denominator coefficients [–20 Log B (dB)] is also printed. When the option
for an impulse response is exercised, the time in seconds (M/FS) and the im-
pulse response of the filter coefficients [C(M)] and denominator coefficients
[D(M)] are printed.

Program Interaction

Filter coefficients generated by this program are used in the recursive
filter in the Subarray Beamformer (SABF) program.

Program Restrictions

Subject to precision requirements, this program is limited to order 20 for lowpass and highpass filters and limited to order 10 for bandpass and bandreject filters.

Comments

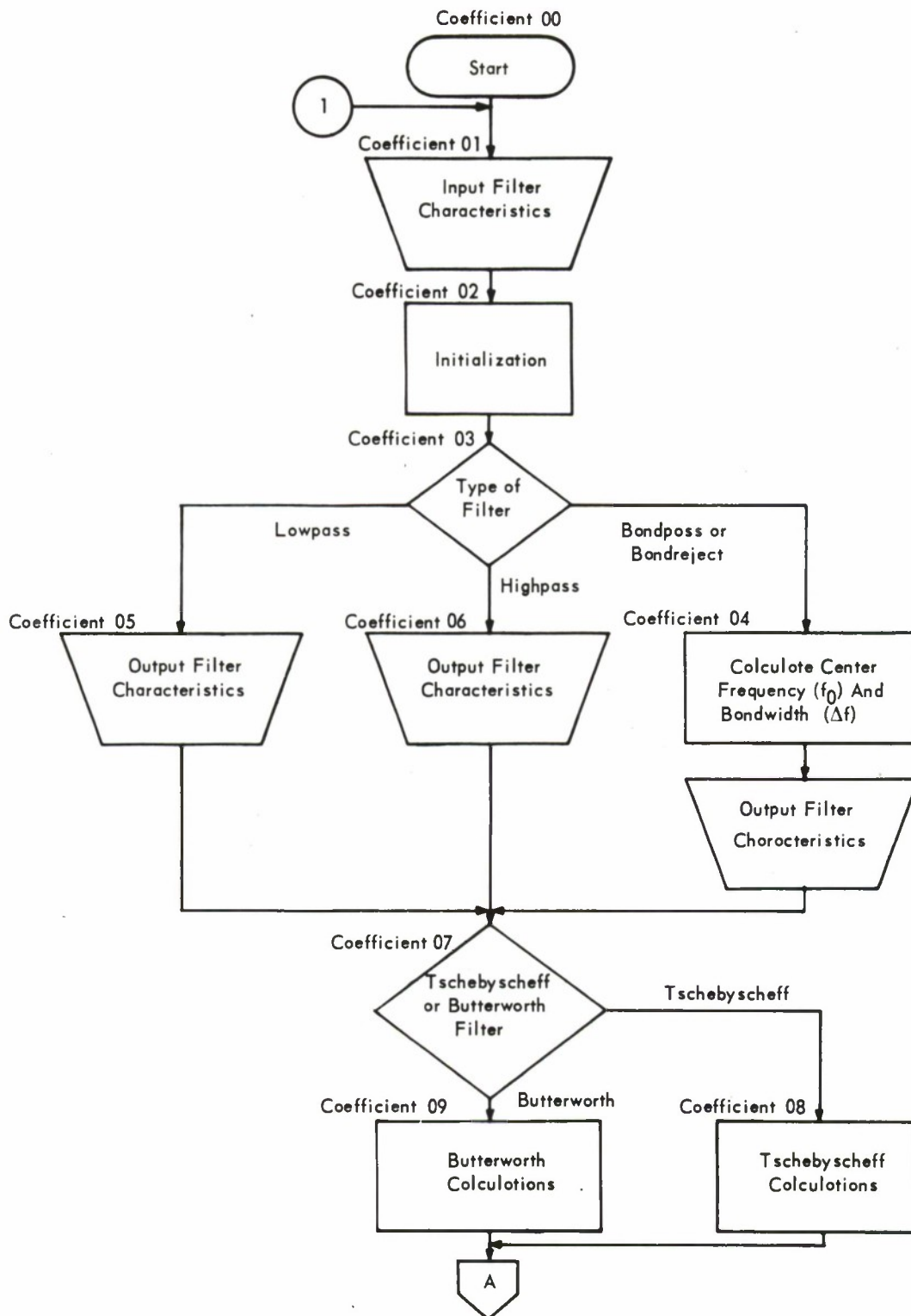This program is written in FORTRAN IV for the IBM 7090.

Figure 4-4. Filter Coefficient (Sheet 1 of 3)
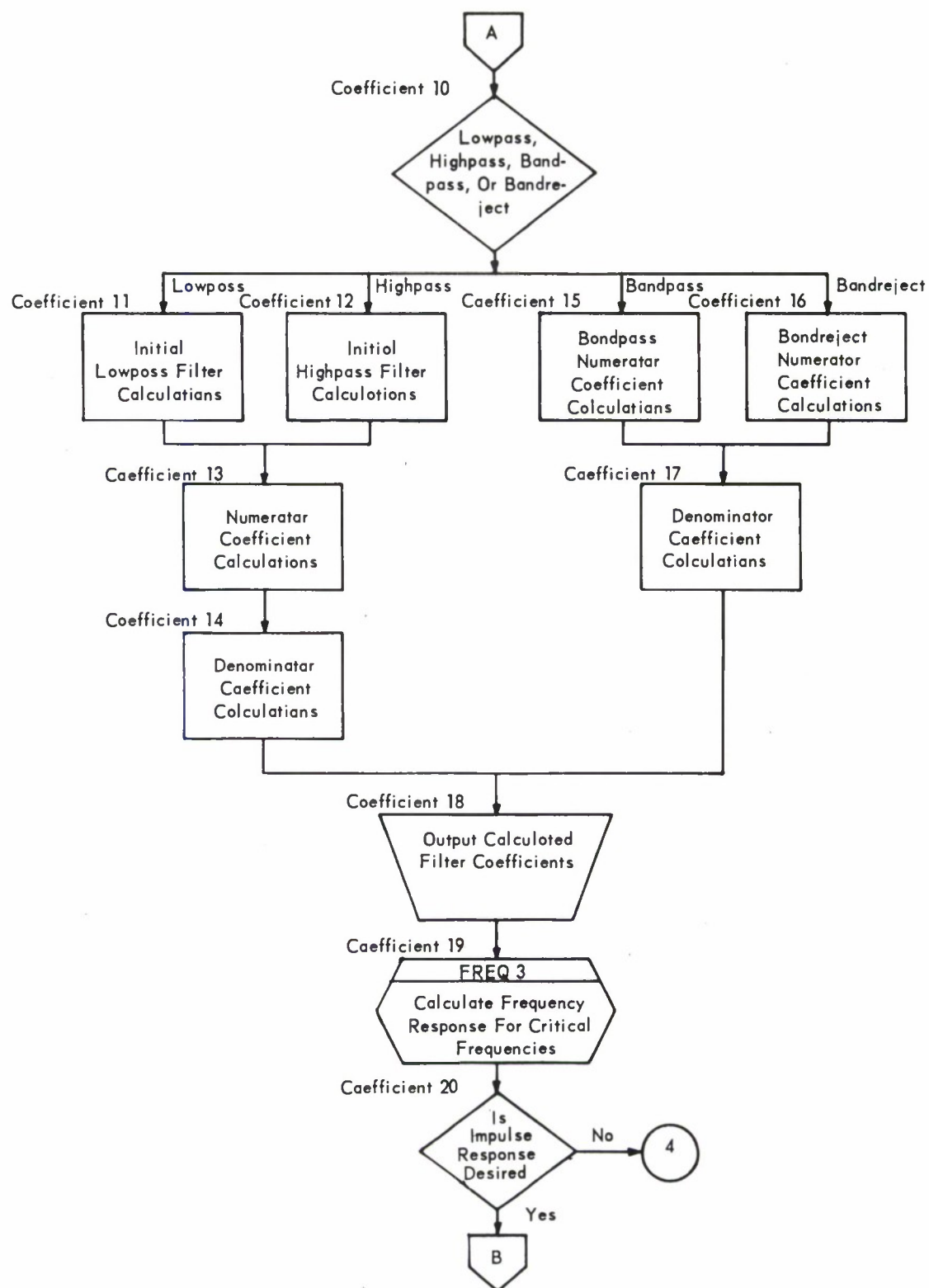
Figure 4-4. Filter Coefficient (Sheet 2 of 3)
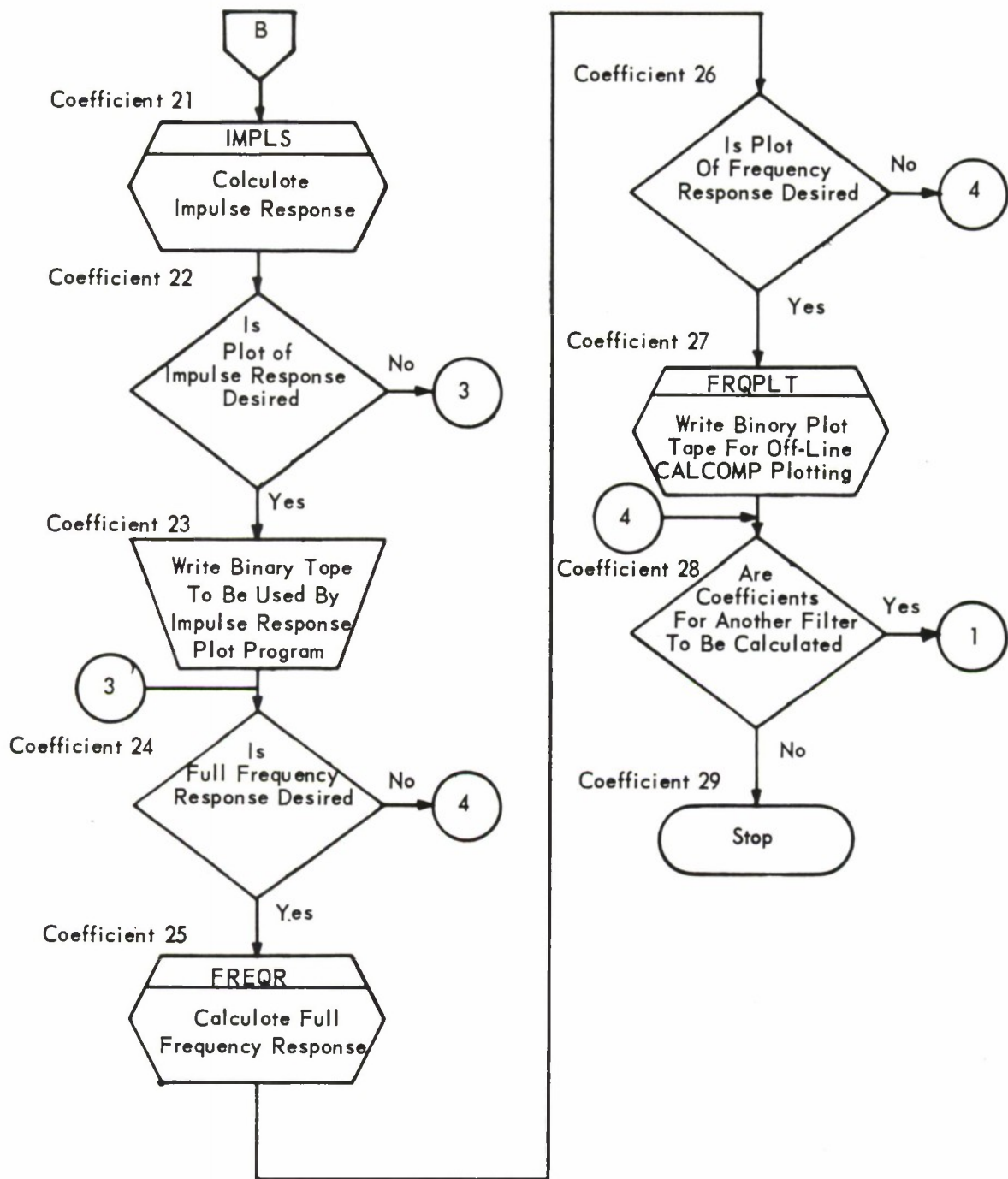
Figure 4-4. Filter Coefficient (Sheet 3 of 3)

4.5   SUBARRAY BEAMFORMER (SABF) (Figure 4-5)

Purpose

This program produces subarray beams which can be used for further processing. The program calculates a variable number of subarray beams for all subarrays for which seismometer data is available on the input tape. In addition, the option to pass the beams through a digital filter is provided, and the point at which each of the beams exceeds a prescribed threshold is computed and recorded.

Description

Input

A LASA edit tape is the main input to the SABF program. In addition to this, seismometer data, control parameters, digital filter parameters, and time delays form other inputs.

Card Input

Data Card 1

Card Column	Field Specification	Variable Name	Sample Value
1-5	I5	NRSKP	1750
6-10	I5	NRPRO	3280
11-15	I5	NSUB	21
16-20	I5	NSBCH	25
21-25	I5	NBPSA	1
26-30	I5	IPHST	21

where

NRSKP   Number of logical records to be skipped before processing

NRPRO   Number of logical records to be processed

NSUB   Number of subarrays on input tape (NSUB ≤ 21)

NSBCH   Number of seismometers per subarray on input tape (NSBCH ≤ 25)

NBPSA   Number of beams to be formed for each subarray (NBPSA ≤ 6)

IPHST   Number of past history records to be maintained for beam-forming (IPHST ≤ 21)

Data Card 2

Card Column	Field Specification	Variable Name	Sample Value
1-5	I5	LCFIL	1
6-10	I5	LCWCH	0
11-15	I5	LCWBM	1
16-20	I5	LCWTP	0
21-25	I5	ITHRES	2400
26-30	I5	IBRATE	10

where

LCFIL   =0, no filter is to be implemented
               =1, filter is to be implemented

LCWCH   =0, seismometer input values not printed
               =1, seismometer input values printed

LCWBM   =0, beam output values not printed
               =1, beam output values printed

LCWTP   =0, process first data tape
               =1, read header from 1st tape, then mount 2nd tape to process

ITHRES   Threshold value to be used on beams

IBRATE   Rate (per second) at which beams are to be formed

Data Card 3

Card Column	Field Specification	Variable Name	Sample Value
11-15	I5	NCENT	1
26-30	I5	NRING(1)	0
41-45	I5	NRING(2)	1

Card Column	Field Specification	Variable Name	Sample Value
56-60	I5	NRING(3)	1
71-75	I5	NRING(4)	1

where

NCENT =0, delete all center seismometers from beamforming process
=1, use all center seismometers in beamforming process

NRING(I) =0, delete B, C and D, E and F, G and H ring of all subarrays from the beamforming process (respectively, I = 1, 4)
=1, use B, C and D, E and F, G and H ring of all subarrays in the beamforming process

Data Card 4A

Card Column	Field Specification	Variable Name	Sample Value
11-15	I5	NSPEC	2

where

NSPEC Number of specific individual seismometers to be deleted from the beamforming process.

Data Card 4B (Necessary if NSPEC > 0)

Card Column	Field Specification	Variable Name	Sample Value
11-15	I5	NSEIS(I) I=1	17
16-20	I5	NSEIS(I) I=2	38
.			
.			
56-60	I5	NSEIS(I) I= NSPEC	521

where

NSEIS Specific seismometer to be deleted from the beamforming process. Ten seismometer channel numbers are recorded on each card so the number of cards required is directly related to the number of individual seismometers to be deleted (NSPEC).

Data Card 5 (Necessary if LCFIL ≠ 0)

Card Column	Field Specification	Variable Name	Sample Value
1-54	54H	(Type of Filter)	Butter-worth B-P .9-1.4 10Hz 3rd order

where

(Type of Filter) 54-character description of type of filter to be implemented

Data Card 6 (Necessary if LCFIL ≠ 0)

Card Column	Field Specification	Variable Name	Sample Value
1-5	I5	NP	6
6-20	E15.8	A0	0.14891068E-02
21-35	E15.8	B0	0.10000000E+01

where

NP Degree of filter—number of cards required to contain the coefficients required for an NP degree filter

A0 First numerator filter coefficient

B0 First denominator filter coefficient

Data Card 7 (Necessary if LCFIL ≠ 0)

Card Column	Field Specification	Variable Name	Sample Value
1-15	E15.8	A(m)	0.053E+01
16-30	E15.8	B(m)	-0.42633238E 01

where

A(m) Numerator filter coefficient

B(m) Denominator filter coefficient

Card Column	Field Specification	Variable Name	Sample Value
1-3	I3	ITD(J, L)	4
4-6	I3	ITD(J, L)	5
.			
.			
73-75	I3	ITD(J, L)	3

where

ITD(J, L) Time delay for the Lth seismometer available on the input tape for the Jth beam.

Since there are 25 time delays provided per card, the number of cards required is directly related to the number of seismometers available and the number of beams to be formed.

Tape Input. The input tapes must be of LASA edit format, and the first tape mounted on physical unit B2 must have a standard edit format header. If the data to be processed begins on a tape which does not have a header, a header tape must be mounted initially and the input variable LCWTP set equal to one. In this situation the header record is read from the first tape, and then a program pause occurs so that the desired tape may be mounted.

Computation

Three main calculations are present in the SABF program—beamforming, filtering, and thresholding.

Beamforming. The computation involved in the beamforming process in SABF is represented by

$$B_{jk}(t) = \frac{1}{I_j} \sum_{i=1}^{NSBCH} f_{ij}(t - N_{ijk}) \cdot wt_{ij} \qquad (4.1)$$

where

I_j	Number of seismometers with weights equal to 1 in jth subarray
i	ith seismometer
j	jth subarray
k	kth beam
t	Current sample time
N_{ijk}	Time delay for ith seismometer for the kth beam in the jth subarray
f_{ij}	LASA edit data from the ith seismometer in jth subarray
wt_{ij}	Weight for the ith seismometer in the jth subarray (equal to either one or zero and used to delete individual seismometers from beam sums)
$B_{jk}(t)$	Resultant subarray beam for the kth beam in the jth subarray
NCH	Number of seismometers per subarray

As indicated in the equation, each beam formed represents a delayed sum of weighted seismometers for a particular subarray. This process is repeated, using a different set of time delays, for each beam formed in that subarray, and then repeated for the total number of subarrays present. The number of beams formed, then, is the product of j and k.

Recursive Filtering. The computation involved in the recursive filtering process in SABF is represented by

$$G_{jk}(t) = \sum_{p=o}^{P} a_{jk}(p) \cdot B_{jk}(t-p) - \sum_{p=1}^{P} b_{jk}(p) \cdot G_{jk}(t-p) \qquad (4.2)$$

where

P	Degree of the filter
j	jth subarray
k	kth beam
t	Current time sample
$a_{jk}(p)$	Filter coefficients
$b_{jk}(p)$	Filter coefficients

$B_{jk}(t-p)$ kth beam formed in the jth subarray at sample time (t-p)

$G_{jk}(t-p)$ kth filtered beam formed in the jth subarray at sample time (t-p)

As the equation indicates, the filtering is performed on the beams formed in SABF. Each beam formed is passed through the same digital filter, and a resultant filtered beam value, $G_{jk}(t)$, for the current time period is produced.

Thresholding. Each beam and filtered beam in SABF is compared with a threshold value provided as input to the program to determine when the threshold is first exceeded. The logic is similar to that incorporated within the Threshold Time Delay program. The threshold information is required by other programs.

Output

Both printed output and magnetic tape output are produced by SABF.

Printed Output. Hard-copy results of this program include such pertinent run parameters as event identification, seismometers used and deleted, number of samples processed, number of beams formed, beamforming rate, delays used in beamforming, filter parameters (if used), and points at which the unfiltered beam and filtered beam values exceeded a threshold. The option also exists to print the center seismometer and beam values obtained throughout the process.

Tape Output. A tape consisting of a header of pertinent execution parameters followed by all unfiltered beam and filtered beam values generated is produced for use by other programs. This tape also includes the value of the center seisometer in each subarray for each sample period considered in the processing. The logical format of the tape is presented on a sample time basis. The center seismometer and unfiltered beams make up one FORTRAN logical record; filtered beams, if produced, make up the next FORTRAN logical record.

Program Interaction

This program requires a LASA edit tape generated by the LASA Tape Edit program. The filter coefficients used are obtained from the results of the Filter Coefficient program. The time delays used are provided by the Threshold Time Delay program. The magnetic tape output serves as input to the LASA Beamformer (LBF) program and to the SABF Power program. The points at which the threshold is exceeded are also used in both of these programs.

Program Restrictions

Data restrictions imposed on this program are

Maximum number of seismometers per subarray	25
Maximum number of beams formed per subarray	6
Highest filter degree	6
Maximum time history of seismometer (sample periods)	21

The above data restrictions can be circumvented for individual computer runs if tradeoffs with other data restrictions are effected.

Specific seismometers to be deleted must be in ascending order numerically when entered on the data cards.

Comments

This program is written in FORTRAN IV except for the subroutine which reads the LASA edit tape. This read routine is written in IBM 7090 MAP language. The program currently runs on the IBM 7090 under control of the IBSYS monitor.
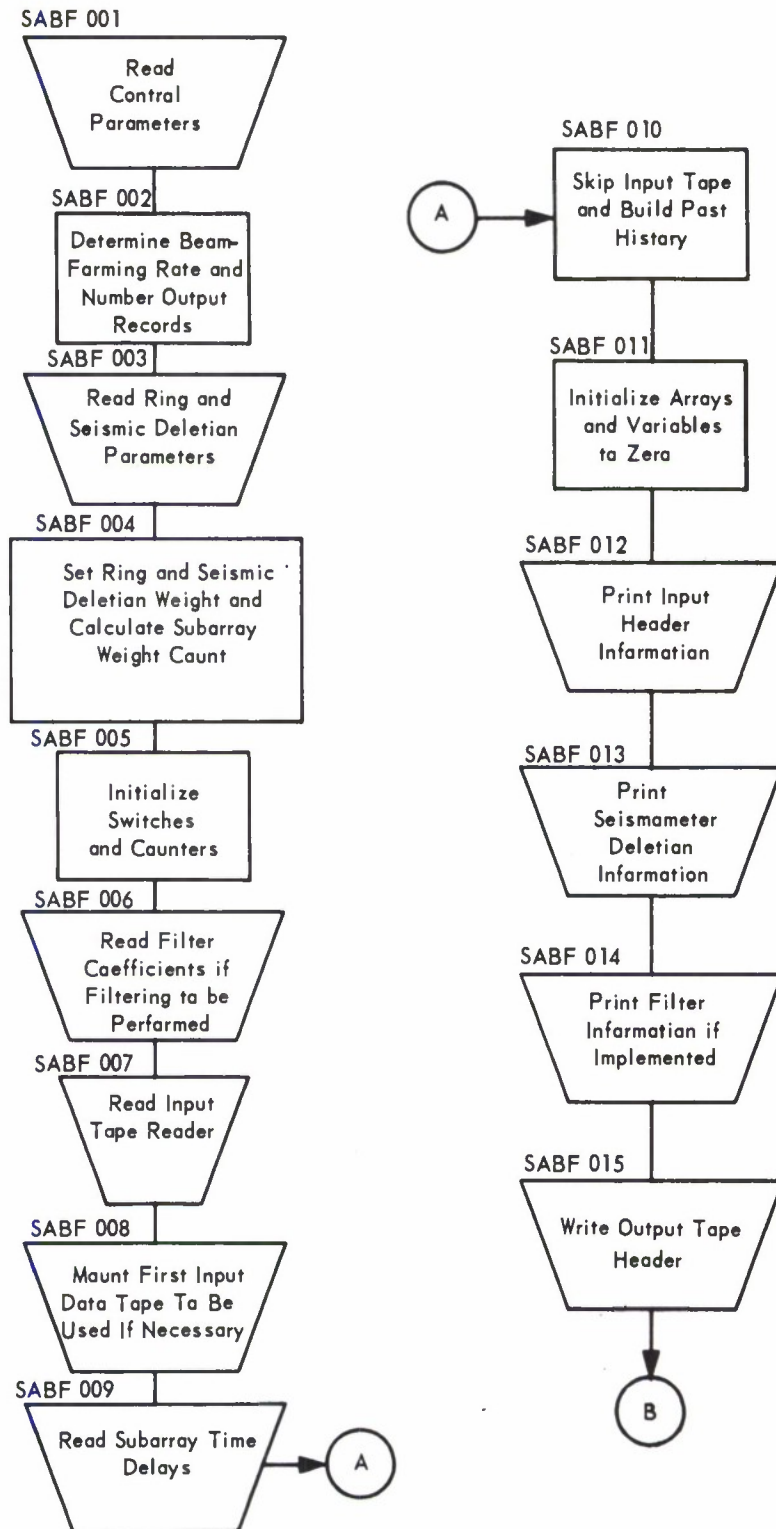
SABF 001

Read
Control
Parameters

SABF 002

Determine Beam-
Forming Rate and
Number Output
Records

SABF 003

Read Ring and
Seismic Deletion
Parameters

SABF 004

Set Ring and Seismic
Deletion Weight and
Calculate Subarray
Weight Count

SABF 005

Initialize
Switches
and Counters

SABF 006

Read Filter
Coefficients if
Filtering to be
Performed

SABF 007

Read Input
Tape Reader

SABF 008

Mount First Input
Data Tape To Be
Used If Necessary

SABF 009

Read Subarray Time
Delays

A

A

SABF 010

Skip Input Tape
and Build Past
History

SABF 011

Initialize Arrays
and Variables
to Zero

SABF 012

Print Input
Header
Information

SABF 013

Print
Seismometer
Deletion
Information

SABF 014

Print Filter
Information if
Implemented

SABF 015

Write Output Tape
Header

B

Figure 4-5. Subarray Beamformer (SABF) (Sheet 1 of 5)

4-41

Figure 4-5. Subarray Beamformer (SABF) (Sheet 2 of 5)

4-42

$$BEAM\,(J,\,K)\;=\;\frac{1}{SUBWT1(J)}\;\sum_{I\,=\,1}^{NSBCH}\;FI\,(I,\,J,\,N\,(I,\,J,\,K)\,)\;\cdot\;WT\,(I,\,J)$$

SABFB

LCFIL: 0

Call SABFF

SEIS (J) = FI (I, J, ILINE)

Write Center Seismometer and SABF Beams
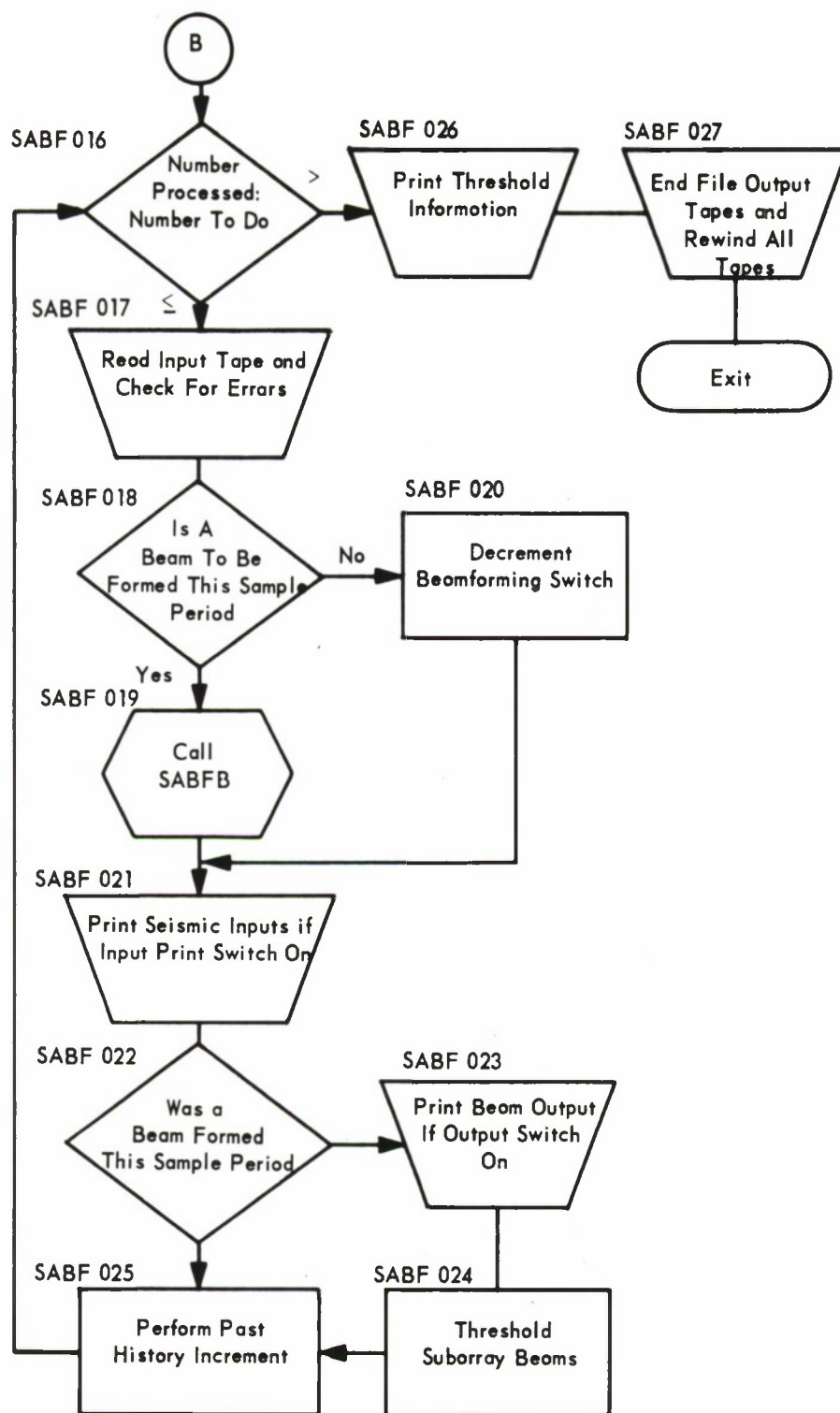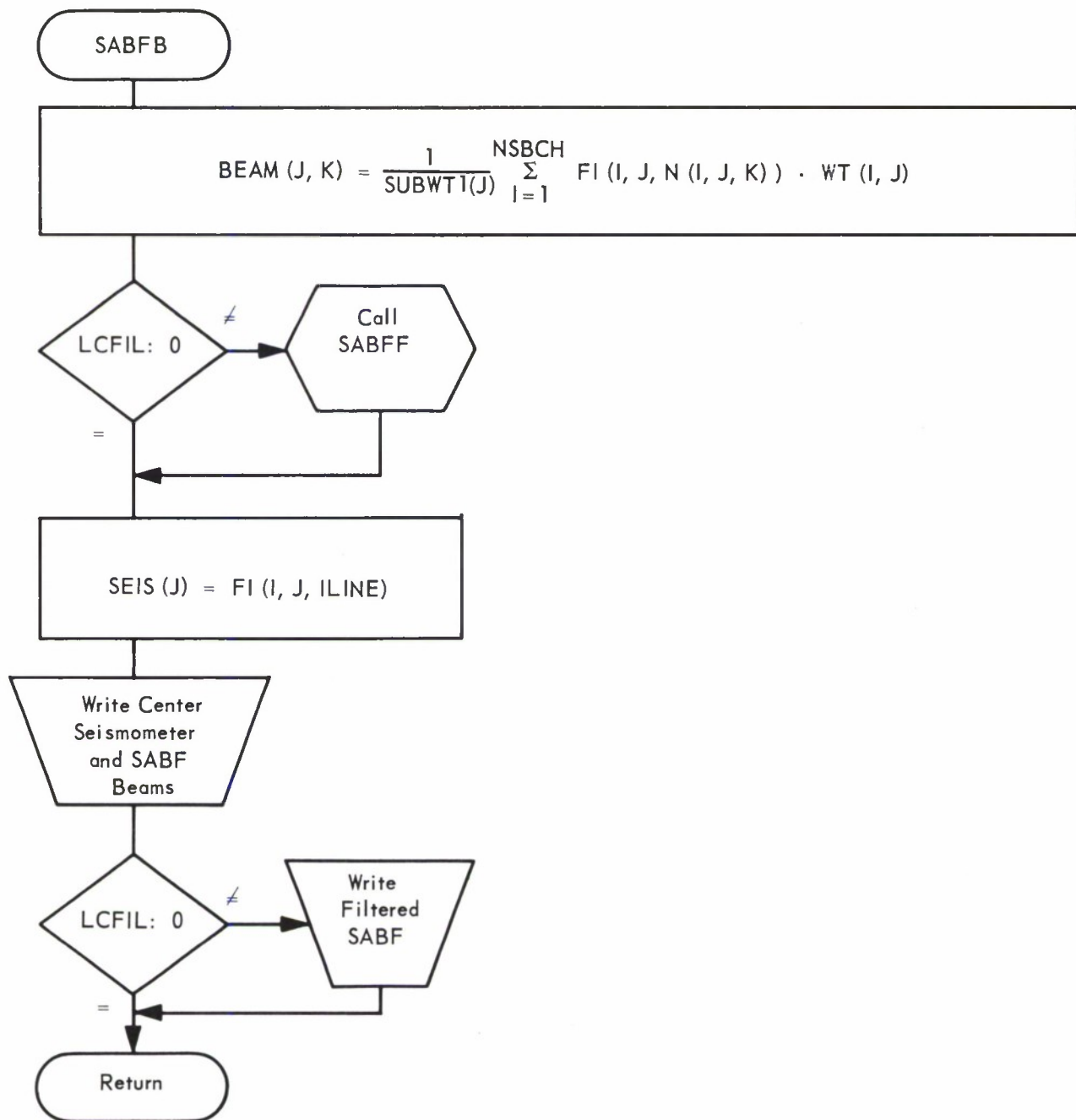
LCFIL: 0

Write Filtered SABF

Return

Figure 4-5. Subarray Beamformer (SABF) (Sheet 3 of 5)

Figure 4-5. Subarray Beamformer (SABF) (Sheet 4 of 5)
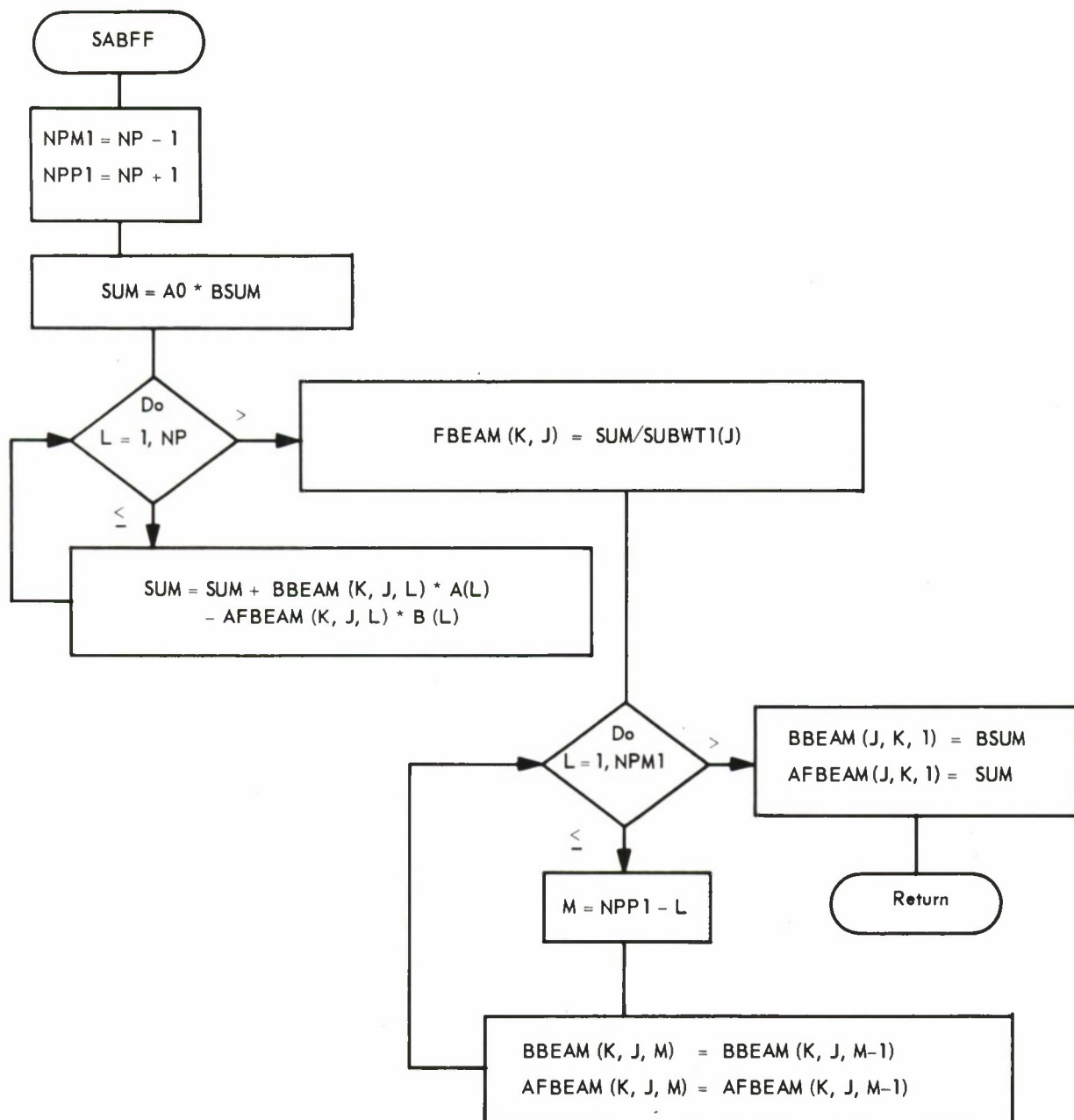
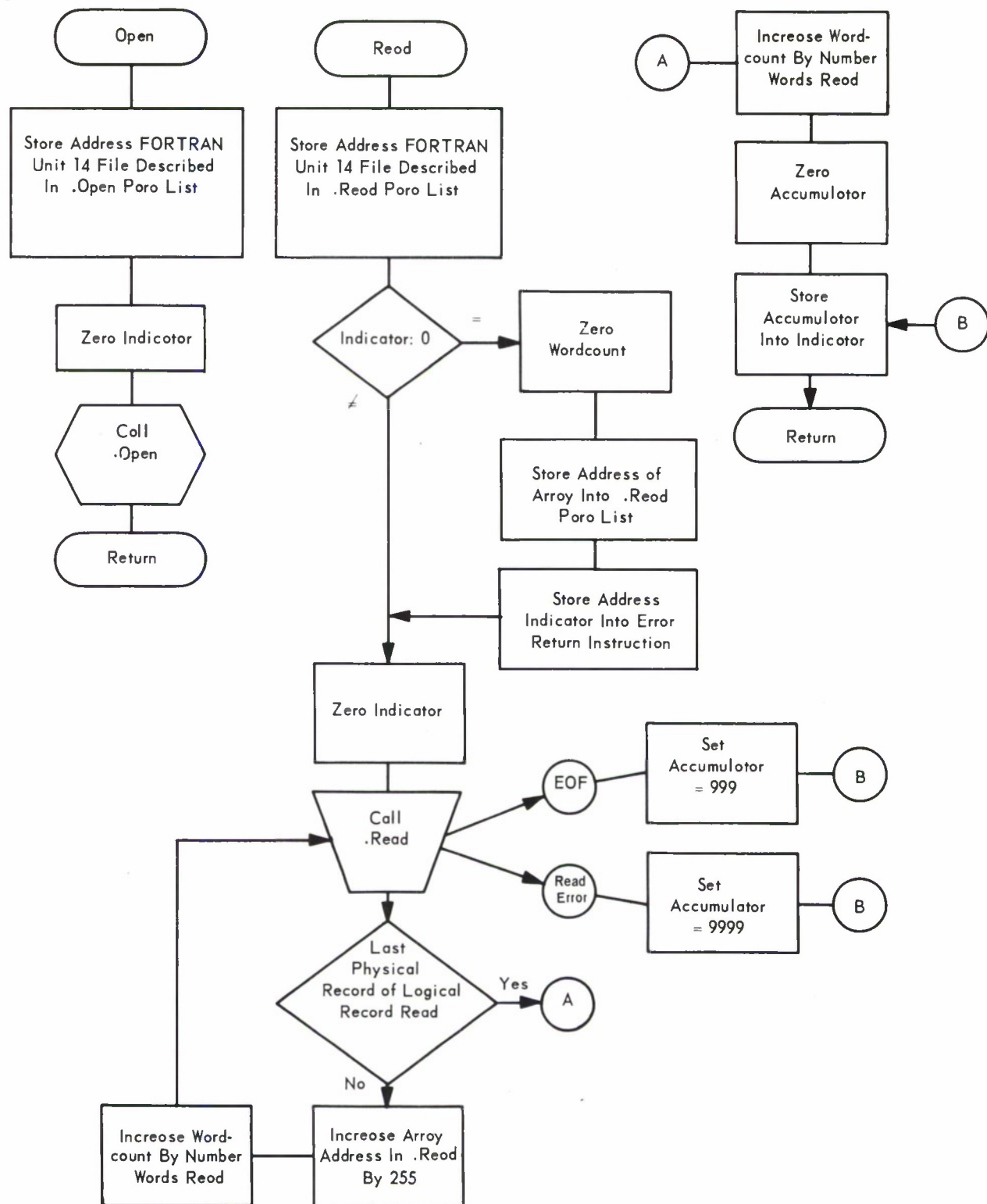Figure 4-5. Subarray Beamformer (SABF) (Sheet 5 of 5)

4-45

4.6 LASA BEAMFORMER (LBF) (Figure 4-6)

Purpose

This program forms a central LASA beam and its associated neighboring beams; they will be available for further processing.

Description

Input

The output tape generated by the Subarray Beamformer (SABF) program containing unfiltered and optionally filtered subarray beam values is the primary input to this program. In addition to this beam tape, the time delays required to form the central and neighboring beams for either the unfiltered or filtered case are supplied by card input.

Card Input

Data Card 1

Card Column	Field Specification	Variable Name	Sample Value
11–15	I5	IPHIST	190
23–30	I5	NRTBP	2000
41–45	I5	ITHRES	2400
56–60	I5	IFTHRS	2400
71–75	I5	IOPTN	500

where

IPHIST   Maximum number of past beam samples necessary for LASA beamforming (IPHIST ≤ 190)

NRTBP   Number of input records to process (if = 0, NRTBP = NRPRO-ISKIP where NRPRO is the number of records available on the input tape)

ITHRES   Unfiltered beam threshold values

IFTHRS   Filtered beam threshold values

IOPTN   =0, do not print LASA beams
                  >0, print beam values for IOPTN time samples
                  =-1, print all beams formed for all time samples

Data Card 2

Card Column	Field Specification	Variable Name	Sample Value
11-15	I5	ISKIP	1200
26-30	I5	LBRATE	10
41-45	I5	LSADEL	2

where

ISKIP   Number of sample periods to skip before processing

LBRATE   Beamforming rate per second (10 or 5)
                  (must be less than or equal to SABF tape rate)

LSADEL   Subarray deletion logic switch
                  =1, no deletion of subarray beams from beamforming
                  =2, deletion of outer ring of subarray beams from beamforming
                     (F ring deleted)
                  =3, deletion of the two outer ring subarray beams from beam-
                     forming (F and G ring deleted)

Data Card 3

Card Column	Field Specification	Variable Name	Sample Value
7-18	F12.6	UX	0.057493
25-36	F12.6	UY	-0.038521
42-45	I4	IM	3
51-54	I4	IN	5

where

UX   Inverse velocity space X coordinate for the beam defined by the
                  time delays on the following card(s)

UY   Inverse velocity space Y coordinate for the beam defined by the
                  time delays on the following card(s)

IM   Incremental subscript identification of coordinates

IN   Incremental subscript identification of coordinates

Data Card 4 (Necessary if preceding UX < 99999.0)

Card Column	Field Specification	Variable Name	Sample Value
1-5	I5	ITD (I, M) M=1	178
6-10	I5	ITD (I, M) M=2	205
.			
.			
65-70	I5	ITD (I, M) M= NSUB I=1 to NBPLA	56

where

ITD (I, M) Time delay for ith subarray for forming LASA beams (for filtered time delays the variable name is IFTD (I, M), and NBPLA would be replaced by NFBPLA)

The reading of a data card type 3 with a UX value greater than or equal to 99999.0 signals the end of the reading of unfiltered time delays. The second such card terminates the reading of filtered time delays. A deck of time delays may be used for the generation of either unfiltered or filtered LASA neighboring beams. Their placement in relationship to the "99999.0 UX cards" clearly signals which type of beam is to be formed. Core restrictions prevent the formation of both unfiltered and filtered beams during the same production run.

Computation

The beamforming process performed by this program is the same as the SABF program beamforming process except that instead of the time delayed sum of seismometer channels, the LASA beams are formed by a time delayed sum of subarray beam channels. The process is performed first for the central beam and then the neighboring beams, using the unfiltered or filtered input subarray beams. The decision to produce unfiltered or filtered beams is determined by the presence or absence of the respective time delays.

The deletion of the one or two outermost rings of subarray beams from beamforming is done with a logic switch for each subarray. The switch is tested before incorporating the subarray beam in the LASA beamforming process.

Additional processing provides the sample period in which each of the LASA beams formed first exceeds a prescribed threshold. The largest absolute beam value computed is also determined.

Output

Both printed output and magnetic tape output are produced by LBF.

Printed Output. The printed control information and data from this program include the following: output tape header data, logic control parameters, input and output beamforming rates, adjusted neighboring beam-time delays, beam values (if desired), thresholding points and values, and maximum absolute beam value computed.

Magnetic Tape Output. A tape consisting of a header of pertinent execution and data parameters followed by either unfiltered or filtered LASA beams for a desired number of samples is produced.

Program Interaction

The subarray beam input to this program will be supplied by the output tape generated by the SABF program. The time delays for the neighboring beams will be supplied by the Neighboring Beam Time Delay Calculations program.

The output of this program, the LASA beam tape, will serve as input to the LBF Power program, and will be used in the LASA beam pattern display process.

Program Restrictions

The total number of beams this program can form is restricted to 600. The maximum time history for each beam is 190 sample periods. Because of the number of beams and the limits of core storage, separately compiled program decks for unfiltered and filtered LBF executions are necessary. The SABF input tape must have been generated at a rate not exceeding 10 samples per second.

Comments

The placement of the time delay control UX cards determines the type of beams (filtered or unfiltered) to be formed and is critical to the performance of the LBF. The incorrect data deck placement for a program deck compiled for the other type of beam input will produce meaningless results.

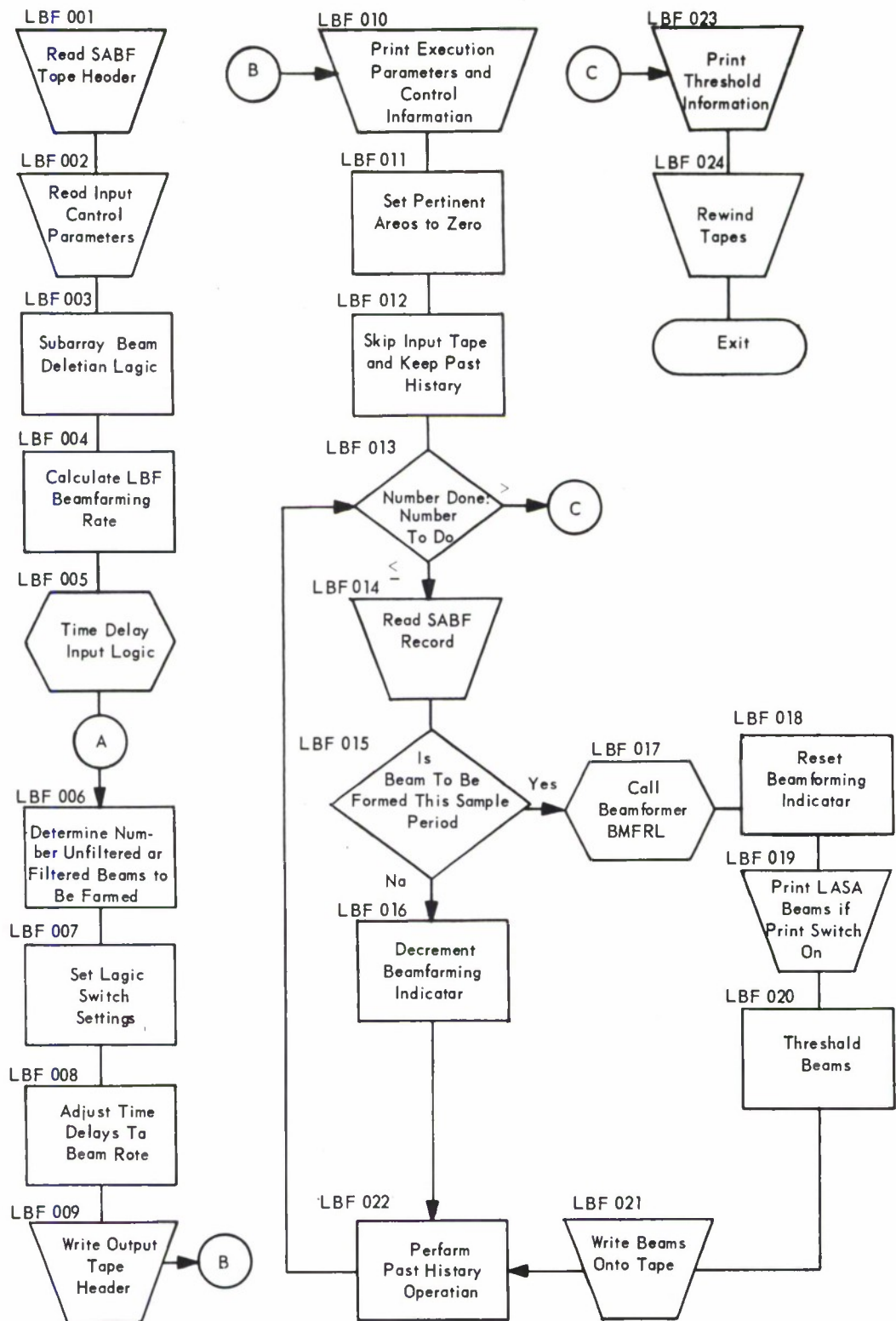This program is written in FORTRAN IV for the IBM 7090.

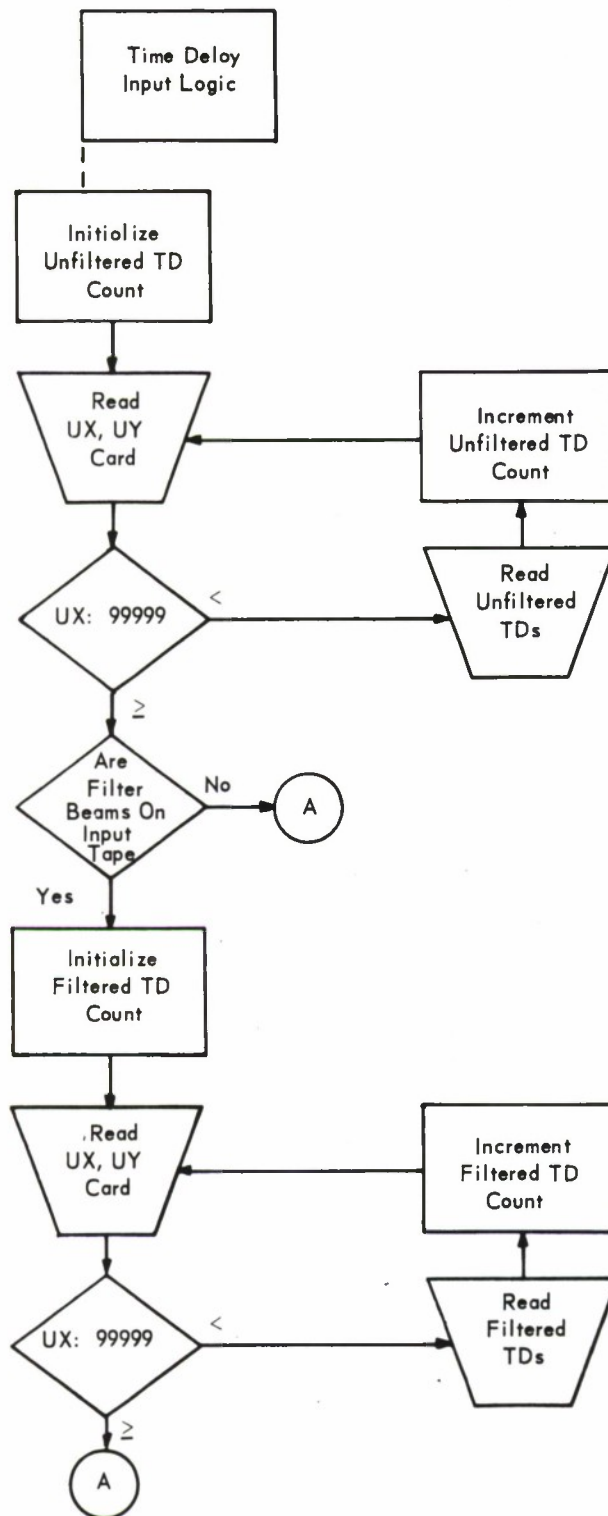Figure 4-6. LASA Beamformer (LBF) (Sheet 1 of 3)

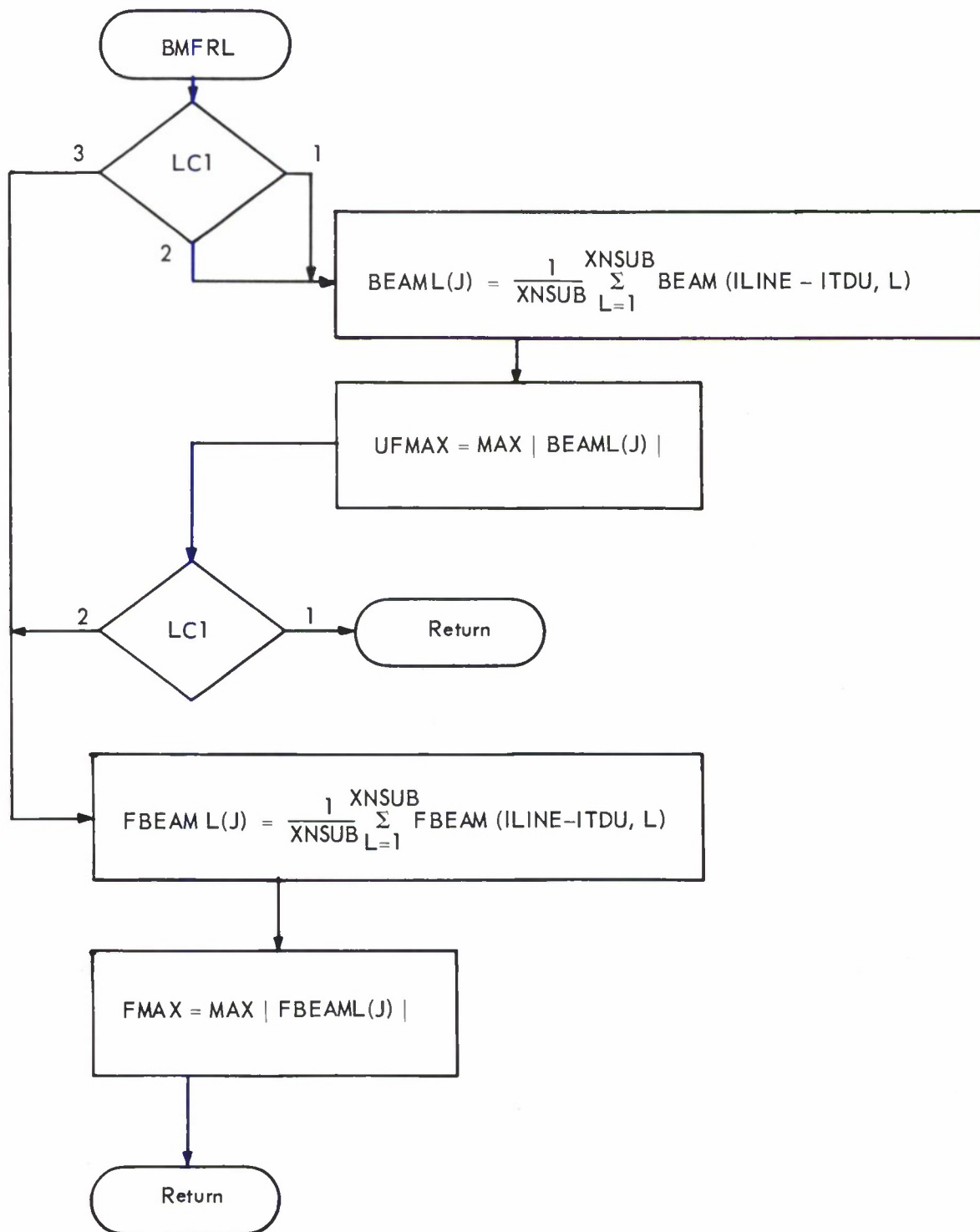4-51

Figure 4-6. LASA Beamformer (LBF) (Sheet 2 of 3)

Figure 4-6. LASA Beamformer (LBF) (Sheet 3 of 3)

4.7 NEIGHBORING BEAM-TIME DELAY (Figure 4-7)

Purpose

This program generates a set of time delays to form a close-packed system of beams in relation to a particular central beam being investigated.

Description

Input

The primary input to this program is the location of the source of the event undergoing analysis. This event location is approximated by the location (in inverse velocity space) of the centerline of the best detection beam. In addition, the arrival time of the wavefront of this event at a set of known locations (e.g., the center seismometer in each subarray of LASA) is needed.

Card Input

Data Card 1

Card Column	Field Specification	Variable Name	Sample Value
1-8	F8.3	X(I)	0004.425
9-16	F8.3	Y(I)	-006.002

where

X(I)   X component of position of the Kth seismometer (or subarray center) in subarray I

Y(I)   Y component of position of the Kth seismometer (or subarray center) in subarray I

Data card 1 is repeated for all 21 subarrays. Each card will give coordinates of the Kth seismometer in a different subarray.

Data Card 2

Card Column	Field Specification	Variable Name	Sample Value
1	I1	KPUNCH	1
2	I1	KPRINT	1

where

KPUNCH   0/1 condition. Do not punch output cards/Punch output cards.

KPRINT   0/1 condition. Print location (U_x, U_y) for each neighboring beam formed and those beams immediately outside the circle of selected area of detection beam uncertainty/Print location (U_x, U_y) only for those beams immediately outside the circle of selected area of detection beam uncertainty.

Data Card 3

Card Column	Field Specification	Variable Name	Sample Value
1-12	F12.6	R3DB	0.001200

where

R3DB   The 3.0 dB radius of an event beam in (U_x, U_y) space

Data Card 4

Card Column	Field Specification	Variable Name	Sample Value
1-12	F12.6	UXC	0.05732
13-24	F12.6	UYC	-0.039163

where

(UXC, UYC)   Inverse-velocity space centerline location of the detection beam

Data Card 5

Card Column	Field Specification	Variable Name	Sample Value
1-12	F12.6	RADCIR	0.013

where

RADCIR   Radius of circle of selected area of detection beam uncertainty

Data Card 6

Card Column	Field Specification	Variable Name	Sample Value
1-12	F12.6	XLST	8.0

where

XLST   An estimated time in seconds greater than any possible delay
(equal to 1/2 maximum travel time across the array)

Data Card 7

Card Column	Field Specification	Variable Name	Sample Value
5-9	F5.2	DELT(I)	-0.02

where

DELT(I)   Arrival time (seconds) at Ith subarray relative to arrival at
center seismometer element

Data card 7 is repeated for all 21 subarrays.

Computation

The equations used in this program are discussed in Appendix D of the
First Quarterly Technical Report (reference 2) and Appendix E.8 of the Second
Quarterly Technical Report (reference 3).

Output

For each beam within the circle of the selected area of detection beam uncertainty (RADCIR), the centerline location of that beam (U_X, U_y) in inverse velocity space (in sec/km) and time delays in seconds required to form this beam are printed out. The centerline locations for these beams immediately outside the circle of selected area of detection beam uncertainty and the total number of beams are also printed out. For all delays to be of the same algebraic sign, as required by the LASA Beamformer program, the magnitude of the calculated first arrival for each neighboring beam must be smaller than the input value XLST.

This program also provides punched output cards in the following format for use by other LASA programs.

Card Output

Output Card 1

Card Column	Field Specification	Variable Name	Sample Value
7-18	F12.6	UX	0.057320
25-36	F12.6	UY	-0.039163
42-45	I4	M	6
51-54	I4	N	-4

where

(UX, UY)   Centerline location of the neighboring beam in inverse velocity space

M, N   Incremental values on the centerline location of the detection beam in inverse velocity space

Output Card 2

Card Column	Field Specification	Variable Name	Sample Value
1-5	I5	ID(2)	162
6-10	I5	ID(20)	165

Card Column	Field Specification	Variable Name	Sample Value
.			
.			
66-70	I5	ID(10)	236

Output Card 3 .

Card Column	Field Specification	Variable Name	Sample Value
1-5	I5	ID(11)	115
6-10	I5	ID(16)	17
.			
.			
31-35	I5	ID(19)	278

where

ID(2), ID(20), ..., ID(19)   Delays for subarrays 1 through 21, respectively

Program Interaction

The location in inverse velocity space of the centerline of the best detection beam, (U_{xc}, U_{yc}) is obtained from the output of the Least Squares Wavefront program. The outputs of the Neighboring Beam Time Delay Calculation program are used by the LASA Beamformer (LBF) program and the Display Address Card program.

Program Restrictions

This program has been arbitrarily restricted to the use of arrival times at 21 known locations.

Comments

This program is written in FORTRAN IV for the IBM System/360. Input arrival times are in order by rings. Output delays are in standard LASA order.
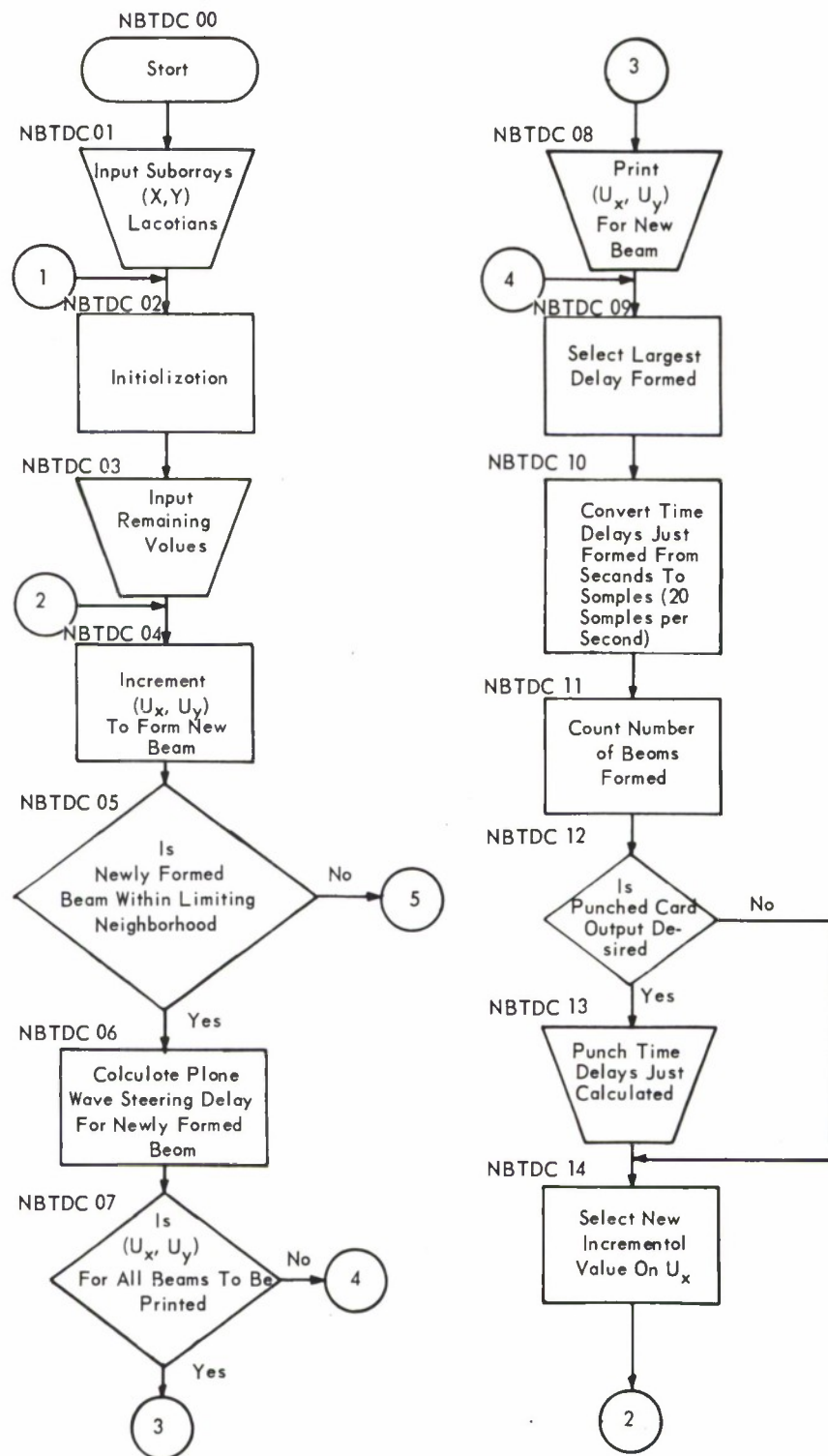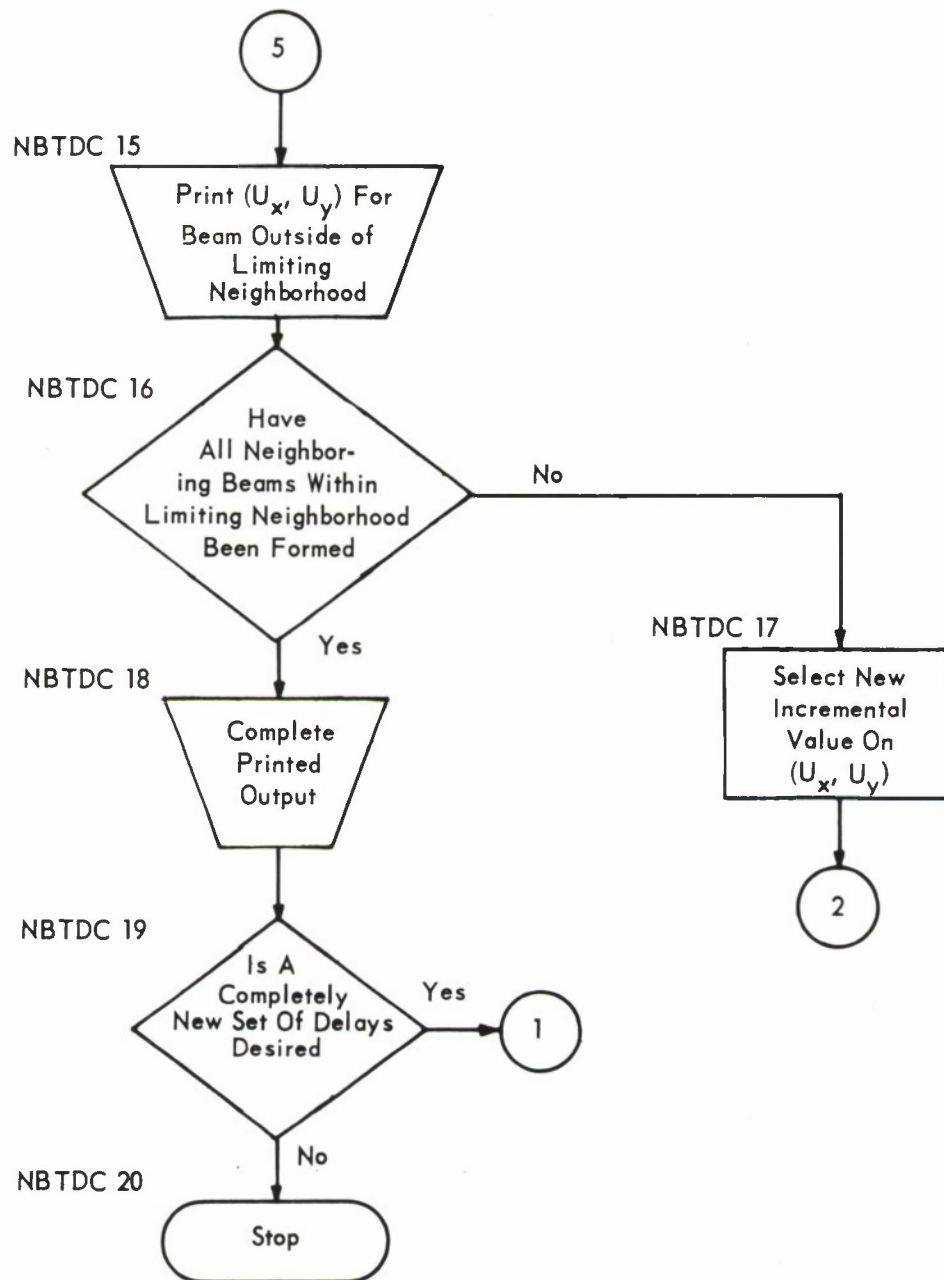
Figure 4-7. Neighboring Beam-Time Delay (Sheet 1 of 2)

Figure 4-7. Neighboring Beam-Time Delay (Sheet 2 of 2)

4.8 SEISMOMETER POWER (Figure 4-8)

Purpose

This program calculates both noise and signal power at the seismometer level for any particular event.

Description

Input

The main input to the program is a LASA edit tape which includes all the seismometer channels which are to be analyzed. This input tape is placed on unit B2.

Additional inputs on data cards include parameters specifying the starting point and duration for both the noise and signal power analysis, and the relative event arrival times at each of the seismometers.

Card Input

Data Card 1 (Format 12A6)—Any comment in columns 1-72 will appear in the printout.

Data Card 2

Card Column	Field Specification	Variable Name	Sample Value
1-6	I6	NCH	525
7-12	I6	NUMN	1700
13-18	I6	NUMS	100
19-24	I6	NBEGS	-14
25-30	I6	NENDN	15
31-26	I6	KSKIP	1
37-42	I6	KSA	21
43-48	I6	KSEIS	25
55-60	I6	INPUT2	1
61-66	I6	KSPS	20

where

NCH	Number of channels (seismometers) on input tape
NUMN	Number of noise samples to be processed
NUMS	Number of signal samples to be processed
NBEGS	Algebraic beginning of signal from threshold in number of samples (-number before threshold; + number after threshold; 0 at threshold)
NENDN	Samples from end of noise to threshold (nonalgebraic—must always be positive, or 0 when noise is to end at threshold)
KSKIP	Number of samples skipped by the seismometer threshold program (add 1 to KSKIP if input tape contains header)
KSA	Number of subarrays on input tape
KSEIS	Number of seismometers in one subarray
INPUT2	For seismometer edit tape, INPUT2 must equal 1. No other capability exists at this time.
KSPS	Samples/second on input tape

Data Card 3

Card Column	Field Specification	Variable Name	Sample Value
1-14	E14.5	CON	0.028E+00
15-28	E14.5	THN	2000. E+00
29-42	E14.5	THS	8192. E+00

where

CON	Input values from tape are multiplied by CON to give desired dimensions (CON = .028 for P_i = nanometers^2/second^2)
THN	Prints out and removes all glitches in noise portion larger than value of THN
THS	Prints out and removes all glitches in signal portion larger than value of THS
	(Set THN and THS = 0 if deglitching is not desired)

<u>Data Cards 4 to 47</u>

All cards have the format 13I6 and contain the following:

Variable Name	Sample Value	Function
ITAB(j)	1403	Sample period number of threshold for each seismometer (comes from Threshold Time Delay program)

Computation

The following equation represents the computation to determine the power in the seismometer data channels.

$$P_i = \frac{1}{N} \sum_{n=1}^{N} \left[a \cdot f_i(n) \right]^2 \tag{4.3}$$

where

N	Number of samples to be included in the power sum
a	Scale factor (converts seismometer data to nanometers)
$f_i(n)$	Value of the ith seismometer at the nth sample period
P_i	Power of the ith seismometer

The formula is used to provide intermediate power values for seismometer 1 (B1 subarray, A0 seismometer) once every 200 samples (10 seconds) for the noise portion, and once every 4 samples (.5 seconds) for the signal portion.

The average power for all the seismometers in a subarray or in the LASA array is given by

$$P_g = \frac{1}{M} \sum_{i=1}^{M} P_i \tag{4.4}$$

where

M	Number of seismometers in group
P_i	Power of the ith seismometer
P_g	Average group power

This program can detect the presence of spikes appearing in the input seismometer data channels. If this option is specified by the appropriate input parameter, all seismometer channels are compared to noise and signal thresholds set by input data cards. If a threshold is exceeded, the particular seismometer channel(s) value is set to zero for that sample, and the effective summation window made smaller by subtracting 1 from N.

Output

Program off-line output consists of several related data blocks. The first block contains a listing of input data card values. Unless otherwise noted, the other data blocks are rectangular arrays with 21 columns of 25 values. Each column represents one subarray of 25 seismometers.

The second data block, in rectangular form, contains the seismometer delay times.

The third data block, in rectangular form, contains the seismometer values for the last sample skipped before noise processing begins.

The fourth-data block, in column form, contains intermediate noise and signal power values for seismometer 1.

The fifth and sixth data blocks, in rectangular form, contain noise and signal power values averaged across each subarray. Signal-to-noise ratio for each subarray is also given.

The seventh data block, in column form, contains average noise and signal power and signal-to-noise ratio across the entire LASA array.

The eighth and ninth data blocks, in rectangular form, contain the standard deviation of noise and signal portions of seismometer movement (nanometers/second).

The last two rows of block nine give the standard deviation of average subarray movement.

Data block ten, consisting of one row, gives the standard deviation of seismometer movement over the entire LASA array.

Data blocks eleven and twelve, in rectangular form, contain the same data as data blocks five and six, expressed in dB relative to one nanometer.

Block thirteen, in column form, contains the same data as data block seven, but recorded in dB relative to one nanometer.

Program Interaction

Input to this program must be a tape recorded in the LASA edit format. System gain can be determined by comparing the results of this program with the results of the Subarray and LASA Beam Power programs.

Program Restrictions

The noise and signal intervals must be separated by one or more sample periods.

Comments
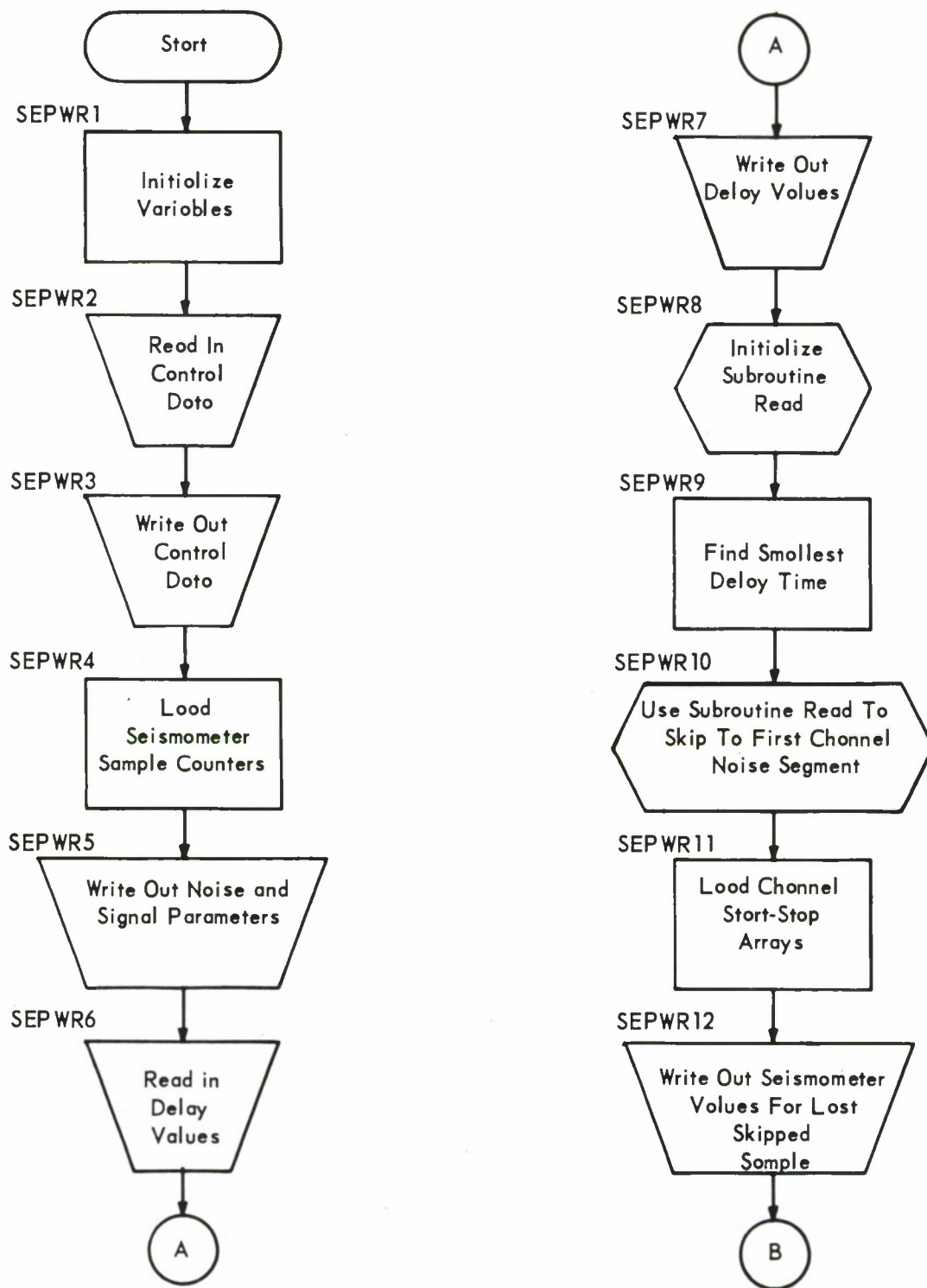
This program is written in FORTRAN IV for the IBM 7090.

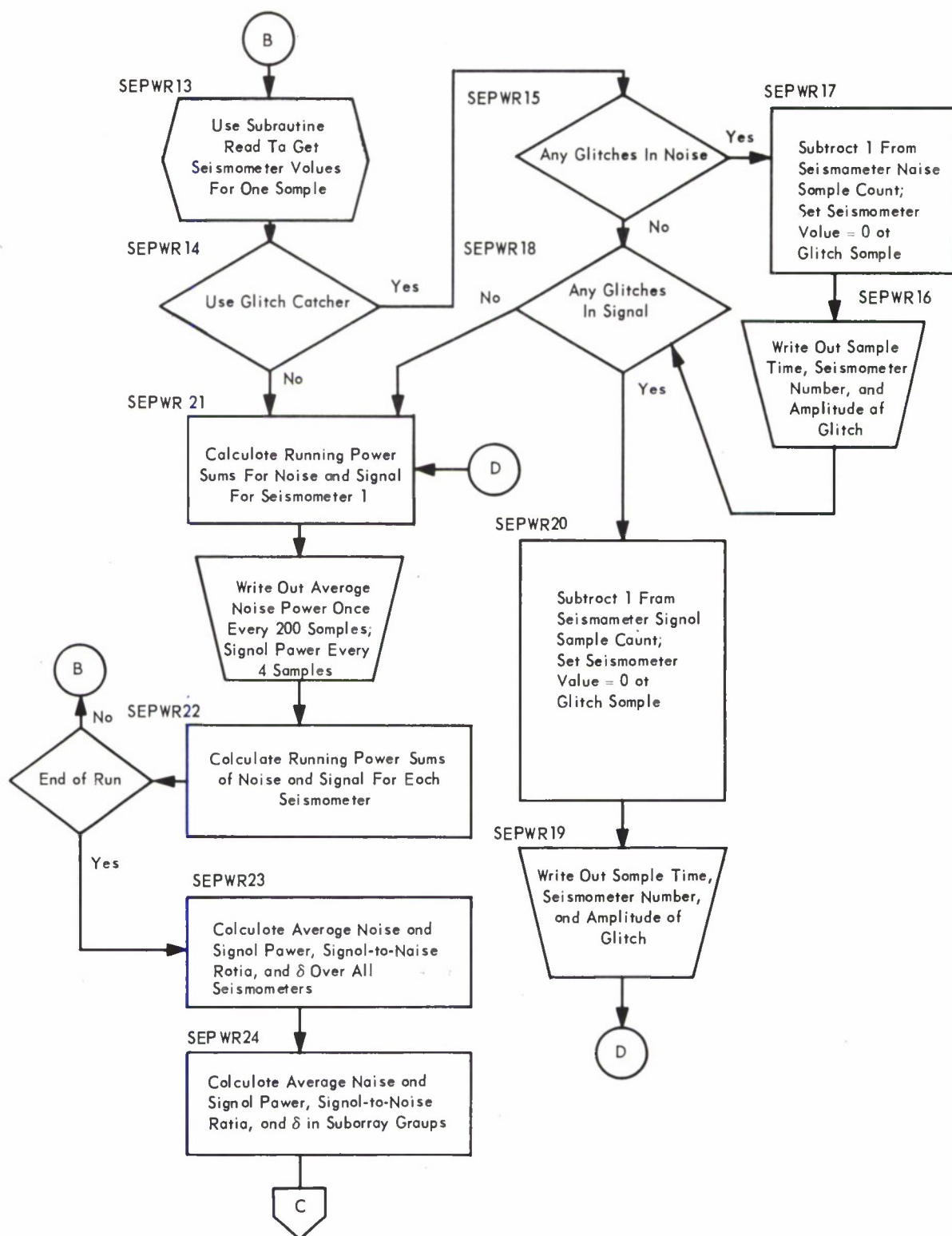Figure 4-8. Seismometer Power (Sheet 1 of 3)

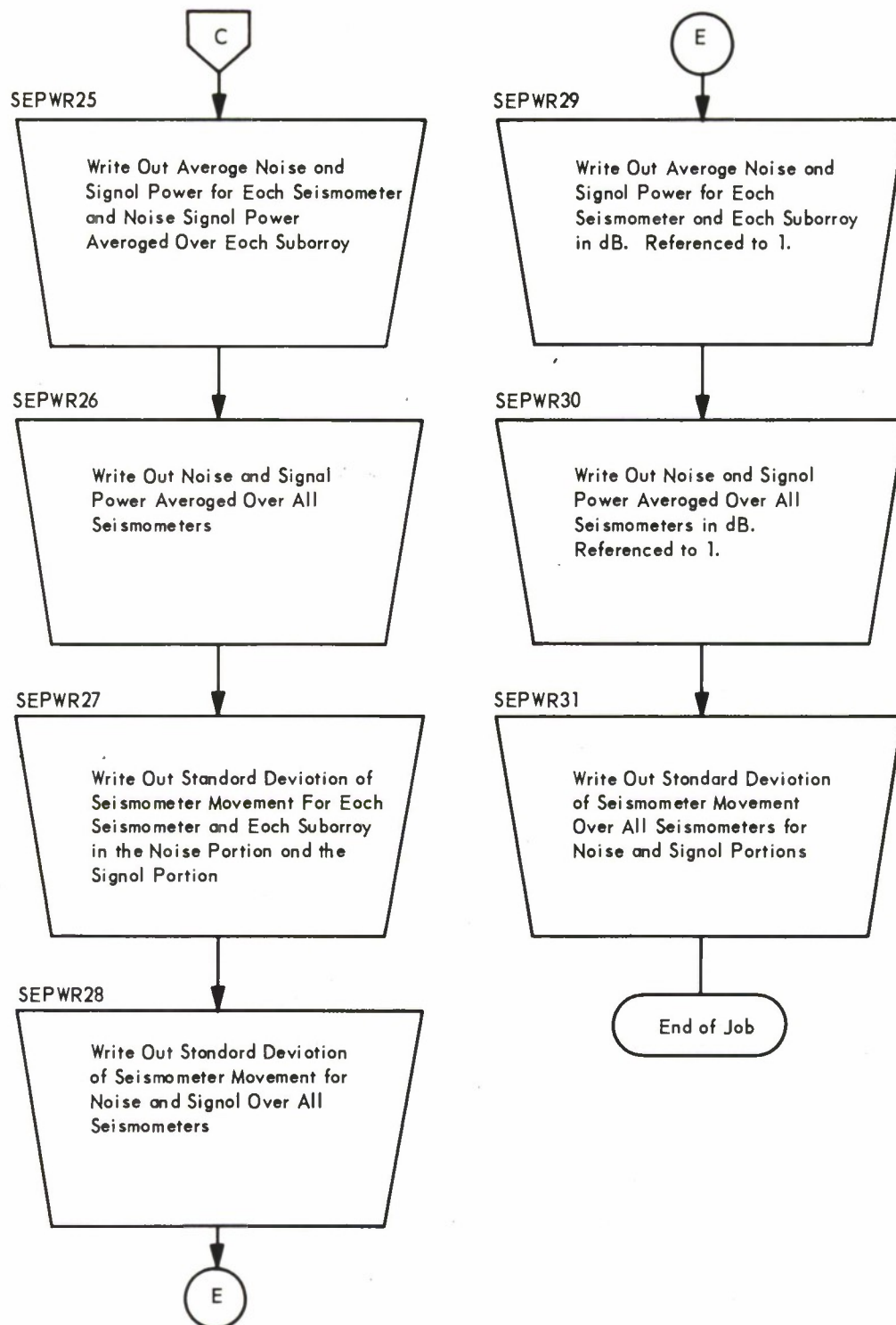Figure 4-8. Seismometer Power (Sheet 2 of 3)

C

SEPWR25

Write Out Average Noise and Signal Power for Each Seismometer and Noise Signal Power Averaged Over Each Suborray

SEPWR26

Write Out Noise and Signal Power Averaged Over All Seismometers

SEPWR27

Write Out Standard Deviation of Seismometer Movement For Each Seismometer and Each Suborray in the Noise Portion and the Signal Portion

SEPWR28

Write Out Standard Deviation of Seismometer Movement for Noise and Signal Over All Seismometers

E

E

SEPWR29

Write Out Average Noise and Signal Power for Each Seismometer and Each Suborray in dB. Referenced to 1.

SEPWR30

Write Out Noise and Signal Power Averaged Over All Seismometers in dB. Referenced to 1.

SEPWR31

Write Out Standard Deviation of Seismometer Movement Over All Seismometers for Noise and Signal Portions

End of Job

Figure 4-8. Seismometer Power (Sheet 3 of 3)

4.9   SUBARRAY BEAM POWER (Figure 4-9)

Purpose

This program calculates noise and signal power present in the beams formed by the Subarray Beamformer program (SABF).

Description

Input

The primary input to this program is the tape generated by the SABF program. This tape includes unfiltered and filtered beam values formed over some specified period of time. Other input values include parameters indicating points at which noise and signal analysis is to begin, duration of both noise and signal power analysis, and the points at which each beam present on the tape exceeded some prescribed threshold in the SABF program.

Card Input

Data Card 1

Card Column	Field Specification	Variable Name	Sample Value
1-5	I5	IPHST	300
6-10	I5	ISNTS	010
11-15	I5	INDUR	1700
16-20	I5	ISDUR	52
21-25	I5	ISPS	20
26-30	I5	IPTRB	40
31-35	I5	IDUMP	1

where

IPHST   Number of sample periods retained for subarray beam past history. This value must be less than 301.

ISNTS   Number of subarray beam samples between the end of the noise analysis and the start of the signal analysis

4-69

INDUR   Number of subarray beam samples to be included in the noise power calculations

ISDUR   Number of subarray beam samples to be included in the signal power calculations

ISPS   Rate at which the subarray beams were formed

IPTRB   Count of sample periods by which the start of the signal analysis may be perturbed

IDUMP   Binary switch for the program. When equal to one, intermediate power sums are printed every 20 seconds for noise and every .2 seconds for signal. When equal to zero, no intermediate power sums are printed.

Data Card 2 - 4

Card Column	Field Specification	Variable Name	Sample Value
1-10	I10	ITH (i)	3047
11-20	I10	ITH (i)	3253
21-30	I10	ITH (i)	3248
31-40	I10	ITH (i)	3153
41-50	I10	ITH (i)	3088
51-60	I10	ITH (i)	3097
61-70	I10	ITH (i)	3029

where

ITH(i)   Record number on the subarray beam input tape at which the ith subarray beam exceeded a preset threshold value. Note that there are 7 subarrays per card, so three input cards are required to provide data for 21 subarrays.

Magnetic Tape Input. The magnetic tape generated by the Subarray Beam-former program is an input tape for this program. It is a binary tape and must be mounted on FORTRAN logical unit 13.

Computation

The main computations in this program are the power calculations and standard deviation performed on both noise and signal portions of the filtered and unfiltered beams present on the input tape.

The computation to determine the power of a beam is represented by

$$P_j = \frac{1}{N} \sum_{n=1}^{N} \left[a \cdot B_j(n) \right]^2 \qquad (4.5)$$

where

N	Number of samples to be included in the power sum
a	Scale factor (.028) to convert the subarray beam values to nanometers
$B_j(n)$	Value of the jth subarray beam at the nth sample
P_j	Power of the jth subarray beam

In addition to the power calculations on an individual beam basis, the average beam power for all subarrays present, $\bar{P}$, and the associated standard deviations are calculated. This process is done first for the unfiltered and then the filtered beams.

The logic flow of the program begins with reading the header record of the subarray beam tape. This procedure provides pertinent parameters such as the number of subarrays, the number of beams per subarray, a binary switch indicating the availability of filtered subarray beams on the tape, and the number of records available for processing. The data cards described in the card input section are then read by the program.

Pertinent run parameters are calculated by the program. All power analysis is performed relative to the point at which signal thresholds were exceeded on each subarray beam. If the noise analysis is to end 5 seconds before the threshold value, it will end at that point for all channels by using time delay values in a manner similar to the way they are used in beamforming. The threshold values then provide the necessary information by which the starting points and duration for both signal and noise power calculations are to be performed. If filtered beams are available for processing, their noise and signal power will be computed over identical time periods relative to the unfiltered beams.

Once the noise and signal power calculations have been performed over the desired time intervals, the average subarray beam power and standard deviation is computed relative to all the subarrays considered. The data is computed and recorded for both unfiltered and filtered beams (if available).

Output

The output of this program is a list of the individual unfiltered beam power sums (P_j) and 10 log (P_j) for both noise and signal. In addition, the average noise and signal power for the unfiltered beams with the associated standard deviation is presented.

The same output is recorded for the filtered beams.

An optional output is provided which presents the intermediate noise power every 20 seconds and the intermediate signal power every 0.2 seconds.

Program Interaction

This program requires a SABF output tape containing subarray beam values over some specified period of time. In addition, the output of the SABF provides data indicating the start of the event for each beam recorded on the SABF output tape.

The resultant powers calculated in this program can be compared to a similar power analysis at both the seismometer level and the LASA beam level to indicate overall system gain.

Program Restrictions

This program is designed to process only one unfiltered and one filtered beam per subarray, and expects the beam input values to be contained on a single tape. The selection of the starting points for both the noise and signal analysis, as well as the duration of both, must be done with some caution to ensure that the required amount of data is present on the beam input tape.

Comments

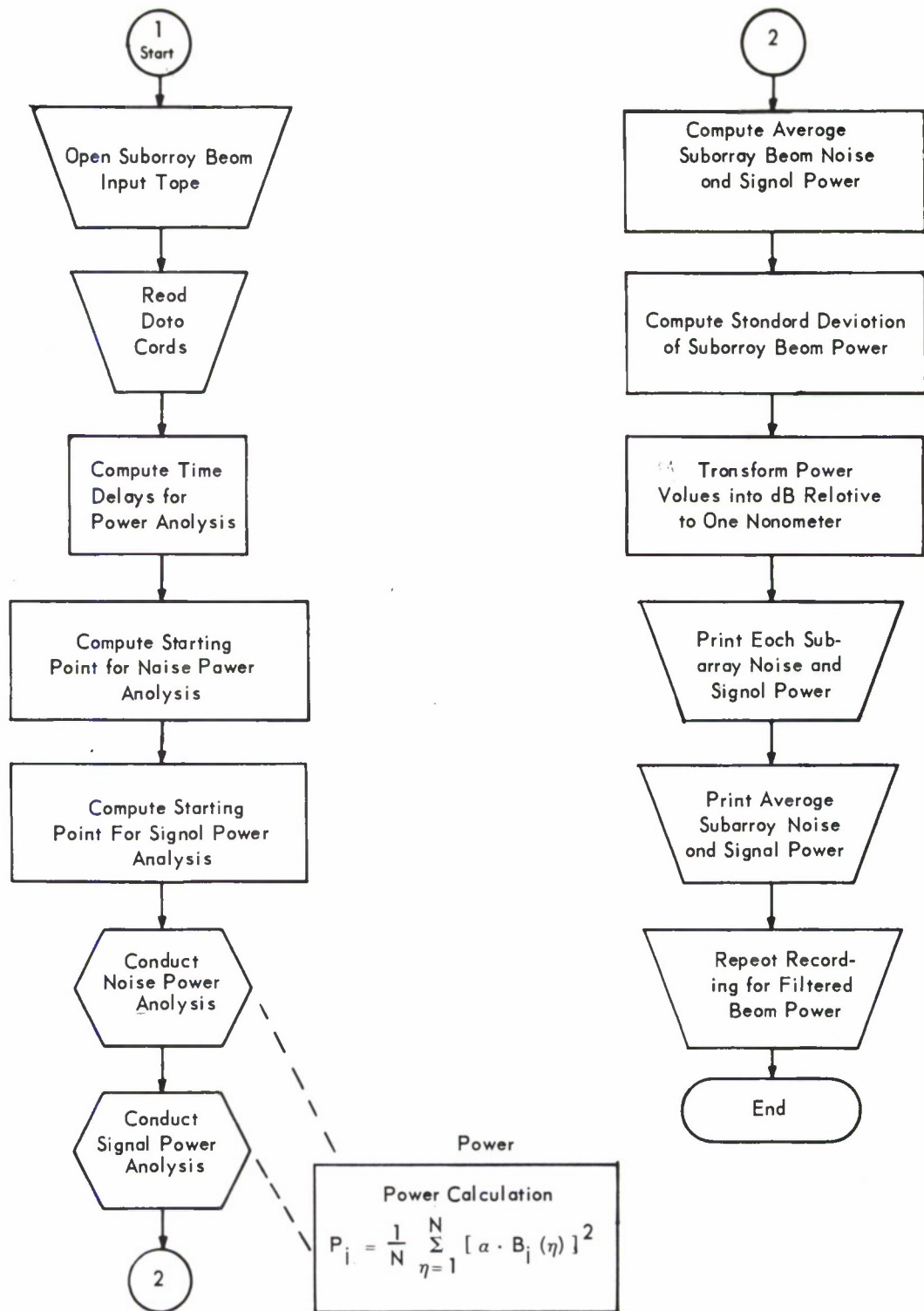This program is written in FORTRAN IV for the IBM 7090.

Power Calculation

$$P_i = \frac{1}{N} \sum_{\eta=1}^{N} [\, \alpha \cdot B_i\,(\eta)\,]^2$$

Figure 4-9. Subarray Beam Power

4.10 LASA BEAM POWER (Figure 4-10)

Purpose

This program is designed to calculate noise and signal power present in LASA beams. The LASA beams may be either unfiltered or filtered, and their values are obtained from the LASA Beamformer program. The LASA beam power analysis data may be compared with similar power analysis data at both the seismometer level and subarray level to indicate overall system gain.

Description

Input

Both card and tape input data are required for this program as described below in detail.

Card Input

Data Card 1

Card Column	Field Specification	Variable Name	Sample Value
1-5	I5	ISNTS	5
6-10	I5	INDUR	425
11-15	I5	ISDUR	20
16-20	I5	ISPS	5
21-25	I5	IPTRB	4
26-30	I5	LC2	0
31-35	I5	IDUMP	1
36-40	I5	IDRN	99
41-45	I5	IDRS	0

where

ISNTS   Number of consecutive beam samples between the end of the noise and the beginning of the signal power calculations

INDUR   Number of beam samples to be used in the noise power analysis

ISDUR	Number of beam samples to be used in the signal power analysis
ISPS	LASA beam sampling rate (samples per second)
IPTRB	Number of beam samples between that sample at which the beam signal threshold was first exceeded and the start of the actual signal power analysis
LC2	Processing option flag. If given a value of 0, power analysis for only the center LASA beam will be performed. If given a value of 1, power analysis of all LASA beams will be performed.
IDUMP	Output option flag used to request intermediate power sums for both noise and signal. If given a value of 0, no intermediate power sums will be printed. If given a value of 1, intermediate power sums will be printed.
IDRN	Number of samples between each successive printing of intermediate power sums for noise analysis. For example, if it is desired to have an intermediate power sum printed every tenth sample, then IDRN = 9. This parameter is of no significance if IDUMP = 0.
IDRS	Number of samples between each successive printing of intermediate power sums for signal analysis (see IDRN)

Data Card 2

Card Column	Field Specification	Variable Name	Sample Value
1-10	I10	ITHUB(1) or ITHFB(1)	2301
11-20 . . . 61-70	I10 . . . I10	ITHUB(2) or ITHFB(2) : : ITHUB(7) or ITHFB(7)	2559 2231

where

ITHUB(k)	Sample number at which unfiltered LASA beam k first exceeded the signal threshold
ITHFB(k)	Sample number at which filtered LASA beam k first exceeded the signal threshold

4-75

A single data card 2 may consist of no less than one and not more than seven entries specifying a sample number at which a beam exceeded the signal threshold. Each entry is an integer of no more than 10 significant digits. Whether processing unfiltered or filtered LASA beams, the data deck should contain as many data cards as are required to specify the threshold sample numbers for all beams processed. The threshold sample numbers must be entered consecutively according to their corresponding beam numbers. If both unfiltered and filtered beams are to be processed, then the threshold data deck for unfiltered beams should precede that for the filtered beams. Threshold sample numbers for the LASA beams are generated as hard-copy output by the LASA Beamformer program.

Tape Input. Tape input consists of a LASA beam tape, for a given event, generated by the LASA Beamformer program. It is a 7090 FORTRAN compatible binary tape. This tape should be mounted on FORTRAN logical unit 14 at 800 BPI.

Computation

The power in the kth LASA beam computed over an interval of N beam samples is given by

$$P_k = \frac{1}{N} \sum_{j=1}^{N} c \left[B_k(j) \right]^2 \tag{4.6}$$

where

$B_k(j)$ jth sample of LASA beam k, either filtered or unfiltered

c   Conversion factor to convert beams to nanometers

In addition, power is expressed in dB relative to one nanometer by

$$dB(P_k) = 10 \log_{10}(P_k). \tag{4.7}$$

Output

Selected parameters obtained from the LASA beam tape header and data card 1 will be printed. These parameters include the

1. Number of unfiltered and/or filtered LASA beams whose values are recorded on the LASA beam tape

2. Number of samples per beam available on the LASA beam tape

3. Sampling rate

4. Number of samples used in noise analysis and signal analysis

5. Sample numbers for the beginning and end of both noise and signal power analysis for each unfiltered and/or filtered beam processed.

If IDUMP = 1, intermediate values of power expressed in nanometers squared and dB relative to one nanometer will be tabulated for both noise and signal, together with the elapsed time in seconds. These values will be recorded for each unfiltered and/or filtered beam processed.

Total power will be printed after the noise and signal analysis has been completed for all unfiltered and/or filtered beams processed.

Program Interaction

The LASA beam tape is generated by the LASA Beamformer program.

The sample number at which each LASA beam first exceeds the signal threshold is provided by the same program. The LASA beam power analysis results may be compared with similar power analysis data at both the seismometer and subarray levels to indicate overall system gain.

Program Restrictions

None

Comments

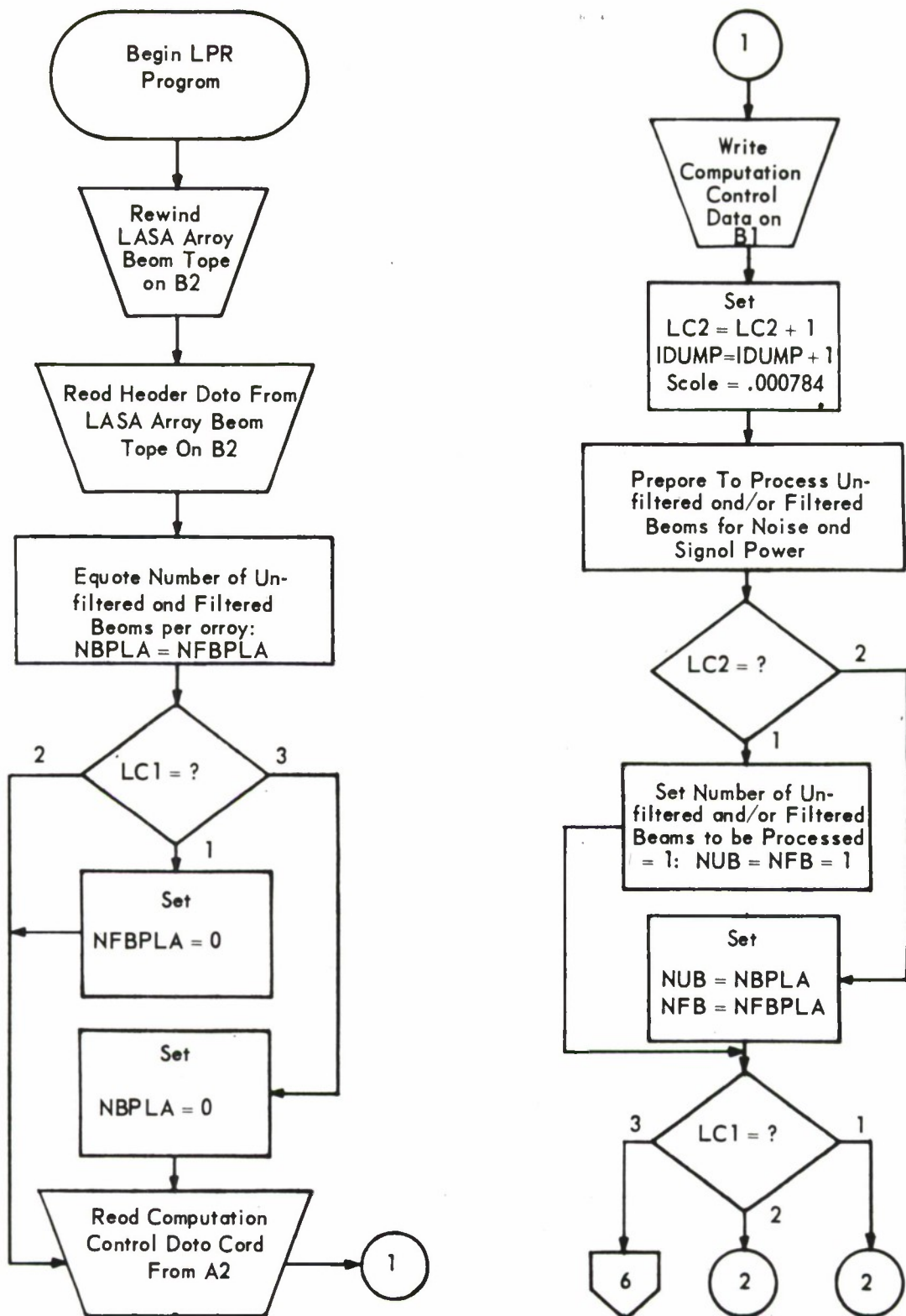This program is written in FORTRAN IV for the IBM 7090.

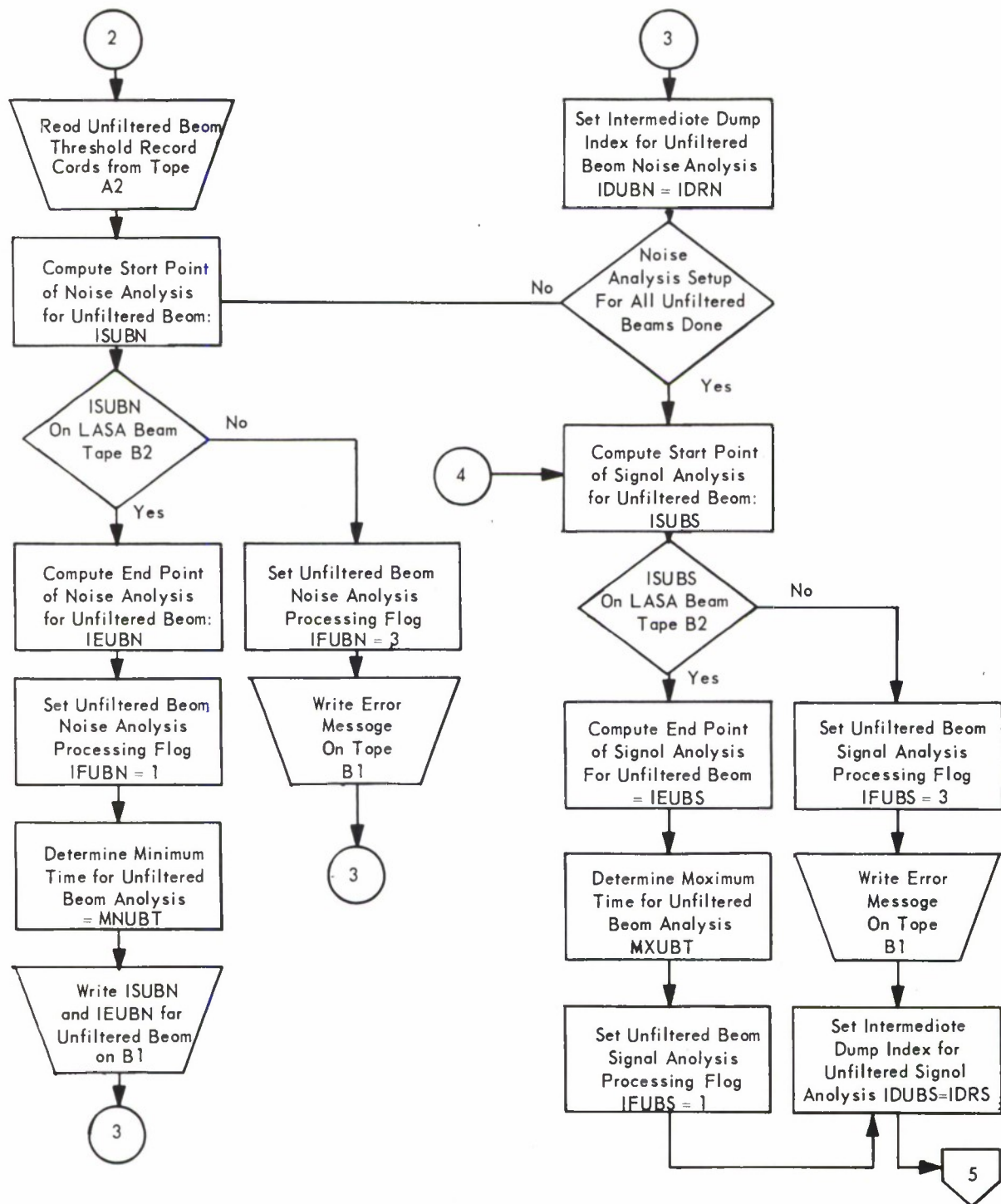Figure 4-10. LASA Beam Power (Sheet 1 of 6)
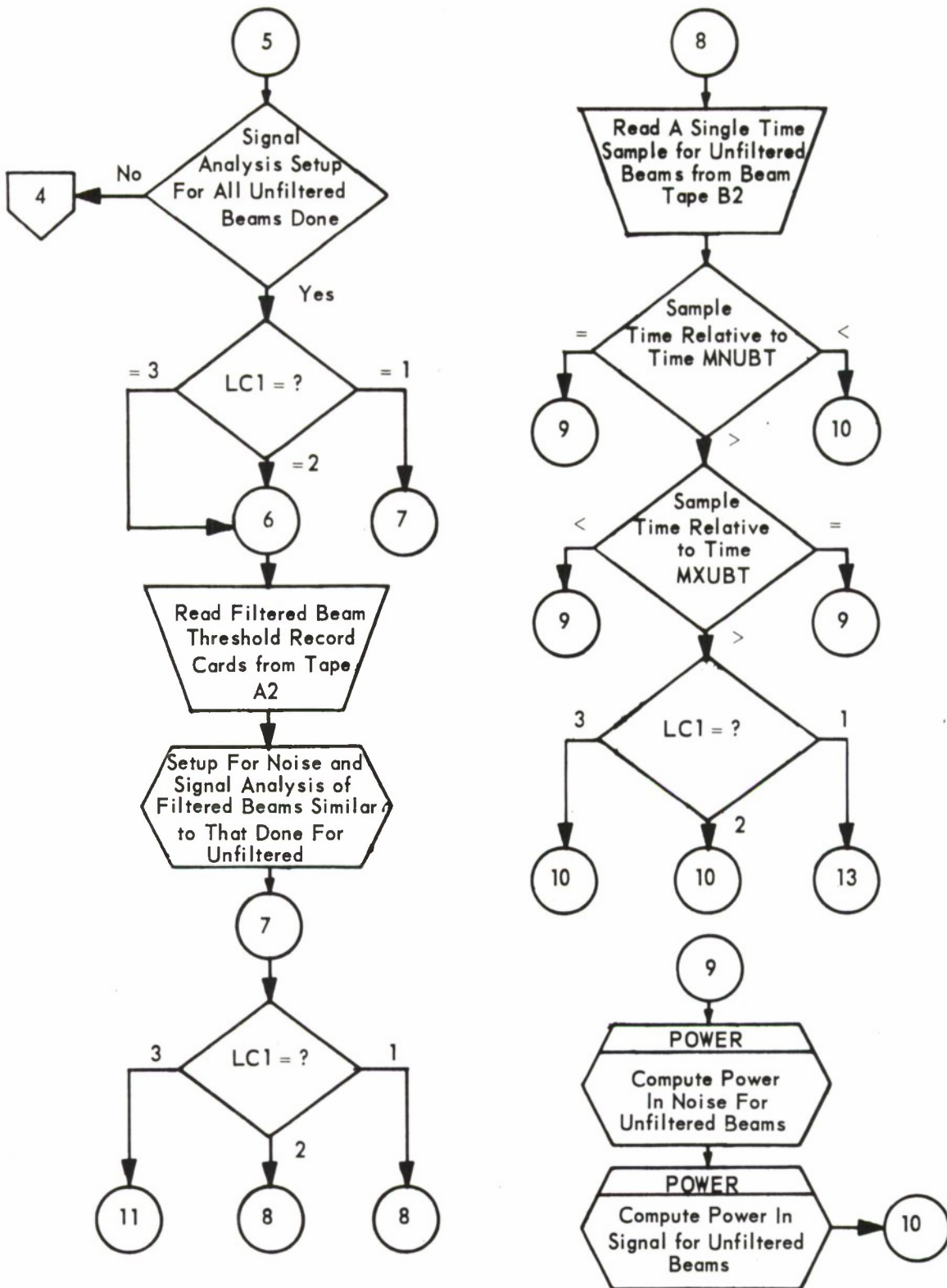
Figure 4-10. LASA Beam Power (Sheet 2 of 6)

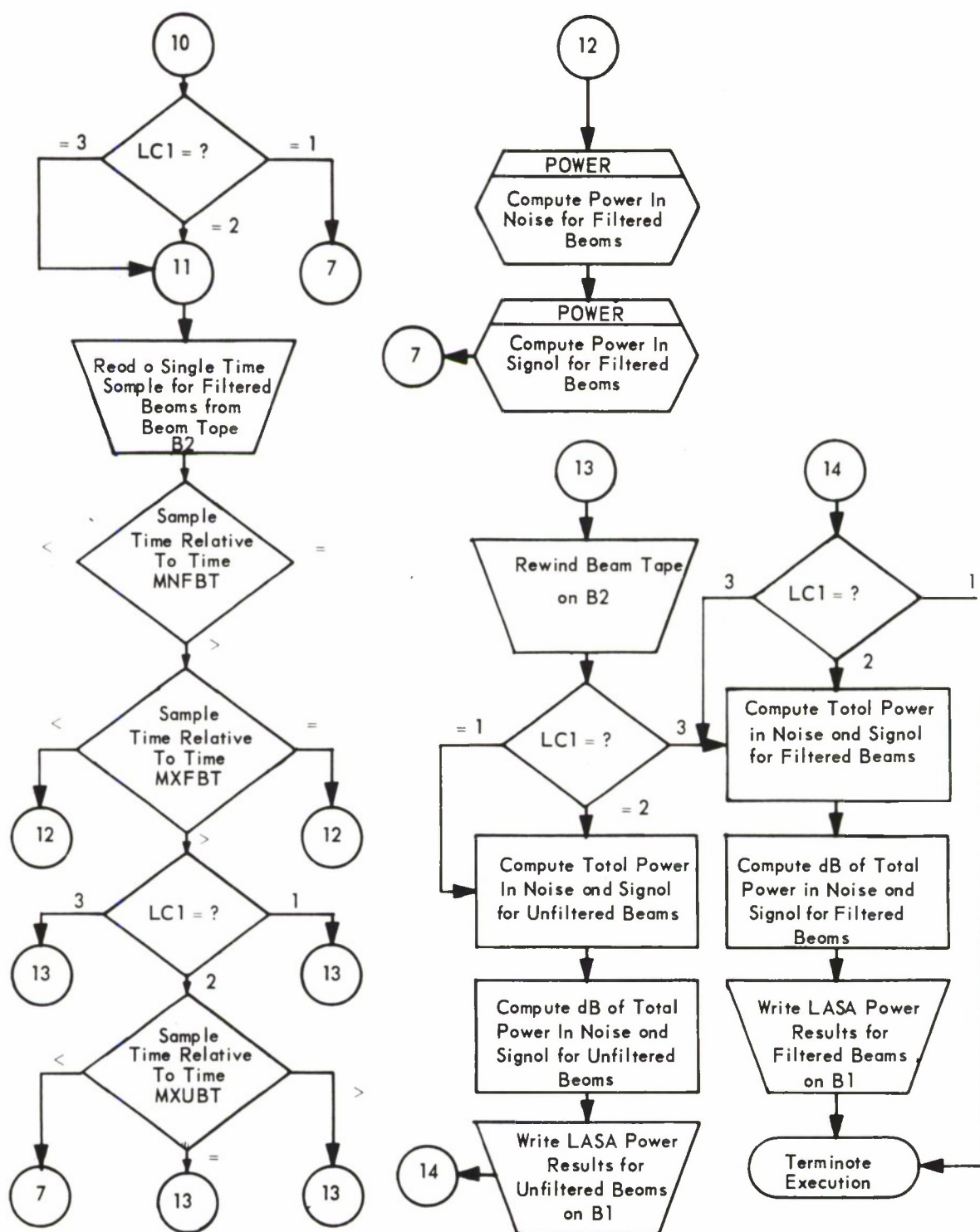Figure 4-10. LASA Beam Power (Sheet 3 of 6)
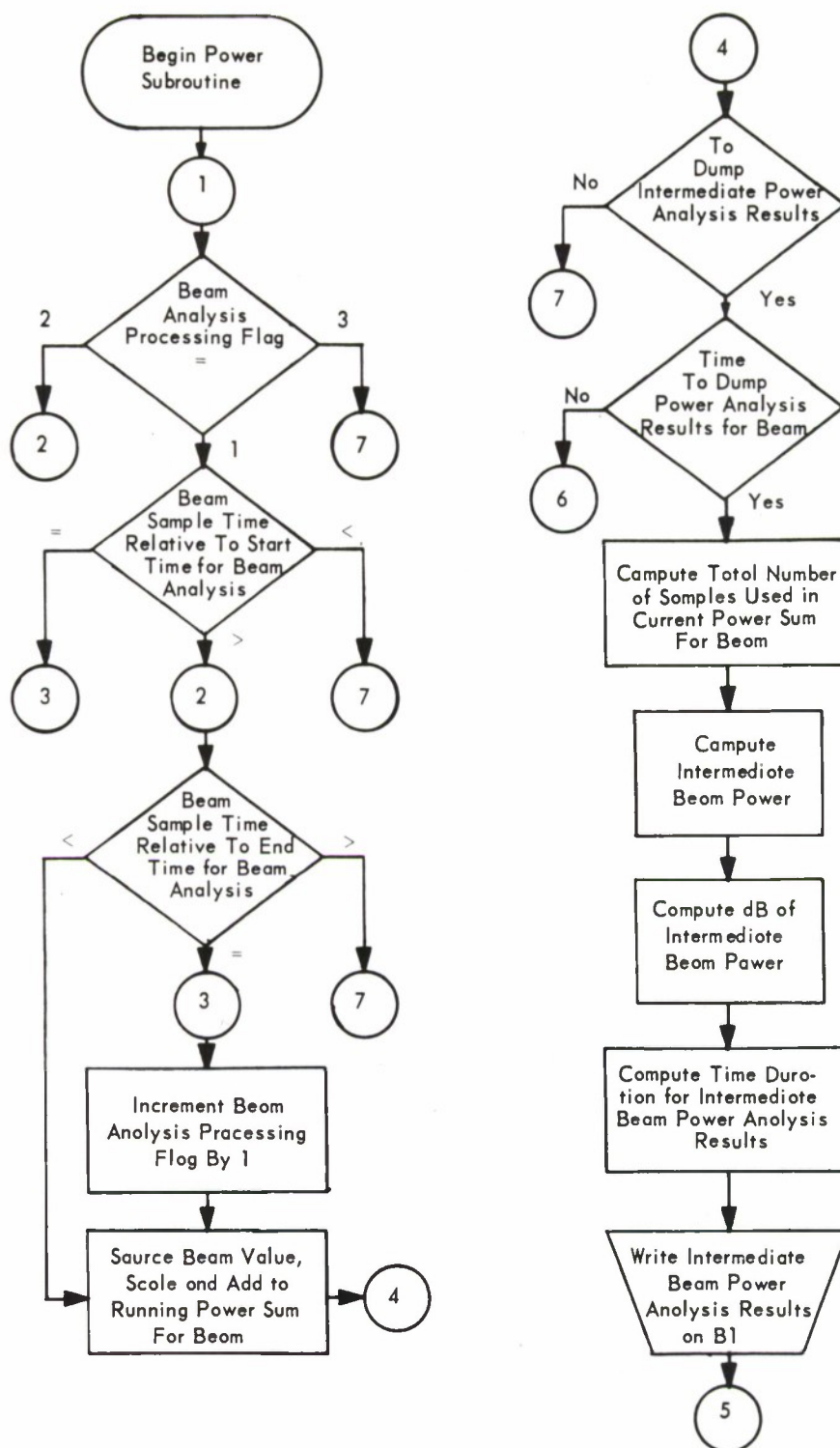
Figure 4-10. LASA Beam Power (Sheet 4 of 6)

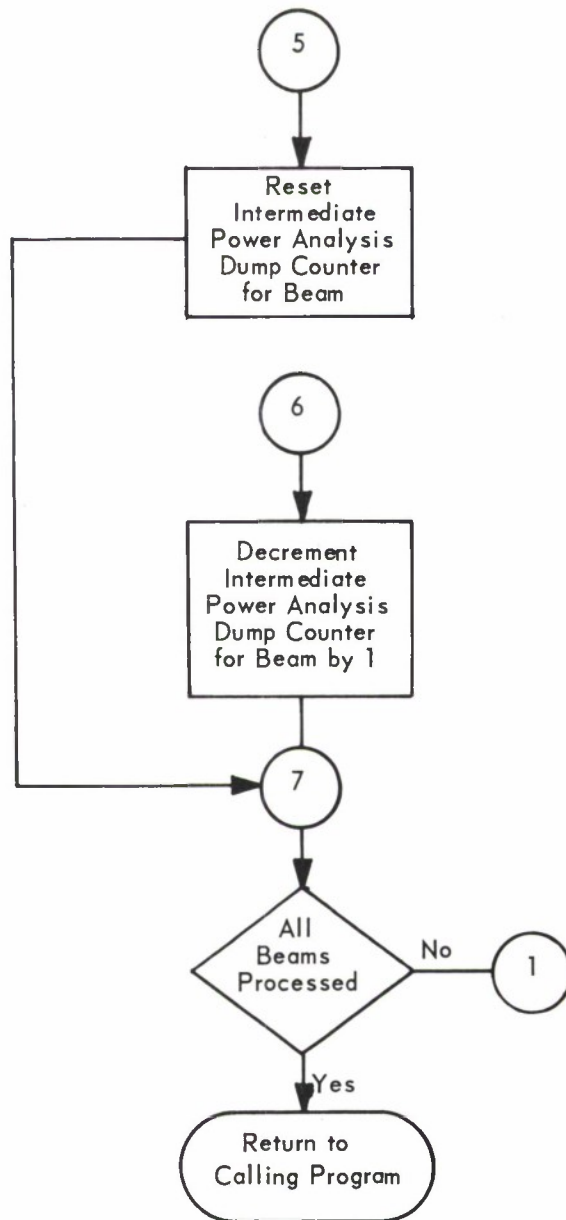Figure 4-10. LASA Beam Power (Sheet 5 of 6)

Figure 4-10. LASA Beam Power (Sheet 6 of 6)

4.11 THRESHOLD TIME DELAY (Figure 4-11)

Purpose

This program provides the approximate time delays required to form beams in the Subarray Beamformer program. No attempt is made to seek maximum gain or to minimize losses.

Description

Input

The primary input to this program is a selected LASA edit tape(s) containing an event of sufficient magnitude to permit the successful execution of the threshold logic. Other pertinent run parameters, such as the threshold value, are provided by input data cards.

Card Input

Data Card 1

Card Column	Field Specification	Variable Name	Sample Value
11-15	I5	IST	1000
26-30	I5	IEND	3800
41-45	I5	NOCHAN	525
56-60	I5	ISKIPH	0
71-75	I5	NTHRS	2400

where

IST   First data record to be thresholded

IEND   Last data record to be thresholded

NOCHAN   Number of seismometers which are to be thresholded (NOCHAN ≤ 525)

ISKIPH   Input tape header indicator
= 0, header exists and will be read
> 0, header does not exist (1st record is data)

NTHRS   Threshold value to be used

Data Card 2

Card Column	Field Specification	Variable Name	Sample Value
11-46	6A6	EVENT	Longshot Explosion (10/29/65)

Data Card 3A1 (Necessary if ISKIPH > 0)

Card Column	Field Specification	Variable Name	Sample Value
1-5	I5	NCH	525

where

NCH   Number of seismometers on tape (NCH ≤ 525)

Data Card 3A2 (Necessary if NCH ≠ 525)

Card Column	Field Specification	Variable Name	Sample Value
1-5	I5	JCH(K) K=1	1
6-10	I5	JCH(K) K=2	2
.			
.			
.			
66-70	I5	JCH(K) K= NCH	525

where

JCH(K)   Specific seismometer channels available on the input tape(s). Fourteen seismometer channel numbers are recorded on each card so the number of cards is directly related to the number of channels on the tape.

Data Card 3B (Necessary if ISKIPH = 0 and NOCHAN $\neq$ NCH from header)

Card Column	Field Specification	Variable Name	Sample Value
1-5	I5	ICH(K)	1
6-10	I5	ICH(K)	2
.			
.			
66-70	I5	ICH(K)	525

where

ICH(K)   Specific seismometer on which thresholding is desired. Fourteen seismometer channel numbers are recorded on each card so the number of cards is directly related to the number of channels which are to be thresholded.

Tape Input. The input tape(s) in LASA edit format is mounted on FORTRAN logical unit 14 at 800 BPI. The first input tape need not have a header record. This would be the case if it were desirable to begin thresholding on other than the first tape of sequentially generated LASA edit tapes.

If IEND is not equal to the record count when the end of the current input tape is encountered, an on-line message instructs the operator to mount the next input reel. A program pause occurs at this point. In this manner multireel thresholding is accomplished.

Computation

The initial processing of the program is the introduction of control parameters and tape header information (if available). With these variables the program determines if all desired seismometers are on the data tape, and notes any discrepancy.

After positioning the input tape to the desired point in time, the program searches for the first sample period at which each desired seismometer exceeds the prescribed threshold. Once each seismometer has exceeded the threshold, time delays (on a subarray basis) are obtained by computing the

difference in sample periods between the time each seismometer within a subarray exceeded the threshold and the time the center seismometer in the subarray exceeded the threshold. The time delay for the ith seismometer in the jth subarray is

$$TD \; (i, \; j) = THC \; (j) - TH \; (i, \; j) + T \; (j) \tag{4.8}$$

where

THC(j)   Sample period time in which the center seismometer in the jth subarray exceeded the threshold.

TH(i, j)   Sample period time in which the ith seismometer in the jth subarray exceeded the threshold.

T(j)   Sample period bias for the jth subarray.

The bias term in the computation provides the means by which all delays have the same algebraic sign.

Output

The sample period times at which each seismometer exceeded the threshold, as well as the time delays for each seismometer relative to its associated subarray, are printed.

Program Interaction

The time delays generated by this program are used in the Subarray Beamformer (SABF) program to form subarray beams.

Program Restrictions

None

Comments

This program is written in FORTRAN IV for the IBM 7090. The read subroutine used to read the LASA edit tapes is written in IBM 7090 MAP language.

Because of the occurrence of corrupt data, the thresholds may trigger and generate incorrect time delays. This has proved useful in the detection of "glitches," and the time delays are easily adjusted by investigation of the data.
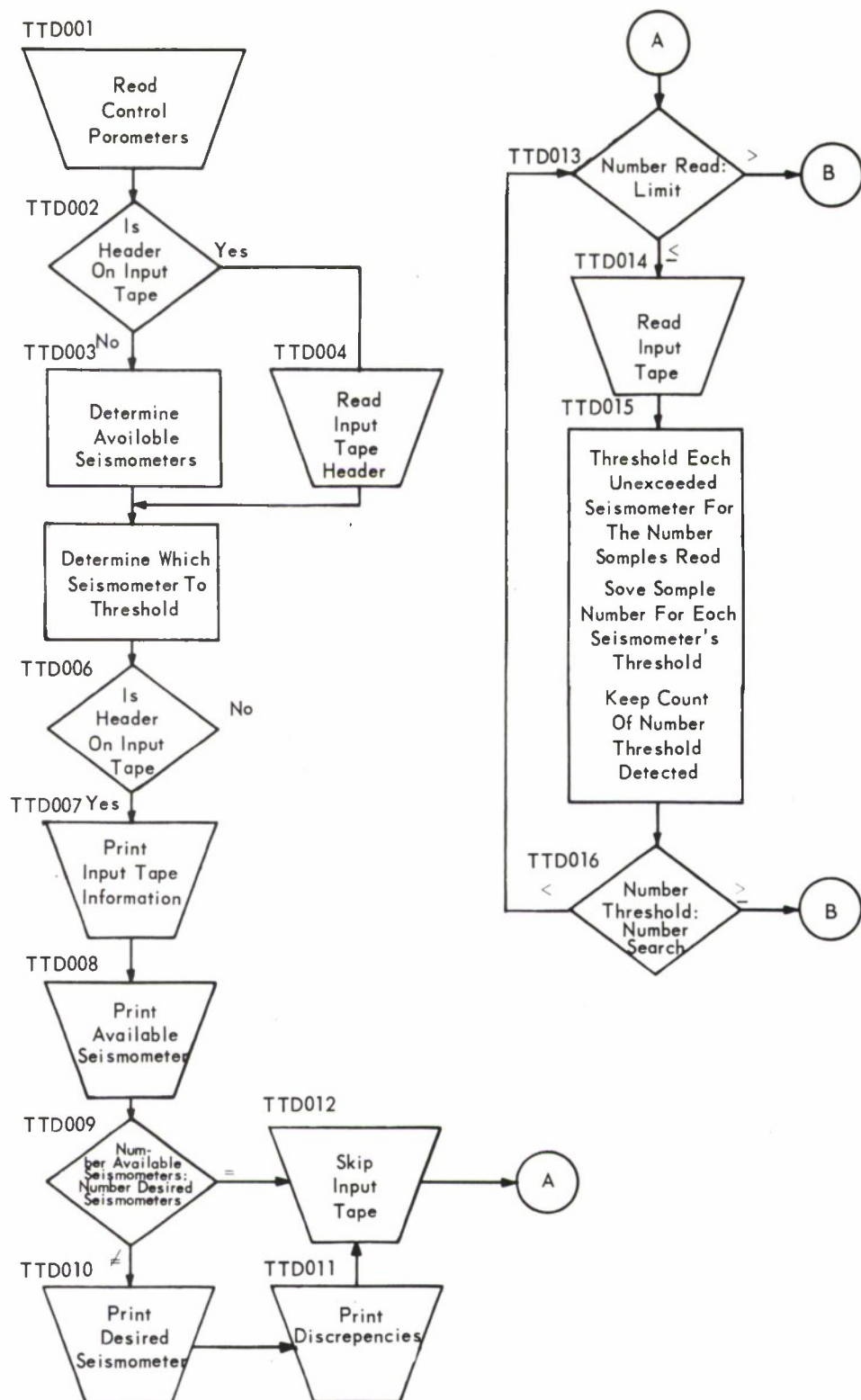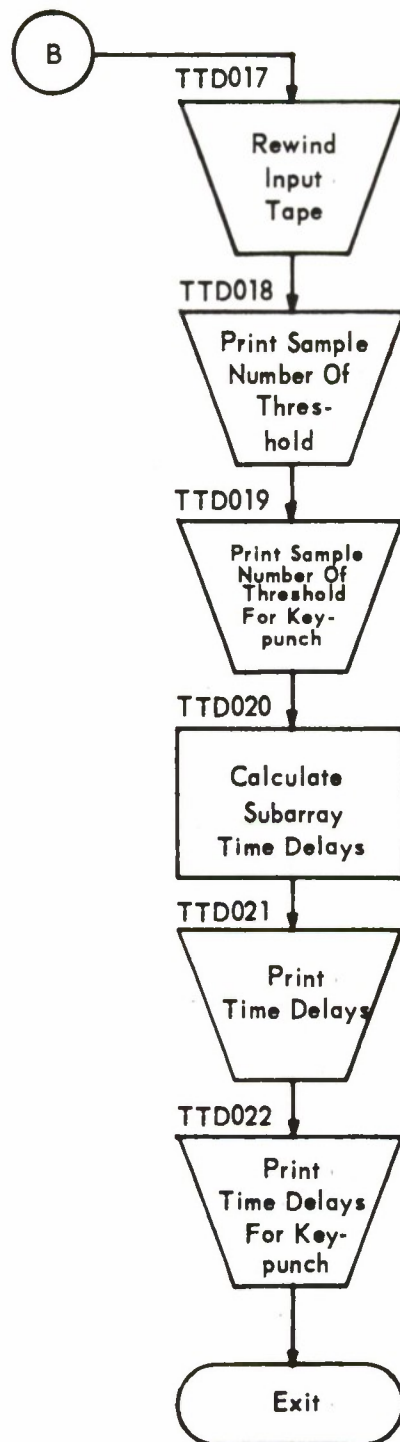
Figure 4-11. Threshold Time Delay (Sheet 1 of 2)

Figure 4-11. Threshold Time Delay (Sheet 2 of 2)

4.12   SUBARRAY PLOT (SAPLOT) (Figure 4-12)

Purpose

This program plots seismometer data from a selected subarray for a variable period of time. The resultant plot provides a visual representation of the seismometer activity during the selected time period.

Description

Input

Seismometer data is obtained from a LASA edit tape, while control parameters and other pertinent data, such as the selected subarray identification, are read from cards.

Card Input

Data Card 1

Card Column	Field Specification	Variable Name	Sample Value
11-28	3A6	EVENT	Longshot (10/29/65)
31-35	I5	ISKIPH	1
36-40	I5	NCH	525

where

EVENT	18-character description of the plot
ISKIPH	= 0, header exists on first input tape ≠ 0, header does not exist on first input tape
NCH	Number of seismometers on input tape

Data Card 1B (Necessary if ISKIPH ≠ 0 NCH ≠ 525)

Card Column	Field Specification	Variable Name	Sample Value
1-5	I5	JCH(I)	1
6-10	I5	JCH(I)	3
.			
.			
66-70	I5	JCH(I)	525

where

JCH(I) Specific seismometer channels on the input tape. Fourteen seismometer channel numbers are recorded on each card so the number of cards is related to the number of channels on the input tape.

Data Card 2

Card Column	Field Specification	Variable Name	Sample Value
11-12	I2	ISUBA	21
14-15	I2	NSUBA(I) I=1	1
.			
.			
74-75	I2	NSUBA(I) I=ISUBA	21

where

ISUBA   Number of subarrays to plot ($1 \leq$ ISUBA ≤ 21)

NSUBA   Specific subarray to plot (1 to 21)

Data Card 3

Card Column	Field Specification	Variable Name	Sample Value
1-10	F10.2	DSKIP	12.05
11-20	F10.2	PSEC	132.00
21-30	F10.2	ABSMAX	8191.
31-35	I5	NOTAPE	1

where

DSKIP   Amount of time to skip on input reel in seconds (20 samples/sec)

PSEC   Amount of time to process from input reel in seconds (must be a multiple of 22 seconds)

ABSMAX Absolute maximum value of vertical (x) axis

NOTAPE Number of input tapes to be used

Tape Input. The input tape(s) must be in LASA edit format and must be mounted on FORTRAN logical unit 14. The first input tape need not have a header. This situation would be signified by the appropriate setting of the input variable ISKIPH.

Computation

The program determines the desired vertical axis scale from card inputs, and then positions the data tape to the specified sample period. The reading of the LASA edit tape then begins for the specified number of time samples. After each read, the seismometer values of the selected subarray are extracted. The array of seismometer data obtained is placed on tape by the Calcomp subroutines in the proper format for subsequent plotting. The plotting continues until the specified number of time samples have been read.

The program may then select a different subarray and, by repositioning the input tape(s) to the specified first sample, may repeat the process for a different subarray.

Output

Both printed and tape outputs are produced by the program.

Printed Output. This program prints a message each time it completes a subarray plot.

Magnetic Tape Output. The magnetic tape(s) produced by the program on physical unit A6 at 200 BPI is in the prescribed format for off-line plotting on a Calcomp plotter.

Program Interaction

The program requires a tape of the LASA edit format as input.

Program Restrictions

Seismometer values are read and plotted in 440 sample blocks with a limit of 6 blocks to a plot page. Since the seismometer values are not plotted until a full array of 440 samples is read, it is necessary to have PSEC equal to increments of 440 samples so as not to lose seismometer values.

The ability to initialize a new page and continue to plot up to seven pages exists. The program may also plot up to 21 subarrays in a single execution, and any of these subarrays may be repeated or occur in any order.

Comments

This program is written in FORTRAN IV and the read subroutine in MAP. It is run under the IBSYS Operating System on the IBM 7090.

The plotting is done on a Calcomp Model 563 digital incremental plotter, whose plot limits are 30 inches by 120 feet.
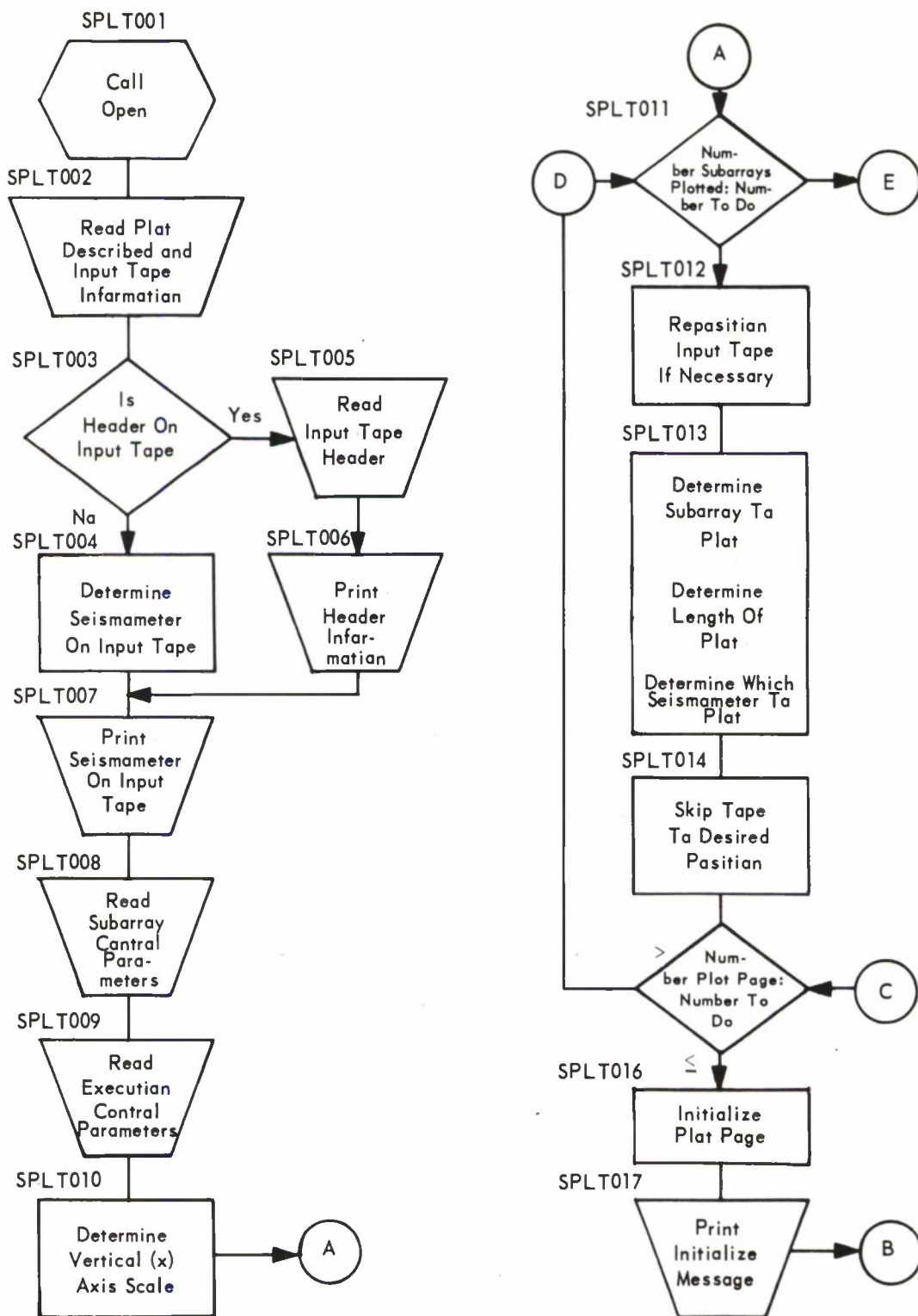
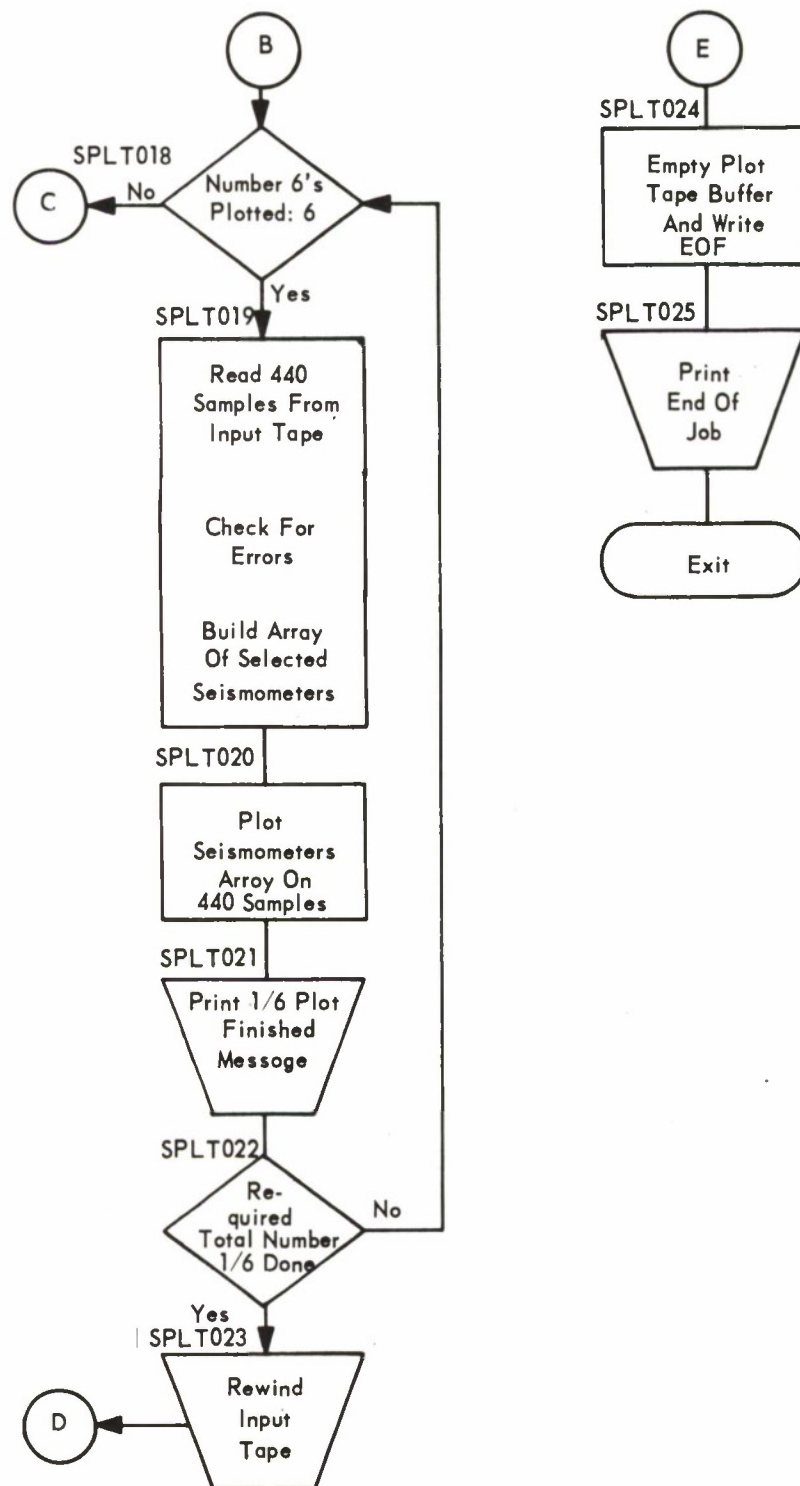Figure 4-12. Subarray Plot (SAPLOT) (Sheet 1 of 2)

Figure 4-12. Subarray Plot (SAPLOT) (Sheet 2 of 2)

4.13   BEAM PATTERN DISPLAY (Figure 4-13)

Purpose

This program prepares input tapes for use on the Experimental Display.

Description

Input

Input consists of parameter cards specifying the action desired, address cards specifying location of beams on the display face, and magnetic tapes containing LASA beams. The input cards follow the program deck.

Card Input

Data Card 1

Card Column	Variable Name	Sample Value
2 – 5	BMCNT	0151
10	TPCNT	1
12 – 15	RATE	1
37 – 40	ISKP	90
42 – 45	TAPECNT	300
49 – 50	COPYCNT	˙10

where

BMCNT	Number of beams per time sample
TPCNT	Number of input tapes
RATE	Number of 50 millisecond displays generated for each time sample
ISKP	Number of time samples to skip before processing begins
TAPECNT	Total number of output records to be produced (i.e., RATE times number input records to be processed)
COPYCNT	Number of copies of the entire time period to be made on the output tape

The display face consists of 32 rows and 32 columns numbered from zero to 31, top to bottom, left to right. This data card contains a row-column address for each beam. Each card contains a maximum of 12 addresses and there may be any number of these cards.

Data Card 2

Card Column	Variable Name	Sample Value
2 - 6	LOC1	15, 15
8 - 12	LOC2	15, 16
.		
.		
68 - 72	LOCn	05, 11

where

LOC1   The row-column address of beam one

LOC2   The row-column address of beam two, etc

Tape Input (may be a 7- or 9-track tape). The input tape consists of physical records of a maximum of 105 characters and a minimum of 12 characters, having been written with a FORTRAN format of 15F7.0. More than one physical record may be necessary to accommodate all beams.

The tape must also contain a header record of 30 tape characters. Characters 7-12 of this header record must contain the number of beams per time sample. (This tape is presently assigned to 7-track unit 181.)

Computation

The beam values are read and converted to display intensities through use of a table containing data limits for each intensity level.

Output

The output is a 9-track tape for use on the Experimental Display. A single physical record is 6150 characters in length and contains six frames

of display data. The tape will contain the number of copies of the display sequences that were requested by COPYCNT.

The program will also type messages for the operator concerning mounting tapes, etc. Output is on the IBM System/360 tape drive 183; the work tape is unit 184.

Program Interaction

The magnetic tape input is produced by the LASA Beamformer program and a reformatting process. The address cards are produced by the Display Address Card program.

Program Restrictions

Only one output reel can be produced per input request.

Comments

This program was written in assembler language for the IBM System/360. It is presently designed to operate using the Basic Programming Support System.
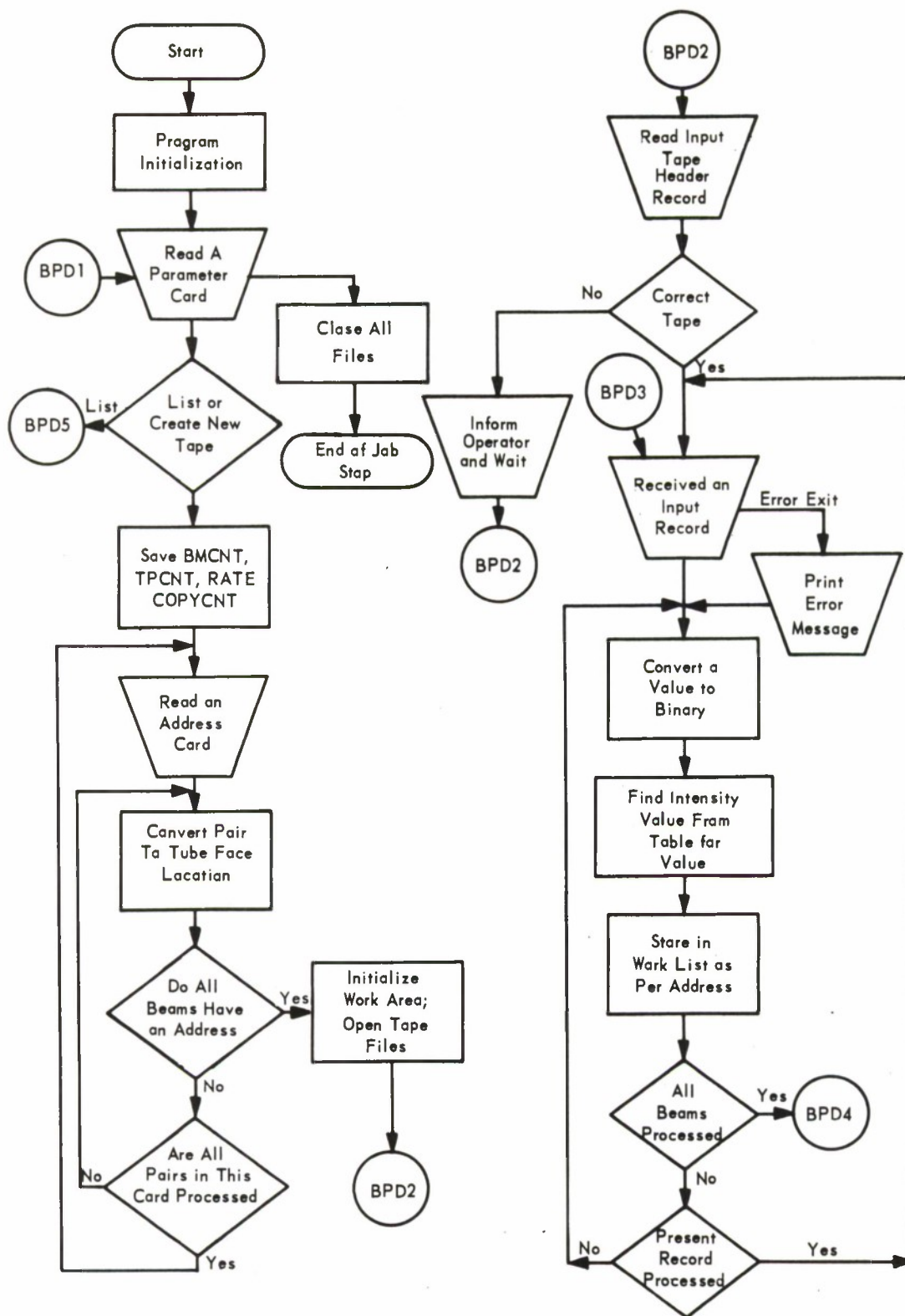
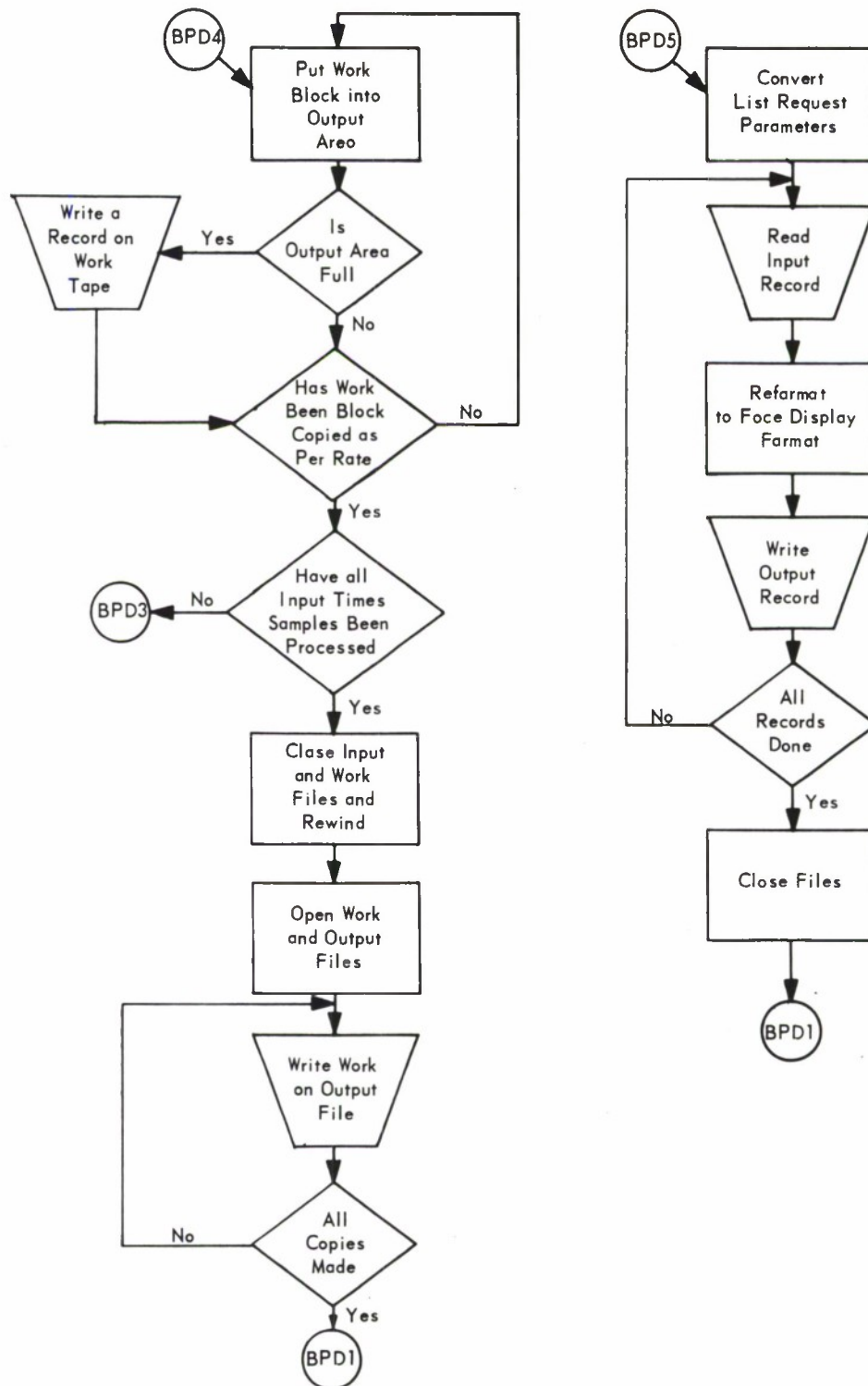Figure 4-13. Beam Pattern Display (Sheet 1 of 2)

Figure 4-13. Beam Pattern Display (Sheet 2 of 2)

4.14   DISPLAY ADDRESS CARD (Figure 4-14)

Purpose

This program is used to generate the address cards necessary for use by the Beam Pattern Display program.

Description

Input

The input to this program consists of the output deck from the Neighboring Beam Time Delay Calculations program.   Three cards are used to represent each beam, although the contents of the last two cards are ignored.   The first data card for each beam has the following format:

Card Input

Card Column	Field Specification	Variable Name	Sample Value
7 – 18	F12.6	UX	0.057493
25 – 36	F12.6	UY	-0.038521
42 – 45	I4	M	0
51 – 54	I4	N	0

Up to 1024 beams can be used as input. The last beam is followed by a blank card.

Computation

The first beam (first three cards) is read and the UX, UY, M, and N values are saved.   An internal matrix which corresponds to the display face is zeroed.   The rest of the beam inputs are read and assigned a sequence number starting with 2.   As each beam is read, its sequence number is placed in the matrix at the row and column address computed as

$$\text{ROW} \quad\;\; = 16 + (\text{UY}(1) - \text{UY}(I)) * 1000 \tag{4.9}$$
$$\text{COLUMN} = 16 + (\text{UX}(I) - \text{UX}(1)) * 1000$$

where UX (1) and UY (1) are the coordinates of the first beam and UX(I) and UY(I) are the coordinates of the Ith beam. If any ROW or COLUMN address is negative or greater than 32, the associated beam is ignored. The first beam is assigned the coordinates ROW = 16, COLUMN = 16.

The matrix is now compressed so that all zero entries are removed from the center of the matrix. The first beam is held invariant at the center of the matrix. Four loops are used, one for each quadrant of the matrix.

Following the compression process, the row and column indexes are sorted by ascending beam sequence number. Any zero matrix entry is ignored and missing sequence numbers are omitted. The list of UX, UY, M, N, ROW and COLUMN entries are printed in ascending sequence. The ROW and COLUMN entries are punched in ascending sequence in the format required for the Beam Pattern Display program.

Output

The outputs are given in the Computation section above. The output deck is suitable for input to the Beam Pattern Display program.

Program Interaction

The input to this program is the output of the Neighboring Beam program. The output of this program serves as part of the input to the Beam Pattern Display program.

Program Restrictions

Any velocity coordinates which initially place the beam off the display face are ignored.

Comments

This program was written in FORTRAN IV for use on an IBM System/360.
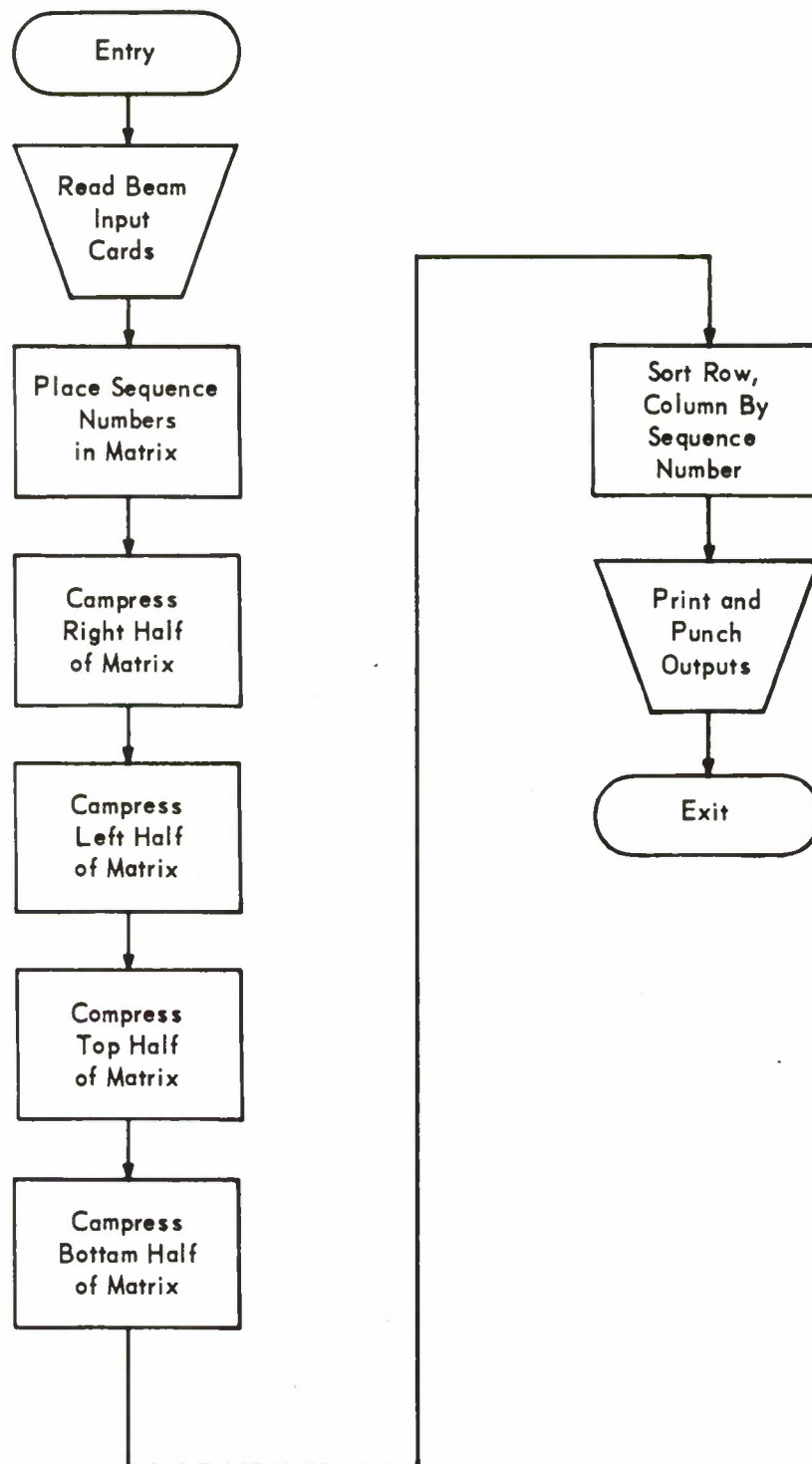
Figure 4-14. Display Address Card

4.15   LEAST SQUARES PLANE AND QUADRATIC WAVEFRONT (Converted Study Program) (Figure 4-15)

Purpose

This program calculates the direction and speed, and thereby the approximate azimuth and range, of the wavefront corresponding to a given set of arrival times at a set of known locations by calculating the best-fitting plane wavefront and quadratic wavefront corresponding to these arrivals. For the linear case, an attempt is made to correct the arrival times for curvature as a function of range.

Description

Input

Card Input

Data Card 1

Card Column	Field Specification	Variable Name	Sample Value
1 - 2	I2	N	21

where

N   Number of array elements or subarrays whose centers are treated as single elements (N $\leq$ 25)

Data Card 2

Card Column	Field Specification	Variable Name	Sample Value
1 - 2	I2	NIT	5

where

NIT   Number of iterations to perform on plane wavefront calculations

Data Card 3

Card Column	Field Specification	Variable Name	Sample Value
1 - 2	I2	KPUNCH	1

where

KPUNCH   1/0 condition. Punch output cards which are used in Steering Delay Anomalies program/Do not punch output cards.

Data Card 4

Card Column	Field Specification	Variable Name	Sample Value
1 - 2	A2	ARRAY(1)	B1
3 - 4	A2	ARRAY(2)	B2
.			
.			
.			
41 - 42	A2	ARRAY(N)	A0

where

ARRAY(1)   Name of subarray 1

ARRAY(2)   Name of subarray 2

     .

     .

ARRAY(N)   Name of subarray N

Data Card 5

Card Column	Field Specification	Variable Name	Sample Value
1 - 10	F10.0	R0	13528.0
11 - 20	F10.0	R1	-46116.0
21 - 30	F10.0	R2	-1000000.0
31 - 40	F10.0	R3	0.0
41 - 50	F10.0	RE	6370.0

where

R0 ⎞
R1 ⎟
R2 ⎬ Constants
R3 ⎠

RE   Radius of earth

Data Card 6

Card Column	Field Specification	Variable Name	Sample Value
1 - 8	F8.3	X(1)	4.425
9 - 16	F8.3	Y(1)	-6.022

where

X(1)   X component of the position of Kth seismometer (or subarray center) in subarray 1

Y(1)   Y component of the position of Kth seismometer (or subarray center) in subarray 1

Note: Card 6 is repeated for all N seismometers in the order specified by data card 4. Each card will give coordinates of Kth seismometer in a different subarray.

Data Card 7

Card Column	Field Specification	Variable Name	Sample Value
1 - 2	I2	ICWT(1)	3

where

ICWT(1)   Number of the seismometer whose weight is to be changed to zero. Additional seismometer numbers can be records in columns 3-4, 5-6 ... 49-50. (If no weights are to be changed, data card 7 will be blank.)

Data Card 8 (Teledyne card format)

Card Column	Field Specification	Variable Name	Sample Value
1 - 2	I2	IMONTH	11
3 - 4	I2	IDAY	23
5 - 6	I2	IYEAR	65
7 - 8	I2	IHOUR	15
9 - 10	I2	IMIN	58
11 - 14	F4.1	ASEC	16.3
15 - 19	A5	ALAT	18.4N
20 - 25	A6	ALONG	123.7E
26 - 28	I3	IDEPTH	243
29 - 31	F3.1	AMAG	2.5
32 - 36	I5	IRANGE	13250.
37 - 39	I3	IAZMTH	120
40	A1	CORD	C
41 - 71	3A8, A7	DCMT(I),I=1,4	CHILE
72 - 77	I6	NUMESD	000100

where

IMONTH Month of event

IDAY Day of event

IYEAR Year of event

IHOUR Origin time, hours

IMIN Minutes

ASEC Seconds

ALAT Latitude to nearest tenth of degree (N or S for north or south)

ALONG Longitude to nearest tenth of degree (E or W for east or west)

IDEPTH Depth to nearest kilometer

AMAG Magnitude

IRANGE Output field distance from A0 subarray to epicenter

IAZMTH Output field distance from A0 to event

CORD C/D condition. Compression/Dilation

DCMT(I),
 I=1,4   Comments

NUMSED   Event number (ESD number for the event)

Data Card 9

Card Column	Field Specification	Variable Name	Sample Value
1 - 2	I2	(Hour)	
3 - 4	I2	(Minute)	
5 - 9	F5.2	ATIME(I)	58.24
72 - 77	I6	(Event Number)	
79 - 80	I2	(Subarray)	

where

ATIME(I)   Arrival time (seconds) at Ith subarray. Only information in columns 5 - 9 is used by the program. (Time recorded in hours and minutes must be the same for all. If one time is 6 min. 10.3 sec. and another is 5 min. 55.2 sec., they must be given as 5 min. 70.3 sec. and 5 min. 55.2 sec., respectively. Additional events will have data cards as per format of cards 8 and 9, and will follow cards of previous event.)

Computation

The Least Squares Plane and Quadratic Wavefront program accepts a set of seismometer (or subarray center) locations with corresponding arrival times and weights. It calculates a least squares best-fitting quadratic wavefront surface of the form

$$t_k = p + X_k U_x + Y_k U_y + \alpha X_k^2 + 2\beta X_k Y_k + \gamma Y_k^2 \qquad (4.10)$$

by determining p, U_x, U_y, α, β, and γ to minimize the sum of the squares of the residuals or deviations from the quadratic surface, i.e.,

$$\Sigma_k (t_k - t)^2 = \text{Minimum.} \qquad (4.11)$$

4-109

Nomenclature

X_k, Y_k X and Y components of the position of the Kth seismometer (or subarray center)

t_k Arrival time of a wavefront at the Kth seismometer

w_k Weighting to be attached to the arrival time t_k in calculations

(U_x, U_y) Inverse velocity speed coordinates

U Reciprocal speed $= (U_x{}^2 + U_y{}^2)^{1/2}$

Calculations

Replace

$$X_k \text{ by } X_k - \frac{\Sigma W_k X_k}{\Sigma W_k}$$

$$Y_k \text{ by } Y_k - \frac{\Sigma W_k Y_k}{\Sigma W_k}$$

$$t_k \text{ by } t_k - \frac{\Sigma W_k t_k}{\Sigma W_k}$$

The parameters defining the quadratic surface are obtained by solving the following matrix equation.

$$
\begin{bmatrix}
\Sigma w_k & 0 & 0 & \Sigma w_k X_k^2 & \Sigma w_k X_k Y_k & \Sigma w_k Y_k^2 \\
0 & \Sigma w_k X_k^2 & \Sigma w_k X_k Y_k & \Sigma w_k X_k^3 & \Sigma w_k X_k^2 Y_k & \Sigma w_k X_k Y_k^2 \\
0 & \Sigma w_k X_k Y_k & \Sigma w_k Y_k^2 & \Sigma w_k X_k^2 Y_k & \Sigma w_k X_k Y_k^2 & \Sigma w_k Y_k^3 \\
\Sigma w_k X_k^2 & \Sigma w_k X_k^3 & \Sigma w_k X_k^2 Y_k & \Sigma w_k X_k^4 & \Sigma w_k X_k^3 Y_k & \Sigma w_k X_k^2 Y_k^2 \\
\Sigma w_k X_k Y_k & \Sigma w_k X_k^2 Y_k & \Sigma w_k X_k Y_k^2 & \Sigma w_k X_k^3 Y_k & \Sigma w_k X_k^2 Y_k^2 & \Sigma w_k X_k Y_k^3 \\
\Sigma w_k Y_k^2 & \Sigma w_k X_k Y_k^2 & \Sigma w_k Y_k^3 & \Sigma w_k X_k^2 Y_k^2 & \Sigma w_k X_k Y_k^3 & \Sigma w_k Y_k^4
\end{bmatrix}
\begin{bmatrix}
P \\ U_x \\ U_y \\ \alpha \\ 2\beta \\ \gamma
\end{bmatrix}
=
\begin{bmatrix}
0 \\ \Sigma w_k t_k X_k \\ \Sigma w_k t_k Y_k \\ \Sigma w_k t_k X_k^2 \\ \Sigma w_k t_k X_k Y_k \\ \Sigma w_k t_k Y_k^2
\end{bmatrix}
\tag{4.12}
$$

The reciprocal speed u is given by

$$U = \sqrt{U_x{}^2 + U_y{}^2} \, .$$

(4.13)

The azimuth to the event is given by

$$AZI = 270° - \tan^{-1} \frac{U_y}{U_x} \quad \text{for } U_x > 0$$

(4.14)

$$AZI = 90° - \tan^{-1} \frac{U_y}{U_x} \quad \text{for } U_x < 0$$

$$AZI = 0° \qquad\qquad \text{for } U_x = 0 \text{ and } U_y \geq 0$$

$$AZI = 90° \qquad\qquad \text{for } U_x = 0 \text{ and } U_y < 0$$

The range to the event is given by an approximate quadratic fit to the results of ray tracing.

$$R = 13528 - 46116 \, U - 10^{-6} U^2 .$$

(4.15)

The second derivatives with respect to time for range, range and azimuth, and azimuth are given by

$$\frac{d^2 \text{(range)}}{dt^2} = \frac{2}{U^2} \left(\alpha U_x{}^2 + 2B U_x U_y + \gamma U_y{}^2 \right)$$

$$\frac{d^2 \text{(range - azi)}}{dt^2} = \frac{2}{U^2} \left[(\gamma - \alpha) U_x U_y + \beta (U_x{}^2 - U_y{}^2) \right]$$

(4.16)

$$\frac{d^2 \text{(azimuth)}}{dt^2} = \frac{2}{U^2} \left(\alpha U_y{}^2 - 2\beta U_x U_y + \gamma U_x{}^2 \right) .$$

Output

The printed output generated by this program is discussed in Section 3.4 of this report.

Card Output

Output Card 1

Card Column	Field Specifications	Variable Name	Sample Value
1 - 15	15H	(Constant)	ESD Event No. =
16 - 21	I6	NUMESD	318
30 - 60	3A8, A7	DCMT(I), I = 1,4	Fox Island
73 - 78	I6	NUMESD	318
79 - 80	I2	(Constant)	00

where

NUMESD   Event number (ESD number for the event)

DCMT(I)   Comments (see input data card 8, columns 41 - 71)

Output Card 2

Card Column	Field Specifications	Variable Name	Sample Value
1 - 2	I2	I	16
3 - 11	F9.2	W(I)	1.0
12 - 21	F10.4	DELTO(I)	0.0321
22 - 31	F10.4	DELT(I)	0.0318
32 - 41	F10.4	DLTQUD(I)	0.0317
73 - 78	I6	NUMESD	318
79 - 80	I2	I	16

where

I	Ith element (usually the center seismometer of the Ith subarray)
W(I)	Weighting factor > 0 (usually 1.0)
DELTO(I)	Time deviation from plane wavefront for Ith element
DELT(I)	Time deviation after range corrections
DLTQUD(I)	Time deviation from quadratic wavefront
NUMESD	Event number

Data card 2 is repeated for all elements with weight > 0.

<u>Output Card 3</u> (Blank card) – Indicates the end of the output of data cards 2.

<u>Output Card 4</u>

Card Column	Field Specification	Variable Name	Sample Value
1 – 4	I4	NUMESD	318
5 – 14	F10.6	W1	0.060130
15 – 20	F6.1	AZIDEG	318.1
21 – 40	E20.8	D2TRAN	-0.3935201 E-04
41 – 60	E20.8	D2TAZI	0.10267138 E-04
61 – 80	E20.8	D2TRAZ	-0.35568413 E-04

where

NUMESD	Event number
W1	Inverse phase velocity
AZIDEG	Calculated azimuth to event
D2TRAN	Second-time derivative with respect to range
D2TAZI	Second-time derivative with respect to azimuth
D2TRAZ	Second-time derivative with respect to range-azimuth

Program Interaction

The punched output from this program (deviations of the actual arrivals from the best-fitting plane or quadratic wavefront) is used as input to the Seismic Steering Delay Anomalies program. The calculated inverse velocity space coordinates are used by the Neighboring Beam program.

Program Restrictions

To determine a plane wavefront, the arrival times at three different locations must be available for the event; five arrival times are needed to determine a quadratic wavefront. The program is arbitrarily restricted to the use of a maximum of 25 arrival times.

Comments

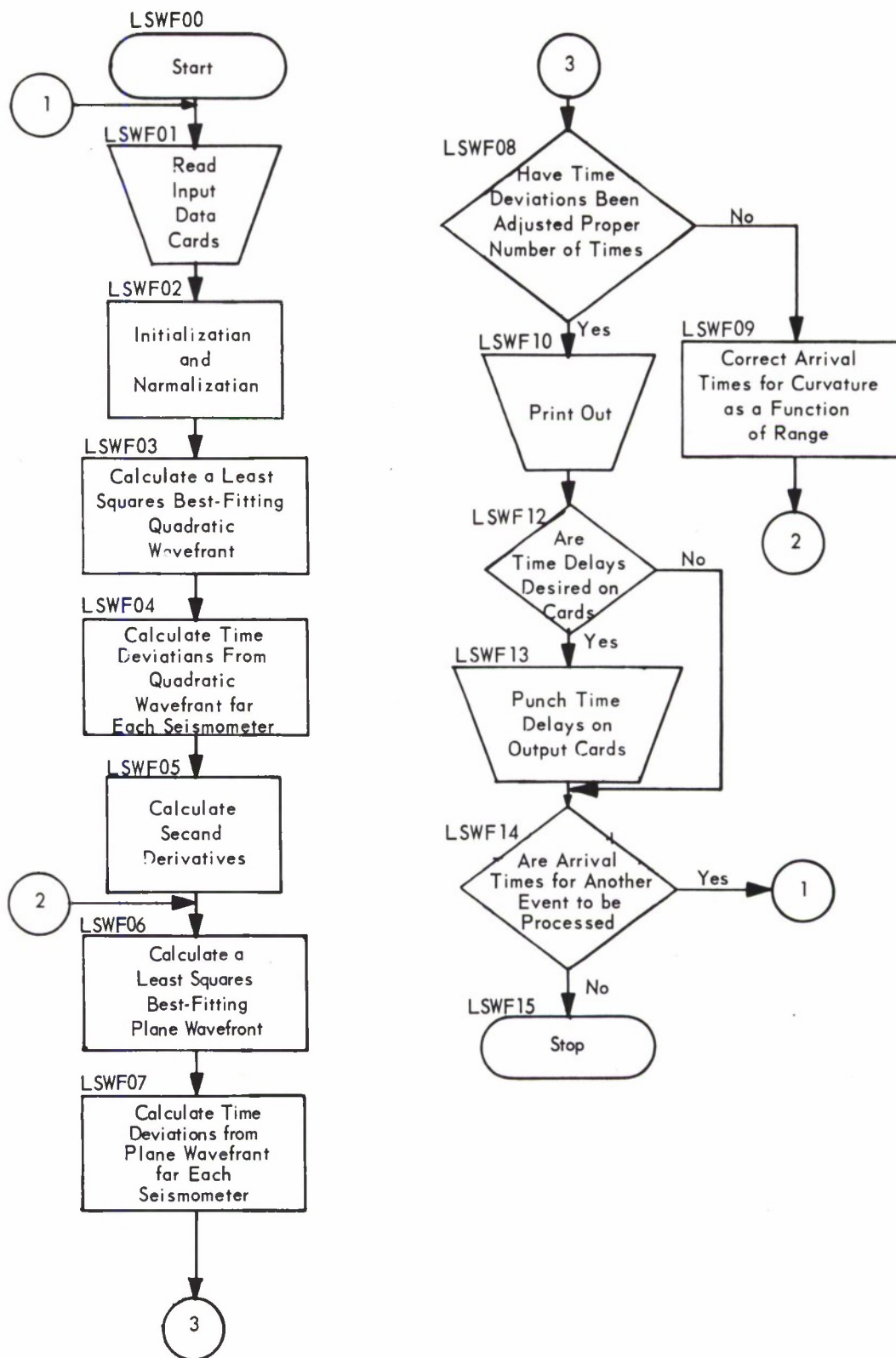This program is written in FORTRAN IV for the IBM System/360.

Figure 4-15. Least Squares Plane and Quadratic Wavefront

4.16   CROSS-COVARIANCE OF SEISMIC DATA CHANNELS (Figure 4-16)

Purpose

This program computes and plots the cross-covariance of two seismic data input channels (seismometers or beams).

Description

Input

Input consists of cards to specify type and quantity of input data, cards to specify what segments of data are to be used for computation and plotting, and any of three forms of data tapes.

Card Input

Data Card 1

Card Column	Field Specification	Variable Name	Sample Value
1 - 3	I3	IS(1)	1
5	I1	IFORM	1
7	I1	ITAPE	2
9	I1	IHEAD	2
11 - 20	F10.2	T1(1)	67.25
21 - 30	F10.2	T2(1)	130.20
31 - 33	I3	IS(2)	525
35	I1	JFORM	3
37	I1	JTAPE	1
39	I1	JHEAD	1
41 - 50	F10.2	T1(2)	103.50
51 - 60	F10.2	T2(2)	157.45
66 - 70	I1	INC	1

where

IS(1)	Number of seismometer or beam for first data segment
IFORM	Indicates type of input tape for first data segment 1 – LASA edit (on FORTRAN logical unit 14 at 800 BPI) 2 – Seismic Data Laboratory Format (on FORTRAN logical unit 15 at 556 BPI) 3 – LASA beam (on FORTRAN logical unit 03 at 800 BPI)
ITAPE	Opening procedure for first segment input tape 1 – Rewind and use tape previously mounted on unit indicated by IFORM 2 – Mount a new tape (a card containing a message to the operator must follow the parameter card if a new tape is to be mounted) 3 – First data segment is same as previous first data segment read. IS(1), T1(1), and T2(1) must be in the card exactly as it was in the previous control card which caused the data to be read.
IHEAD	Logic flag to indicate presence of header record in first segment tape 1 – No header record on tape 2 – Header record on tape
T1(1)	Starting time of first segment to be read (in seconds from beginning of first tape in the file)
T2(1)	Ending time of first segment
IS(2)	Number of seismometer or beam for second data segment
JFORM	Type of input tape for second data segment (see IFORM)
JTAPE	Open procedure for second segment input tape 0 – Both first and second data segments are on same tape 1 – Reuse tape on JFORM unit 2 – Mount new tape (a message must follow parameter card and message card for first segment, if any) 3 – Second segment is same as previous second segment (or no second segment is to be read, i.e., only an auto-covariance will be requested)
JHEAD	Similar to IHEAD but refers to second segment
T1(2)	Starting time for second segment
T2(2)	Ending time for second segment
INC	Number of records to next observation to be read 1 – All records to be read 2 – Every other record to be read.

Data Card 2

Card Column	Field Specification	Variable Name	Sample Value
5	I1	LS(1)	1
6 - 15	F10.2	TM0(1)	75.45
16 - 25	F10.2	TM1(1)	65.45
26 - 35	F10.2	TM2(1)	90.45
40	I1	LS(2)	2
41 - 50	F10.2	TM0(2)	125.40
51 - 60	F10.2	TM1(2)	120.35
61 - 70	F10.2	TM2(2)	150.05
71	I1	IPOS	1
72 - 73	I2	LAST	-1

where

LS(I)   Indicates which data segment specified on the input data card is to be used (1 or 2)

TM0(I)   Time (seconds) at which a peak is expected (used only for annotation but must be within the range of TM1 and TM2)

TM1(I)   Beginning time of the segment to be computed and plotted

TM2(I)   Ending time of the segment

IPOS   Indicates that a rectified plot of the covariance curve is to be plotted: 1 - no, 2 - yes

LAST   Indicates action to be taken after processing the present request:
blank or 0 - Next parameter card is another computation card
           1 - Next card is an input parameter card
         -1 - End of job.

I   Indicates first or second plotting segment

Input Tapes

The LASA edit and LASA beam tape formats have been discussed in previous sections. The Seismic Data Laboratory Tape is in IBM 7090 internal format (36-bit integers) with 120 words per record and 10 records per file.

Computation

The cross-covariance formulas,[12] where A_i, $i = 1, \ldots, n$, and B_i, $i = 1, \ldots, m$, are two sets of data and $n \leq m$, are

$$R_j = \left(\sum_{i=1}^{T} A_i * B_{i+j-1} \right) / T - (\text{Average } A * \text{Average } B); \qquad (4.17)$$
$$j = 1, \ldots, m$$

where

$$T = \text{minimum } (n, m-j+1),$$

$$\text{Average } A = \left(\sum_{i=1}^{m} A_i \right) / n,$$

$$\text{Average } B = \left(\sum_{i=1}^{m} B_i \right) / m;$$

and

$$S_j = \left(\sum_{i=1}^{T} A_{i+j-1} * B_i \right) / T - (\text{Average } A * \text{Average } B); \qquad (4.18)$$
$$j = 1, \ldots, n$$

where

$$T = n - j + 1.$$

Output

The output consists of a Calcomp plotter tape which results in an annotated graph of each seismometer and the cross-covariance curve.

Program Interaction

None

Program Restrictions

The total size of selected segments read cannot be longer than 7200 samples. (This would be a total of six minutes of LASA data if the sample rate were 20 samples per second.)

Comments

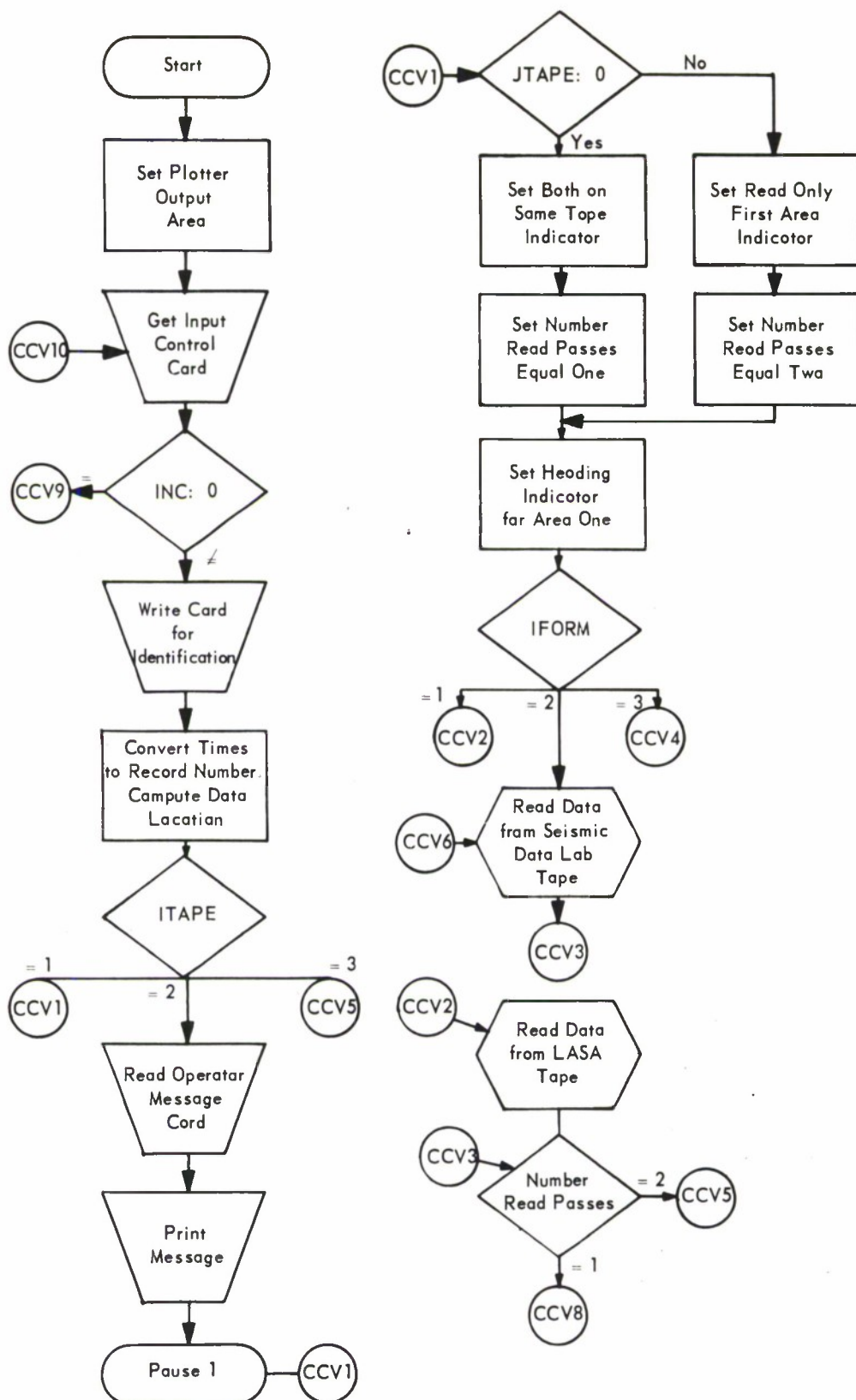This program is written in FORTRAN IV for the IBM 7090.

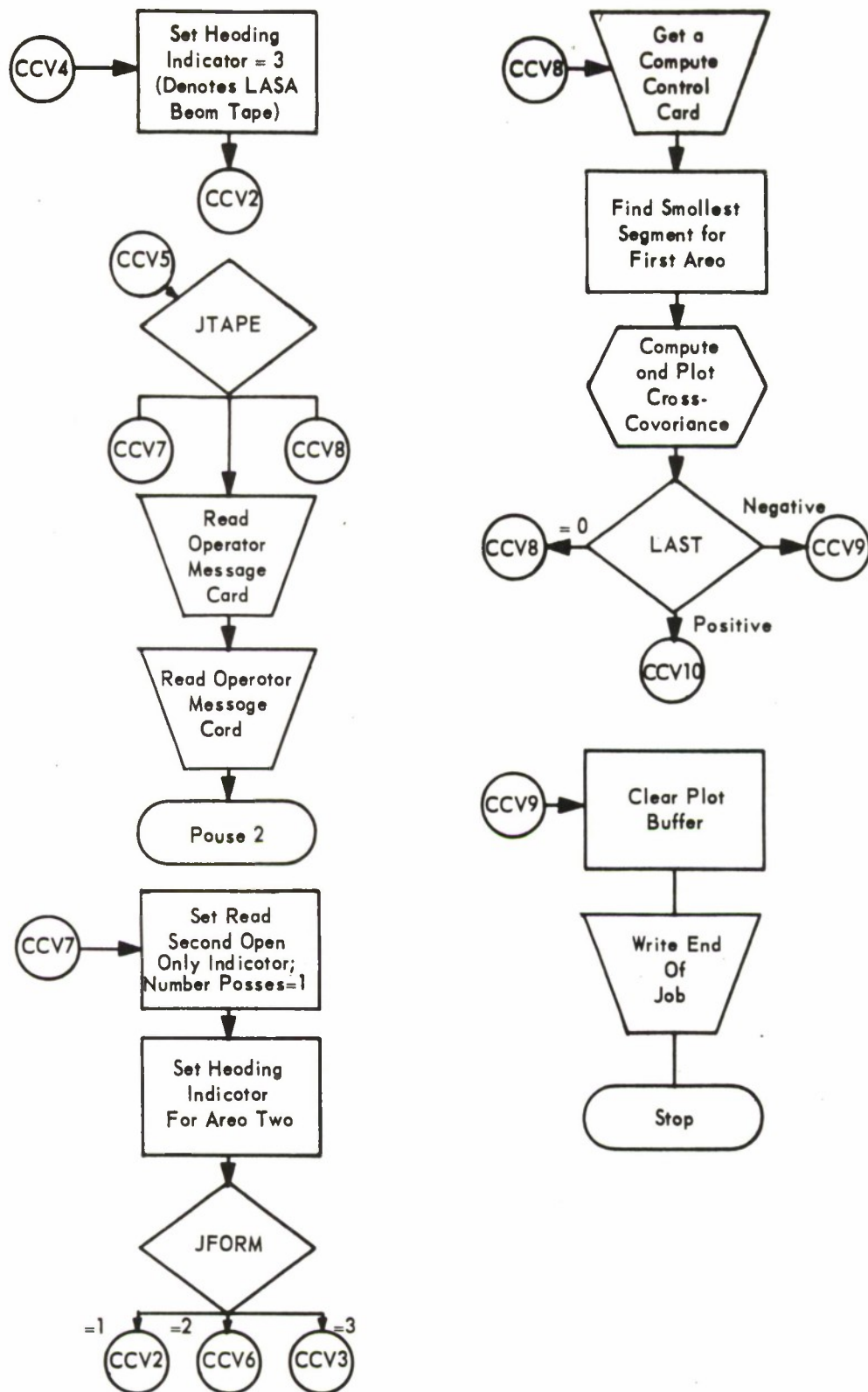Figure 4-16. Cross-Covariance of Seismic Data Channels (Sheet 1 of 2)

Figure 4-16. Cross-Covariance of Seismic Data Channels (Sheet 2 of 2)

4.17   POWER SPECTRA ANALYSIS (PSA)   (Figure 4-17)

Purpose

This program calculates the Fourier transform of time traces obtained from LASA edit seismometer tapes, LASA subarray beam tapes, or LASA array beam tapes. Each trace may consist of N real data samples where N is taken as a power of two. From the Fourier transform of a given trace, the program computes the phase angle, signal power, energy-density, dB of power, and dB of energy density spectra with respect to angular frequency. Optional plots of either energy-density or the dB of energy-density may be obtained at the discretion of the user.

All of the above calculations are performed on two seismometers, two subarray beams, or two array beam traces at a time. The traces may be for the same seismometer or beam taken over different intervals of time, or for different seismometers or beams taken over the same or different intervals of time. Different time intervals may be disjoint or overlapped; however, the length of both intervals and the sampling rate must be the same. The program will operate on a single seismometer or beam trace at a time but with some loss in efficiency.

Description

Input

Card Input. Card input consists of one or more sets of control cards. Each set of control cards contains a data card 1 followed by one or more data cards 2.

Data Card 1

Card Column	Field Specification	Variable Name	Sample Value
1 - 2	I2	NREEL	2
3 - 8	A6	IREEL(1)	2240
9 - 14	A6	IREEL(2)	2241
15 - 20	A6	IREEL(3)	
21 - 22	I2	LEVEL	0
23 - 24	I2	IPLOT	0

where

NREEL   Number of input tape reels not exceeding three

IREEL(1) Identification number of the first reel of tape. This tape must contain a header record according to the format of a LASA edit seismometer tape, LASA subarray beam tape, or LASA array beam tape. This reel number will appear in an on-line message to the operator concerning tape mounting.

IREEL(2) Identification number of the second reel of tape (if any). This tape should contain a continuation of data recorded on the first reel.

IREEL(3) Identification number of the third reel of tape (if any). This tape should contain a continuation of data recorded on the second reel.

LEVEL   Logic flag indicating the level of data recorded on the input tape; it assumes any one of three values:

0 for LASA edit seismometer tape

1 for LASA subarray beam tape

2 for LASA array beam tape

IPLOT   Logic flag indicating whether or not the plotting option is exercised by the user on subsequent data cards, and assumes one of two values:

0 for no plotting

1 for plotting

If a value of 1 is specified, an on-line message to the operator is given, requesting that an output tape be mounted on unit A6 for subsequent recording of data for off-line plotting on a Calcomp plotter.

Data Card 2

Card Column	Field Specification	Variable Name	Sample Value
1 - 2	I2	M	9
3 - 12	F10.3	Q	0.028
13 - 22	F10.3	DTIME	0.050
23 - 32	F10.3	DZ	0.000
33 - 34	I2	LCPR	3
35 - 36	I2	LCPL	2
37 - 39	I3	NS1	1
40 - 44	I5	NRSS1	2000
45 - 47	I3	NS2	22
48 - 52	I5	NRSS2	3500
53 - 54	I2	IPLOTE	1
55 - 56	I2	LCB	1
57 - 58	I2	JOBE	1

where

M
Indicates that the time trace for each of the seismometers or beams specified on this card should consist of 2^M data samples where $3 \leq M \leq 12$

Q
Input quantum in nanometers

DTIME
Time increment in seconds between successive data samples of the time traces specified. This should correspond with the recording rate of the input tape or tapes being used. The notation ΔT will be used in referring to this parameter.

DZ
Filter recursive time increment. The notation ΔZ will be used in referring to this parameter.

LCPR
A logic choice for printing program input and output data; it assumes any one of four values:

0 - Header and time trace data obtained from the input tapes and power spectra analysis output data are not to be printed

1 - Only the header and time trace data obtained from the input tapes is to be printed

2 - Only power spectra analysis output data is to be printed

3 - Header and time trace data obtained from the input tapes and power spectra analysis output data are to be printed

LCPL	A logic choice for plotting; it assumes any one of three values:
	0 – No plots are desired
	1 – Plot of energy–density is desired for the seismometers or beams specified on this card
	2 – Plot of the dB of energy–density is desired for the seismometers or beams specified on this card

NS1	Data word number per logical record (sample) associated with the LASA seismometer or beam upon whose trace a power spectra analysis is to be performed. For example, if a LASA edit seismometer tape is being used, then a data word number of 39 would refer to seismometer B1 of subarray F1. A knowledge of the logical record format for the LASA edit seismometer tape, LASA subarray beam tape, or a LASA array beam tape (whichever is being used) is essential in the proper selection of this data word number.

NRSS1	Number of logical records (samples) to be skipped before transmitting trace data for seismometer or beam NS1

NS2	See NS1; similar to NS1 but related to the second of the two traces to be analyzed

NRSS2	See NRSS1; similar to NRSS1 but related to NS2

IPLOTE	This flag is used to indicate the continuation or termination of plotting requests for the current set of control cards; it assumes one of two values:
	0 – Continue writing plots on the plot output tape on unit A6.
	1 – Upon completion of computations requested on this card, no further plots are to be written on the current plot output tape on unit A6. This setting causes an end-of-file mark to be recorded on the current plot output tape. The tape will be rewound and unloaded.
	This flag should be 0 if IPLOT = 0 on data card 1.

LCB	A logic choice flag for processing LASA subarray or array beams; it assumes one of two values:
	0 – Unfiltered beam trace data is to be processed for the beams specified on this card
	1 – Filtered beam trace data is to be processed for the beams specified on this request card

JOBE	This flag indicates the continuation or termination of the current set of control cards; it assumes one of two values:
	0 – Data card 2 is not the last card of the current set of control cards
	1 – Data card 2 is the last card of the current set of control cards. Therefore, the next control card to be read will be either data card 1 or an end-of-file.

Tape Input. Tape input consists of up to three reels of tape containing trace data to be used in power spectra computations requested in each set of control cards described above. For a given set of control cards, the tape may be either LASA edit seismometer tapes, LASA subarray beam tapes, or LASA array beam tapes, as indicated by the LEVEL flag on the data card 1 for the set.

Each tape must be an IBM 7090 FORTRAN compatible binary tape recorded at 800 BPI. Each tape, beginning with the first, should be mounted on unit B2. On-line messages to the operator concerning the mounting of each tape are given as they are needed. The first tape of a multireel setup must contain a header record.

If IPLOT = 1 on data card 1, a scratch tape must be mounted on unit A6 at 200 BPI.

Computation

Given a set of $N = 2^M$ real data samples $X(j)$, $j=0, 1, \ldots, N-1$, the program computes the set of $\frac{N}{2} + 1$ complex coefficients $A(k)$, $k=0, 1 \ldots, \frac{N}{2}$ of the skewed complex Fourier series

$$X(j) = \sum_{k=0}^{N-1} [A(k) W^{jk}] \; ; j = 0, 1, \ldots, N-1 \tag{4.19}$$

where $W = \exp(2\pi i/N)$, $i = \sqrt{-1}$. The $A(k)$ coefficients are found by the inverse formula

$$A(k) = \frac{1}{N} \sum_{j=0}^{N-1} [X(j) W^{-jk}] \; k = 0, 1, \ldots, \frac{N}{2}. \tag{4.20}$$

The Cooley-Tukey (reference 11) algorithm is employed in the calculations. In the above equations, $X(j)$ refers to the value of the jth data sample of the time trace. This data sample is assumed to be for time $T(j) = j\Delta T$. Similarly, $A(k)$ refers to the kth complex transform value of the time trace corresponding to a frequency value of $F(k) = k \cdot \Delta F$ where $\Delta F = 1/N \cdot \Delta T$, or alternately, $W(k) = 2\pi F(k)$. Since the trace data used is real, $A(n-k) = \tilde{A}(k)$ for $k = 1, 2, \ldots,$

$(N/2)-1$ and only $A(0)$ through $A(\frac{N}{2})$ are computed. $A(0)$ and $A(\frac{N}{2})$ are always real.

Having obtained the values of $A(k)$, $k=0, 1, \ldots, N/2$, the following computations are performed.

Phase Angle Spectrum $\theta(k)$

$$\theta(k) = \tan^{-1}[\operatorname{Im} A(k) / \operatorname{Re} A(k)] \quad ; k = 0, 1, \ldots, \frac{N}{2} \tag{4.21}$$

where $\operatorname{Re} A(k)$ and $\operatorname{Im} A(k)$ are the real and imaginary parts of $A(k)$, respectively.

Signal Spectrum $S(k)$

$$S(k) = \begin{cases} Q \sqrt{B(k)} \; ; & k = 0 \text{ and } \frac{N}{2} \\ 2Q \sqrt{B(k)} \; ; & k = 1, 2, \ldots, \frac{N}{2} - 1 \end{cases} \tag{4.22}$$

where $B(k) = [\operatorname{Re} A(k)]^2 + [\operatorname{Im} A(k)]^2$.

Power Spectrum $P(k)$

$$P(k) = \begin{cases} Q^2 B(k); & k = 0 \\ 2Q^2 B(k); & k = 1, 2, \ldots, \frac{N}{2} - 1 \\ \frac{1}{2}Q^2 B(k); & k = \frac{N}{2} \end{cases} \tag{4.23}$$

Energy-Density Spectrum $D(k)$

$$D(k) = \begin{cases} \left[\dfrac{N\Delta t}{\pi}\right] P(k); & k = 0 \text{ and } \frac{N}{2} \\ \left[\dfrac{N\Delta t}{2\pi}\right] P(k); & k = 1, 2, \ldots, \frac{N}{2} - 1 \end{cases} \tag{4.24}$$

Power (in dB) Spectrum $LP(k)$

$$LP(k) = 10 \log_{10} P(k); \quad k = 0, 1, \ldots, \frac{N}{2} \tag{4.25}$$

Energy-Density (in dB) Spectrum LD(k)

$$LD(k) = \begin{cases} LP(k) + \log_{10} \dfrac{N\Delta t}{\pi} & ; k = 0 \text{ and } \dfrac{N}{2} \\[2ex] LP(k) + \log_{10} \dfrac{N\Delta t}{2\pi} & ; k = 1, 2, \ldots, \dfrac{N}{2} - 1 \end{cases} \qquad (4.26)$$

Aggregate Power AP

$$AP = \sum_{k=0}^{\frac{N}{2}} P(k) \qquad (4.27)$$

Aggregate Power (in dB) LAP

$$LAP = 10 \log_{10} AP \qquad (4.28)$$

Angular Frequency (in dB) LW(k)

$$LW(k) = \begin{cases} 20 \log_{10} (W(k)) & ; k = 1, 2, \ldots, \dfrac{N}{2}, Z = 0 \\[2ex] 20 \log_{10} \tan \left(\dfrac{\Delta Z W(k)}{2} \right) & ; k = 1, 2, \ldots, F, Z \neq 0 \end{cases} \qquad (4.29)$$

where F is the greatest integer function of $N\Delta t/2\Delta Z$.

Output

Output may be tabular and/or graphical at the discretion of the user.

Tabular Output. The parameters NREELS, IREEL(1), IREEL(2), IREEL(3), and IPLOT, obtained from a given data card 1, are listed at the time the card is read.

The parameters M, Q, DTIME, DZ, LCPR, LCPL, NS1, NRSS1, NS2, NRSS2, IPLOTE, LCB, and JOBE, obtained from a given data card 2, are listed at the time the card is read.

If the LCPR flag of a given data card 2 indicates that tabulation of input data is desired, header and selected trace data obtained from the input tapes specified will be printed. The tabulation of each data sample per trace will include its sample index and time reference. Header data will be listed only upon the first reference to the selected tapes.

If the LCPR flag of a given data card 2 indicates that tabulation of output data is desired, the spectra computed for each specified time trace will be printed. Each spectra value is associated with its corresponding frequency index and frequency. The tabulation of power spectra analysis includes k, $F(k)$, $W(k)$, $A(k)$, $S(k)$, $\theta(k)$, $P(k)$, $LW(k)$ and $LP(k)$.

Plot Output. Plot output is generated and written on the plot output tape on unit A6 provided IPLOT = 1 on data card 1 and LCPL = 1 or 2 on the current data card 2. If LCPL = 1, a plot of $W(k)$ vs $D(k)$ is created for each time trace specified. If LCPL = 2, a plot of $LW(k)$ vs $LD(k)$ is created. Calcomp plot routines and the plot output tape may be used as direct input to a Calcomp 563 Digital Incremental Plotter, using 22-inch wide plain paper.

Program Interaction

LASA edit seismometer tapes are generated by the LASA Tape Edit program; LASA subarray beam tapes are generated by the Subarray Beamformer program; LASA array tapes are produced by the LASA Beamformer program.

Program Restrictions

All program restrictions are indicated in the above section.

Comments

This program is written in FORTRAN IV for the IBM 7090.

Although plot options and routines are currently in the program, their final form is still subject to change. It is therefore recommended that the plot options not be exercised at this time.

Approximate execution time for the power spectra analysis of two time traces is 4 minutes, including the printing of both input and output data.
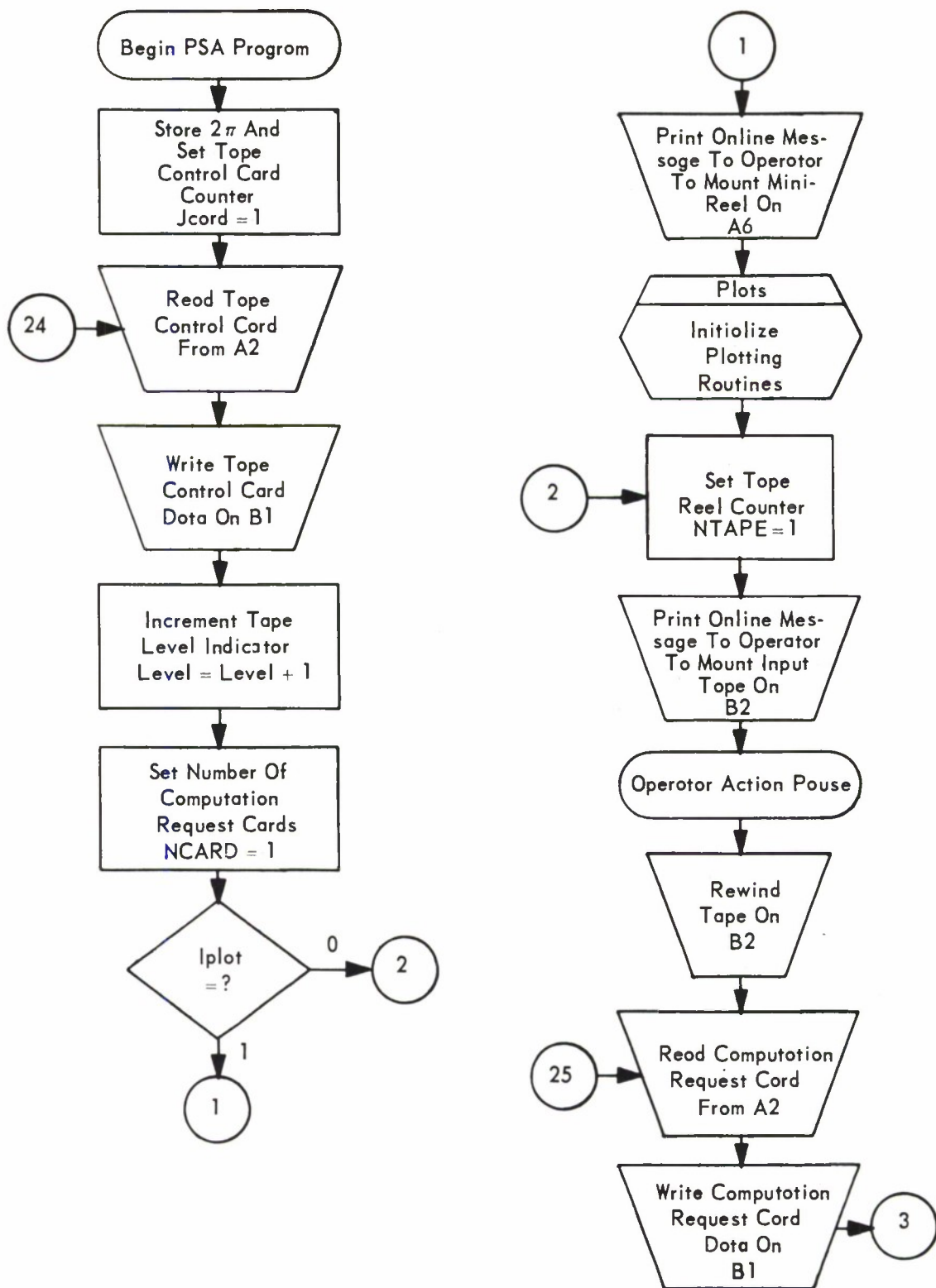
Figure 4-17. Power Spectra Analysis (PSA) (Sheet 1 of 8)
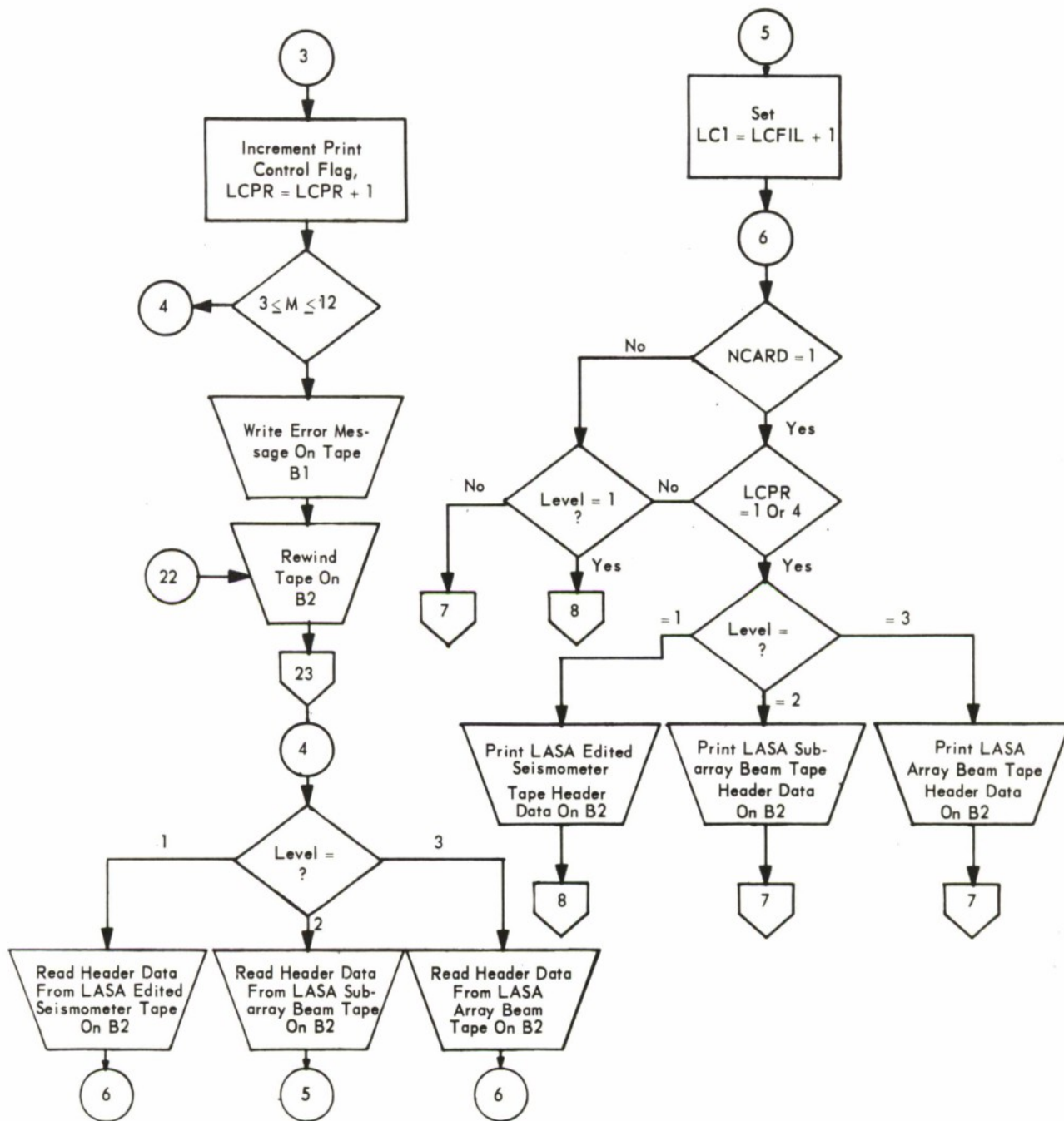
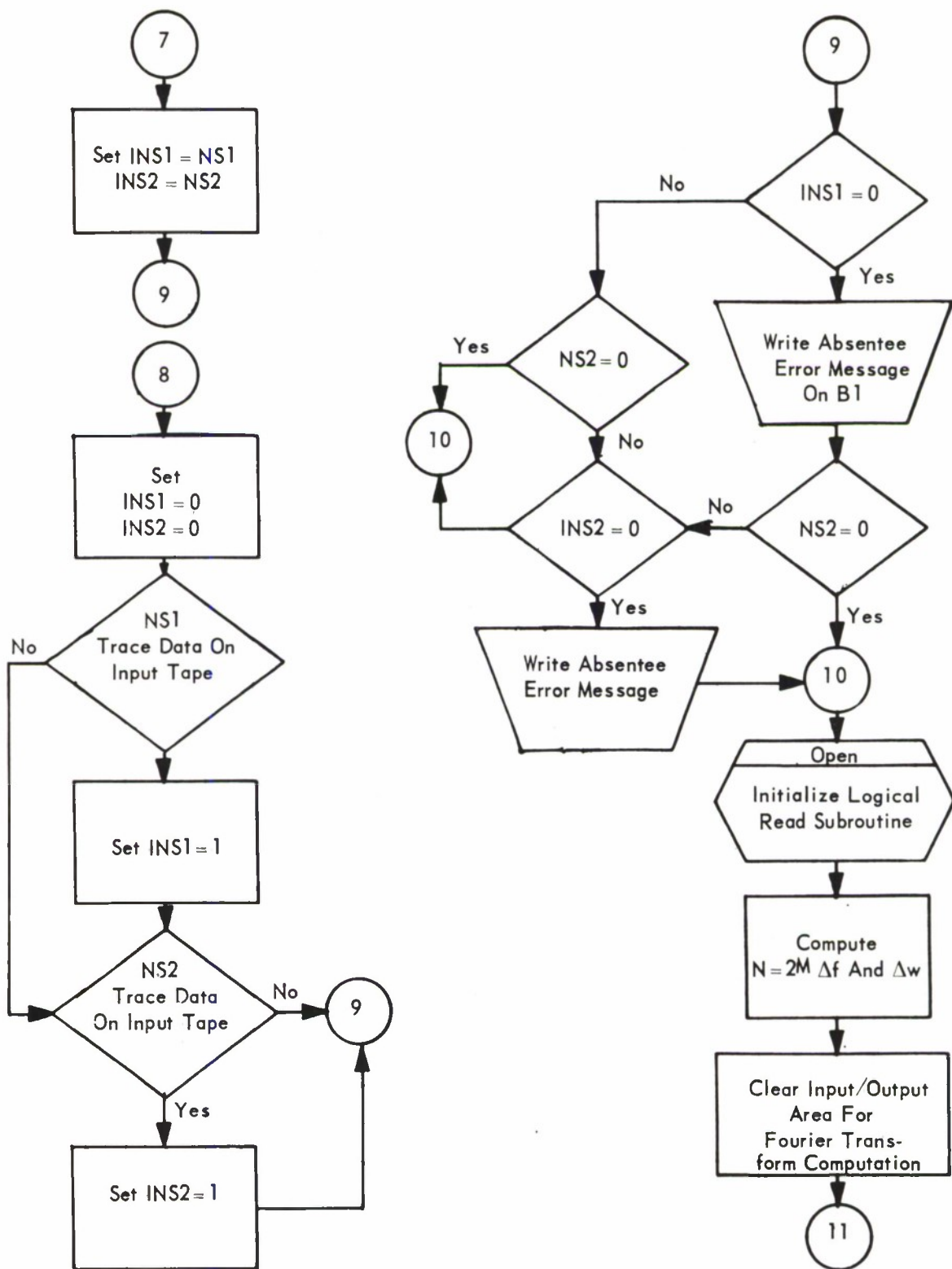Figure 4-17. Power Spectra Analysis (PSA) (Sheet 2 of 8)

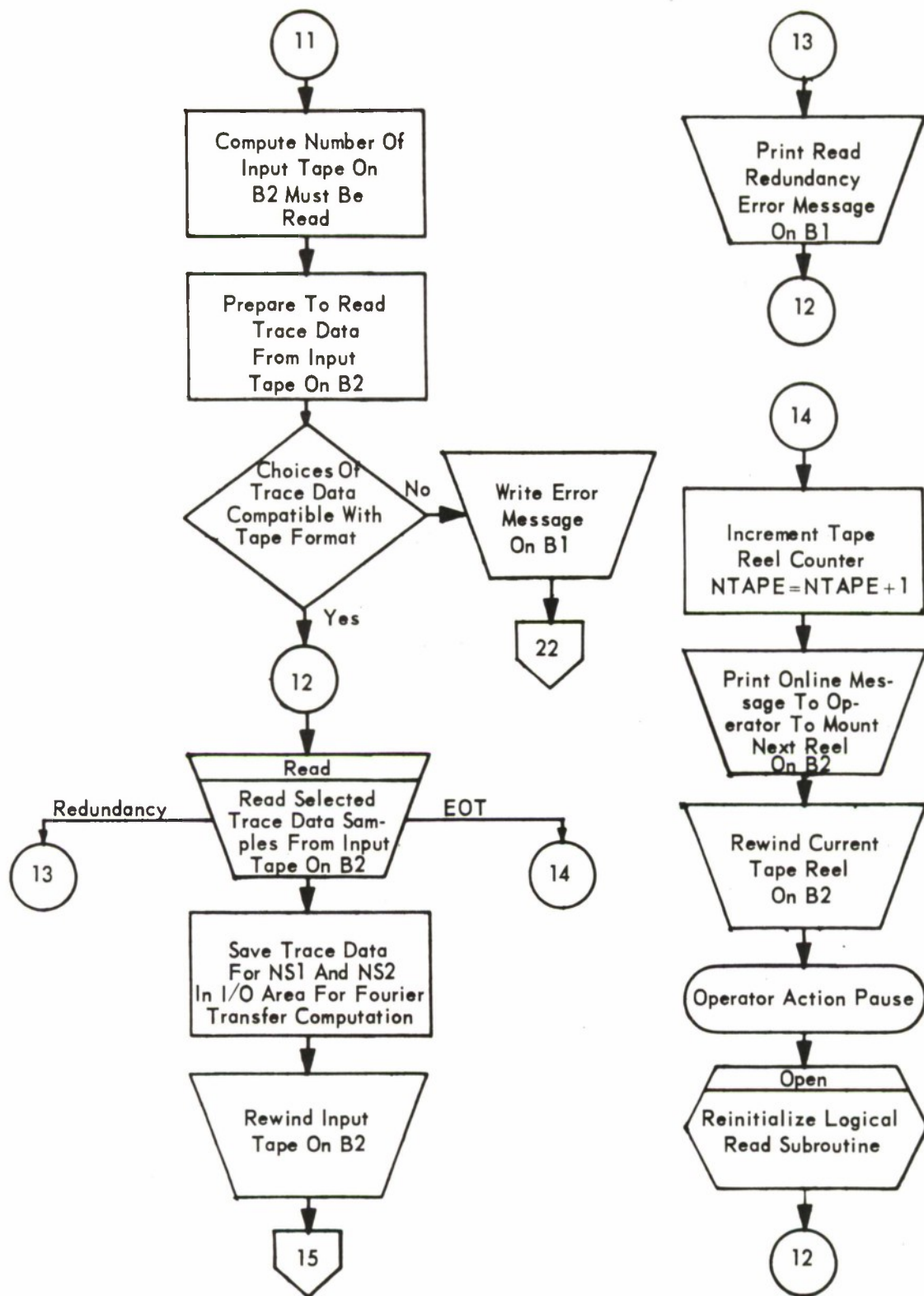Figure 4-17. Power Spectra Analysis (PSA) (Sheet 3 of 8)

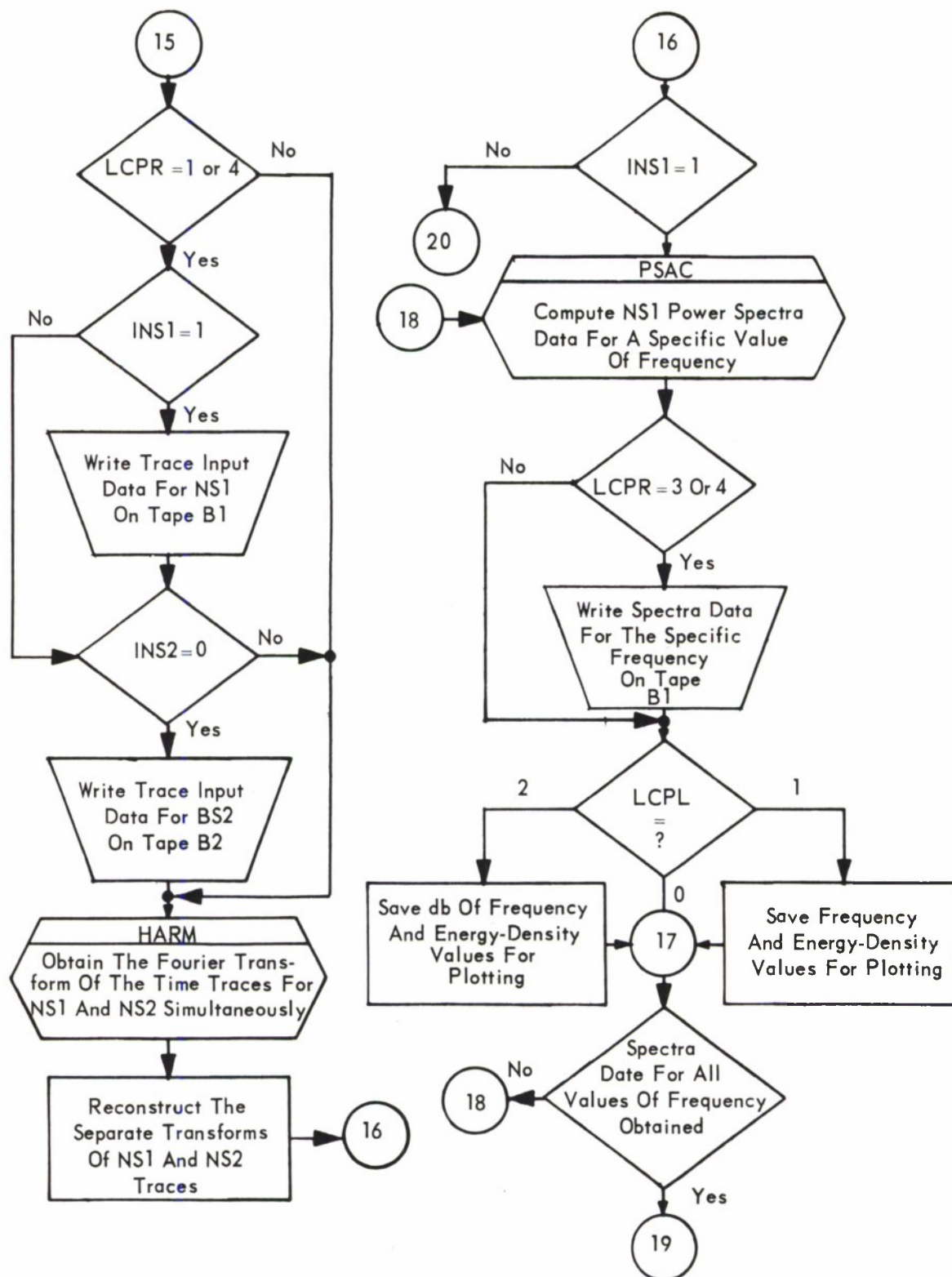Figure 4-17. Power Spectra Analysis (PSA) (Sheet 4 of 8)

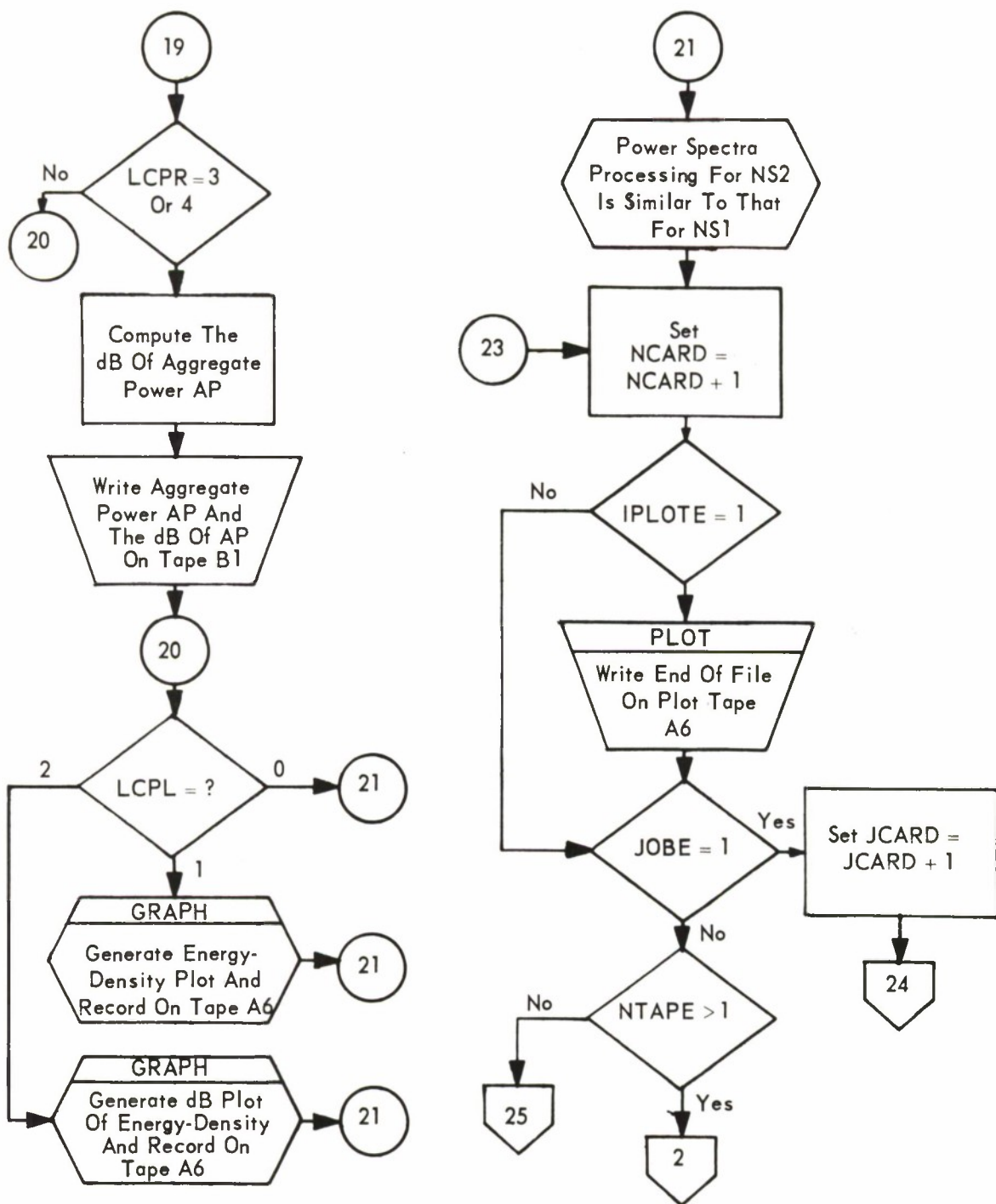Figure 4-17. Power Spectra Analysis (PSA) (Sheet 5 of 8)

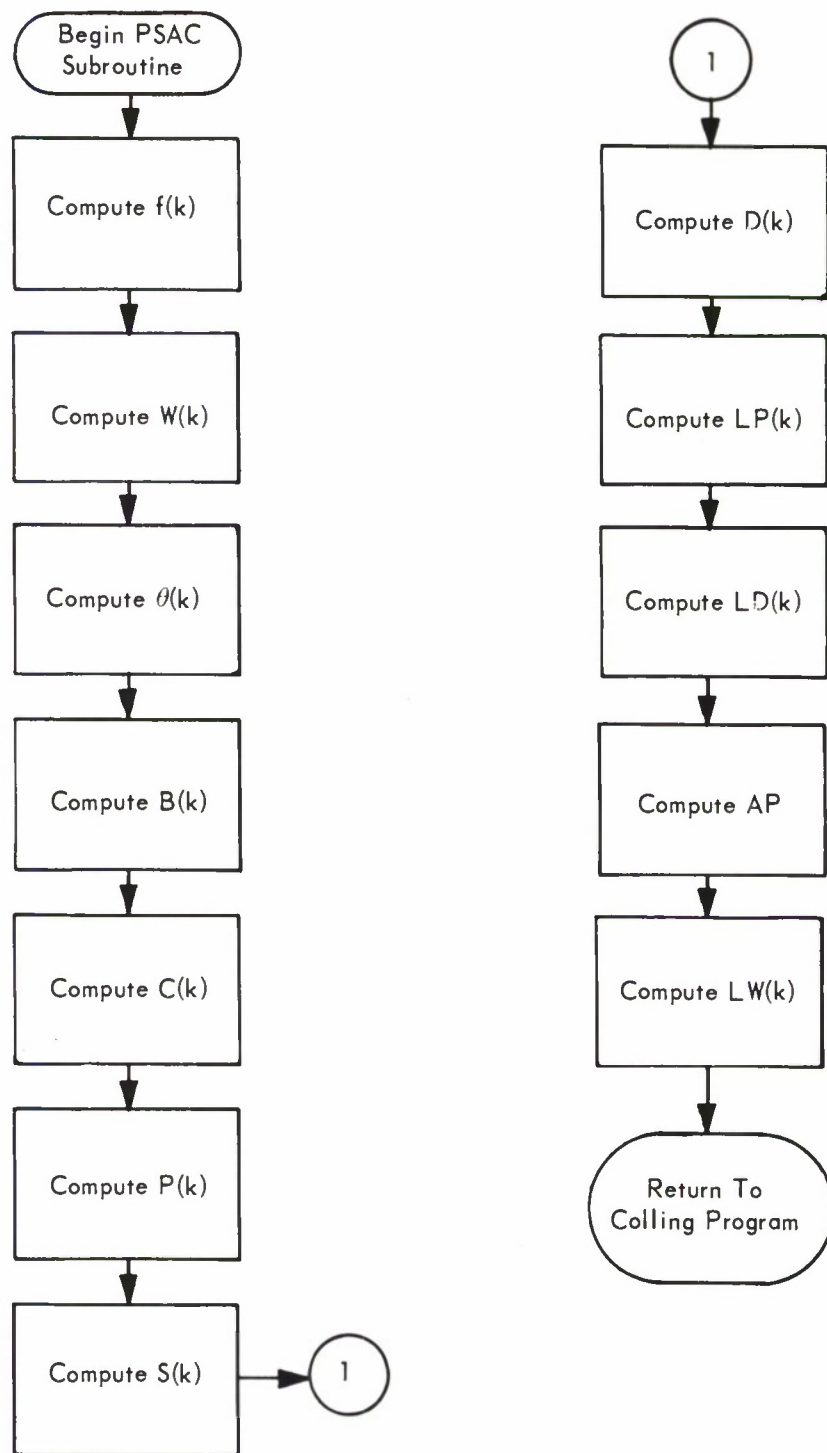Figure 4-17. Power Spectra Analysis (PSA) (Sheet 6 of 8)

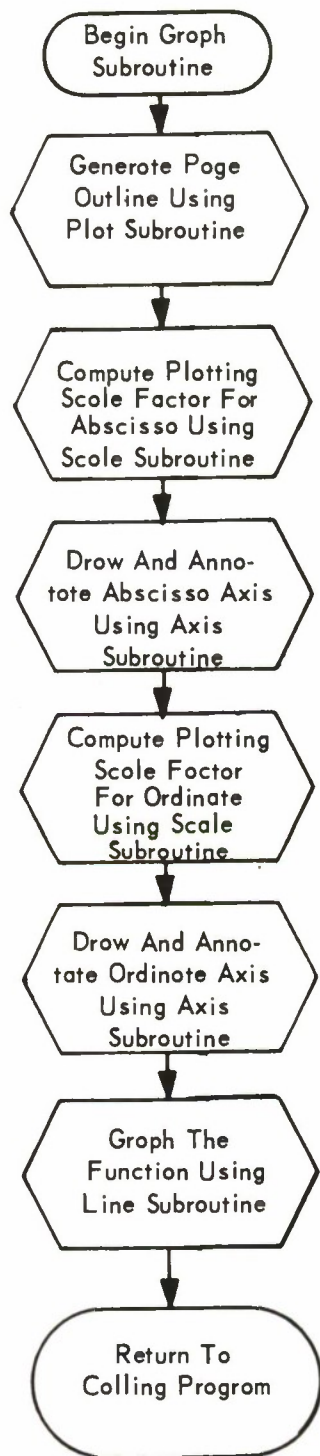Figure 4-17. Power Spectra Analysis (Sheet 7 of 8)

Figure 4-17. Power Spectra Analysis (Sheet 8 of 8)

4.18   SEISMIC RAY TRACE

Purpose

This program calculates the angular range, travel time, and inverse phase speed for both the direct and surface reflected rays, and repeats this calculation for arbitrary equal increments of Snell's constant over any desired range of values.

Description

Input

This program requires a number of layers, N, and for each layer, the radius and velocities at upper and lower boundaries. The source position is defined to be at the upper boundary of any layer with the receiver at the surface.

Card Inputs

Data Card 1

Card Column	Field Specification	Variable Name	Sample Value
1 – 2	I2	K	4
3 – 5	I3	M	1
6 – 14	F9.4	CMIN	220.0000
15 – 23	F9.4	CMAX	840.0000
24 – 32	F9.4	DLTAC	5.0000
33 – 34	I2	IRD	1

where

K	Number of layers ≤ 95
M	Source position defined to be at upper boundary of Mth layer (note: M ≤ K)
CMIN	Minimum value to use for Snell's constant
CMAX	Maximum value to use for Snell's constant

DLTAC   Increment value on Snell's constant

IRD   1/0 condition. Run will use all new data cards/Run will use new data from cards 1 and 2 of this run, data from cards 3 and 4 supplied by last run. (If only one ray trace is to be made, set IRD = 1.)

Data Card 2

Card Column	Field Specification	Variable Name	Sample Value
1	blank		
2 - 49	48H	(Descriptive data)	K to geography conversion 6/13/66)

Data Card 3

Card Column	Field Specification	Variable Name	Sample Value
1	blank		
2 - 24	23H	(Descriptive data)	Velocity profile 2

Data Card 4

Card Column	Field Specification	Variable Name	Sample Value
1 - 10	F10.3	RL(I)	5920.000
11 - 20	F10.3	RL(I)	9.000
21 - 30	F10.3	RU(I)	6370.000
31 - 40	F10.3	VU(I)	7.000

where

RL   Radius of lower boundary of Ith layer

VL   Speed at lower boundary of Ith layer

RU   Radius of upper boundary of Ith layer

VU   Speed at upper boundary of Ith layer

(Data card 4 is repeated for each layer)

Computation

This program was written under the LASA Signal Processing Study (reference 1) and has been converted to System/360 FORTRAN IV.

Output

For each layer, the radius in km at the lower (RL) and upper (RU) boundaries, the velocities in km/sec at the lower (VL) and upper (VU) boundaries, the velocity gradient (G) in sec^{-1}, and the zero-radius velocity (V0) in km/sec are printed. For each value of Snell's constant (C) in sec, the angular distance in degrees and km of both the direct ray (ADR and XDR) and reflected ray (ARFL and TRFL), inverse phase speed (VH-1) in sec/km, and radius of deepest penetration (RMIN) in km are recorded.

Program Interaction

Relation of inverse phase speed to range is used in the Inverse Velocity Space Mapping program.

Program Restrictions

In its current form, the program is restricted to a maximum of 95 layers. The source position must be at the upper boundary of one of the 95 layers.

Comments

This program is written in FORTRAN IV for the IBM System/360.

REFERENCES

1. "Large Aperture Seismic Array Signal Processing Study," IBM Final Report, Contract No. SD-296, 15 July 1965.

2. "LASA Signal Processing, Simulation, and Communications Study," IBM First Quarterly Technical Report, ESD Hanscom Field, Contract No. AF 19(628)-5948, ARPA Order No. 800, 27 May 1966.

3. "LASA Signal Processing, Simulation, and Communications Study," IBM Second Quarterly Technical Report, ESD Hanscom Field, Contract No. AF 19(628)-5948, ARPA Order No. 800, May-August 1966.

4. Edward F. Chiburis, "LASA Travel-Time Anomalies for Various Epicentral Regions," Seismic Data Laboratory of Teledyne, Inc., SDL Report No. 159, 13 September 1966.

5. Harold Jeffreys and K. E. Bullen, Seismological Tables, Burlington House, 1958.

6. Ragazzini and Franklin, Sampled Data Control Systems, McGraw Hill, 1959.

7. J. T. Tou, Digital and Sampled Data Control Systems, McGraw Hill, 1959.

8. K. Steiglitz, "The General Theory of Digital Filters with Applications to Spectral Analysis," New York University Laboratory for Electroscience Research, TR 400-99, 1963.

9. E. A. Guillemin, Synthesis of Passive Networks, Wiley, 1957.

10. Rader and Gold, "Digital Filter Design Techniques," Lincoln Laboratories, ESD-TDR-65-593, December 1965.

11. J. W. Cooley and J. W. Tukey, "An Algorithm for the Machine Calculation of Complex Fourier Series," Mathematics of Computation, Vol. 19, April 1965.

12. J. R. Healy and B. P. Bogert, "System/360 Scientific Subroutine Package Programmer's Manual," IBM Corporation, Form C20-0205.

DOCUMENT CONTROL DATA - R&D

(Security classification of title, body of abstract and indexing annotation must be entered when the overall report is classified)

1. ORIGINATING ACTIVITY *(Corporate author)*	2a. REPORT SECURITY CLASSIFICATION
International Business Machines Corporation 18100 Frederick Pike Gaithersburg, Maryland 20760	Unclassified
	2b. GROUP N/A

3. REPORT TITLE

LASA SIGNAL PROCESSING, SIMULATION, AND COMMUNICATIONS STUDY

4. DESCRIPTIVE NOTES *(Type of report and inclusive dates)*

Final Report (February 1966-January 1967)

5. AUTHOR(S) *(Last name, first name, initial)*

None

6. REPORT DATE	7a. TOTAL NO. OF PAGES	7b. NO OF REFS
March 1967	394	

8a. CONTRACT OR GRANT NO	9a. ORIGINATOR'S REPORT NUMBER(S)
AF 19(628)-5948	ESD-TR-66-635
b. PROJECT NO	
c	9b. OTHER REPORT NO(S) *(Any other numbers that may be assigned this report)*
d	

10. AVAILABILITY/LIMITATION NOTICES

Distribution of this document is unlimited.

11. SUPPLEMENTARY NOTES	12. SPONSORING MILITARY ACTIVITY
	Directorate of Planning and Technology, Electronic Systems Division, AFSC, USAF, L. G. Hanscom Field, Bedford, Mass. 01730

13. ABSTRACT

In this final report, the "LASA Signal Processing, Simulation, and Communications Study" results are described in detail.

A summary of our findings correlates the results with factual detail reported earlier. Signal processing is discussed; further system and simulation studies are reported; suggested system implementation is extended; and the set of simulation programs used in this study is presented.

DD FORM 1 JAN 64 **1473**

14. KEY WORDS	LINK A		LINK B		LINK C	
	ROLE	WT	ROLE	WT	ROLE	WT

INSTRUCTIONS

1. ORIGINATING ACTIVITY: Enter the name and address of the contractor, subcontractor, grantee, Department of Defense activity or other organization (corporate author) issuing the report.

2a. REPORT SECURITY CLASSIFICATION: Enter the overall security classification of the report. Indicate whether "Restricted Data" is included. Marking is to be in accordance with appropriate security regulations.

2b. GROUP: Automatic downgrading is specified in DoD Directive 5200.10 and Armed Forces Industrial Manual. Enter the group number. Also, when applicable, show that optional markings have been used for Group 3 and Group 4 as authorized.

3. REPORT TITLE: Enter the complete report title in all capital letters. Titles in all cases should be unclassified. If a meaningful title cannot be selected without classification, show title classification in all capitals in parenthesis immediately following the title.

4. DESCRIPTIVE NOTES: If appropriate, enter the type of report, e.g., interim, progress, summary, annual, or final. Give the inclusive dates when a specific reporting period is covered.

5. AUTHOR(S): Enter the name(s) of author(s) as shown on or in the report. Enter last name, first name, middle initial. If military, show rank and branch of service. The name of the principal author is an absolute minimum requirement.

6. REPORT DATE: Enter the date of the report as day, month, year; or month, year. If more than one date appears on the report, use date of publication.

7a. TOTAL NUMBER OF PAGES: The total page count should follow normal pagination procedures, i.e., enter the number of pages containing information.

7b. NUMBER OF REFERENCES: Enter the total number of references cited in the report.

8a. CONTRACT OR GRANT NUMBER: If appropriate, enter the applicable number of the contract or grant under which the report was written.

8b, 8c, & 8d. PROJECT NUMBER: Enter the appropriate military department identification, such as project number, subproject number, system numbers, task number, etc.

9a. ORIGINATOR'S REPORT NUMBER(S): Enter the official report number by which the document will be identified and controlled by the originating activity. This number must be unique to this report.

9b. OTHER REPORT NUMBER(S): If the report has been assigned any other report numbers (either by the originator or by the sponsor), also enter this number(s).

10. AVAILABILITY/LIMITATION NOTICES: Enter any limitations on further dissemination of the report, other than those imposed by security classification, using standard statements such as:

(1) "Qualified requesters may obtain copies of this report from DDC."

(2) "Foreign announcement and dissemination of this report by DDC is not authorized."

(3) "U. S. Government agencies may obtain copies of this report directly from DDC. Other qualified DDC users shall request through

_____ ."

(4) "U. S. military agencies may obtain copies of this report directly from DDC. Other qualified users shall request through

_____ ."

(5) "All distribution of this report is controlled. Qualified DDC users shall request through

_____ ."

If the report has been furnished to the Office of Technical Services, Department of Commerce, for sale to the public, indicate this fact and enter the price, if known.

11. SUPPLEMENTARY NOTES: Use for additional explanatory notes.

12. SPONSORING MILITARY ACTIVITY: Enter the name of the departmental project office or laboratory sponsoring (paying for) the research and development. Include address.

13. ABSTRACT: Enter an abstract giving a brief and factual summary of the document indicative of the report, even though it may also appear elsewhere in the body of the technical report. If additional space is required, a continuation sheet shall be attached.

It is highly desirable that the abstract of classified reports be unclassified. Each paragraph of the abstract shall end with an indication of the military security classification of the information in the paragraph, represented as (TS), (S), (C), or (U).

There is no limitation on the length of the abstract. However, the suggested length is from 150 to 225 words.

14. KEY WORDS: Key words are technically meaningful terms or short phrases that characterize a report and may be used as index entries for cataloging the report. Key words must be selected so that no security classification is required. Identifiers, such as equipment model designation, trade name, military project code name, geographic location, may be used as key words but will be followed by an indication of technical context. The assignment of links, rules, and weights is optional.

GPO 886-551